Development of Electrochemiluminescent Sensors as Screening Tools for the Identification of Drug Species within Complex Matrices for Forensic Investigations

A thesis submitted in fulfilment of the requirements for the degree of Doctor of Philosophy

Kelly Brown MChem

Supervisors:

Dr. Lynn Dennany

Dr. Pamela Allan-McMurray

Department of Pure and Applied Chemistry

University of Strathclyde

2020

This thesis is the result of the authors original research. It has been composed by the author and has not been previously submitted for examination which has led to the award of a degree.

Signed: 

Date: 10th December 2020

“You will see there is so much we don’t understand. And the only thing we know is things don’t always go to plan”

Simba (The Lion King 1994)

Acknowledgments

There are so many people on both sides of the hemisphere I am grateful to, without which my PhD experience would not have been the same or half as enjoyable.

Firstly, I would like to express my sincerest thanks to my supervisor Lynn, your unwavering support, guidance and constant encouragement have been invaluable over the past three years. Your easy-going approach and emergency coffee breaks have helped me hugely throughout this process. Without you I would not be here now.

I must also express my thanks to my second supervisor Pamela, your kind nature and constant cheer are inspiring, from my Master thesis till now your support has been amazing in guiding me towards the completion of my PhD.

I would also like to thank all the members of our research group, your support throughout the ups and downs of PhD life have kept me going, and especially for the constant supply of cakes, biscuits and sweets without which (I would be a dress size smaller) the afternoon slump in the office would not be the same. But I must especially thank Julien, you are the best Post-Doc anyone could ask for, your constant support and encouragement are why I'm still here, you are always there to listen to me rant, a tough job I'm sure. I owe you many a Raspberry Cooler Juju.

To my Rotten Bananas, I don't know how I would have done this without you guys. Alex you are the ray of sunshine we all need in our down days and Sayali you provide us with the guidance and grounding we need to keep going. Our morning, mid-day and afternoon tea breaks were my saviour, and the constant supply of memes, jokes and banter are invaluable.

Finally, to my family, friends (especially Amanda) and Joe, your love, laughter and constant support were key to seeing me through this journey, you have been there for me every step of the way since and your ability to put up with me is amazing I cannot thank you all enough. Mum and Dad, I would not be here without you both, through high school, my MChem and now my PhD you have always encouraged me to go for my dreams and never give up (even if I am a "Sponger") and so I must dedicate this thesis to you both. And Bailey you might have no idea what's going on but your cheeky antics, smiling puppy face and knowing when I've need a hug have gotten me through the last few months.

Abstract

Alternative substances of abuse such as novel psychoactive substances (NPS) still pose a significant public health risk, despite increased legislative controls. Therefore, the ability to identify such substances is vital in order to limit their circulation. Current screening methods are often inadequate for NPS and incompatible with a range of complex matrices. As such, it has become necessary to develop a robust screening methodology, applicable to a range of matrices. To this extent, the development of an electrochemiluminescent (ECL) sensor is detailed within, utilising the traditional $[Ru(bpy)_3]^{2+}$ luminophore. The developed sensor was successfully applied for the detection of tropane alkaloids, atropine and scopolamine, at forensically and clinically relevant concentrations within commercial drink samples (tonic water and Coca-Cola®), herbal plant material and biological fluids including human serum, artificial saliva, urine and sweat. Focus was placed upon the ability of the sensor to be utilised by non-experts outwith a laboratory facility. Hence, all analysis was performed without extraction, purification or separation strategies. The abrasive ECL technique developed, allowed direct detection of the alkaloids, following collection from a roughened skin surface and mechanical application of herbal material, without any surface damage or signal detriment observed. Finally, increased specificity was coined through the development of pH controlled ECL, which facilitated the detection and quantification of scopolamine, in the presence of atropine through suppression of its emission. This provided greater specificity previously unachievable with single luminophore ECL analysis.

Publications

K. Brown, P. Allan, P. S. Francis and L. Dennany, J. Electrochem. Soc., 2020, 167, 166502.

K. Brown, C. Jacquet, J. Biscay, P. Allan and L. Dennany, Analyst, 2020, 145, 4295-4304.

This paper is presented within Chapter Five of this thesis.

K. Brown, C. Jacquet, J. Biscay, P. Allan and L. Dennany, *Anal. Chem.*, 2020, **92**, 2216-2223.

This paper is presented within Chapter Six of this thesis.

K. Brown and L. Dennany, in *Forensic Analytical Methods*, The Royal Society of Chemistry, 2019, DOI: 10.1039/9781788016117-00115, pp. 115-139.

The publication is contained within Chapter One of this thesis.

K. Brown, M. McMenemy, M. Palmer, M. J. Baker, D. W. Robinson, P. Allan and L. Dennany, *Anal. Chem.*, 2019, **91**, 12369-12376.

This paper is presented within Chapter Four of this thesis.

A. J. Stewart, **K. Brown** and L. Dennany, *Anal. Chem.*, 2018, **90**, 12944-12950.

D. W. Robinson, **K. Brown**, P. Allan, M. J. Baker L. Dennany *et al.,* PNAS, 2020 *(in press) Proc. Natl. Acad. Sci., 2020, 117, 31026.*

K. Brown and L. Dennany, in *Challenges in Detection Approaches for Forensic Science,* The Royal Society of Chemistry, 2020 *(in press)*
The publication is contained within Chapter One of this thesis.

K. Brown and L. Dennany, in *Chapter 00093. Electrochemical sensors for new challenges*, Encyclopedia of Sensors and Biosensors, 2020 *(under editorial review as of Oct 2020)*

Presentations

Oral:

75th RSC Analytical Biosciences Group 75th Anniversary Annual General Meeting, Online Meeting, November 2020: *"Electrochemiluminescent Sensors as Screening Tools within Complex & Biological Matrices"*

7th Analytical Biosciences Early Career Researcher Meeting, Glasgow, March 2020: *"Making Light Work of Biological Matrices: Electrochemiluminescent Sensors as a Drug Detection Strategy for Biological Matrices"*

17th ISEAC & 3rd ECL 2019, Changchun, China, August 2019: *"Mixed Luminophore ECL for the Differentiation Between Analytes of Similar Chemical Structure"*

Carnegie Scholars Gathering 2019, Glasgow, February 2019: *"Forensic Electrochemistry: Shinning a Light on the Future of Drug Detection"*

Poster:

71st Annual Meeting of the International Society of Electrochemsitry, Online Meeting, August 2020: *"Does the Salt Really Matter? Impact of the Counterion Upon ECL Signals"*

RSC Twitter Poster Conference 2020, Online Meeting, March 2020: *"Electrochemiluminescent Sensors: A Move in the Light Direction for New Drug Detection"*

7th Analytical Biosciences Early Career Researcher Meeting, Glasgow, March 2020: *"Hallucinogens and How to Find Them: Rapid Drug Detection Utilising Electrochemiluminescent Sensors"*

CSOFS Student Conference,Glasgow, December 2019: *"Electrochemiluminescence: Lighting the way for the Future of Drug Detection"*

Electrochem 2019,Glasgow, August 2019: *"Disposable Electrochemiluminescence (ECL) Based Sensor for Rapid Drug Screening"*

STEM for Britain Finalist 2019, London, March 2019: *"Forensic Electrochemistry: Lighting the Way for Future of Drug Detection"*

BrightSparks Symposium 2018, Manchester, August 2018: *"Electrochemical Detection of Tropane Alkaloids Atropine and Scopolamine"*

8th EAFS 2018, Lyon, August 2018: *"Electrochemical Detection of Tropane Alkaloids"*

Scotland and North of England Electrochemistry Symposium (RSC Butler Meeting), Aberdeen, April 2018: *"Electrochemical Assessment for the Detection of New Illicit Substances"*

Carnegie Scholars Gathering 2018, Edinburgh, February 2018: *"Electrochemical Assessment of the Psychoactive of New Illicit Substances"*

Abbreviations

ΔE_p	Peak-to-peak separation
2-AI	2-aminondane
2C	2,5-dimethoxyphenethylamines
4-CMC	4-chloromethcathinone
4-MEC	4'-methyl-N-ethylcathinone
4-MMC	4-methylmethcathinone or mephedrone
A.U	Arbitrary units
ACN	Acetonitrile
ATR-FTIR	Attenuated total reflectance Fourier transform infrared spectroscopy
ATS	Amphetamine type stimulants
BSA-Au NC	Bovine serum albumin-stabilised gold nanoclusters
CB1/CB2	Cannabinoid receptors
CCD	Charged couple device
CE	Capillary electrophoresis
CE	Counter electrode
CL	Chemiluminescence
cP-ELISA	Competitive paper-based enzyme-linked immunosorbent assay
CV	Cyclic voltammetry
D_{CT}	Charge transfer coefficient
DLLME	Dispersive liquid-liquid microextraction
dMRM	Dynamic multiple reaction monitoring
E	Potential
EC	Electrochemical
ECL	Electrochemiluminescence
ELISA	Enzyme-linked immunosorbent assay
Ep_a	Anodic peak potential

Ep_c	Cathodic peak potential
EtOH	Ethanol
EWA	Early warning advisory
FT-IR	Fourier transform infrared spectroscopy
FWHM	Full width half maximum
GC	Glassy carbon
GC-MS	Gas chromatography mass spectrometry
HOMO	Highest occupied molecular orbital
HPLC	High performance liquid chromatography
HPLC-MS	High performance liquid chromatography mass spectrometry
Ip_a	Peak anodic current
Ip_c	Peak cathodic current
ISF	Interstitial fluid
LC-MS	Liquid chromatography mass spectrometry
LC-MS/MS	Liquid chromatography tandem mass spectrometry
LC-QqQ-MS/MS	Liquid chromatography triple quadrupole tandem mass spectrometry
$LiClO_4$	Lithium perchlorate
LOD	Limit of Detection
LSD	Lysergic acid diethylamide
LUMO	Lowest unoccupied molecular orbital
MAL	Methallylescaline
MDMA	3,4-Methylenedioxymethamphetamine
MLCT	Metal-to-ligand charge-transfer
MPA	Methiopropamine
MWCNT	Multi-walled carbon nanotubes
NaCl	Sodium Chloride
NMR	Nucelar magnetic resonance

NPS	Novel psychoactive substances
PCA	Principal component analysis
PCP	Phencyclidine
PL	Photoluminescence
PLS-DA	Partial least squares discriminant analysis
PLSR	Partial least squares regression
PMT	Photomultipler Tube
PSA	Psychoactive substances act
RBG	Red-Blue-Green
RE	Reference electrode
RSD	Relative standard deviation
$[Ru(bpy)_3]^{2+}$	Tris-(2,2′-bipyridyl)-ruthenium(II)
$Ru(bpy)_3]^{2+}].Cl_2.6H_2O$	Tris (2,2′-bipyridyl)-dichlororuthenium(II) hexahydrate
S-route	Singlet route
S/B	Signal to blank
SC	Synthetic cannabinoid
Sc-HBr	Scopolamine hydrobromide
SCE	Saturated calomel electrode
SERS	Surface enhanced Raman spectroscopy
SLE	Supported liquid extraction
SPE	Screen printed electrodes
ST-route	Singlet-triplet route
T-route	Triplet-triplet annihilation route
Δ^9-THC	Δ^9-tetrahydrocannabinol
UK	United Kingdom
UNODC	United nations office on drugs and crime
UV	Ultraviolet
WE	Working electrode

Table of Contents

CHAPTER ONE

INTRODUCTION AND GENERAL LITERATURE REVIEW

“ Just because it’s what’s done, doesn’t mean it’s what should be done”

Cinderella (Cinderella 1950)

This chapter comprises of publications:

K. Brown and L. Dennany, in Forensic Analytical Methods, The Royal Society of Chemistry, 2019, pp. 115-139. (Primary author)

DOI: 10.1039/9781788016117-00115

K. Brown and L. Dennany, in Challenges in Detection Approaches for Forensic Science, 2021. (Primary author)

In press, publication in January 2021

1.1 Introduction

New or novel psychoactive substances (NPS), often misleadingly referred to as “legal highs”, are a diverse range of purposely designed pharmacological analogues of controlled substances which mimic their ‘parent’ compound user effects. Through the alternation of chemical structure to produce these NPS, the compounds themselves often lie outwith the traditional drug legislation in place.[1, 2] A formal definition of NPS can be found within the 2014 New Psychoactive Substances Report provided by the United Kingdom (UK) government which defines them as; “Psychoactive drugs, newly available in the UK, which are not prohibited by the United Nations Drug Conventions but which may pose a public health threat comparable to that posed by substances listed in these conventions.”[3] With their availability and legitimate routes of purchase and consumption, a marked increase in their abuse was globally observed, furthered by the growing online market and adaptability of these compounds to circumvent legislation.[4] What’s more the terminology, “legal high”, used in combination with branded packaging and availability in high street stores leads to the misconception that these substances offer a lower risk alternative to traditional illicit substances. With NPS marketed as not for human consumption, often under the guise of bath salts or plant food, manufacturers were able to bypass the strict legislation in place for food products adding a further degree of risk to the consumer.[1, 3, 5, 6] A number of NPS were initially developed by utilising failed pharmaceutical drug campaigns, with expired patents providing clandestine chemists with a diverse range of structures and synthetic routes to exploit.[1] However, little is

known about their pharmacology and long-term health effects, although paranoia, psychosis and seizures have all been reported.[1, 3, 6-8] Often the potency of these NPS is far greater than their controlled counterpart resulting in frequent overdoses amongst users, as witnessed with within the synthetic cannabinoid (SC) drug class. SCs were designed to mimic the psychoactive effects of Δ^9-tetrahydrocannabinol (THC), through virtue of their structural similarities.[9, 10] Δ^9-THC is the main component responsible for the psychoactive effects of cannabis as a result of its agonist action toward the cannabinoid receptors (CB1 and CB2). While Δ^9-THC is considered a partial agonist toward these receptors, SC often display full agonist behaviour toward the CB1 and CB2 receptors.[9, 10] This greater potency thus accounts for the enhanced psychoactive effects experienced by users of these substances compared with cannabis.[11]

NPS have rapidly become a global phenomenon, present within 120 countries with 950 substances reported to the United Nations Office on Drugs and Crime (UNODC) Early Warning Advisory (EWA) system as of December 2019.[12] Despite various attempts by government bodies to increase the legislative control on these substances, they still pose a major threat to public health with a significant number of deaths attributed to their use each year. With the UK government introducing a blanket ban on their use in the form of the 2016 Psychoactive Substances Act (PSA), it was hoped their prevalence would decline however with 713 deaths attributed to NPS use within the UK

alone in 2018, it is evident they still pose a significant risk to the public despite these legislative measures.[13, 14]

It has become increasingly important to recognise that drugs cannot be simply defined as those traditional illicit substances or these NPS but also must include legal or medicinal substances. Often the terminology of drugs or drug use leads to the presumption of illicit substance abuse, such as heroin or cocaine. However, the dictionary definition of a drug as "a medicine or other substance which has physiological effect when ingested or otherwise introduce into the body" highlights how this terminology should cover a range of different substances.[15] Therefore, it becomes more correct to include, alcohol, tobacco, medicines and even poisons within this category. Moreover, with criminality considered one of the major factors toward the classification of a drugs of abuses' potential harm to society it becomes clear that substances outwith this common connotation should also be considered as a contributing factor.[16] With substances such as Rohypnol™ [17-19], atropine[20-22] and scopolamine[17, 23-28] amongst others increasingly used to facilitate criminal activity including; sexual assault, theft and attempted murder, a more diverse approach must be taken by forensic practitioners and policymakers to tackle alternative substance abuse.

Therefore, it has become increasingly important to consider more than just NPS when considering the challenges faced by the forensic community in regard to alternative drug substances. This chapter will primarily focus upon

the detection strategies and their corresponding challenges for the analysis of alternative psychoactive drugs. Secondly how their detection is further hindered by their incorporation into complex matrices will be considered. With reliable detection strategies applicable to a variety of alternative and complex matrices limited, it is hoped to highlight the potential of alternative approaches, primarily electrochemical techniques, and how their intrinsic benefits will aid in the expansion of their use as a potential screening methodology within the forensic arena.

The versatility of electrochemical sensing methods lends itself well to a wide range of applications across a diverse range of fields.[29-32] Electrochemical sensors are particularly amenable for forensic analysis. The portability, sensitivity and minimal sample preparation required, makes them ideally suited for at-scene, point-of-care and evidential analysis, particularly as a screening tool during the initial phases of an investigation.[33] With their continued development leading to increased specificity and their ability to facilitate direct detection within complex sample matrices, including biological fluids, expansion of their applications within the forensic environment is inevitable. Flexibility in choice of electrode material alongside surface functionalisation facilitates easy sensor fabrication for targeted analyte detection, thereby improving sensor specificity as well as offering versatility of their applications, dictated through the surface modification. The increased use of screen-printed electrodes (SPE) offers a mechanism for the reduction of cross contamination risk as a result of their disposability, in addition to an

ease of surface modification for targeted detection during their manufacturing process, increasing their commercialisation potential. The incorporation of different species for surface modification has never been simpler or more attainable, with facilities allowing fabrication of electrodes in-house now widely available. Portable potentiostats (now widely available) in combination with disposable SPE and minimal sample preparation facilitates on-site and point-of-care analysis, a key goal within forensic research. By enabling the rapid identification of substances, the police and forensic investigators are able to make informed decisive investigative decisions, whilst also minimising any potential for cross contamination or evidence destruction during transportation between crime scenes and forensic laboratories where full characterisation and analysis is performed.

Electrochemical methods are however unlikely to entirely replace the traditional gold-standard analytical techniques currently employed within forensic analysis. This is partly due to the complex and diverse range of sample matrices, often requiring the employment of a range of techniques for sample analysis coupled with the legal requirements necessary for presentation within courts. However, electrochemical sensors do offer a viable portable technique, whose employment at crime scenes or as screening devices would ultimately improve forensic investigative tools.

1.2 Traditional Detection Methodologies

With the continued increase in alternative drug abuse and related deaths, it is vital that these substances can be readily identified to limit their circulation. Moreover, the ability to rapidly identify these substances is vital across a range of environments including, seized goods analysis, clinics for the monitoring of substance abuse, post-mortem examinations and criminal casework. Hence an increased importance has been placed upon the development of effective and efficient detection methods. Despite conventional methods used for traditional illicit substance identification offering reliable and often unparalleled detection strategies, these are often incomplete or incompatible with a number of NPS. Their inability to address this global phenomenon utilising traditional approaches is further emphasised when considering that the well-established screening techniques, primarily consisting of the colorimetric presumptive tests which offer class identification, are incompatible with the majority of complex matrices and rely upon the subjectivity of colour identification to assign a class.[34] Furthermore, the vast numbers of NPS analogues and their extensive metabolism, with little to no structural difference can lead to false identifications, particularly within biological fluids where metabolites are often used to determine the parent drug. Various detection strategies available are reliably used for traditional illicit substance detection and have a common place within forensic laboratories. Such techniques include; hyphenated chromatographic and mass spectrometry systems[35-43], nuclear magnetic resonance (NMR)[44-46], Fourier transform infrared spectroscopy (FT-IR)[47, 48] and Raman

spectroscopy.[49-51] In recent years these techniques have shown promise for the detection of NPS and alternative drug substances. The following sections will discuss the advantages and limitations of such techniques for the identification of these species within complex matrices, including biological fluids.

1.2.1 Chromatographic Methods

Hyphenated chromatographic methods largely remain the gold standard within forensic analysis for compound identification and are currently the recommended detection strategy by the Scientific Working Group for the Analysis of Seized Drugs (SWGDRUG).[52] Most often, within the forensic arena, these separation strategies are coupled with mass spectrometry for the identification of unknowns via their characteristic fragmentation patterns. The vast number of NPS and their corresponding metabolites present within biological fluids, often found within a forensic case, requires instrumentation that is highly sensitive and offers a good degree of specificity. Traditional chromatographic methods employed for the detection and confirmation of NPS include gas chromatography mass spectrometry (GC-MS) and liquid chromatography tandem mass spectrometry (LC-MS/MS). These methodologies have been successfully applied to a range of biological fluids including blood, urine and oral fluid (i.e. saliva), all of which are forensically and toxicologically relevant matrices. GC-MS is widely regarded as the most established technique within forensic analysis and as such is an obvious contender for the detection of NPS.[42]

In 2016 Geyer *et al.*[53] demonstrated the power of GC-MS through the qualitative identification of 13 diphenidines class NPS alongside some of the common adulterants including benzocaine and caffeine.[53] Through a simple solvation and injection methodology they were able to successfully resolve all adulterants and diphenidines within a 43-minute analysis time, despite their almost indistinguishable chemical structures.[53] By removing any derivatisation procedures, commonly required prior to GC-MS analysis, the complexity, analysis time and cost were significantly reduced. In addition, the authors then described the quantitive power of their methodology, through analysis of individual and mixed samples of two purchased dipheidine derivatives at concentrations comparable to the quoted vendor values.[53] Although this direct analysis methodology demonstrated a strong proof-of-concept for the detection of these structurally similar NPS derivatives, their methodology was only applied to drugs in their powdered forms. Rather it would be more beneficial if biological samples were analysed to establish the success of such a simple GC-MS methodology toward complex matrix analysis. Geyer *et al.*[53] offer a simplistic GC-MS methodology which showed promise for the identification of NPS within forensic analysis. Proposing the potential of such techniques for employment as rapid screening methodologies, may however be premature. Without the assessment of the capability of such a methodology for alternative NPS classes, in addition to its compatibility with biological matrices its applicability to a variety of different forensic matrices remains unknown. Although the removal of the

derivatisation procedures has simplified the methodology, the instrument requirements mean such techniques still require fully dedicated laboratory facilities, and as such can never be considered truly portable.

The detection of NPS within biological matrices is faced with several challenges. Not only is there extensive metabolism of NPS, often resulting in structurally identical metabolites arising from different parent NPS compounds, but the constant production of NPS by clandestine chemists with varying structures poses a significant challenge to forensic toxicologists. In addition, the vast majority of NPS are incompatible with the current immunoassay screening methods, often producing false positives as a result of immunoassay cross reactivity. As such, there remains a sizeable gap in the forensic arena for screening protocols applicable to NPS. Chromatographic methods make up the vast majority of the methodologies currently proposed, however, whether GC-MS or LC-MS is used, samples require pre-treatment or extraction prior to analysis to remove the target species from the biological matrix.[35-39, 54, 55] As a result the proposed methodology is incompatible for applications outwith a fully equipped lab with experienced personnel, decreasing throughput in turn with an increase in analysis time, cost and reagent consumption. Factors which screening methodologies are traditionally employed to minimise.

Mercieca *et al.*[42] attempted to overcome the aforementioned limitations by employing dispersive liquid-liquid microextraction (DLLME), which allowed for

the simultaneous derivatisation of compounds alongside a rapid low cost extraction procedure. Using hexyl chloroformate, Mercieca *et al.*[42] flash derivatised a range of NPS classes including amphetamine-type stimulants, synthetic cathinones, phenehtylamines and ketamines, successfully resolving all analytes including positional isomers.[42] Their methodology, summarised in Figure 1.1, can be performed in under 22 minutes, with a 6 minute preparation time and 15 minute chromatographic analysis time. Moreover, the authors have not only demonstrated this method under ideal conditions, they have also shown its ability to separate 26 compounds within both human urine and whole blood.[42] This is a significant advantage as it addresses the limitation of chromatographic methods previously described, which only demonstrated the ability to separate out compounds within ideal non-biological matrices. As forensic cases often involve toxicological samples it is vital that any developed methodology is applicable both to pure samples and a variety of biological matrices. As such the methodology proposed by Mercieca *et al.*[42] offers a relatively high throughput, method in comparison to traditional chromatographic methods, and has proven success in the analysis of real-case samples identifying 3,4-Methylenedioxymethamphetamine (MDMA), ketamine and norketamine in whole blood.[42]

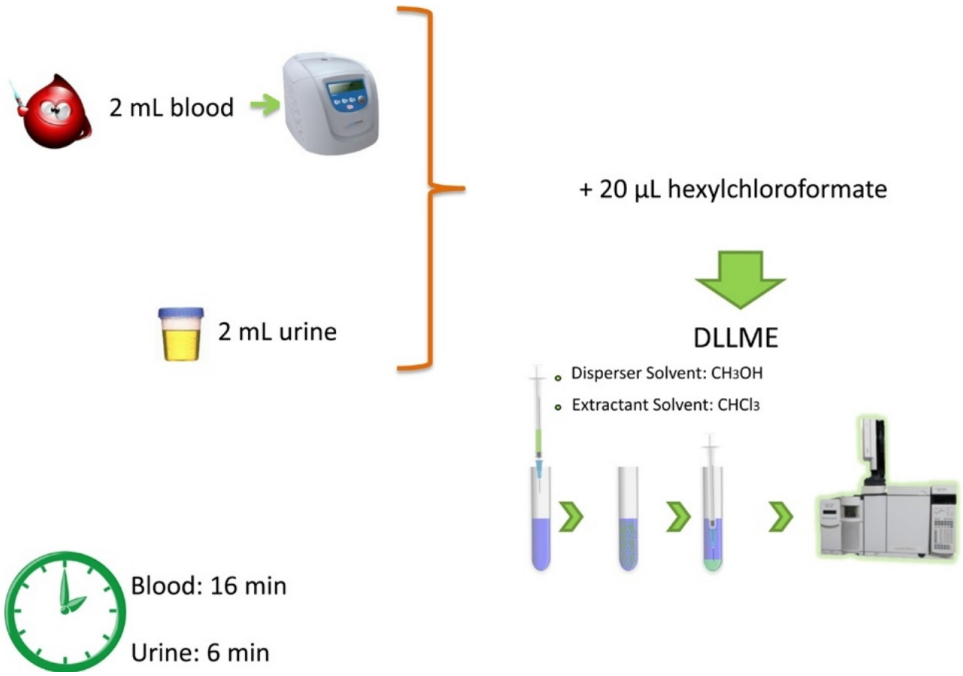

Figure 1.1: Schematic summary of the DLLME and chromatographic separation procedures of Mercieca *et al.*[42] for the analysis of NPS within urine and whole blood samples. Reproduced from ref. 42 with permission from Elsevier, Copyright 2018.

A prevalent constraint amongst many of the currently developed NPS detection methodologies is the narrow range of NPS classes which are typically focused upon, with many solely concentrating upon one group of NPS structures.[35, 38, 53-55] Without considering all classes the impact upon resolution from co-eluting species, including other NPS classes, common illicit substances and adulterants cannot be ascertained. Moreover with continually evolving structural changes and over 500 new NPS analogues reported over the last decade, it is impossible for forensic services and manufacturers to maintain a current and working reference library.[52, 56] As

such, the task of developing and maintaining positive screening methodologies even more improbable. However, recent developments in chromatographic technologies may present a solution to such problems. The use of liquid chromatography triple quadrupole tandem mass spectrometry (LC-QqQ-MS/MS) in combination with a dynamic multiple reaction monitoring (dMRM) mode has shown a huge amount of promise in the assessment of vast numbers of NPS, illicit substances and prescription adulterants. The methodology proposed by Kimble and DeCaprio[43], summarised in Figure 1.2, was successfully employed for the qualitative identification of over 800 NPS, alongside common licit and illicit substances.[43] Moreover, the authors were able to quantify 80 NPS which did not co-elute. Although these are incredibly impressive numbers of identifiable NPS, the 10-fold decrease from 800 to 80 between qualification and quantification highlights serious limitations faced by chromatographic methods due to the significant numbers of NPS and their corresponding metabolites. However, this does not discredit the huge impact the employment of such a methodology can offer the forensic community. Using a dMRM method allowed for the identification of species that elute at similar retention times but possess different transitions, hence facilitating the identification of over 800 NPS, metabolites and adulterants, even within the complex matrix of human urine.[43] To validate this methodology, the authors obtained toxicological case samples and analysed them with their developed methodology and database. The results were largely consistent with those obtained during the traditional forensic analysis, but also highlighted the

presence of additional NPS not initially detected through the routine screening methodologies employed.[43]

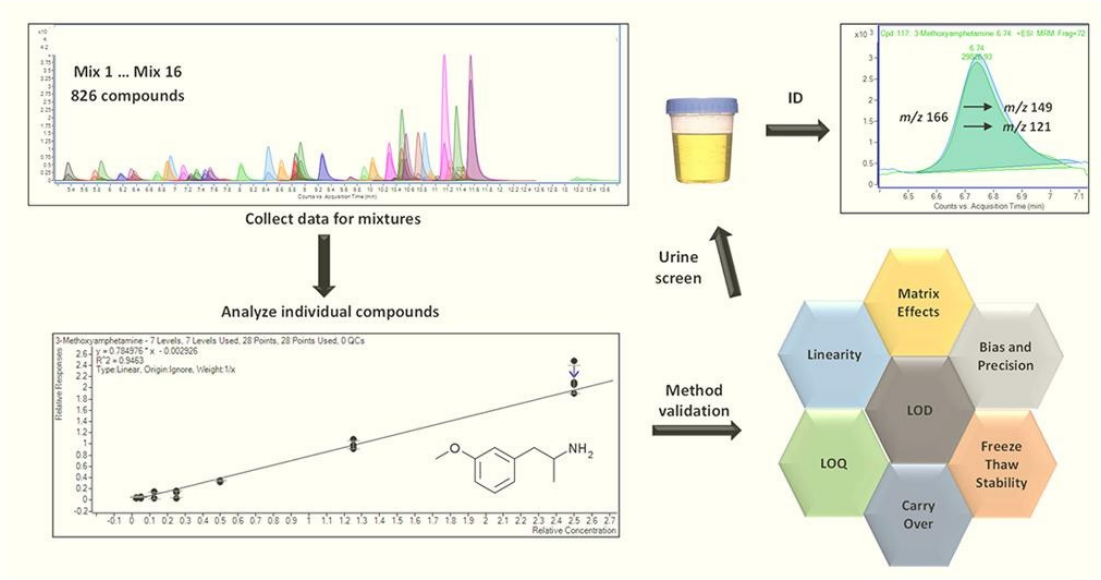

Figure 1.2: Schematic summary of the dMRM and LC-QqQ-MS/MS methodology from Kimble and DeCaprio[43] for the analysis of over 800 NPS within urine. Reproduced from ref. 43 with permission from Elsevier, Copyright 2019.

The use of dMRM in combination with LC-QqQ-MS/MS by Kimble and DeCaprio[43] has highlighted how continued advancements in chromatography have the potential to address a number of the disadvantages facing current screening methodologies. This is highlighted through consideration of the ability to detect NPS original not found within the case samples. Moreover, the authors simple “dilute-and-shoot” method for urine samples negates the need for any extraction procedures. Although no alternative biological matrices were tested using their methodology, it stands to reason that if combined with the DLLME proposed by Mercieca *et al.*[42] the combination of

the two would offer a rapid screening procedure for a huge number of NPS; even those with similar retention times. Although these developments represent a step forward in tackling the challenge of NPS detection, particularly within biological matrices, they still fail to offer a low-cost methodology with expensive and specialist equipment required coupled with expert knowledge of the techniques. Moreover, both LC-MS and GC-MS techniques require fully dedicated laboratory facilitates, with access to gas cylinders including nitrogen and helium thus making them unsuited for at-scene analysis or within other environments where drug screening is performed on site, such as border patrol or airport security. While the need for reference standards remains imperative for chromatographic analysis, although a number of reference standards are widely available from manufacturers, the diversity of NPS and continual growth make it almost impossible for reference standard manufacturers to sustain an active and complete reference library.[52, 56]

1.2.2 Spectroscopic Methods

Spectroscopic methods including Raman and IR have become increasingly popular within forensic analysis.[57-59] This can be attributed to the recent advances within instrumentation, which has resulted in a rise in the miniaturisation of traditional benchtop instruments toward handheld portable systems ideal for at-scene analysis.[59] Not only this but when paired with statistical analysis methods such as chemometrics, the ability to build large libraries based upon a compound's spectroscopic fingerprint, which can be

stored within the instrumentation for rapid identification, makes these spectroscopic devices increasingly powerful analytical tools.[59] When combined with their non-destructive nature and wide range of compatible matrices they appear to offer a viable alternative for the detection of NPS satisfying a number of the requirements not met by the more traditional chromatographic methods.

One distinct advantage of spectroscopic techniques is the ability to directly analyse samples, negating the need for sample extraction. This is in contrast to the sample preparation procedures typically required for chromatographic methods. As such spectroscopic techniques offer an increased sample throughput with a decrease in reagent consumption and often analysis cost. The ability to directly analyse samples comes to the forefront when the analysis of blotter papers, typically impregnated with psychedelics, is performed. Traditional methods for the analysis of blotter papers requires the extraction of substances form their surface, destroying the sample in the process. Neto[57] demonstrated the power of attenuated total reflectance Fourier transform infrared spectroscopy (ATR-FTIR) for the direct analysis of such a complex matrix.[57] Using ATR-FTIR, Neto[57] was successfully able to directly detect a range of psychedelic NPS, known as NBOMEs, from blotters surface. Neto[57] assigned the spectra collected from the blotters to IR spectral libraries for the identification of present NPS. However, the cellulose/paper and plastic polymer backgrounds of the blotters hindered a number of measurements, swamping the signals obtained. Of the 72 blotters analysed,

this method returned only 9 positive NBOME blotters, with the remaining returned as negative for the presence of the NPS.[57] It therefore becomes apparent that the use of ATR-FTIR for complex matrices is hindered by the matrix effects, which can dominate the spectra obscuring peaks resultant from the presence of NPS. However, the power of the technique comes when combined with chemometric analysis methods. Through the employment of deconvolution followed by multiclass discriminant analysis the number of blotters returned as positive for the presence of the NPS increased to 39.[57] A summary of the statistical analysis performed by Neto[57] is shown in Figure 1.3. Through the employment of these statistical analysis methods, Neto[57] was able to further classify the NPS present into NBOMEs, lysergic acid diethylamide (LSD) and methallylescaline (MAL), with a specificity of 94% and sensitivity of 82% reported.[57] To determine the accuracy of the ATR-FTIR assignment, GC-MS and LC-MS were employed. The results demonstrated a strong agreement with the ATR-FTIR assignment following deconvolution, although, highlighted the limited ability of IR to assign the different NBOMEs within the class with a number of misassignments noted and false negatives returned when the illicit substance LSD was present.[57] Neto[57] has highlighted the potential of ATR-FTIR for direct NPS detection within a complex blotter matrix, through this work. However, the limitations as a result of matrix effects are clear and the requirement for an adequate chemometric model is highlighted to avoid false class assignments or false negatives. As noted by Neto[57] one of the major limitations faced by his methodology is the lack of reference standards available to build the required chemometric models.

Hence although offering a non-destructive and rapid analysis method, the lack of available reference standards, as is also observed with chromatographic methods, remains a significant challenge that has yet to be addressed. As a result the employment of chemometric methods within the forensic arena for NPS detection remains low.

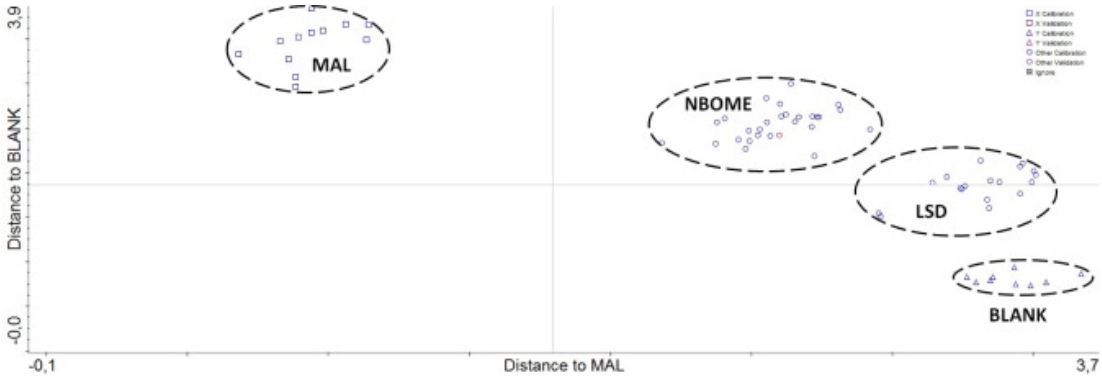

Figure 1.3: Plot of Mahalanobis distances following classification of MAL, NBOME, an LSD after calibration of the discriminant analysis method to classify blotters. Reproduced for ref. 57 with permission from Elsevier, Copyright 2015.

In 2017 Pereria *et al.*[58] attempted to improve upon the methodology of Neto[57], by employing ATR-FTIR alongside a supervised classification model, using partial least squares discriminant analysis (PLS-DA) for the classification of a range of psychedelics, including NBOMEs, LSD, 2,5-dimethoxyphenethylamine (2C-H) and MAL.[58] Of particular note is the fact that Pereria *et al.*[58], similarly to Neto[57] described issues regarding miss assignment of NBOME classes and the classification of some LSD samples as blanks. This becomes obvious when consulting the classification plots for

each of the NPS classes, shown in Figure 1.4, whereby all classes except LDS are grouped above the threshold away from the other classes.[58] This therefore raises the question over the sensitivity of the method, with Pereria *et al.*[58] stating that the false negatives for LSD are attributed to the low concentrations of LSD present upon the blotter papers in comparison to the other NPS classes analysed. A further limitation is highlighted by the inability of this model to identify new species, assigning them as blanks, as they are not included within the model. Similarly, if previously unencountered compounds share similar functionalities to the NBOME, 2C-H or MAL structural classes then it would be falsely assigned to the closest matching class, hence resulting in false positives.[58]

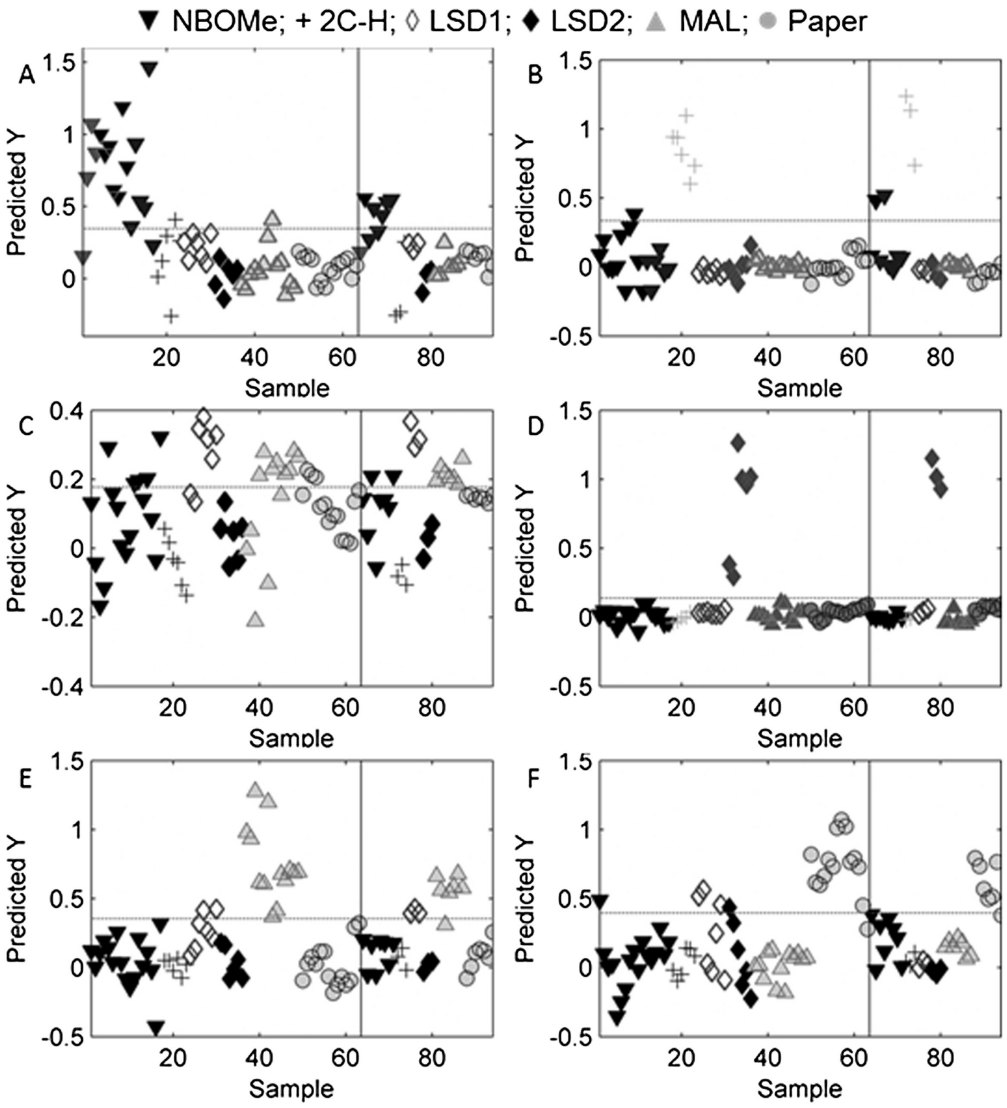

Figure 1.4: Classification plots for (A) NBOMe, (B) 2C-H, (C) LSD1, (D) LSD2, (E) MAL, and (F) paper/blank. The horizontal line indicates the threshold value, while the vertical line splits training and test samples. Reproduced from ref. 58 with permission from Elsevier, Copyright 2017.

With analysis in under 2-minutes reported[58] and the non-destructive nature of FT-IR maintaining the samples' integrity for further analysis, its employment within forensic analysis is seemingly obvious. Yet despite this, there is limited literature currently available upon the detection of NPS via FT-IR, with those reported focusing solely upon the NBOME class when present within blotter papers. As such, the current literature fails to address any potential problems with the detection of NPS within alternative matrices including biological fluids. This may be largely attributed to the interference effects of the matrix background. FT-IR analysis of drugs within biological fluids including saliva and blood is hindered by the strong absorbance of these matrices as a result of their composition including the high-water content, a known hindrance of IR analysis.[60, 61] As such the background matrix effects prevent the acquisition of any fine structural details which would allow for the identification of species such as NPS within the samples. Although possible to address these issues through the use of microfluidic devices to transfer the drug species into an IR translucent matrix[60] or perform extraction procedures to remove the species from the matrix, this often requires expert knowledge of appropriate sample preparation procedures negating the benefits of the portability and the non-destructive nature of the technique.

One solution with the potential to overcome the aforementioned problems faced by IR for the analysis of NPS comes in the form of the complementary spectroscopic technique Raman. Raman has become increasingly popular within forensic analysis, with a number of portable instruments commercially

available and already in employment for illicit drug screening procedures. Hence their expansion into NPS detection is not unlikely in the near future. Moreover, the ability to offer improved sensitivity through the employment of surface enhanced Raman spectroscopy (SERS) makes this technique even more appealing for trace analysis.[62] Proof-of-concept studies on the use of Raman for NPS detection have shown some promising results, particularly within complex matrices. Unlike IR which suffers from a lack of sensitivity within aqueous matrices, the same is not seen with Raman and as such a number of groups have demonstrated the ability to detect NPS within biological matrices through Raman spectroscopy.[62]

In 2017 Mostowtt and McCord[62] demonstrated the power of SERS, utilising a portable Raman instrument for the identification and differentiation of four structurally similar synthetic cannabinoids within urinary samples.[62] In contrast to the IR methodologies aforementioned, chemometric analysis was not required, while species assignment was no longer restricted to high-level class identification. Instead, the obtained spectra were manually compared and contrasted with each SC producing a unique Raman spectrum at toxicologically relevant concentrations.[62] For urinary analysis however a supported liquid extraction (SLE) procedure was required prior to sample analysis. The SLE procedure detailed includes a 20 minute extraction process involving a solid silica support and dichloromethane washes.[62] Although through this process Mostowtt and McCord[62] were able to obtain signals comparable to those obtained within an ideal matrix, such extraction

procedures negate the idea of a portable system. SLE requires a fully equipped laboratory facility, while the use of dichlorormethane prevents at-scene analysis.

As previously discussed the investigation of a single class of NPS compounds is insufficient to assess any proposed methodologies for potential employment within the forensic arena. Recent reports on the application of SERS to a range of different NPS does however highlight the potential to use this technique for the discrimination of different structural types. However, manual comparison methods for the assignment of compounds is not feasible given the huge variety of NPS which exist. This is again where chemometric analysis offers a huge degree of power. Muhamadai *et al.*[50] sufficiently demonstrated this by combining a portable SERS method with principal component analysis (PCA) for discrimination of methcathinones, aminoindanes, dipehnidines and synthetic cannabinoids.[50] Discrimination of the four different structural classes was investigated both in solid and aqueous solution by Raman and SERS, the results of which are found within the PCA plots shown in Figure 1.5 (a) and (b). Although able to achieve a good degree of discrimination between the different structural classes, both Raman and SERS analysis displayed some overlap with the different classes due to their similar chemical structures.[50] The application of a second chemometric model in the form of partial least squares regression (PLSR) was then employed to determine the detection limits within aqueous solutions. However, despite SERS being recognised for its superior

sensitivity, the detection limits achievable only lie within the mM region, with a LOD reported between 2 mM to 51 mM.[50] Such concentration ranges however cannot compete with the chromatographic methods or offer the sensitivities required to be toxicologically relevant. However, in spite of this Muhamadai *et al.*[50] were able to simultaneously monitor 4-methylmethcathinone (4-MMC) and its two metabolites; nor-mephedrone and 4-methylephedrine in both water and human urine. Unlike the method of Mostowtt and McCord[62], Muhamadai *et al.*[50] were able to obtain SERS within urine without any sample preparation. Hence their method could indeed be translated to at-scene analysis and considered truly portable. On the whole Muhamadai *et al.*[50] were able to demonstrate the suitability of SERS for the direct analysis of urine samples for the detection and discrimination of NPS and their metabolites.[50] However, the high detection limits signify that such methodologies could not be considered for NPS detection, without further sensitivity improvements.

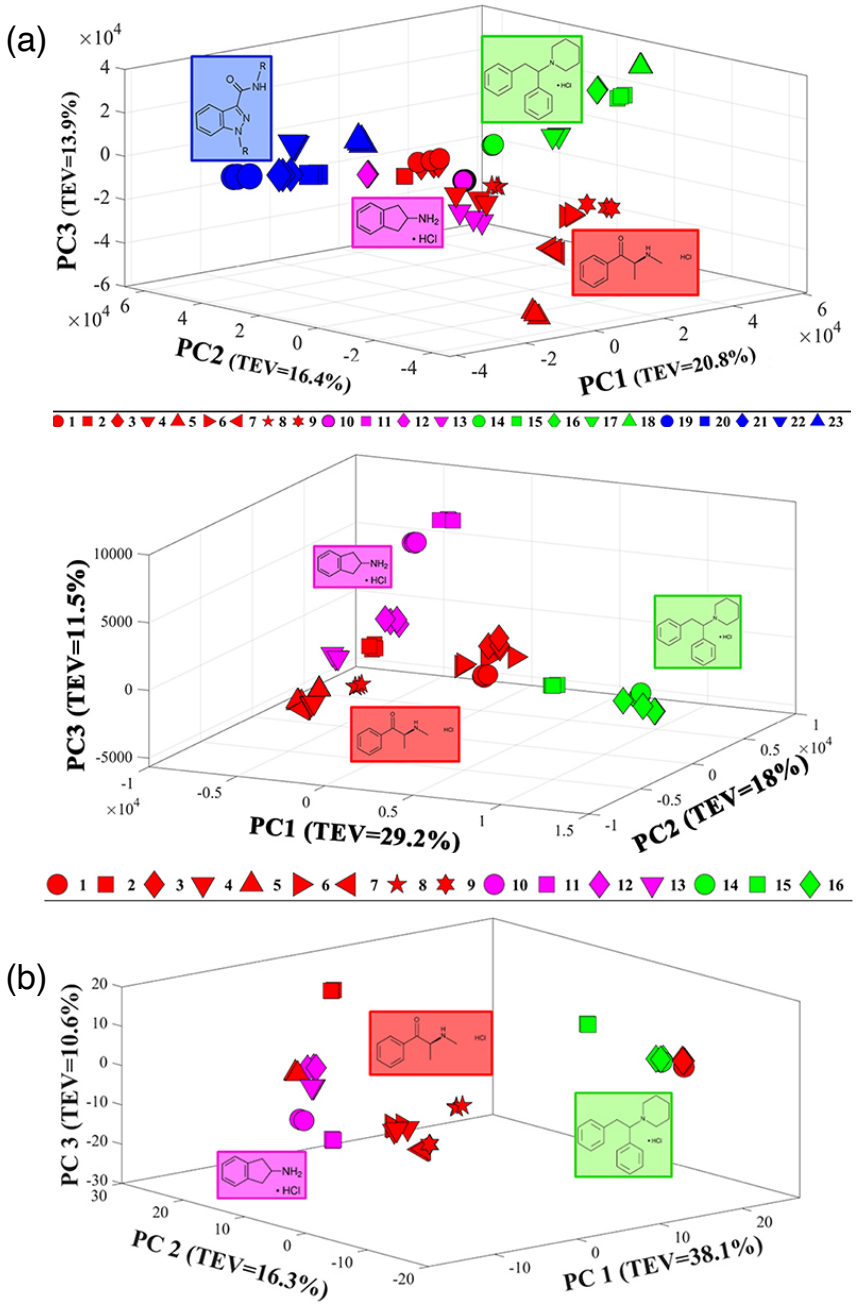

Figure 1.5: (a) PCA plots obtained from Raman spectra collected in solid powder form (top) and aqueous (0.1M) (middle), with structural classes indicated by colourings with methcathinones denoted in red, aminoindanes in purple, dipehnidines in green and synthetic cannabinoids in blue. (b) PCA plots from SERS analysis with methcathinones denoted in red, aminoindanes in purple, dipehnidines in green. Reproduced from ref. 62 with permission from Muhamadali, Watt, Xu, Chisanga, Subaihi, Jones, Ellis, Sutcliffe and Goodacre, Copyright 2019.

With manufacturers continually developing and advancing instrumentation, a new field of portable Raman instruments combined with portable mass spectrometers have been recently coined. Fedick *et al.*[51] reported the use of such instrumentation detailing a paper-based SERS system in combination with paper spray mass spectrometry, summarised in Figure 1.6, for the detection of fentanyl one of the most prevalent NPS.[51] Using a commercially available SERS paper-based substrate, samples were analysed directly via spotting 10 μL of the liquid sample onto the substrate or via mechanically wiping the substrate, wet with 10 μL of methanol, over a surface containing fentanyl.[51] The ability to detect fentanyl from plastic, metal and glass via mechanical application of the sensor is a huge step toward field portability, where negating the need for sample preparation is of great importance. As such, this methodology addresses a number of the challenges currently faced. Of note is not the ability of the authors to detect fentanyl, but the ability to identify fentanyl within a heroin mix in a 1:1 and 10:1 heroin to fentanyl ratio, solely using the portable Raman system.[51] The authors discuss how further sensitivity improvements could be achieved if a separation strategy or statistical deconvolution method was employed to the collected Raman spectra. However, by employing the mass spectrometer as a secondary confirmation technique they were able to detect fentanyl in the presence of heroin down to a 100:1 ratio.[51] What's more, the ability to detect five different fentanyl analogues was achieved, with each producing a characteristic Raman spectrum allowing for identification in-field. Once again however the lack of reference standards would limit the potential of this application.

Although only fentanyl analogues were discussed within this contribution, the authors highlight a wider problem with such an approach. For species to be identified via their Raman spectra, each new fentanyl analogue or in fact NPS would need to be added to the internal database housed within the portable spectrometer. As such identification of NPS not previously encountered would be limited. However, Raman facilitates rapid class identification and hence provides an equivalent to the current presumptive tests offered for traditional illicit substances used in-field.

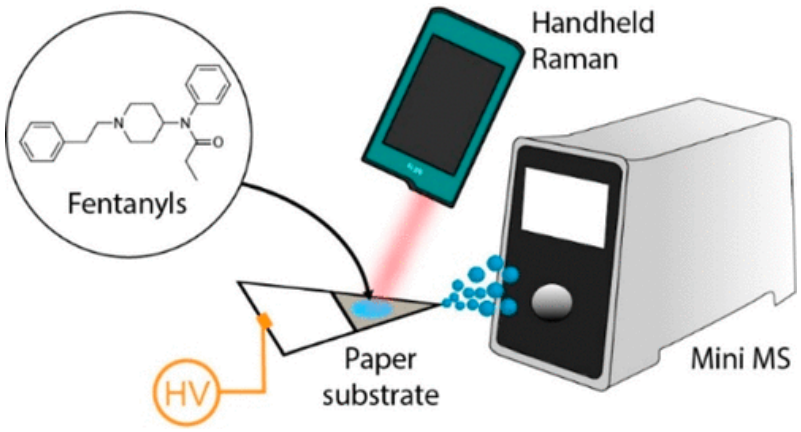

Figure 1.6: Schematic summary of the paper based SERS and paper spray mass spectrometry, utilised by Fedick *et al.*[51] for the detection of fentanyl and its analogues. Reprinted with permission from ref. 51. Copyright 2020, American Chemical Society.

On the whole, spectroscopic techniques stand to offer a viable solution for the detection of NPS. They offer commercially available field portable instruments, and as demonstrated above, often do not require sample preparation to be performed. As a result, spectroscopic techniques are well positioned for implementation into field analysis. A fact further highlighted by the current utilisation of commercial Raman instruments for illicit substance detection at border security. However, as with chromatographic techniques, they still suffer from the lack of available reference standards and as such the databases which can be housed within the instrumentation for compound identification are often incomplete in regard to NPS. Moreover, few have currently demonstrated the applicability of these techniques for the analysis of complex matrices, particularly biological fluids. While the employment of statistical analysis methods have allowed for the discrimination of some different structural compounds from one another, to date there has not been an intensive investigation into a wider range of NPS classes, hence specificity of these techniques toward different NPS classes is unknown. As such, the applicability of spectroscopic techniques for the analysis of mixed or adulterated samples is at present unknown.

1.3 Alternative Detection Methodologies

Despite chromatographic and spectroscopic methods' largely regarded as the primary analytical techniques for the detection of NPS within the forensic field, there is an increased interest in new and alternative methodologies. Although lesser known amongst the wider analytical community techniques including, electrochemistry, immuno-sensors and microchip electrophoresis have recently demonstrated a strong capability for the detection of NPS. As such, it is important to consider such techniques and their ability to address the challenges currently facing NPS detection.

1.3.1 Colorimetric Techniques

Although a number of the traditional colorimetric presumptive tests are inadequate for NPS detection, in recent years alternative versions of such methods have been proposed to specifically target NPS.[63-67] One such method was proposed by Merli *et al.*[67] and describes a colorimetric test for the detection of indole based synthetic cannabinoid AB-001. A modified version of the Ehrlich reagent (p-N,N-dimethylaminobenzaldehyde), in which the volatile hydrochloric acid component was removed, was immobilised upon a solid silica support forming the sensing system.[67] In contrast to the traditional colorimetric tests, widely recognised to suffer from subjectivity, Merli *et al.*[67] utilised a smartphone camera to obtain the red, green and blue (RGB) values of the colour produced as a result of the interaction between the SC and the Ehrlich reagent. Through this methodology, the authors

proposed a simplistic quantification method for the identification of AB-001. A range of SC standards dissolved in ethyl acetate were used to prepare the calibration curve shown in Figure 1.7 through monitoring the change in the intensity of green light; in contrast the intensities of the red and blue light were observed to remain constant.[67] Quantification of AB-001 between 10 and 50 μg was achieved by utilising a simple colour change, monitored via a smart phone camera. This methodology cannot be discounted, as its simplistic nature and ability to not only identify the target SC but also quantify its presence, using a widely available device such as a smart phone is of marked interest.[67] Of more significance however is the ability of this methodology to be performed upon the herbal materials which SCs are typically distributed upon. Investigation of tabaco and damiana leaf, known SC supports, produced a notable colour change, thus demonstrating the ability of this methodology to negate potential matrix interference.[67] Furthermore, a number of common interferent species also investigated, including fellow indole containing SC JWH-018 and JHW-302 and a number of other psychotropic adulterants, again produced no notable no colour change of note. The remarkable specificity of this simplistic colorimetric methodology toward the AB-001 SC.[67] However, the specificity toward the adamantoyl-based SC can also be considered a limitation of the proposed methodology; an ideal presumptive test would aim to identify a class of substances, and in its current format this colorimetric test could ultimately lead to false negatives if other structural SC were present. Ultimately Merli *et al.*[67] have demonstrated that the adaption of colorimetric tests for NPS

identification cannot be discounted, and further they addressed the limitation of traditional colorimetric tests through the removal of the subjectivity surrounding colour identification. As such, continued development of such colorimetric testing may be a viable option for future employment for rapid NPS detection, even within herbal matrices.

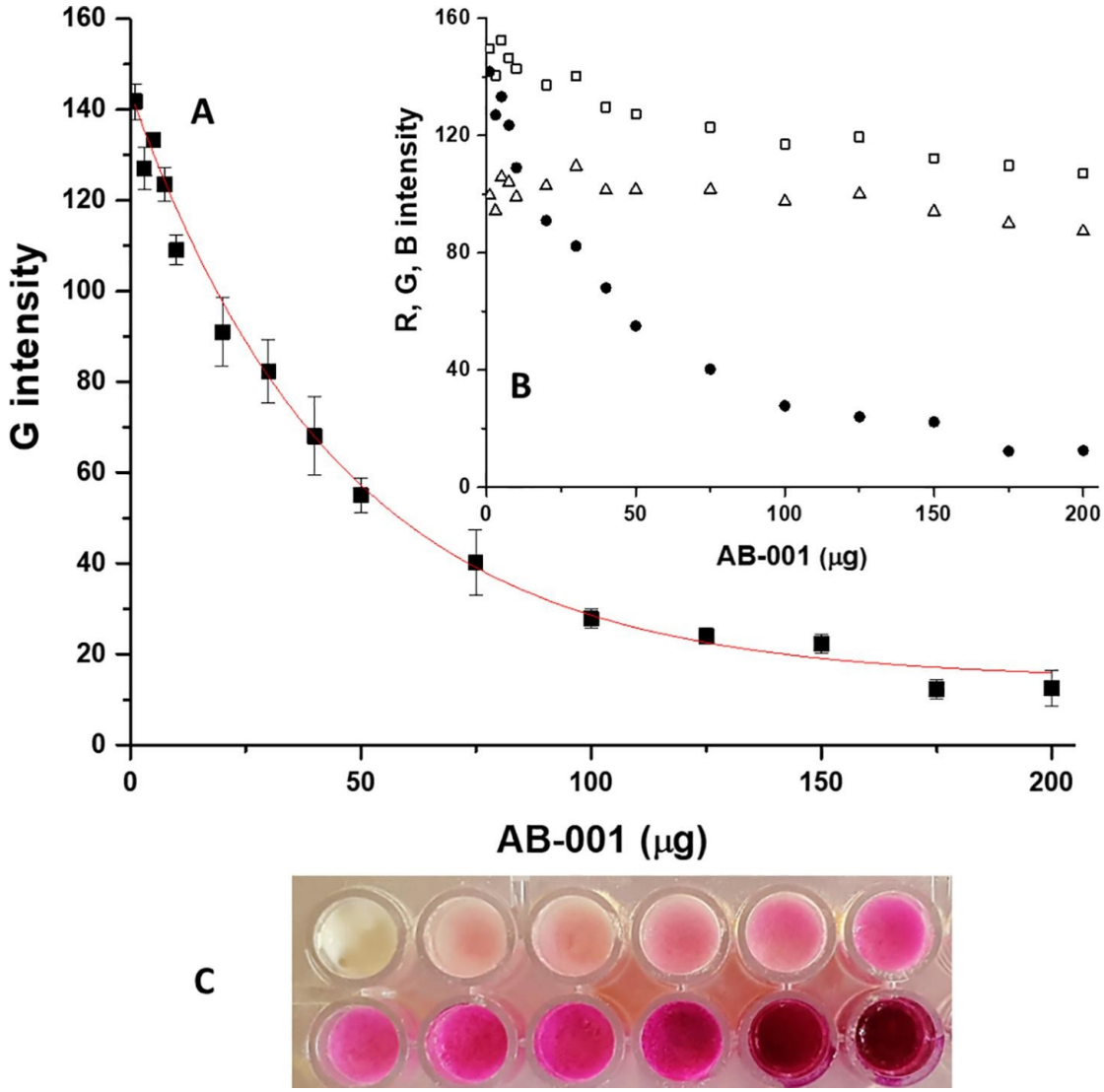

Figure 1.7: Variation in the values with increasing concentration of AB-001. a) shows the relationship between green values and AB-001 concentration between 1-200 μg b) relationship between RGB values obtained from the smart phone digital images with AB-001 concentrations, where R: squares, G:circles and B: triangles and c) colour obtained within wells in which 0, 1, 2, 5, 10, 25, 50, 75, 100, 150 and 200 μg of AB-001 were added respectively. Reproduced from ref. 62 with permission from Elsevier, Copyright 2019.

An alternative to the traditional chemical-based colorimetric testing was proposed by Yen *et al.*[68] who developed a methodology utilising a photoluminescence (PL) probe formed via bovine serum albumin-stabilised gold nanoclusters (BSA-Au NC).[68] A colour change from red to dark blue in the presence of cathinone's was observed under UV interrogation with the developed probe. Using this methodology Yen *et al.*[68] could not only identify cathinone 4-chloromethcathinone (4-CMC) but could also quantify it within aqueous solutions. This quantification method relies upon the measurement of the PL spectra of the sample, monitoring the decrease in the intensity of the emission peak at 650 nm as the 4-CMC concentration is increased, achieving a linear range between 0.48 to 7.5 mM and a LOD of 0.14 mM.[68] However, such a monitoring method would require the use of a spectrofluorimeter and thus confines this methodology to a laboratory environment. Of more interest is therefore portable qualitative identification, utilising a UV torch and smartphone camera to illuminate and record the emission respectively. Utilising this portable system, the authors were able to identify by eye the presence of 4-CMC.[68] Unsurprisingly this qualitative method decreased the sensitivity, increasing the detection limit to 10 mM. However from the images presented (refer to Figure 1.8) it can be seen that even at 5 mM a switch from an intense pink colouration toward a purple colouring is visible.[68] The authors could indeed improve this assignment and remove the subjectivity through the employment of a smartphone application to determine the RGB values of their obtained images as was performed by Merli *et al.*[67]

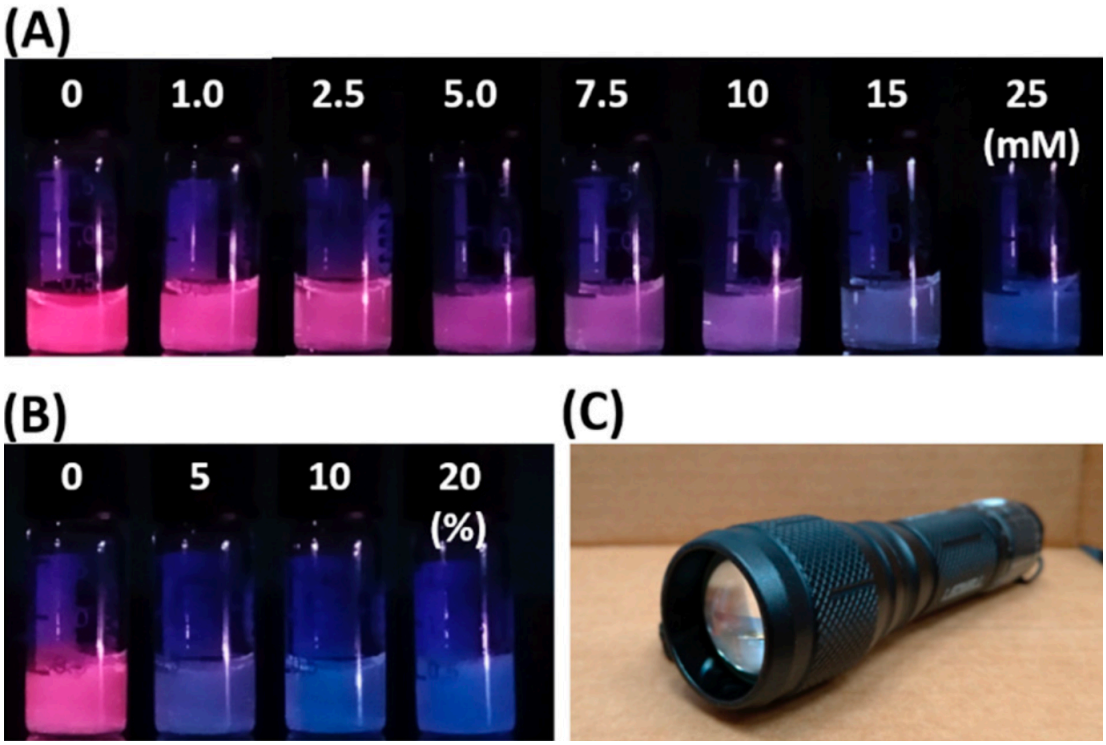

Figure 1.8: (A) PL images obtained with BSA-Au NC probe with increasing concentrations of 4-CMC, showing the colour change from pink to blue and the 10 mM changing point identified by the authors. (B) PL images were obtained with BSA-Au NC probe with increasing concentration of 4-CMC (%w/w) in the presence of glucose ranging from 100% to 80%. (C) UV torch used to collect the PL images. Reproduced from ref. 68 with permission from Sensors. Copyright 2019.

Of more note however is the selectivity offered by this methodology, as demonstrated through the interference study which took into consideration interference effects from common diluents such as glucose and fructose in addition to alternative illicit substances and NPS including heroin, cocaine, methamphetamine and ketamine. Through their inference study the authors identified that their BSA-Au NC probe not only displayed a specificity toward 4-CMC but toward the cathinone class in general. This was further demonstrated through the application of the probe to a number of seized samples, which were tested using the BSA-AU NC probe with GC-MS confirmation. Of the 20 real case samples tested by the authors, 4 produced positive results indicating the presence of a cathinone species (2,3,11 and 16 within Figure 1.9), later identified as ephylone, butylone, 4-chloro-*N,N*-dimethylcathinone and a mixture of dibutylone and 4-chloro-*N,N*-dimethylcathinone, all of which belong to the cathinone class. All remaining samples tested negative, see Figure 1.9, with GC-MS confirming the lack of cathinones present, hence illustrating strong specificity of the developed colorimetric test. Despite the strong proof-of-concept for cathinone detection demonstrated by Yen *et al.*[68], all analysis was performed within aqueous based solutions. As such it cannot be ascertained if such a methodology would be applicable to more complex matrices including biological fluids or drinks samples, many of which possess an intrinsic colour or indeed produce their own photoluminescence and as such may interfere with the desired colour changes of interest.

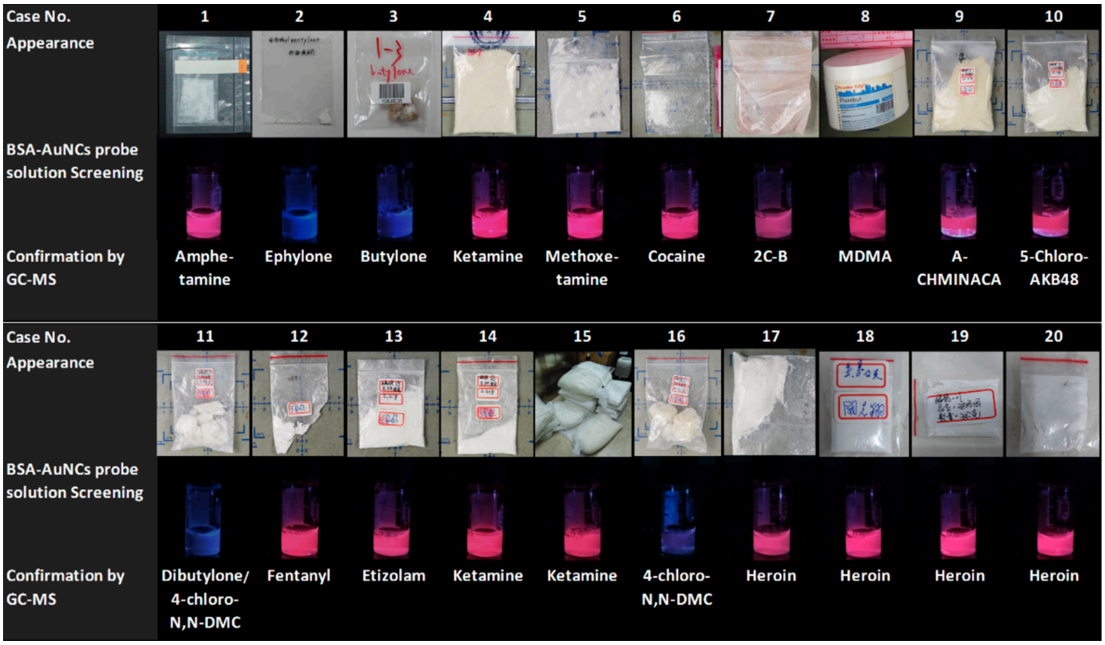

Figure 1.9: Screening results from 20 seized street and smuggling samples, with screening performed utilising the BSA-Au NC probe, with GC-MS used for species confirmation. Reproduced from ref. 68 with permission from Sensors. Copyright 2019.

1.3.2 Immunoassay Methods

Colorimetric testing, despite the improvements made by the aforementioned methods, still largely suffer from an incompatibility with biological fluids, particularly whole blood whose natural red colouring can dominate and obscure any observable colour change within a sample. However, one technique which could address the limited matrix compatibility of colorimetric methods as creening methods within biological matrices are immunoassays. Immunoassays are widely employed for clinical and toxicological drug screening with minimal sample preparation and a high degree of

automation.[56] Although a range of commercially available immunoassay kits are available for traditional drug substances' this is not currently the case for NPS. As with the analytical techniques previously discussed, the huge variety of NPS structures and continual manufacturer of new compounds, makes it virtually impossible to develop and manufacturer specific immunochemical tests in line with demand.[56] Although some commercial kits are now available for the detection of SC in urine and oral fluid, including ThermoFisher's CEDIA® UR-144/XLR-11 assay and NarcoCheck® K2 rapid test strip, the same cannot be said of other NPS classes. One concern surrounding the use of immunoassay testing is the observed cross reactivity. This is a particular concern with regard to NPS, which could be falsely identified as alternative illicit substances. An extensive study on the cross reactivity of 94 NPS with five commercially available immunoassay kits, for amphetamine, methylamphetamine, ecstasy and phencyclidine (PCP) detection, was performed.[69] The ultimate goal was to determine the suitability of commercially available immunoassay kits, manufactured for traditional illicit substances, for NPS detection. The authors focused upon amine containing species, utilising immunoassay kits for the identification of traditional illicit substances containing the amine functionality and focusing on the detection of amine containing NPS classes; 2,5-dimethoxyamphetamines, 2,5-dimethoxyphenethylamines (2C), β-keto amphetamines, substituted amphetamines, piperazines, α-pyrrolidinopropiophenones, tryptamines and PCP analogues.[69] Of the 94 NPS tested, 80 produced a colour change indicating a positive result with at least one of the commercially available kits,

while none of the NPS investigated produced a positive result across all five of the immunoassay kits. Of more interest however was the observation that a number of the tested NPS, including 4-methylmethcathinone (mephedrone) and 1,4-dibenzylpiperazine, were observed to produce a positive result with only one of the amphetamine testing kits, while generating a negative with the others.[63] As such a large degree of uncertainty remains over the potential of exploiting cross reactivity to facilitate the use of traditional drug immunoassay kits for NPS detection. What's more the authors did not consider the potential impact of matrix effects, diluents or adulterants when exploiting the potential of cross reactivity. Before the implementation of such a methodology could be widely considered, a much greater understanding of cross reactivity across a range of commercially available kits and NPS classes would be necessary. A database and guidance upon the desired colour changes indicative of the presence of a NPS classes wold be essential for practitioners to minimise the impact of subjectivity upon colour identification.

Rather than rely upon cross reactivity, Chen *et al.*[70] described the manufacture of a paper-based immunosorbent-based approach for the detection of ketamine. Utilising competitive paper-based enzyme-linked immunosorbent assay (cP-ELISA), the authors developed a portable low-cost device capable of the colorimetric detection of ketamine within an oral fluid.[70] Their design allowed for the pre-manufacture and storage of the test device

making it ideal for roadside or at-scene testing. In addition by utilising a smartphone camera to record the colour change they not only negate the subjectivity associated with colour identification but facilitate semi-quantitive as well as qualitative analysis. Using an in-house developed smartphone application, they concluded that monitoring the ratio of the red-blue intensity present within the cP-ELISA reaction, produced a response which was not only concentration dependent but also produced the most identifiable change, as demonstrated within Figure 1.10.[70] Interestingly the authors investigated the impact of the inclusion of a filtration step prior to the analysis of oral fluid. Although filtration was observed to improve the LOD 10-fold (0.03 ng mL^{-1} cf. 0.3 ng mL^{-1} for unfiltered), removal of the filtration step increases the usability and portability of the developed system.[70] Improvement in the LOD with filtration can likely be attributed to the removal of interferent effects as a consequence of non-specific binding. Yet without filtration, the detection limit achieved could still be considered clinically relevant, particularly for roadside testing, the target application of the authors.[70] Assessment of the sensor via a blind study of 90 clinical samples comprising of 50 negative and 40 positives for ketamine was performed. Using their simplified sensor, and without any prior sample preparation, they were able to assign 36 positive samples and 46 negative samples, with their paper-based cP-ELISA, offering a sensitivity of 90% and specificity of 92%.[70] These promising results highlight the possibility to use such methodologies for the rapid and low-cost screening of NPS directly within biological fluids. Moreover, for the first time the strength of the proposed methodology is

demonstrated through the analysis of real-life clinical samples. However, once again the authors solely focused the study upon one specific NPS, in this instance ketamine, while failing to investigate any potential interferent effects form other NPS or traditional illicit substances. Hence no certainty regarding the sensor's specificity in the presence of different NPS classes or indeed those structurally similar to ketamine is presented. This is of course fundamental information required before any testing methodology could be introduced into the field for forensic or toxicological analysis.

Although the argument stands that immunoassays could offer an obvious alternative for the detection of NPS within toxicological samples in particular, to date their remain limited studies to validate such a claim.[56, 69, 70] The limited studies available suggest these techniques do demonstrate promise for NPS detection, however further testing of different NPS classes within a variety of sample matrices would be required. The huge number of structural variants of NPS currently hinder the development of suitable and specific antibody-antigen combinations for use within immunoassays. Uncertainty surrounding the cross reactivity between not only parent NPS and traditional illicit substances but also their corresponding metabolites exists, particularly when considering that different NPS classes are known to produce structurally identical or similar metabolites. Currently, cross reactivity is negated through the employment of a second additional screening method, typically LC-MS or GC-MS. However, it therefore stands to reason that chromatographic

methods would instead be employed solely, offering all the required data rather than as a secondary screening analysis. This would in turn limit cost and reduce analysis time but also provide the ability to identify any unknown or new NPS which might be within a sample, that would not be detected via immunoassay analysis. As such, before immunoassays could be seriously considered for wide-scale employment for the detection of NPS, far greater and more extensive research is required, particularly to identify suitable antibody-antigen combinations for the huge variety of NPS classes available.

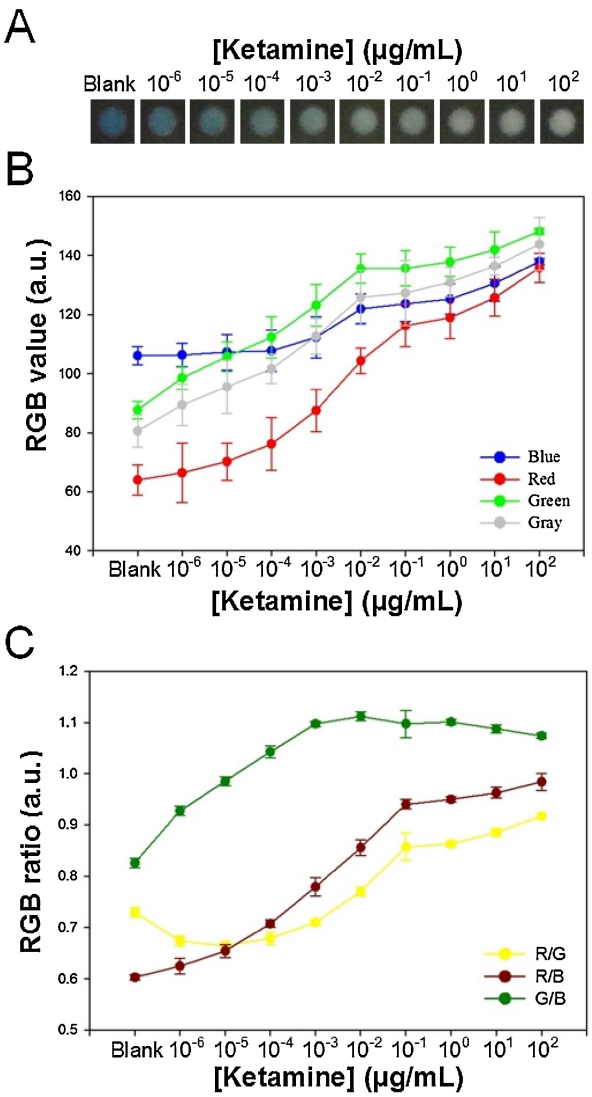

Figure 1.10: Analysis of cP-ELISA sensing system generated image to obtained the red (R), green (G) and blue (B) colour values from images taken of the paper platform (N=5). (a) shows the colorimetric results for ketamine analysis on the paper platform, (b) the corresponding R, G, B and grey values from this image and (c) the R/G, R/B and G/B ratios of ketamine analysis with values determined by ImageJ software. The concentration of ketamine antibody and ketamine HRP were 88.9 μg mL^{-1} and 0.33 x diluted, respectively with a heating temperature of 40 ^{o}C and 30 second wash time. Reproduced from ref. 70 with permission from Elsevier, Copyright 2019.

1.3.3 Electrochemical Sensors

Electrochemical sensors are highly amenable toward forensic analysis. Not only do they show tremendous portability, with a huge increase in wearable on-body sensors in recent years, but they have proven success in the detection of forensically relevant substances including, illicit drugs, poisons and NPS within a variety of complex matrices including herbal material, commercial beverages and biological fluids.[71-77] One of the earliest reported cases of the electrochemical detection of NPS dates back to 2014, when Smith *et al.*[7] described how a range of synthetic cathinones could be irreversibly oxidised upon graphite screen printed electrode (SPE), glassy carbon and boron-doped diamond electrodes, resulting in a characteristic anodic peak at +1.0 V vs saturated calomel electrode (SCE).[7] With the SPE sensor offering the highest anodic current and lowest over potential, it is clear even during some of the first reported cases of electrochemical NPS detection, portable systems were already at the forefront of the developed methodologies. The sensor designed by the authors although able to successfully detect synthetic cathinones, caffeine and benzocaine individually, lacked the required specificity for identification of the individual species when present within a mixed matrix, as would be encountered within street samples.[7] The subsequent year the authors proposed a further electrochemical sensor for the detection for mephedrone (4-MMC), and 4'-methyl-*N*-ethylcathinone (4-MEC).[78] Here uniquely the authors developed a sensor utilising a one pence coin (post 1992 mint) as the working electrode, alongside a platinum wire counter and SCE reference.[78] The design of the

working electrode is detailed within Figure 1.11 and was fabricated such that the geometry of the working electrode area remained consistent but facilitated the switching of the coin, post measurement to create a disposable system.[78] The copper oxide within the coin produced a singular oxidation peak at -0.01 V (vs SCE) and two reduction peaks at -0.4 and -0.6 V (vs SCE). The authors proposed that mephedrone could be indirectly detected via monitoring the reduction in the oxidation peak intensity, where mephedrone adhesion blocks the active working electrode surface, hindering its electro-activity. A decrease in oxidation peak intensity with an increase in mephedrone concentration was observed with an R^2 value reported at 0.97, and a LOD of 0.56 μg mL^{-1}.[78] However, this indirect detection methodology lacks any specificity, as demonstrated through their analysis of 4-MEC which produced the same effect upon the oxidation peak as observed with mephedrone.[78] Detection through a decrease in oxidation peak intensity due to the physical adsorption of species onto the electrode surface is an unselective process and would result no matter the species present. Although their sensor was novel and inexpensive to produce, it is ultimately unsuitable for implementation into forensic analysis, where it is vital to minimise the possibility of false positives, provide high species specificity or at minimum drug class identification is required.

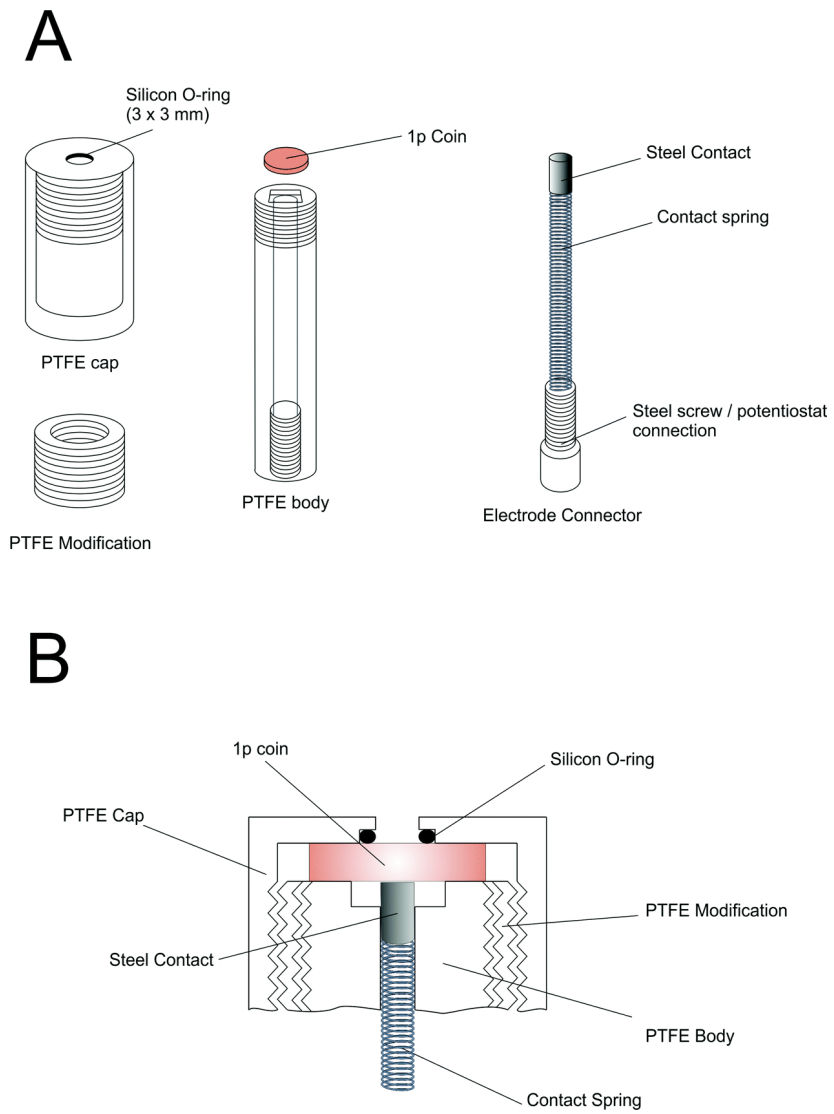

Figure 1.11: Schematic diagram of the one pence coin working electrode construction, with the polytetrafluoroethylene (PTFE) housing which holds the coin in position during analysis, accurately defining the electro-active area. (b) Cross-section of the assembled electrode which is inserted into solution for analysis. Reproduced from ref.78 with permission from the Royal Society of Chemistry.

Although these early reports highlighted the viability of forensic electrochemistry for NPS detection it was clear that much work was still required to improve specificity, widen compatible sample matrices and expands the classes of NPS which could be identified. Since these early reports, electrochemical techniques have been applied to an array of different NPS including synthetic cocaine[5], phenethylamines[79], piperazine[80] and synthetic cannabinoids.[81] Despite the typical lack of specificity, indirect electrochemical detection methods for NPS have drawn some interest. In addition to Fang *et al.*[78], Cumba *et al.*[5] also proposed an indirect electrochemical detection method for the detection of synthacaine. Synthacaine or synthetic cocaine primarily consists of a mixture of central nervous system stimulants, with methiopropamine (MPA) predominantly detected within UK samples.[5] Cumba *et al.*[5] investigated a range of different techniques for the analysis of synthacaine street samples, know to contain MPA and 2-aminondane (2-AI).[5] As is the case with many NPS, the authors report how traditional presumptive tests, although valid on the individual components of pure samples when applied to real-life mixtures produced unreliable results.[5] Raman spectroscopy, although able to reliably detect 2-AI, was unsuited for the detection of MPA as a result of the significant fluorescence background which prevented the acquisition of useable spectra.[5] Proposing a viable on-site detection method, Cumba *et al.*[5] applied linear sweep voltammetry together with SPE to address the limitations of the presumptive and Raman spectroscopic analysis. Utilising a graphite SPE, direct oxidation of MPA was observed with an irreversible oxidation peak at

+0.94 V (vs Ag/AgCl).[5] In contrast, 2-AI did not display any electrochemical behaviour across the scanned potential range of 0.2-1.6 V.[5] As with Raman spectroscopy, the ability to identify only a singular component within the mixed matrix is not a viable technique for use within forensic analysis. However, by employing an indirect detection method using *N,N'*-(1,4-phenylene) dibenzenesulfonamide as a mediator, a substance which chemically reacts with MPA and 2-AI to form secondary species which can subsequently be electrochemically reduced, allowed for the simultaneous detection of both MPA and 2-AI within mixed matrices.[5] The species produced were then reduced at the graphite SPE at -0.16 V (2-AI) and -0.36 V (MPA). Using their indirect system the authors were able to successfully analyse mixed MPA and 2-AI samples for the detection of both components with detection limits down to 0.49 μM and 0.07 μM respectively.[5] The methodology developed was validated through the comparison of electrochemical analysis of street samples to the validated HPLC method, with good correlation between both methods with concentrations within ±0.35% for MPA and ±0.78% for 2-AI observed.[5] Cumba *et al.*[5] therefore, demonstrated the potential strength of indirect electrochemical methods for NPS detection. However the authors failed to assess any potential interferents from other adulterants or diluents which may be encountered within street samples, hence their methodology cannot be fully evaluated for implementation into forensic analysis within its current format. However, this does not discount their proposed indirect methodology for future applications,

as a result of the greater specificity, displayed compared with indirect electrochemical methods previously reported.

The electrochemical detection of NPS within biological fluids was initially reported in 2018 when Razavipanah *et al.*[82] discussed the detection of synthetic cathinone, mephedrone, within human urine and serum samples.[82] Utilising an electrochemically imprinted sensor, the authors highlighted the need for point-of-care devices able to provide rapid and reliable detection of NPS. The electrochemical sensor combined a nanocomposite of gold nanoparticles and functionalised multi-walled carbon nanotubes within a sol-gel molecular-imprinted polymer and polytyramine.[82] The film produced was then electrochemically deposited upon a glassy carbon electrode and the template from the polymer matrix removed prior to analysis. The sensor developed was highly sensitive, with detection limits for mephedrone reported down to 3 nM in both urine and human serum, with no interference effects from the complex matrices reported,[82] a crucial characteristic for point-of-care devices. Although these concentrations lie well within the forensically relevant range for mephedrone, a lack of investigation into the impact of other drug species or indeed metabolites that would be present within these biological matrices' was not conducted. As such, although the developed sensor highlighted the promise of such electrochemical methodologies for utilisation within NPS sensing devices for application to biological matrices, further assessment into their specificity is necessary to determine their suitability for applications within the forensic arena.

Synthetic cannabinoids make up one of the most prevalent NPS classes, and as such are the largest group of substances currently monitored by the EU early warning system.[83] Common functional groups within SC structures include the indoles and indazoles. This functionally provides SC with a high degree of electro-activity, making them ideal for electrochemical detection. As such, electrochemical sensors could offer a viable detection method for this specific NPS class. Dronova *et al.'s*[81] investigation of the SC class revealed a number of the indole and indazole containing SC displayed irreversible oxidation peaks upon boron-doped diamond, glassy carbon and platinum electrodes across a potential range of +0.7 to +2.7 V (vs Ag/AgCl).[81] Glassy carbon electrodes showed the lowest sensitivity to this class with boron-doped diamond displaying the greatest, while platinum electrodes facilitated oxidation at the lowest overpotentials.[81] To prove the applicability of their system to real-world applications, the authors performed analysis within an artificial saliva matrix, replicating sample conditions likely to be encountered during roadside testing.[81] Application of anodic pre-treatment to the boron-doped diamond electrode facilitated the lowest detection limits, down to the nM range at the least positive potentials. Further to this initial proof-of-concept, the authors described the detection of SCs within herbal material, a common matrix utilised for their distribution.[81] In spite of the interference such a matrix has previously shown within colorimetric analysis, the electrochemical sensor here did not suffer from the same interference effects.[81] The authors were, therefore, able to demonstrate the potential of their standard cell setup for a two-tiered approach required for the forensic

detection of SC. Yet the lack of specificity between different indole and indazole species, with their similar oxidation potentials, prevented the identification of multiple synthetic cannabinoids when present within a single matrix. Despite their suitability toward electrochemical detection, no further reports of the study of SC with such electrochemical methodologies have been reported to date.

Although there has been significant focus placed upon the development of wearable and portable electrochemical sensors, these have largely concentrated upon applications within the biomedical arena. However, the same principles used within such devices are inherently translatable to the forensic field, as demonstrated through the reported detection of explosives, nerve agents and Δ^9-THC with such devices.[71, 77] It, therefore, stands to reason that such sensors could indeed be easily adapted and applied for the detection of NPS. Barfidokht *et al.*[73] demonstrated this principle reporting upon the detection of the potent synthetic opioid fentanyl. Utilising their developed “lab-on-a-glove” sensor, their system showed similarities to that previously reported by de Jong *et al.*[84] in 2016 for the detection of cocaine. To manufacturer their sensor, Barfidokht *et al.*[73] employed a two-finger sensing system, whereby sample collection was performed upon the thumb with electrochemical sensing performed via the index finger. Using a screen printer, the authors deposited Ag/AgCl ink onto a nitrile glove forming the reference electrode and the connecting pads, with carbon paste used for the working and counter electrodes alongside the thumb sampling pad.[73] For

incorporation of the required conductance to perform the electrochemical methods the authors devised a simple drop casting procedure, where the working electrode was modified via depositing an ionic liquid hydrogel containing multi-walled carbon nanotubes (MWCNT) on to its surface. The gel deposited glove could then be stored for up to two weeks without any loss of stability. To perform measurements, the thumb and index finger of the glove are connected, and square-wave voltammetry was performed via a portable potentiostat attached to the user's wrist. Collected data is relaid back to a smartphone, tablet or laptop remotely via inbuilt Bluetooth connectivity. The complete portable system is shown within Figure 1.12.[73]

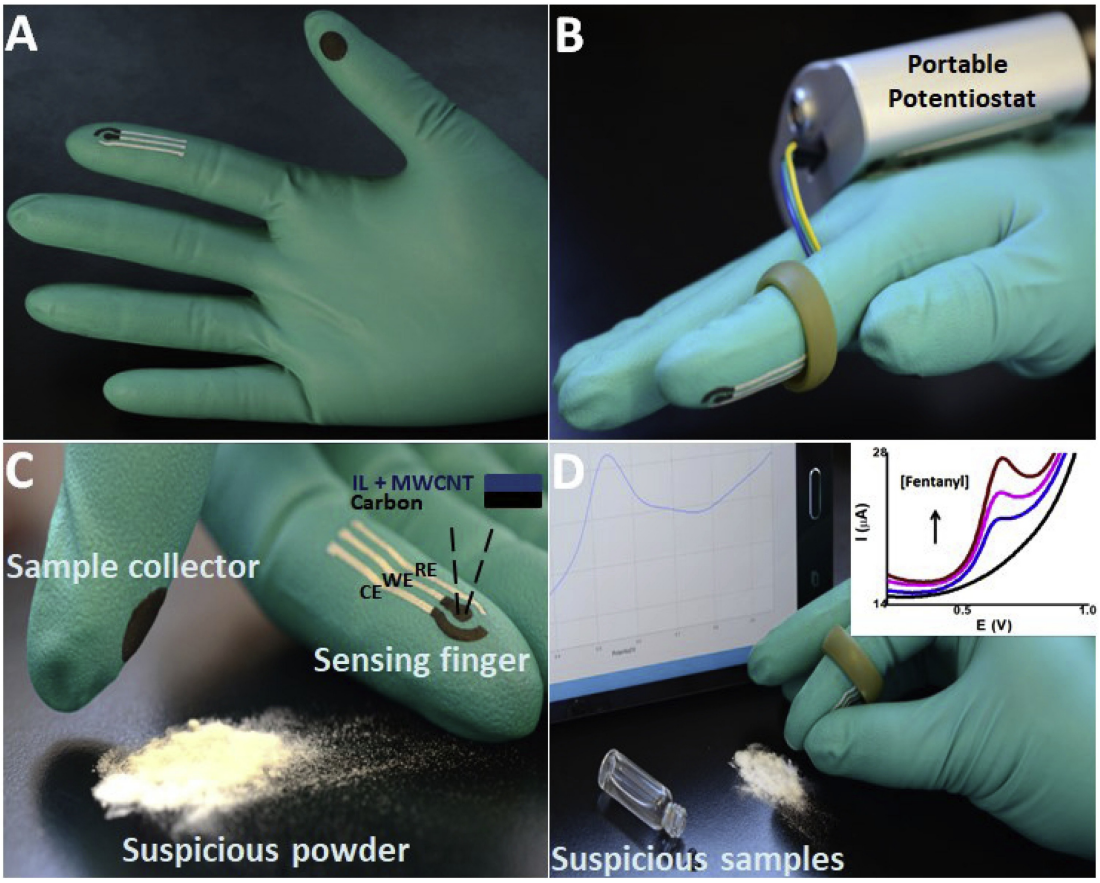

Figure 1.12: Overview of the portable "lab-on-glove" sensor for the on-site detection of fentanyl; (a) photograph of the glove based sensor with the sensing finger (index finger) modified with ionic liquid/MWCNT and sampling finger (thumb) with carbon paste sampling pad shown. (b) Shows the glove-based sensor connected to the portable potentiostat. Electrodes are connected via wires and a modified ring to the PalmSens potentiostat for on-site detection with wireless data relay to a smartphone for rapid analysis. (c) Image shows suspicious sample collection in the powder phase with the sensor. (d) Completion of the electrochemical cell via connection of the thumb (collector) and sensing (index) finger after swiping a powder sample for analysis; inset shows the voltammograms obtained facilitating fentanyl identification in powder/liquid samples. Reproduced from ref. 73 with permission from Elsevier. Copyright 2019.

Fentanyl detection was achieved through monitoring of the single anodic peak observed at +0.65 V (vs Ag/Ag/Cl).[73] The authors investigated sensor performance utilising both buffered liquid samples and more interestingly for the direct analysis of a solid powder. After collecting the powder sample, the index finger containing the electrochemical sensing system with the ionic liquid film electrolyte, and the thumb containing the sample were joined.[73] As can be seen in Figure 1.13 fentanyl could be easily identified from the background when analysis of the raw powdered sample was performed, through the characteristic anodic peak observed. The abrasive voltammetry technique was able to demonstrate that despite lower volumes of electrolyte and sample, trace amounts of the powder could indeed be confidently identified. Not only this but the portable on-site sensor demonstrated a degree of specificity with the analysis of a range of common diluents revealing only acetaminophen and theophylline produced anodic peaks, but outwith the potential window for fentanyl detection and hence would not impact upon fentanyl identification.[73] Further confirmation of sensor specificity can be observed through the analysis of powder and liquid samples containing fentanyl, caffeine, acetaminophen and glucose, as shown in Figure 1.14. The “lab-on-glove” system developed by Barfidokht *et al.*[73] demonstrated a strong proof-of-concept toward a wearable and on-site screening methods for the identification of NPS.[73] Through their abrasive voltammetry method developed, the authors removed the requirement for any sample preparation and hence meets a number of the prerequisites required for such a screening methodology. Although specificity was demonstrated

through the application of the sensor to a number of diluents, they failed to address any possible inference effects from other NPS classes, particularly those with similar amine functionality as fentanyl including its analogues. As is the case in many electrochemical methods, oxidation potentials for a number of species can lie within similar ranges and as such, it would be prudent to ensure this “lab-on-glove” methodology would not suffer from inference from other NPS or indeed illicit substances such as heroin. However, this does not discredit the achievement of the authors to manufacture a sensitive and stable fully portable system, and further investigation of such methodologies might even prove its potential for application to a range of different NPS classes.

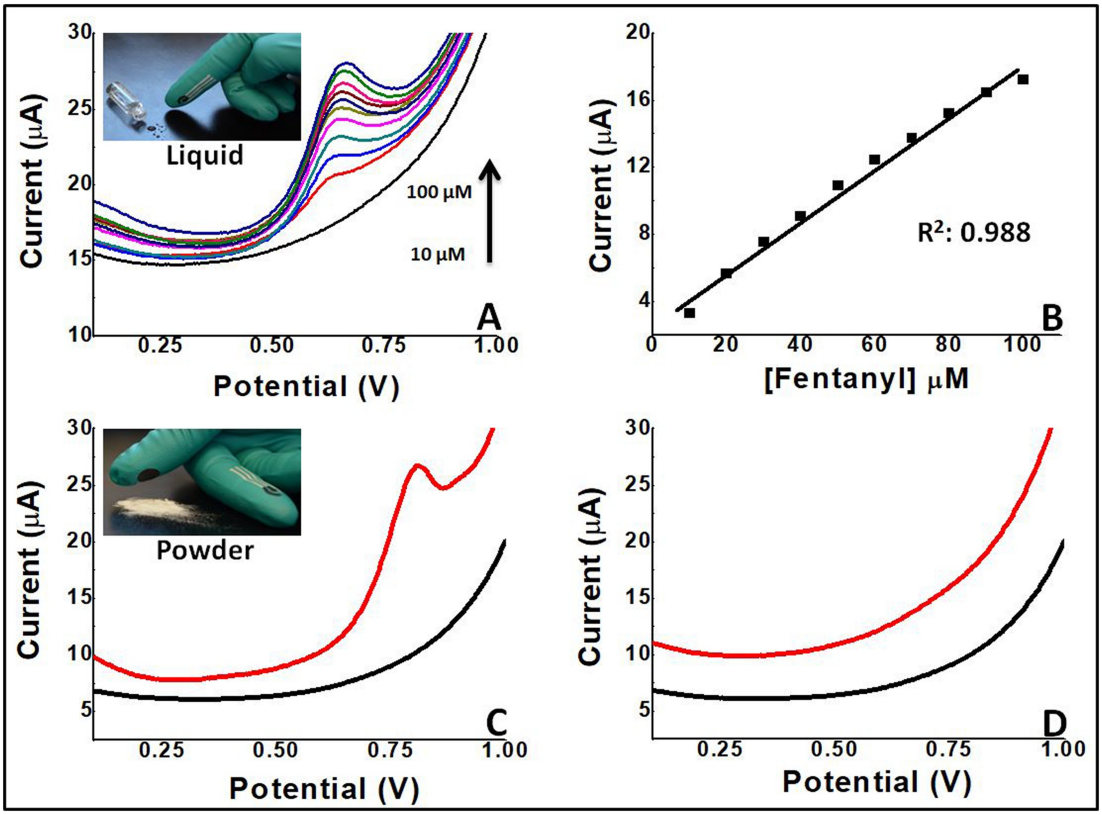

Figure 1.13: Electrochemical characterisation of the glove-based sensor for the detection of fentanyl in liquid and powder form. (a) Shows the square-wave voltammetric response of the sensor with increasing fentanyl concentrations between 10-100 μM in pH 7.4 0.1 M PBS. (b) Shows the corresponding calibration plot from the data obtained in (a). (c) Shows the sensor response to fentanyl powder (red) and the background from the ionic film electrolyte (black). (d) A control experiment with swiping of the surface in the absence of fentanyl (red) and containing fentanyl (black). Reproduced from ref. 73 with permission from Elsevier. Copyright 2019.

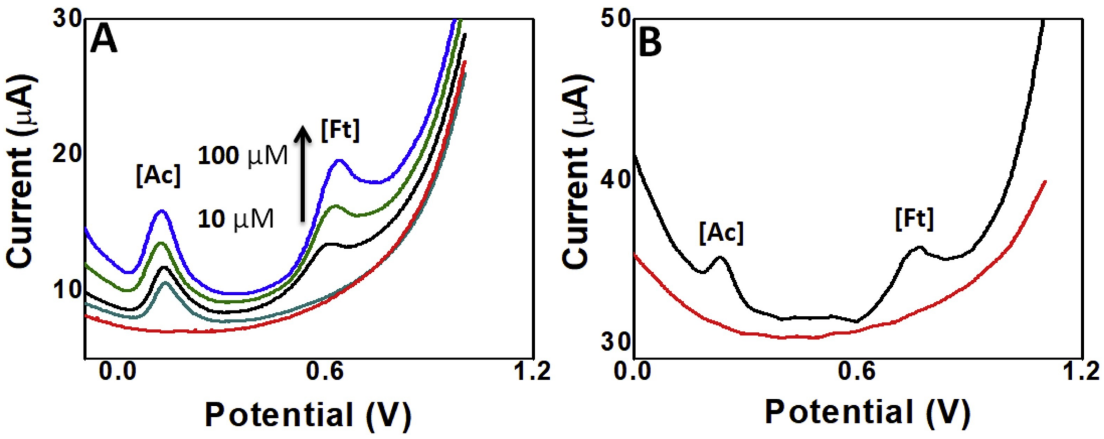

Figure 1.14: Fentanyl response when analysed within a mixture of cutting agents. (a) Shows the square wave voltammetric response of liquid fentanyl (Ft) across a concentration range of 10-100 μM (black to blue), alongside 100 μM acetaminophen (Ac), caffeine and glucose in PBS. (b) Fentanyl response in a mixed powder containing 100 μM fentanyl, acetaminophen, caffeine and glucose. Reproduced from ref. 73 with permission from Elsevier. Copyright 2019.

Emerging technology combining electrochemistry with microneedle arrays for the manufacture of wearable sensors, which facilitate continuous monitoring of a compound of interest within the wearer, have gained significant attention in recent years. These needle type sensors monitor compounds within the interstitial fluid (ISF) beneath the skins surface, relaying data remotely to a smartphone, tablet or laptop. In a continuation of fentanyl detection, here the ability to monitor the opioid, in addition to morphine and norfentanyl within a biological matrix is reported.[76] Similarly, to Barfidokht *et al.*[73] the authors monitored fentanyl using its characteristic oxidation at ~ +0.7 V (vs Ag/AgCl) obtained via square-wave voltammetry. Interestingly the sensor offered simultaneous multi-analyte detection, utilising a dual working electrode

system, shown in Figure 1.15, to monitor fentanyl alongside organophosphate nerve agents.[76] To manufacturer the array, electrodes are housed within the hallow point microneedles, where the working electrodes and counter were constructed from carbon paste, while the reference was made from embedding a Ag/AgCl wire into the fourth needle.[76] Unlike Barfidokht *et al.*[73] here the authors assessed the impact of structurally similar opioids upon fentanyl detection, including its metabolic product norfentanyl. Unsurprisingly analysis of morphine, which also possess the electro-active piperidine tertiary amine functionality, relieved an anodic peak at +0.7 V (vs Ag/AgCl), alongside a second oxidation peak at +0.2 V (vs Ag/AgCl).[76] As such the monitoring of fentanyl in the presence of morphine, or indeed any other piperidine tertiary amine containing species, will see the current peak intensity at +0.7 V (vs Ag/AgCl) increase, thus preventing accurate fentanyl quantification.[76] However, the presence of the secondary anodic peak present within morphine would facilitate the discrimination between fentanyl solely present or alongside morphine; where fentanyl itself would only display a singular oxidation peak. However, the production of a second identifying peak may not be present within all piperidine tertiary amine containing species and as such is a significant limitation not addressed by the authors within this contribution. The metabolic product, norfentanyl was observed to produced a cathodic peak at -0.2 V (vs Ag/AgCl).[76] The presence of this peak could therefore offer an alternative potential at which fentanyl consumption could be monitored alongside other structurally similar opioids such as morphine which also produce the anodic peak at +0.7 V (vs Ag/AgCl).[76] The

authors demonstrated the strength of their concept design through the application of the sensor to an agarose tissue-mimicking phantom gel skin model, where they observed a current increase at both working electrodes with an increase in both analyte concentrations, giving a degree of confidence in the developed sensor toward *in-vivo* translation.[76] Despite the complex matrix and the simultaneous multi-analyte detection, no inference or impedance upon the sensor's stability or sensitivity was reported by the authors. Their unique design offers an interesting alternative approach for screening by negating the collection of biological matrices from a suspect but via direct application of the sensor, although a lack of consideration for potential applications toward a range of NPS classes has not been performed.

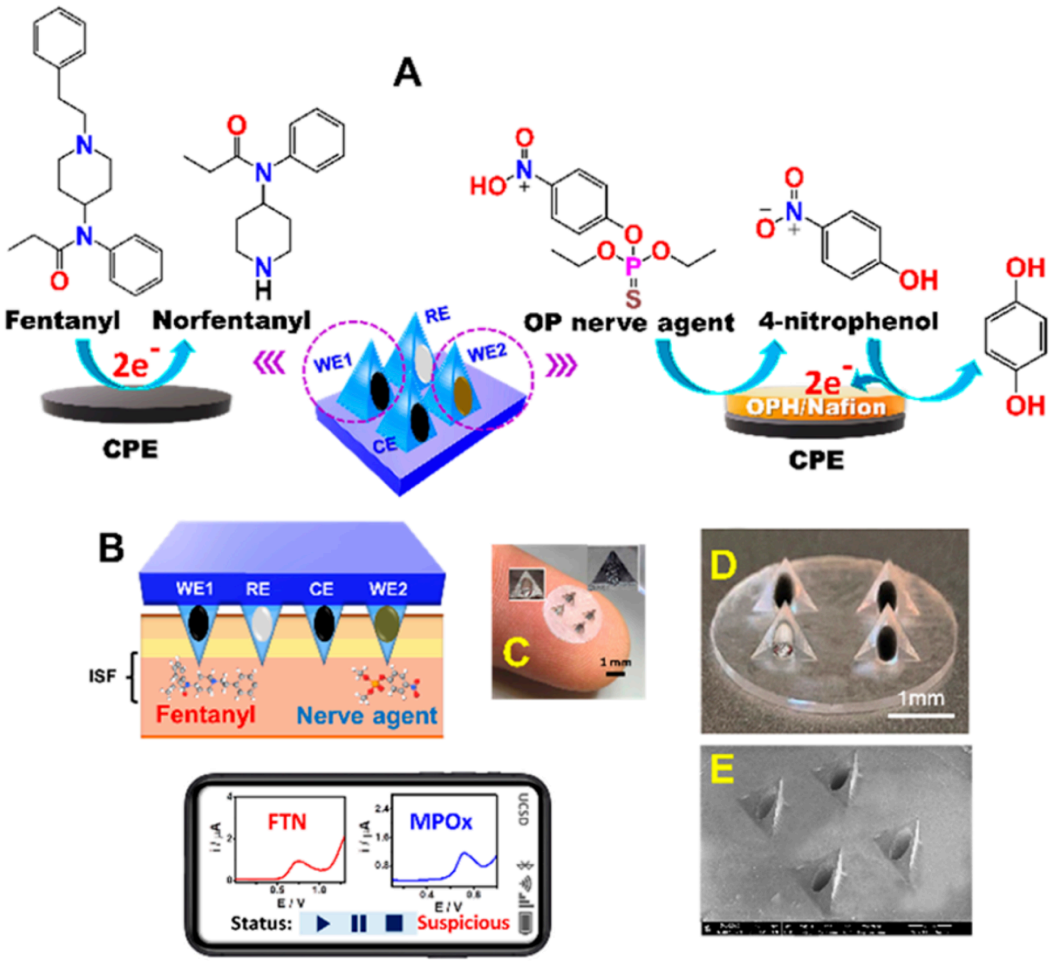

Figure 1.15: Schematic and images of the microneedle sensor array for the simultaneous detection of opioids and nerve agents. (a) Schematic of fentanyl and nerve agent reactions at the two working electrodes. (b) Schematic of the microneedle array for the simultaneous minimally invasive dual-threat detection, with wireless data relay to smartphone, (c,d) Optical images of the microneedle array. (e) SEM image of the four hollow point microneedles. Reprinted with permission from ref. 76. Copyright 2020 American Chemical Society.

Although a number of different NPS classes have displayed redox behaviour which would allow for their monitoring via electrochemical methods, there still remains a lack of assessment of a number of different NPS classes via a singular electrochemical method. Synthetic cathinone's and their metabolites are one of the more extensively studied NPS classes with electrochemical methods.[7, 78, 82, 85] Previous reports have shown their oxidation upon graphite screen printed electrodes[7, 85], glassy carbon[7], boron doped diamond[7] and molecularly imprinted nanocomposite films[82], all of which displayed oxidation peaks at ~ +1.0 V (vs Ag/AgCl/SCE).[7, 78, 82, 85] Moreover, their detection has been achieved in a variety of complex matrices including urine and human serum.[7, 82, 85] However, few reports investigate their detection alongside alternate drug classes or other forensically relevant compounds. In contrast, other NPS classes such as synthetic cannabinoids have been rarely studied with only a single report to date on their electrochemical detection.[81] Although in recent years there has been an increase in the studies of synthetic opioids such as fentanyl, a wider range of classes both individually and within mixed samples, require investigation to fully assess the potential of electrochemical sensors for wider employment as screening methodologies. The possibility to utilise more unusual but nevertheless forensically relevant substances, which possess similar structural functionality to NPS may offer a viable alternative to assess the applicability of developed electrochemical methods toward forensic applications. Such substances could include a range of poisons such as atropine[21, 31, 86] and scopolamine[17, 23, 87, 88] or traditional illicit substances.[5, 84, 89, 90]

Alongside NPS abuse, alternative compounds not traditionally considered as substances of abuse are now being utilised due to their accessibility. This includes recreational abuse alongside criminal use, where they are utilised to facilitate crimes such as sexual assault, robbery or murder. One such group of interest is the naturally occurring tropane alkaloids, atropine and scopolamine, which share structural similarities to cocaine. *Atropa belladonna, Datura* and *Mandrake* all share these deadly tropane alkaloids, yet their growth is uncontrolled in many countries, with the plants encountered amongst a number of easily accessible locations including domestic gardens.[91, 92] Pharmaceutical products containing these substances can often be purchased without a medical prescription.[26] Atropine and scopolamine are anticholinergic hallucinogens, as a result of their antagonists' actions toward the acetylcholine receptors, gifting them their hallucinogenic properties.[26, 91, 92] Criminal abuse of these tropane alkaloids is not a modern phenomenon, with one of the most widely known cases of atropine poisoning occurred in Edinburgh in 1994. Dr Paul Agutter, a biology professor at Edinburgh Napier University at the time, attempted to murder his wife by spiking her gin and tonic with the deadly alkaloid. Agutter subsequently attempted to evade the police by diverting suspicion from himself by lacing multiple bottles of branded tonic, before returning the laced bottles to a local supermarket shelf. This successfully created mass panic when a number of people in the Edinburgh area subsequently fell ill initially averting suspicion from himself.[20, 93] Similarly, the use of scopolamine for drug-facilitated robberies and sexual assaults can be traced back to the

1950s. Cases are largely concentrated in the South American continent but incidents involving scopolamine have been more recently encountered in Norway, Spain and the UK.[17, 23-26, 28] Scopolamine renders the consumer into a submissive "zombie" like state, where they demonstrate a high degree of obedience as a result of the reduction in declarative memory.[26] This resultant zombie like trance is abused by criminals to persuade their victims to willingly perform illegal tasks or surrender their valuables, with no recollection of events once the drug has been excreted from their system.[23, 26] Victims have been dosed through a number of methods including, inhalation, ingestion or even topical adsorption, where one case detailed the presence of scopolamine contained within moisturising creams.[23] Such cases prompted Ramdani *et al.*[21] to investigate the electrochemical detection of the alkaloid within spiked drink samples. Fabricated in house via the printing of carbon paste onto a flexible polyester substrate, Ramdani *et al.*[21] constructed a graphite SPE sensor for the detection of atropine. Using their sensor, the authors were able to detect atropine down to concentrations of 18.4 μM within diet Coca-Cola® with only micro-litre sample volumes required.[21] Exclusively utilising cyclic voltammetry via a portable potentiostat, the authors achieved detection at a forensically relevant range, within a complex matrix of the carbonated drink.[21] Ramdani *et al.*[21] provided a strong proof-of-concept for the detection of atropine within commercial drinks; however much work is still required to assess the viability of the alkaloids detection within a wider range of sample matrices. As noted by the authors, other species intrinsic to these complex matrices can interfere with substance detection, such as

quinine. Quinine a fellow alkaloid found within tonic water, undergoes comparable electro-activated oxidation at the tertiary amine functional group within the heterocyclic nitrogen ring system present within both species.

For the detection of poisons such as atropine and scopolamine or date rape drug Rohypnol™, methodologies which offer rapid results but can also be performed at-scene or at a patients bedside is crucial. The rapid excretion of such species makes their detection after 24 hours significantly challenging.[17, 92] This is where electrochemical methods begin to strongly challenge the more traditional analytical techniques. Instrument portability with minimal sample volumes facilitates the development of point-of-care or in-field analysis methods offering almost instantaneous results. The lack of or minimal sample preparation required with some samples, such as spiked drinks able to behave as their own electrolyte, further enhance the applicability and ease of use of these techniques toward on-site analysis.[18] The best approach for the detection of species involved within drug-facilitated crimes or sexual assaults would afford the opportunity to develop for a two-pronged approach. Firstly, where samples are taken directly from the suspected crime scene which might include the victim's drink; and secondly, where samples are taken directly from the victim, such as urine, sweat or blood within a hospital setting.

Agutter may have chosen atropine as a result of its poor detection within bodily fluids; however, since his murder attempt in 1994, a number of

electrochemical methods have demonstrated the ability to successfully detect the poison within complex matrices including urine[86, 94-96] and human serum.[95, 96] The ability to electrochemically detect atropine indicates that scopolamine, a closely related tropane alkaloid, could be successfully detected employing the same methodologies. This was recently proven by Da Costa *et al.*[88] who demonstrated an in-field detection strategy for scopolamine within urine and a variety of alcoholic and non-alcoholic drinks.[88] As was observed with quinine and atropine, the two sister tropane alkaloids oxidise within the same potential range as a result of their electrochemical behaviour arising from the tertiary amine group present within their tropane ring functionality housed within both compounds. The ability to apply the same methodologies to species with similar electrochemical and structural properties allows for the application of those already developed to a wider range of species with ease. For example, cocaine a fellow tropane alkaloid and one of the highest abused illicit substances possesses the same tropane functionality as atropine, scopolamine and quinine. It hence stands to reason that the methodologies developed for cocaine could be applied to other tropane alkaloid species and vice versa. This can be advantageous when considering more well known species, such as cocaine have a extensive literature base already in place.[84, 89, 97-100]

Although there are obvious advantages of the ability to apply developed methodologies to new species of similar structure, it also introduces problems

with regard to specificity and the ability to differentiate between those structurally similar species. Increasing specificity of electrochemical techniques is however not an insurmountable limitation. Often, modified working electrodes are used to avoid or overcome interference effects from species with similar redox potentials. For example, Asturias-Arribas *et al.*[89] employed carbon nanotubes, immobilised upon a carbon SPE to facilitate greater separation between the overlapping peaks of cocaine and some of its common adulterants; codeine, paracetamol and caffeine.[89] De Oliveira *et al.*[97, 98] modified carbon paste[97], glassy carbon[98] and platinum electrodes[98] with a uranyl Schiff base for the determination of cocaine negating interference effects from the presence of lidocaine and procaine.[97, 98] Further specificity has been coined through the use of bio-based sensors, where highly selective species such as single stranded aptamers or antibodies are employed.[99-101] The general principles of bio-based sensors are depicted in Figure 1.16. The aptamer is observed to selectively bind to the target species, such as cocaine, which results in the production of a signal but will not bind to any of the common adulterants or diluents, even those of similar structure.[99] Alternative methodologies to improve specificity are observed through the pairing of electrochemical techniques to form a dual detection system, such as through the employment of the light emitting technique electrochemiluminescence (ECL). ECL has the potential to improve specificity through a number of methods including; the incorporation of different metal luminophores, with the possibility of different metals offering alternative reactivity with the desired species.[102-105] Or through the

exploitation of multi electrode arrays combined with the inherent control of emission and subsequently detector positioning could also show promise in the improvement of specificity. Alternatively, the application of a separation strategy prior to detection can also be considered, although this comes at the cost of portability. However, it is worth noting that it is unlikely that any electrochemical screening methods would not be followed by confirmatory analysis. Thus, any interfering species would be ultimately identified during these subsequent testing procedures, allowing for electrochemical methodologies to focus upon screening and hence portable applications.

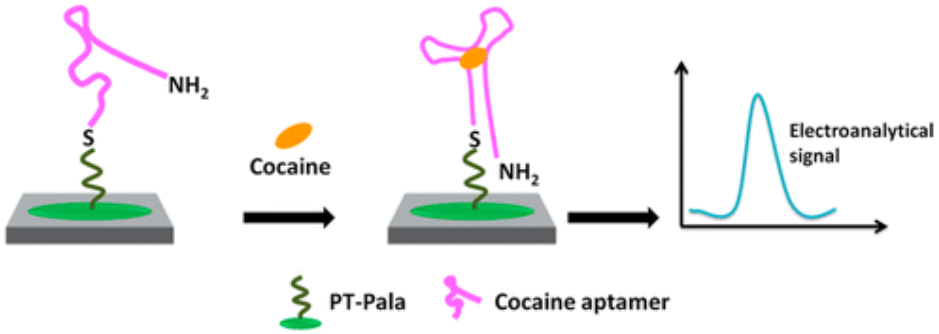

Figure 1.16: Schematic representation of aptamer principles, showing the selective detection of cocaine. Reproduced from ref. 99 with permission from American Chemical Society, Copyright 2016.

As with the previously discussed techniques, in order for electrochemical methods to be utilised as screening methodologies, a database of the expected oxidation or reduction potentials of different NPS classes alongside the predicted number of redox peaks produced would be needed. Ideally such a system could be incorporated into the instrumentation, as is observed

with the portable Raman systems previously discussed, however such technology has yet to be coined. Furthermore, the challenge regarding the ability to source reference standards remains, which would be required to construct such a database. Electrochemistry offers the advantage of high-level class identification, as a result of chemical functionality producing similar redox behaviours across different species. As such, in contrast to the highly specific immunoassay methods, which fail upon structural alternation of compounds, electrochemical sensors remain valid if the electro-active functionality is maintained, despite changes to the peripheral structure. What's more, electrochemical sensors can be easily adapted to facilitate the detection of new compounds within a drug class, an intrinsic advantage as a result of the flexibility in the choice of electrode material and the possibility to employ indirect and alternative detection strategies, such as ECL. It could therefore be argued that a tentative class identification could be assigned to a previously unencountered NPS through comparison of its observed redox behaviour. Although it is likely that electrochemical methods would be primarily employed as screening tools, their strong correlation in comparison to validated HPLC[5] and LC-MS/MS[82] methods demonstrates the possibility for the employment of such methodologies for future quantitative analysis utilising portable instrumentation with less reagent consumption and hence lower operating costs. As such, the argument stands that electrochemistry could offer a more viable alternative, compared with other analytical methodologies, particularly as an analytical screening tool. This is only heightened by its proven application to a wide range of matrices, availability

of screen printed electrodes and commercially available portable potentiostats alongside micro-litre sampling volumes and minimal sample preparation requirements. Furthermore, direct comparison of electrochemical methodologies to the currently utilised colorimetric tests, which cannot be applied to complex matrices including herbal material and biological fluids, sees electrochemical sensors offer improved sensitivity, reliability and ease of use. Yet more research across a wider range of NPS classes is required to determine if they display redox behaviour is necessary to fully assess the suitability of such techniques. While their specificity can often hinder their applications for detection of structurally similar compounds, further development of different strategies to improve specificity, will inevitability reduce the limitations this might impose. Electrochemical sensing can therefore provide vital information in the initial stages of investigations, while rapid in-field testing allows for analysis to be performed during the “golden hour” window, a time where potential contamination or destruction of evidence is at a minimum.

1.4 Project Aims

This project aims to develop a novel electrochemical screening sensor for the detection of alternative illicit substances, primarily focusing upon the tropane alkaloid class. The ideal objective is the development of a portable sensing system for use outwith a laboratory facility which is compatible with a variety of complex matrices. The focus will be initially placed upon the development and optimisation of an electrochemiluminescence (ECL) sensor, which utilises the traditional and hence widely available luminophore tris(2,2′-bipyridine)ruthenium(II) ($[Ru(bpy)_3]^{2+}$) as detailed within chapter three. Sensor development will prioritised reproducibility and reliability for alkaloid detection, with an emphasis on ease of use alongside minimal reagent consumption and rapid results; all prerequisites required for employment within a forensic arena. Once the sensing system has been developed and optimised for the detection of tropane alkaloids, a shift in focus will be made toward its application for analysis within complex matrices. Current screening methodologies lack compatibility across a range of sample matrices often restricted to pure samples, and as such prevent a single in-field testing system. This project aims to address this limitation, faced by not only forensic practitioners but also within border patrol and good seizure analysis. This will be achieved through the development of an ECL sensing system compatible with a variety of matrices, including herbal material and biological fluids, discussed within chapters four and five. Finally investigations will be performed to tackle the issue of specificity, faced by a number of portable screening methodologies and in particular ECL systems. Methodologies to

improve this characteristic, as discussed within chapter six, primarily focus upon procedures which are suited to in-field analysis or can be applied during sensor fabrication, ensuring increased specificity does not compromise instrument portability or ease of use.

1.5 References

1. S. Beharry and S. Gibbons, *Forensic Sci. Int.*, 2016, **267**, 25-34.
2. J. Neicun, M. Steenhuizen, R. van Kessel, J. C. Yang, A. Negri, K. Czabanowska, O. Corazza and A. Roman-Urrestarazu, *PLOS ONE*, 2019, **14**, e0218011.
3. Home Office and N. Baker, New psychoactive substances review: report of the expert panel, https://www.gov.uk/government/publications/new-psychoactive-substances-review-report-of-the-expert-panel, (accessed 13th October, 2017).
4. F. Schifano, L. Orsolini, G. Duccio Papanti and J. M. Corkery, *World Psychiatry*, 2015, **14**, 15-26.
5. L. R. Cumba, A. V. Kolliopoulos, J. P. Smith, P. D. Thompson, P. R. Evans, O. B. Sutcliffe, D. R. do Carmo and C. E. Banks, *Analyst*, 2015, **140**, 5536-5545.
6. Home Office, New Psychoactive Substances (NPS) resource pack, https://www.gov.uk/government/publications/new-psychoactive-substances-nps-resource-pack, (accessed 12th October, 2017).
7. J. P. Smith, J. P. Metters, C. Irving, O. B. Sutcliffe and C. E. Banks, *Analyst*, 2014, **139**, 389-400.
8. J. P. Smith, J. P. Metters, O. I. G. Khreit, O. B. Sutcliffe and C. E. Banks, *Anal. Chem.*, 2014, **86**, 9985-9992.
9. V. J. Koller, G. J. Zlabinger, V. Auwärter, S. Fuchs and S. Knasmueller, *Arch. Toxicol.*, 2013, **87**, 1287-1297.
10. European Monitoring Centre for Drug and Drug Addiction, Perspectives on Drugs: Synthetic cannabinoids in Europe, http://www.emcdda.europa.eu/publications/pods/synthetic-cannabinoids_en, (accessed 9th March, 2020).
11. Z. D. Cooper, Current Psychiatry Reports, 2016, **18**, 52.
12. United Nations Office on Drugs and Crime, UNODC Early Warning Advisory on New Psychoactive Substances, https://www.unodc.org/LSS/Page/NPS, (accessed 9th March, 2020).
13. National Records of Scotland, Drug-related deaths in Scotland in 2018, 2019.
14. United Nations Office on Drugs and Crime, UNODC Early Warning Advisory on New Psychoactive Substances, https://www.unodc.org/LSS/Announcement/Details/2d667984-8928-47d4-ae0c-3a9aed85b639, (accessed 9th March, 2020).
15. Oxford Dictonary, Oxford English Dictonary, https://www.lexico.com/definition/drug, (accessed 9th March, 2020).
16. Royal Society for Public Health, *Taking a New Line on Drugs*, 2016.
17. O. M. Vallersnes, C. Lund, A. K. Duns, H. Netland and I.-A. Rasmussen, *Clin. Toxicol.*, 2009, **47**, 889-893.
18. J. P. Smith, J. P. Metters, D. K. Kampouris, C. Lledo-Fernandez, O. B. Sutcliffe and C. E. Banks, *Analyst*, 2013, **138**, 6185-6191.
19. F. Tseliou, P. Pappas, K. Spyrou, J. Hrbac and M. I. Prodromidis, *Biosens. Bioelectron.*, 2019, **132**, 136-142.
20. D. Johnson, Atropine, https://www.chemistryworld.com/podcasts/atropine/6546.article, (accessed 9th November, 2018).
21. O. Ramdani, J. P. Metters, L. C. S. Figueiredo-Filho, O. Fatibello-Filho and C. E. Banks, *Analyst*, 2013, **138**, 1053-1059.
22. J. Carlier, E. Escard, M. Péoc'h, B. Boyer, L. Romeuf, T. Faict, J. Guitton and Y. Gaillard, *J. Forensic Sci.*, 2014, **59**, 859-864.
23. J. Sáiz, T. D. Mai, M. L. López, C. Bartolomé, P. C. Hauser and C. García-Ruiz, *Sci. Justice*, 2013, **53**, 409-414.
24. E. Le Garff, Y. Delannoy, V. Mesli, V. Hédouin and G. Tournel, *Forensic Sci. Int.*, 2016, **261**, e17-e21.

25. K. J. Lusthof, I. J. Bosman, B. Kubat and M. J. Vincenten-van Maanen, *Forensic Sci. Int.*, 2017, **274**, 79-82.
26. S. Reichert, C. Lin, W. Ong, C. C. Him and S. Hameed, *Canadian family physician Medecin de famille canadien*, 2017, **63**, 369-370.
27. L. Fernández-López, M. Falcón Romero, G. Prieto-Bonete, C. Pérez-Martínez, J. Navarro-Zaragoza, D. Suarez and A. Luna Maldonado, *Forensic Sci. Int.*, 2018, **287**, e10.
28. BBC News, Woman in court over alleged murder and poisoning, https://www.bbc.co.uk/news/uk-england-london-51123944, (accessed 6th April, 2020).
29. W. Miao, *Chem. Rev.*, 2008, **108**, 2506-2553.
30. L. Hu and G. Xu, *Chem. Soc. Rev.*, 2010, **39**, 3275-3304.
31. A. Zhang, C. Miao, H. Shi, H. Xiang, C. Huang and N. Jia, *Sens. Actuators B*, 2016, **222**, 433-439.
32. M. Rizwan, N. Mohd-Naim and M. Ahmed, *Sensors*, 2018, **18**, 166.
33. L. Shaw and L. Dennany, *Curr. Opin. Electrochem.*, 2017, **3**, 23-28.
34. C. Banks and J. Smith, *The Analytical Scientist*, 2016, 41-43.
35. D. Ammann, J. M. McLaren, D. Gerostamoulos and J. Beyer, *J. Anal. Toxicol.*, 2012, **36**, 381-389.
36. F. Vaiano, F. P. Busardò, D. Palumbo, C. Kyriakou, A. Fioravanti, V. Catalani, F. Mari and E. Bertol, *J. Pharm. Biomed. Anal.*, 2016, **129**, 441-449.
37. V. A. Boumba, M. Di Rago, M. Peka, O. H. Drummer and D. Gerostamoulos, *Forensic Sci. Int.*, 2017, **279**, 192-202.
38. J. A. Michely, S. D. Brandt, M. R. Meyer and H. H. Maurer, *Anal. Bioanal. Chem.*, 2017, **409**, 1681-1695.
39. C. Montesano, G. Vannutelli, V. Piccirilli, M. Sergi, D. Compagnone and R. Curini, *Talanta*, 2017, **167**, 260-267.
40. C. Ricardo Leal, S. Márcia Maria Portela de and O. Celinalva da Silva Lima, *Brazilian Journal of Forensic Sciences, Medical Law and Bioethics*, 2017, **6**, 247-257.
41. A. T. Caspar, J. B. Gaab, J. A. Michely, S. D. Brandt, M. R. Meyer and H. H. Maurer, *Drug Test. Anal.*, 2018, **10**, 184-195.
42. G. Mercieca, S. Odoardi, M. Cassar and S. Strano Rossi, *J. Pharm. Biomed. Anal.*, 2018, **149**, 494-501.
43. A. N. Kimble and A. P. DeCaprio, *Forensic Chem.*, 2019, **16**, 100189.
44. G. McLaughlin, N. Morris, P. V. Kavanagh, J. D. Power, J. O'Brien, B. Talbot, S. P. Elliott, J. Wallach, K. Hoang, H. Morris and S. D. Brandt, *Drug Test. Anal.*, 2016, **8**, 98-109.
45. L. Ernst, K. Brandhorst, U. Papke, A. Altrogge, S. Zodel, N. Langer and T. Beuerle, *Forensic Sci. Int.*, 2017, **277**, 51-58.
46. L. H. Antonides, R. M. Brignall, A. Costello, J. Ellison, S. E. Firth, N. Gilbert, B. J. Groom, S. J. Hudson, M. C. Hulme, J. Marron, Z. A. Pullen, T. B. R. Robertson, C. J. Schofield, D. C. Williamson, E. K. Kemsley, O. B. Sutcliffe and R. E. Mewis, *ACS Omega*, 2019, **4**, 7103-7112.
47. K. McCrae, S. Tobias, K. Tupper, J. Arredondo, B. Henry, S. Mema, E. Wood and L. Ti, *Drug Alcohol Depend.*, 2019, **205**, 107589.
48. S. Oldenhof, A. ten Pierick, J. Bruinsma, S. Eustace, J. Hulshof, J. van den Berg and M. Hoitink, *Drug Test. Anal.*, 2020, **12**, 152-155.
49. E. Gerace, F. Seganti, C. Luciano, T. Lombardo, D. Di Corcia, H. Teifel, M. Vincenti and A. Salomone, *Drug Alcohol Rev.*, 2019, **38**, 50-56.
50. H. Muhamadali, A. Watt, Y. Xu, M. Chisanga, A. Subaihi, C. Jones, D. I. Ellis, O. B. Sutcliffe and R. Goodacre, *Front. Chem.*, 2019, **7**.
51. P. W. Fedick, F. Pu, N. M. Morato and R. G. Cooks, *J. Am. Soc. Mass Spectrom.*, 2020, **31**, 735-741.

52. D. Pasin, A. Cawley, S. Bidny and S. Fu, *Anal. Bioanal. Chem.*, 2017, **409**, 5821-5836.
53. P. M. Geyer, M. C. Hulme, J. P. B. Irving, P. D. Thompson, R. N. Ashton, R. J. Lee, L. Johnson, J. Marron, C. E. Banks and O. B. Sutcliffe, *Anal. Bioanal. Chem.*, 2016, **408**, 8467-8481.
54. S. Kneisel and V. Auwärter, *Journal of mass spectrometry*, 2012, **47**, 825-835.
55. L. M. Huppertz, S. Kneisel, V. Auwärter and J. Kempf, *Journal of Mass Spectrometry*, 2014, **49**, 117-127.
56. S. Graziano, L. Anzillotti, G. Mannocchi, S. Pichini and F. P. Busardò, *J. Pharm. Biomed. Anal.*, 2019, **163**, 170-179.
57. J. Coelho Neto, *Forensic Sci. Int.*, 2015, **252**, 87-92.
58. L. S. A. Pereira, F. L. C. Lisboa, J. C. Neto, F. N. Valladão and M. M. Sena, *Microchem. J.*, 2017, **133**, 96-103.
59. W. R. de Araujo, T. M. G. Cardoso, R. G. da Rocha, M. H. P. Santana, R. A. A. Muñoz, E. M. Richter, T. R. L. C. Paixão and W. K. T. Coltro, *Anal. Chim. Acta*, 2018, **1034**, 1-21.
60. P. Wägli, Y.-C. Chang, A. Homsy, L. Hvozdara, H. P. Herzig and N. F. de Rooij, *Anal. Chem.*, 2013, **85**, 7558-7565.
61. D. J. Rowe, D. Smith and J. S. Wilkinson, *Sci. Rep.*, 2017, **7**, 7356.
62. T. Mostowtt and B. McCord, *Talanta*, 2017, **164**, 396-402.
63. K. E. Toole, S. Fu, R. G. Shimmon, N. Kraymen, S. Taflaga and A. Forensic, *Microgram J*, 2012, **9**, 27-32.
64. T. M. Scott, J. K. Yeakel and B. K. Logan, *Drug Test. Anal.*, 2014, **6**, 959-963.
65. G. Musile, L. Wang, J. Bottoms, F. Tagliaro and B. McCord, *Anal. Methods*, 2015, **7**, 8025-8033.
66. E. Cuypers, A.-J. Bonneure and J. Tytgat, *Drug Test. Anal.*, 2016, **8**, 136-140.
67. D. Merli, A. Profumo, S. Tinivella and S. Protti, *Forensic Chem.*, 2019, **14**, 100167.
68. Y.-T. Yen, T.-Y. Chen, C.-Y. Chen, C.-L. Chang, S.-C. Chyueh and H.-T. Chang, *Sensors*, 2019, **19**, 3554.
69. L. E. Regester, J. D. Chmiel, J. M. Holler, S. P. Vorce, B. Levine and T. Z. Bosy, *J. Anal. Toxicol.*, 2014, **39**, 144-151.
70. C.-A. Chen, P.-W. Wang, Y.-C. Yen, H.-L. Lin, Y.-C. Fan, S.-M. Wu and C.-F. Chen, *Sens. Actuators B*, 2019, **282**, 251-258.
71. J. R. Sempionatto, R. K. Mishra, A. Martín, G. Tang, T. Nakagawa, X. Lu, A. S. Campbell, K. M. Lyu and J. Wang, *ACS Sensors*, 2017, **2**, 1531-1538.
72. A. J. Stewart, K. Brown and L. Dennany, *Anal. Chem.*, 2018, **90**, 12944-12950.
73. A. Barfidokht, R. K. Mishra, R. Seenivasan, S. Liu, L. J. Hubble, J. Wang and D. A. Hall, *Sens. Actuators B*, 2019, **296**, 126422.
74. K. Brown, M. McMenemy, M. Palmer, M. J. Baker, D. W. Robinson, P. Allan and L. Dennany, *Anal. Chem.*, 2019, **91**, 12369-12376.
75. K. Brown, C. Jacquet, J. Biscay, P. Allan and L. Dennany, *Anal. Chem.*, 2020, **92**, 2216-2223.
76. R. K. Mishra, K. Y. Goud, Z. Li, C. Moonla, M. A. Mohamed, F. Tehrani, H. Teymourian and J. Wang, *J. Am. Chem. Soc.*, 2020, **142**, 5991-5995.
77. R. K. Mishra, J. R. Sempionatto, Z. Li, C. Brown, N. M. Galdino, R. Shah, S. Liu, L. J. Hubble, K. Bagot, S. Tapert and J. Wang, *Talanta*, 2020, **211**, 120757.
78. F. Tan, J. P. Smith, O. B. Sutcliffe and C. E. Banks, *Anal. Methods*, 2015, **7**, 6470-6474.

79. A. F. B. Andrade, S. K. Mamo and J. Gonzalez-Rodriguez, *Anal. Chem.*, 2017, **89**, 1445-1452.
80. S. A. Waddell, C. Fernandez, C. C. Inverarity and R. Prabhu, *Sensing and Bio-Sensing Research*, 2017, **13**, 28-39.
81. M. Dronova, E. Smolianitski and O. Lev, *Anal. Chem.*, 2016, **88**, 4487-4494.
82. I. Razavipanah, E. Alipour, B. Deiminiat and G. H. Rounaghi, *Biosens. Bioelectron.*, 2018, **119**, 163-169.
83. European Monitoring Centre for Drugs and Drug Addiction, Fentanils and synthetic cannabinoids: driving greater complexity into the drug situation, http://www.emcdda.europa.eu/system/files/publications/8870/2018-2489-td0118414enn.pdf, (accessed 10th December, 2018).
84. M. de Jong, N. Sleegers, J. Kim, F. Van Durme, N. Samyn, J. Wang and K. De Wael, *Chem. Sci.*, 2016, **7**, 2364-2370.
85. H. M. Elbardisy, A. García-Miranda Ferrari, C. W. Foster, O. B. Sutcliffe, D. A. C. Brownson, T. S. Belal, W. Talaat, H. G. Daabees and C. E. Banks, *ACS Omega*, 2019, **4**, 1947-1954.
86. X.-Y. Yang, C.-Y. Xu, B.-Q. Yuan and T.-Y. You, *Chin. J. Anal. Chem.*, 2011, **39**, 1233-1237.
87. L. Jianguo, C. Yuan and J. Huangxian, *Electroanalysis*, 2007, **19**, 1569-1574.
88. T. da Costa Oliveira, M. H. P. Santana, C. E. Banks, R. A. A. Munoz and E. M. Richter, *Electroanalysis*, 2019, **31**, 567-574.
89. L. Asturias-Arribas, M. A. Alonso-Lomillo, O. Domínguez-Renedo and M. J. Arcos-Martínez, *Anal. Chim. Acta*, 2014, **834**, 30-36.
90. J. McGeehan and L. Dennany, *Forensic Sci. Int.*, 2016, **264**, 1-6.
91. A. Iranbakhsh, M. A. Oshaghi and A. Majd, *Acta Biol. Cracov., Ser. Bot.*, 2006, **48**, 13-18.
92. S. F. Malamed, in *Sedation (Fifth Edition)*, ed. S. F. Malamed, Mosby, Saint Louis, 2010, DOI: https://doi.org/10.1016/B978-0-323-05680-9.00029-1, pp. 316-354.
93. J. Emsley, Molecule of Murder, https://www.chemistryworld.com/feature/molecule-of-murder/3004697.article, (accessed 9th November, 2018).
94. N. F. Atta, A. Galal and R. A. Ahmed, *Int. J. Electrochem. Sci*, 2012, **7**, 10365-10379.
95. H. Bagheri, S. M. Arab, H. Khoshsafar and A. Afkhami, *New J. Chem.*, 2015, **39**, 3875-3881.
96. A. A. Ensafi, P. Nasr-Esfahani, E. Heydari-Bafrooei and B. Rezaei, *Talanta*, 2015, **131**, 149-155.
97. L. S. de Oliveira, M. A. Balbino, M. M. T. de Menezes, E. R. Dockal and M. F. de Oliveira, *Microchem. J.*, 2013, **110**, 374-378.
98. L. de Oliveira, A. dos Santos Poles, M. Balbino, M. Teles de Menezes, J. de Andrade, E. Dockal, H. Tristão and M. de Oliveira, *Sensors*, 2013, **13**, 7668.
99. G. Bozokalfa, H. Akbulut, B. Demir, E. Guler, Z. P. Gumus, D. Odaci Demirkol, E. Aldemir, S. Yamada, T. Endo, H. Coskunol, S. Timur and Y. Yagci, *Anal. Chem.*, 2016, **88**, 4161-4167.
100. R. Oueslati, C. Cheng, J. Wu and J. Chen, *Biosens. Bioelectron.*, 2018, **108**, 103-108.
101. J. C. Vidal, J. R. Bertolín, L. Bonel, L. Asturias, M. J. Arcos-Martínez and J. R. Castillo, *Electroanalysis*, 2016, **28**, 685-694.
102. G. J. Barbante, C. F. Hogan, D. J. D. Wilson, N. A. Lewcenko, F. M. Pfeffer, N. W. Barnett and P. S. Francis, *Analyst*, 2011, **136**, 1329-1338.
103. E. H. Doeven, E. M. Zammit, G. J. Barbante, C. F. Hogan, N. W. Barnett and P. S. Francis, *Angew. Chem.*, 2012, **124**, 4430-4433.

104. H. J. Kim, K.-S. Lee, Y.-J. Jeon, I.-S. Shin and J.-I. Hong, *Biosens. Bioelectron.*, 2017, **91**, 497-503.
105. L. Chen, D. J. Hayne, E. H. Doeven, J. Agugiaro, D. J. D. Wilson, L. C. Henderson, T. U. Connell, Y. H. Nai, R. Alexander, S. Carrara, C. F. Hogan, P. S. Donnelly and P. S. Francis, *Chem. Sci.*, 2019, **10**, 8654-8667.

CHAPTER TWO

THEORETICAL PRINCIPLES

“But how can one possibly pay attention to a book with no pictures in it?”

Alice (Alice in Wonderland 1951)

2.1 Cyclic Voltammetry

Cyclic voltammetry (CV) is a powerful and versatile tool, often employed in the first instance of electrochemical analysis. Its simplicity and speed allow for the rapid determination of the redox potentials of electroactive species and provide information on the thermodynamic and kinetic redox processes involved.[1-4] Electrochemical reactions typically occur as a result of heterogeneous electron transfer between a solid electrode and a solubilised electroactive species contained within an electrolyte solution. Electrodes, made from conductive materials such as gold, platinum or glassy carbon, are connected to an external power supply, known as a potentiostat. The potentiostat applies an external voltage that raises or lowers the potential energy of the electrons housed within the electrode; this potential energy is known as the Fermi level. When a negative external potential is applied the energy of the Fermi level is raised, and upon reaching a energy greater than that of the lowest unoccupied molecular orbital (LUMO) of the electroactive species (A), electron transfer from the electrode to the LUMO of the species occurs, refer to Figure 2.1a. This process is known as reduction. In contrast, application of a positive potential reduces the energy of the Fermi level, and upon reaching an energy below that of the highest occupied molecular orbital (HOMO) of the electroactive species' electron transfer from the HOMO of the species to the electrode is witnessed, resulting in electrochemical oxidation, refer to Figure 2.1b. These redox processes are driven by the energy difference between the electrode and the HOMO and LUMO energies of the electroactive species, with reactions dictated by the thermodynamically favourable pathway.[4]

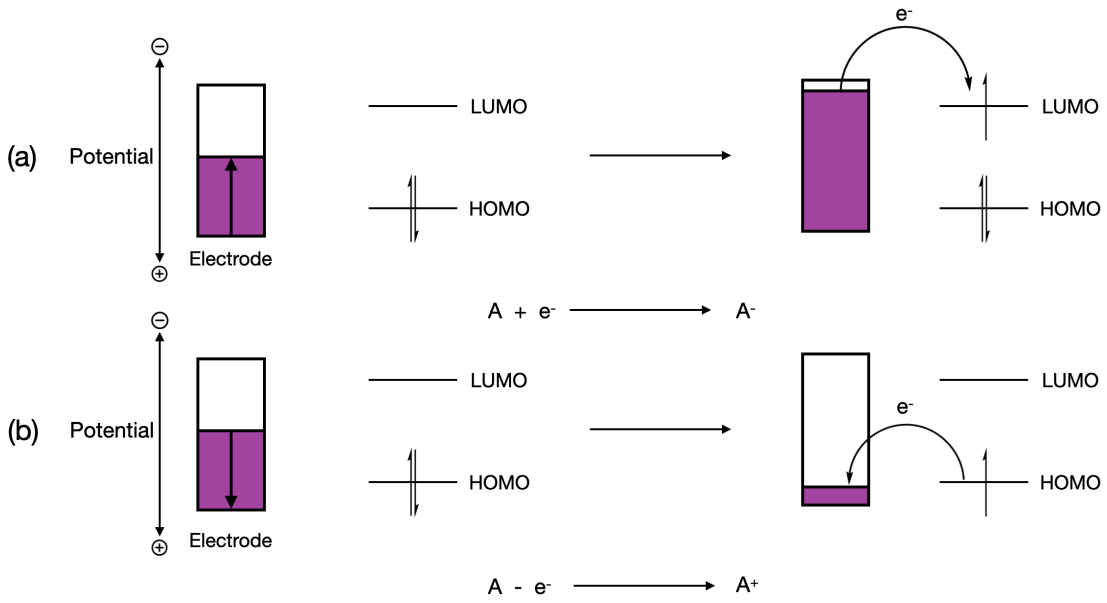

Figure 2.1: Schematic demonstrating how the change in Fermi level energy through the application of an external potential leads to electrochemical (a) reduction or (b) oxidation through heterogeneous electron transfer.

Cyclic voltammetry involves the linear scanning of the potential applied to the working electrode in a triangular waveform, refer to Figure 2.2a. Measurements are typically performed in a three-electrode cell consisting of a working, counter and reference electrode, where the electrochemical reactions of interest occur at the working electrode surface.[4] The potential is swept between two chosen values, referred to as the switching potentials. Voltammograms or cyclic voltammograms are the resulting output from these measurements, and consist of the measured current against the applied potential, see Figure 2.2b.[1, 2, 4] When a positive potential is applied the energy of the Fermi level is decreased and oxidation of the reactant, in the solution immediately surrounding the electrode surface, begins. As this

electrochemical oxidation proceeds the recorded anodic current at the working electrode increases until a maximum value, known as the peak anodic current (i_{pa}), is reached. At the peak anodic current, the solution immediately surrounding the working electrode surface is saturated with the oxidised form of the electroactive species (A_{ox}). As the anodic current increases, and the concentration of the oxidised form of the electroactive species in turn increases, a concentration gradient is established. The concentration gradient between the solution immediately surrounding the working electrode and that within the bulk solution is responsible for diffusion of the analyte to the electrode surface, where oxidation can then occur. With more of the oxidised form of the analyte produced as the potential sweep continues, the resultant concentration gradient drives the analyte (A) from the bulk solution toward the electrode surface via a diffusion process. After reaching the peak anodic current the Nernst diffusion layer surrounding the electrode surface becomes significantly large, such that the flux of the analyte to the electrode surface is no longer sufficient and the reaction becomes mass transport limited. This therefore results in the observed decrease in the anodic current after i_{pa} is reached.[1, 2, 4] When the potential is then reversed and the Fermi level energy is increased, the electrochemical reduction of the accumulative A_{ox} species proceeds. As the reduction reaction continues the cathodic current increases until reaching the peak cathodic current (i_{pc}), where the solution surrounding the electrode surface is now saturated with the analyte , due to its electrochemical reformation.[1, 2, 4]

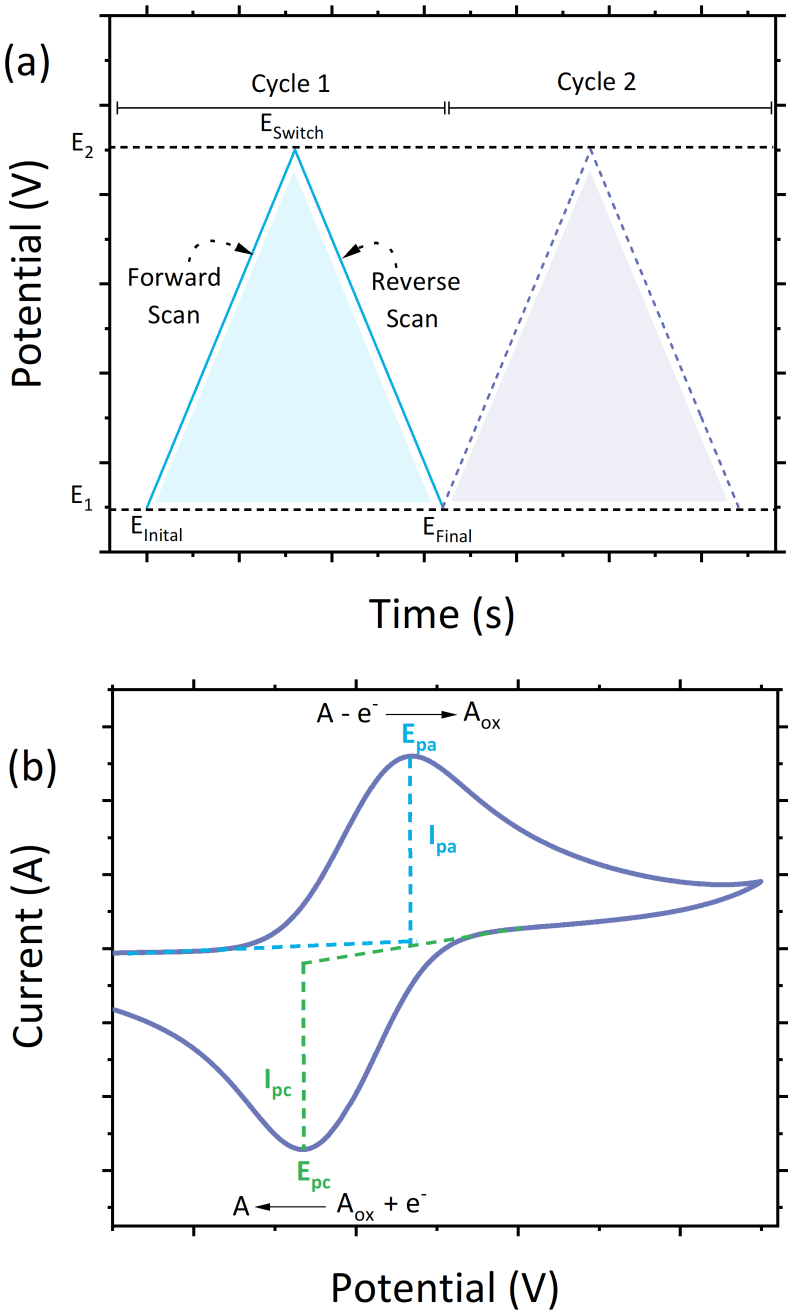

Figure 2.2: (a) Schematic diagram of the typical triangular waveform used to perform CV measurements. (b) Typical resultant CV output voltammogram obtained for a reversible system, where I_{pa} and I_{pc} are the peak anodic and cathodic currents, and E_{pa} and E_{pc} are the anodic peak potential and cathodic peak potential respectively.

The voltammogram profiles and resultant currents measured are influenced by two main properties; the movement of the analyte species to the electrode surface and the electron transfer kinetics between the electrode and the analyte. Analytes are observed to reach the electrode surface through three modes of mass transport; convection, migration and diffusion. Diffusion is the primary process desired within a typical electrochemical system. As such the contributions from convection and migration are negated through the employment of an unstirred solution and a high electrolyte concentration respectively.[4] By using a high electrolyte concentration, analyte migration is minimised by increasing the probability that the electrolyte ions will preferentially migrate to the electrode surface to maintain the charge neutrality of the system.[4] What's more, the use of a high electrolyte concentration ensures that solution resistance toward electron transfer, and hence the Ohmic drop, is minimised.[4] The redox reactions recorded via CV fall into one of three categories; reversible, quasi-reversible and irreversible, as dictated by the system's electron transfer kinetics and the rate of mass transport to the electrode surface.[3, 4] These reaction categories can be visually determined via inspection of the resultant voltammogram profiles, as shown within Figure 2.3. The distinctive 'duck' shape typically associated with CV, details a reversible redox process where the electron transfer kinetics are relatively fast and mass transport to the electrode surface is sufficient, with negligible solution resistance to charge transfer. For reversible systems, giving rise to this distinctive shape, the electrochemical behaviour observed is governed through Fick's and Nernst's laws. Fick's laws detail the diffusional

processes within the electrochemical system. Through consideration of Fick's first and second law, outlined in equations (2.1) and (2.2), we see that the flux of the electroactive species from the bulk solution to the electrode surface is governed by the diffusion coefficient of the species (D), in addition to the concentration of the electroactive species (C) and distance from the electrode surface (x). For reversible systems the current achieved is said to be determined by the rate mass transport of the species to the electrode surface and the corresponding rate of the redox processes. For electrochemically reversible reactions the rate of electron transfer kinetics are said to be far greater than the rate of mass transport to the electrode surface. As such, the Nernstian equilibrium is established at the electrode surface throughout the voltammogram, where concentrations of the redox active species are dictated through the Nernst equation (equation (2.3), where E is the applied potential, E_f^0 is the formal potential, R is the universal gas constant, T is temperature and F is the Faraday constant. For a system operating under ideality the peak to peak separation between the oxidation and reduction peaks (ΔE_p) is minimal. The theoretical ΔE_p value for a solution based system can be determined via equation (2.4), where n is the number of electrons involved in the redox processes. As such, the expected value for a one electron system operating under complete reversibility is observed to be 57 mV at 25 ^oC.[1, 3, 4] For quasi-reversible and irreversible systems, this peak to peak separation value increases while the current maximum decreases, as deviations from ideality are observed. Irreversible systems can be further characterised into two categories; chemically irreversible and electrochemically irreversible. For

chemically irreversible systems only a single peak in the potential region of interest will be observed, as the redox processes result in structural or conformational changes to the redox active species. For reversible solution based systems, said to be under semi-infinite diffusion control, the faradic current is governed by the Randles-Ševćik equation, shown in equation (2.5), where A is the electrode surface area, D is the diffusion coefficient, C is the concentration of the electro-active species and ν is the scan rate.[1, 3, 4]

$$J_i(x) = - D_{(i)} \frac{\partial C_{(i)}(x)}{\partial x} \qquad \text{(equation 2.1)}$$

$$\frac{\partial C_{(i)}}{\partial t} = - D_{(i)} \frac{\partial^2 C_{(i)}(x)}{\partial x^2} \qquad \text{(equation 2.2)}$$

$$E = E_f^0 - \frac{RT}{nF} ln \frac{[Red]}{[Ox]} \qquad \text{(equation 2.3)}$$

$$\Delta E_p = 2.218 \frac{RT}{nF} \qquad \text{(equation 2.4)}$$

$$i_p = 0.446 nFAC \left(\frac{nFDv}{RT} \right)^{\frac{1}{2}} \qquad \text{(equation 2.5)}$$

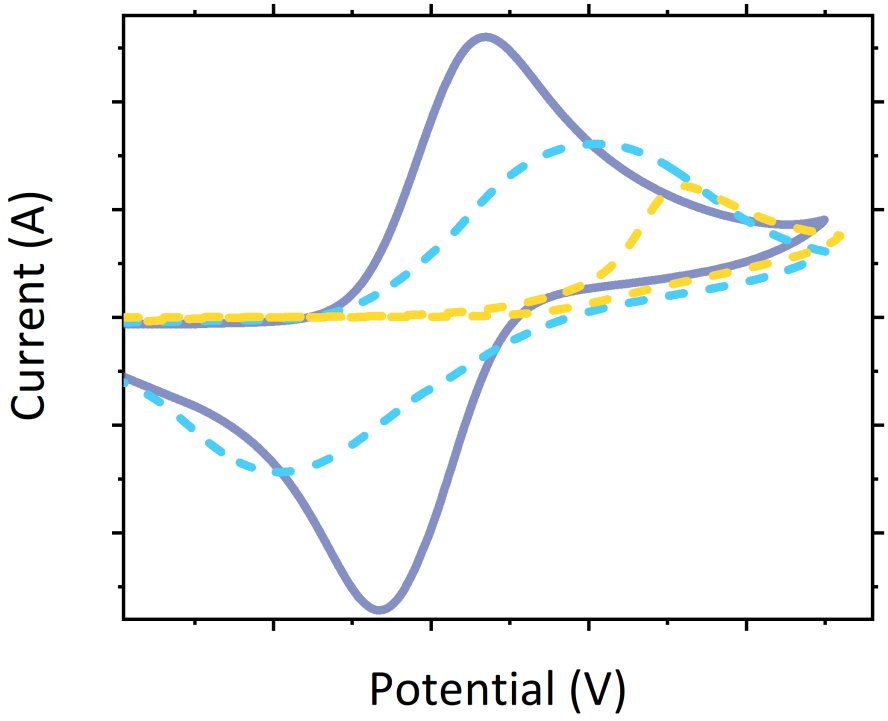

Figure 2.3: Typical CV profiles for reversible (purple solid), quasi-reversible (blue dash) and irreversible (yellow dash) redox processes within solution based systems.

The aforementioned characteristics are intrinsic to a solution based system under semi-infinite diffusion control. However, when the electro-active species are confined to the electrode surface, via surface modifying layers, alternative behaviour is observed. Under these conditions and at sufficiently slow scan rates finite diffusion control is witnessed. Here unlike the peaks observed in Figure 2.3, which display the behaviour of freely diffusing species, the peaks observed for surface confined species are sharp and Gaussian in shape, with no peak to peak separation witnessed, refer to Figure 2.4.[5, 6] This finite diffusion behaviour is a direct result of the fixed

amount of redox active material present at the electrode surface which is now independent of mass transport effects. The removal of the effects of mass transport results in E_{pa} and E_{pc} being equal, therefore ΔE_p is equal to zero and the I_{pa} and I_{pc} values are said to be at unity, where I_{pc}/I_{pa} is equal to one indicating electrochemical ideality in regard to the electron transfer kinetics.[5, 6] For surface confined species' the homogeneity of the surface modification can be evaluated through the full width half maximum height (FWHM) value. FWHM can be determined through equation (2.6), where operation under ideality results in a value of 90.6 mV at 25 ^{o}C for a one electron process.[5-7]

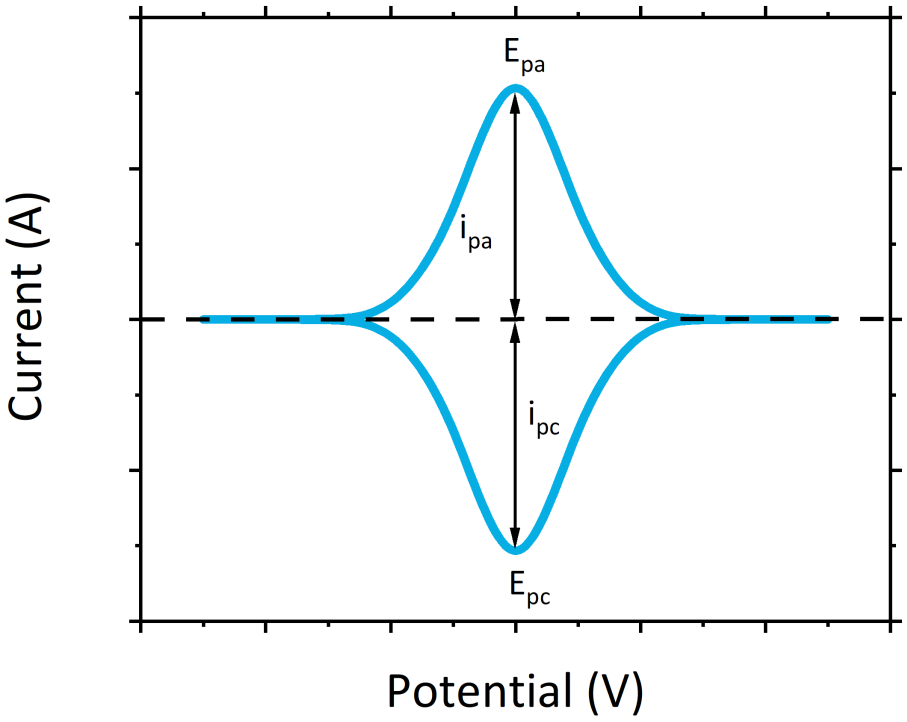

Figure 2.4: Typical CV profile of a reversible redox process for a surface confined species displaying ideal electrochemical behaviour, with sharp Gaussian peaks and ΔEp equal to zero.

$$FWHM = 3.53\frac{RT}{NF}n = \frac{90.6}{n} \qquad \text{(equation 2.6)}$$

For surface confined species the faradic current is determined via equation (2.7), where the surface coverage of the film is considered through the Γ term, which accounts for the total electro-active coverage.[6, 7]

$$i_p = \frac{n^2F^2A\Gamma v}{4RT} \qquad \text{(equation 2.7)}$$

The relationship between the measured faradic current and the scan rate can be used to determine whether a system is under finite or semi-infinite diffusion control, through Randles-Ševćik plots. For systems under semi-infinite diffusion control, the Randles-Ševćik plot of the i_{pa} and i_{pc} values against the square root of the scan rate, will produce a linear relationship. Whilst for finite systems, the Randles-Ševćik plot of the i_{pa} and i_{pc} against the scan rate will produce a linear relationship. For surface confined species at slow scan rates finite diffusion is observed, however as the scan rate is increased there is no longer sufficient time for all the electroactive species present at surface to undergo the redox reactions. As such a tendency toward semi-infinite diffusion control is observed.[4, 6, 7] What's more the relationship between scan rate and peak potential can also provide information of the behaviour of the system. For surface confined species

under finite diffusion the E_{pa} and E_{pc} values should remain constant, while those under semi-infinite diffusion will see a shift in peak potential as the scan rate is increased. This relationship can also be used to determine the whether a system is fully reversible, quasi-reversible or irreversible. If a significant shift in peak potential with an increase in scan rate is observed, then the system is said to be quasi-reversible or irreversible. However, if the system is fully reversible the peak potential should remain approximately constant.[4, 6, 7]

CV is used extensively for the characterisation of electrochemical systems, where distinctive features within the resultant voltammograms allows for a number of characteristics of the electrochemical system to be identified with ease. This includes redox potentials of the analytes of interest, information regarding the electron transfer kinetics and thermodynamics of the redox processes alongside mechanistic information. The speed at which CV can be performed and the wealth of information it provides, have resulted in its widespread employment as the preliminary technique for the investigation of electrochemical systems.[1-4]

2.2 Electrochemiluminescence

Electrochemiluminescence or electrogenerated chemiluminescence (ECL) is a form of photoluminescence produced through the interaction of species generated at an electrode surface. Similar to chemiluminescence (CL) the production of light is the result of highly energetic homogenous electron

transfer reactions, without the requirement of an external light source.[8-12] In contrast to CL, the luminescence produced is not through the controlled mixing of chemical reagents but via the application of an appropriate potential to generate intermediate species, whose interaction leads to luminescence production.[10, 11] Intermediates are generated through the oxidation or reduction of precursors at the electrode surface, one of which, the luminophore, is responsible for the emission of light. These reactive intermediates then undergo highly exo-energetic electron transfer processes, resulting in the formation of an excited state species. Upon relaxation, light at a characteristic wavelength, equivalent to the energy bandgap between the ground and excited state of the luminophore species is emitted.[9, 10, 12, 13] A light detecting device, captures this emission facilitating the use of ECL for analytical applications. Measurements can be recorded, visually such as with a digital camera; spectroscopically typically via a charged coupled device (CCD) spectrometer, allowing for non-subjective colour identification, or ,photo-electronically through the use of a photomultiplier tube (PMT).[9, 10, 12, 13] Typical resultant outputs from each detector system, shown in Figure 2.5, add further flexibility to the technique particularly in terms of its usability, application and device manufacturer, standing only to further its potential within the analytical field.

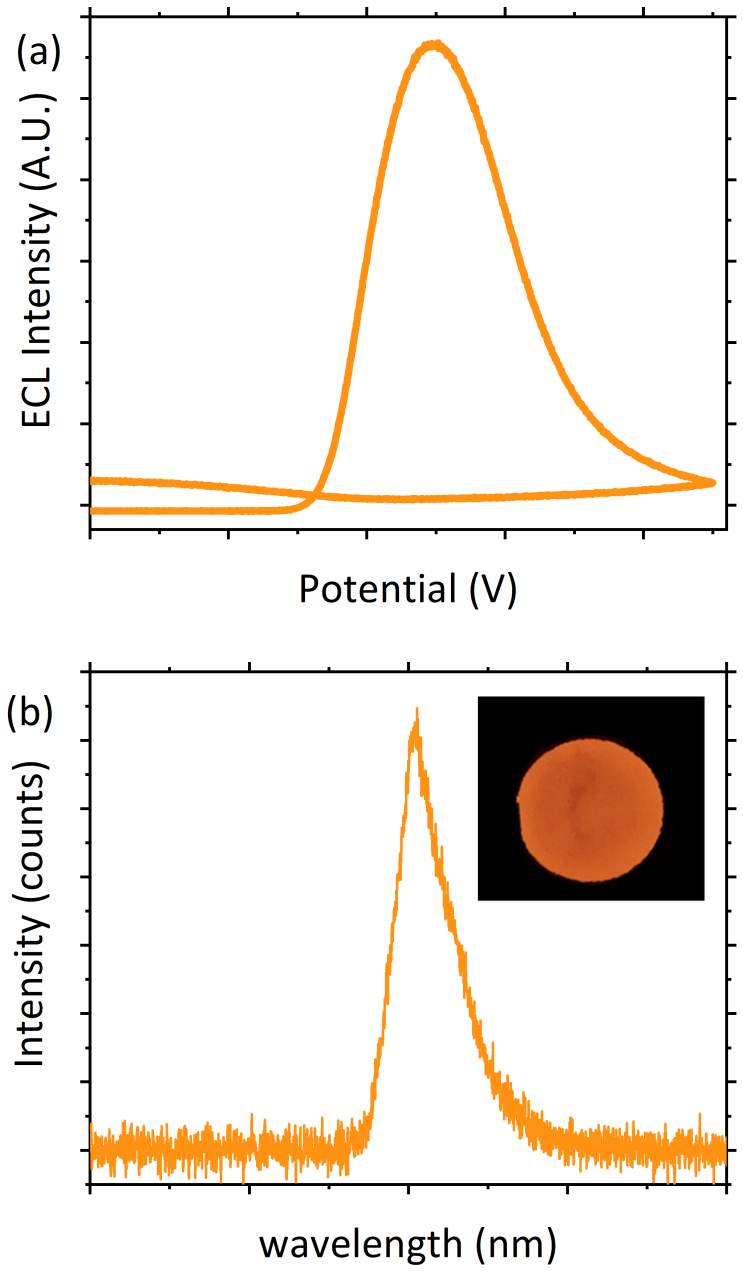

Figure 2.5: Typical resultant outputs from ECL analysis, through (a) photo-electronic detection via a PMT and (b) spectroscopic detection via a CCD with the inset showing emission recorded utilising a digital camera.

The intrinsic advantages of ECL over CL and spectroscopic techniques have seen its successful employment across a wide range of disciplines, including but not limited to clinical diagnostics, biological warfare agent detection, food and water testing and drug analysis.[10, 11, 14-16] ECL can be employed as both a standalone detection system as well as within hyphenated systems, such as HPLC or capillary electrophoresis, were it is primarily employed as an alternative detection system.[14, 15, 17-20] Offering fundamentally simplified instrumentation and increased operational simplicity through the unique removal of an external light source, facilitates compact and lightweight instrumentation avoiding any interference as a result of light scattering or luminescent impurities.[10, 21] One key advantage of ECL to note is the ability to electrochemically generate reactive species *in-situ.* The reactive intermediates or reagents typically required for CL can be extremely unstable, with their short life spans preventing analysis by traditional techniques.[10, 11] ECL electrochemically generates these unstable species at the electrode surface via the oxidation or reduction reactions prior to the production of luminescence. Hence through the electrochemical modification of reagents, reactive species previously unsuitable for CL can now be generated, hence expanding the potential application of ECL based systems over CL. The electrochemical regeneration of reactants, in particular the luminophore at the electrode surface allows for a single species to take part in several ECL cycles This generates a large number of photons during a singular measurement cycle, as such offering superb sensitivity with ranges down to sub-pico-molar possible.[11, 22, 23] As ECL is performed through the

application of a suitable potential to the working electrode surface, its offers control over the generation of the reactive intermediates and the excited states formed, gifting unprecedented control over selectivity and facilitating multi-analyte detection.[11] With the luminescence reaction electrochemically controlled, timing and positioning of the subsequent light emission can be manipulated. As ECL only occurs within the diffusion layer of the working electrode, the emission position and thus detector positioning can be easily controlled, ensuring the maximum number of photos produced are collected, hence improving sensitivity by maximising the signal to noise ratio. Furthermore, selectivity can be enhanced by exploiting detector positioning in combination with multiple working electrodes. Through a position sensitive detector multiple analytes within a sample can be easily detected, through the exploitation of the ability to control where emission occurs.[10, 11] Control over emission timing is another aspect which broadens the applications of ECL, ensuring any necessary reactions are completed prior to initiation of the luminescence mechanism, an aspect particularly important within biosensor fabrication.[10, 12, 21]

ECL can proceed through one of two mechanisms; ion annihilation or the co-reactant pathway. Each mechanism follows a separate pathway, however both involve heterogeneous electron transfer between the electrode and the electroactive species within the system, to produce the required intermediates.[10, 12]

2.2.1 Ion Annihilation

The ion annihilation or annihilation pathway was the primary method which initial ECL studies were based upon following its discovery in the 1960.[24, 25] Annihilation proceeds via the sequential production of both the oxidised and reduced forms of the luminophore species at the electrode surface. The potential is rapidly swept between the values where the luminophore is oxidised and reduced, to produce the anionic and cationic species required to produce luminescence. The annihilation pathway can be summarised by the general principles presented within Scheme 2.1 and can occur between radicals of the same species or within a mixed system, where the radical cations and anions are formed from different parent molecules. Typically, radical ions (for organic luminophores) or the oxidised and/or reduced forms of the parent complex (for inorganic luminophores) annihilate to produce an excited and ground state species.[9, 10, 23, 26] Upon relaxation of the excited state, luminescence is emitted. The luminophore (R) is oxidised, generating the radical cation ($R^{\bullet+}$) which represents a 'hole' in the HOMO of the luminophore, enhancing its oxidative properties. The potential is then switched to that required to generate the radical anion ($R^{\bullet-}$) which represents an unpaired electron within the LUMO of the luminophore, enhancing its reductive properties. The two radical ions then undergoing annihilation, producing an excited state species (R^*) and regeneration of the ground state luminophore R.[9, 10, 23, 26] This process can also occur in reverse, where the species is first reduced and then subsequently oxidised.

Scheme 2.1: General principles of the annihilation pathway

$R - e^- \longrightarrow R^{\bullet+}$	Oxidation at the electrode surface
$R + e^- \longrightarrow R^{\bullet-}$	Reduction at the electrode surface
$R^{\bullet+} + R^{\bullet-} \longrightarrow R + R^*$	Annihilation process leading to formation of excited state
$R^* \longrightarrow R + h\nu$	Emission of excess energy in the form of light

The annihilation process between the cationic and anionic species can proceed via two possible pathways; the thermodynamic pathway and the luminescence pathway.

2.2.1.1 Thermodynamic Pathway

The thermodynamically favourable pathway sees electron transfer occur between the LUMO of the reduced precursor and the HOMO of the oxidised precursor, resulting in the formation of two ground state species. However, the exponentially fast time scale over which electron transfer occurs results in the release of a large amount of energy over a significantly short time scale, which the system would be required to dissipate mechanically, typically through its vibrational modes. This would result in a disruption to the system and as such a kinetic manifestation of the Franck-Condon principle is observed. The Franck-Condon principle states that when a molecule undergoes an electronic transition the nuclear configuration, both in terms momenta and position, experiences no significant change since the mass of nuclei are significantly greater than the mass of an electron.[27] Thus, electron

transfer occurs on an exponentially faster time scale than the nuclei can respond.[27] As a consequence of this principle, the thermodynamically favourable pathway is no longer considered the preferential pathway for electron transfer between the oxidised and reduced precursor species. The probability of the production of an excited state alongside a ground state therefore, becomes the more favourable pathway due to the lower mechanical demand placed upon the system.[9-11, 23, 26]

2.2.1.2 The Luminescent Pathway

The luminescence pathway sees electron transitions occur from the LUMO of the reduced precursor ($R^{\bullet -}$) to the LUMO of the oxidised precursor ($R^{\bullet +}$), which is observed at a slightly lower energy as shown within Figure 2.6. This leads to the generation of a ground state species (R) alongside an excited state species (R*). The luminescence pathway, although thermodynamically less favourable, becomes the more probable transition, as a result of less energy requiring dissipation through the vibrational modes, less mechanical stress is therefore placed upon the system. As such, with electron transfer occurring at a rate exponentially quicker than nuclei rearrangement, this becomes the kinetically favoured route, hence satisfying the kinetic manifestation of the Franck-Condon principle.[9-11, 23, 26, 27]

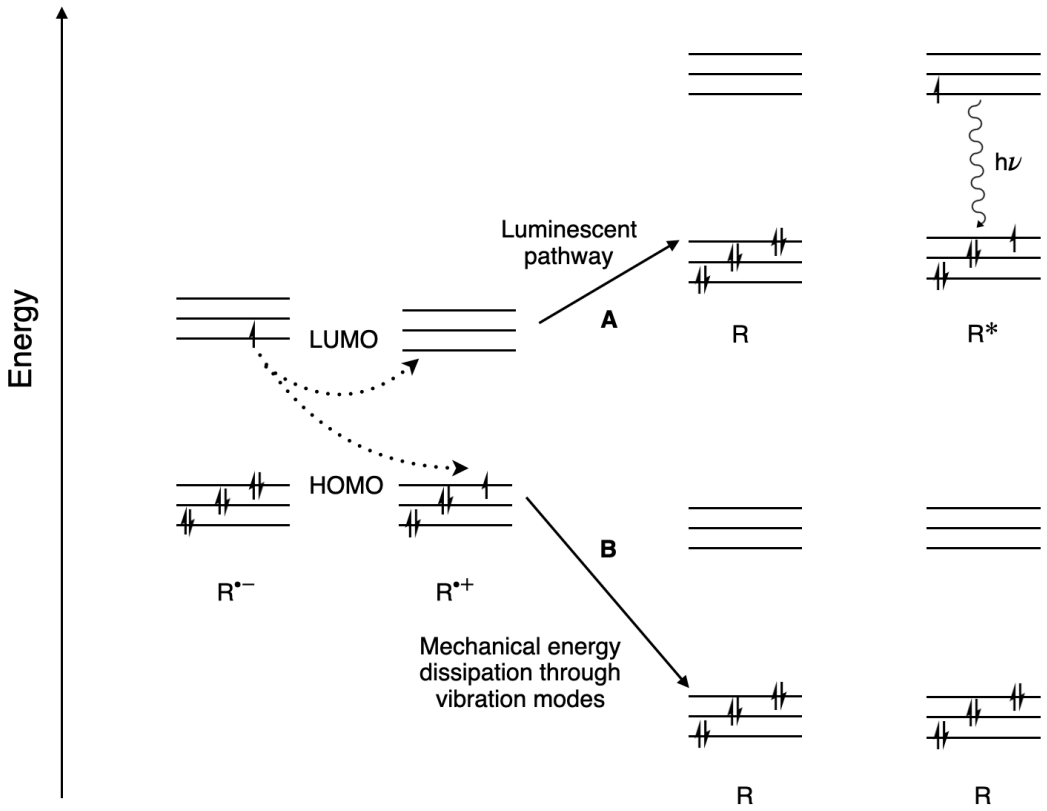

Figure 2.6: Molecular orbital diagram depicting the two alternative pathways which electron transfer can occur between the reduced ($R^{\bullet -}$) and oxidised ($R^{\bullet +}$) precursors. (A) luminescent pathway forming an excited state and ground state species, from which emission is observed and (B) thermodynamic pathway, leading to the formation of two ground state species.

The annihilation of the two radical ions to form the excited state R* can further follow various energetic pathways dependent upon the energy of the system. The route followed is determined by the systems energy and can be typically categorised as the singlet route (S-route) or the triplet-triplet annihilation route (T-route), although the E-route, forming an excimer or exciplex, and ST-route (singlet-triplet route) can also be observed. Figure 2.7 summarises the energy transfer processes of the S-route and T-route by which ECL emission can occur within the annihilation pathway.[10, 11, 23, 26]

The route taken to form the excited state is dictated through the energetics of the homogenous electron transfer reactions and the energy of the excited state. The singlet route is observed when the system is seen to be energy sufficient, here the single excited state ($^1R^*$) is directly formed. However, if the system is energy deficient then the triplet state ($^3R^*$) is formed instead. The annihilation enthalpy is directly related to the energy available to form the excited state and can be determined through equation (2.8), where $-\Delta H_{ann}$ is the annihilation enthalpy, Ep is the peak potential for the electrochemical redox reactions and the constant, 0.16, includes the entropy approximation term ($T\Delta S$) at 25 ^oC, which includes 0.057 eV, accounting for the peak separation for a reversible redox couple for a one electron transfer reaction.[10, 11, 23, 26]

$$-\Delta H_{ann} = E_p(R/R^{\bullet+}) - E_p(R/R^{\bullet-}) - 0.16 \qquad \text{(equation 2.8)}$$

If the annihilation enthalpy is greater than the energy required to form the lowest energy singlet excited state from its ground state then this will directly form via the S-route. Singlet states reside at energies higher than the triplet states and therefore the system requires sufficient energy to promote an electron from the ground state singlet to the first excited state singlet.[10, 11, 23, 26]

If the annihilation enthalpy is less than the energy required to form the lowest energy singlet state but greater than the energy of the triplet state then triplet-triplet annihilation proceeds. Here the system is considered to be energy deficient and thus the singlet excited state cannot be directly formed. Instead, the triplet state is initially formed, which subsequently undergoes further annihilation with a second triplet state, forming a ground and excited singlet state from which emission subsequently occurs. Direct emission from the relaxation of the triplet state is not considered the main mechanism by which T-route ECL occurs, with relaxation from triplet to singlet states a forbidden process. Hence the lifespan of a triplet state is sufficiently greater than that of a singlet state. As such, the triplet state is susceptible to quenching from other species, such as molecular oxygen, present within the system resulting in non-radiative relaxation.[10, 11, 23, 26]

In addition to the S and T-routes, ST and E-routes can also proceed to generate the required excited state. The ST-route is observed when the annihilation entropy is almost indistinguishable from the energy required to

form the lowest excited singlet state. Here the formation of the triplet state $^3R^*$ contributes to the formation of the excited singlet state $^1R^*$ from which emission then occurs.[10] The E-route is observed due to the formation of excited dimers (excimers) or excited complexes (exciplexes), where the complex itself is responsible for the observed emission. These form due to the combination of radical ions, where there is π-orbital overlap. Hence this process is commonly seen in polycyclic aromatic hydrocarbons. E-route emission is seen to be broad, featureless and lower in energy than singlet emission.[10, 26]

The annihilation pathway was the major route adopted during the initial development of ECL, largely owing to its simplicity. Annihilation only requires the presence of an electrolyte, solvent and the ECL species with light generation controlled through potential changes, making the system simplistic and low cost. However, annihilation ECL is restricted to organic solvents, such as acetonitrile. Aqueous solvents are incompatible with annihilation due to the limited potential window preventing both the oxidation and reduction of the luminophore species being achieved.[9, 10, 26]

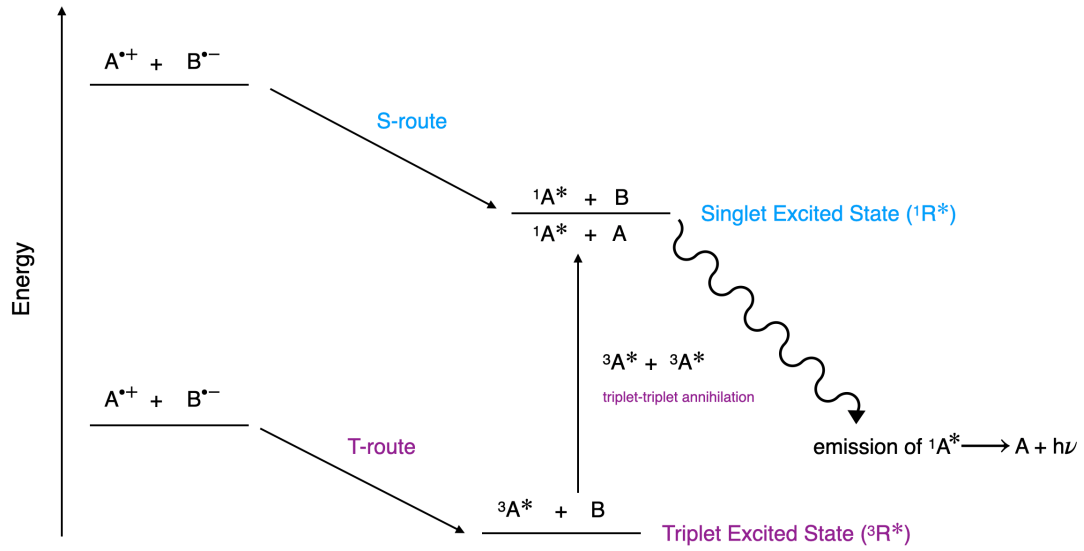

Figure 2.7: Schematic detailing the two primary annihilation routes leading to the formation of the excited state prior to emission. The S-route, is the singlet route seen when the system is energy sufficient and the T-route, is the triplet-triplet annihilation route seen when the system is energy deficient.

2.2.2 Co-reactant Pathway

The co-reactant pathway is now the most commonly employed ECL system.[9, 21, 23, 28] Unlike annihilation, which can be performed using only a singular species, the co-reactant pathway requires two species, with emission occurring due to the interaction between a luminophore and a second species referred to as the co-reactant. Rather than sweeping the potential, a sufficiently cathodic or anodic potential is applied to either oxidise or reduce the species. The radical ions, and resultant intermediates formed from these oxidation or reduction reactions produce the excited state species, which upon relaxation emit the characteristic wavelength of light observed.[9-11, 16, 26] As the co-reactant system only requires the species to be

oxidised or reduced in a single potential step, in contrast to annihilation, it can be performed over smaller potential windows and hence is compatible with aqueous systems. A important property largely responsible for the expansion of ECL applications, particularly within the biomedical field.[10, 21] There are two pathways which co-reactant ECL can occur via; oxidative-reduction or reductive-oxidation, the mechanisms of which are summarised in Scheme 2.2.

The oxidative-reduction pathway proceeds from the application of an anodic potential, resulting in the oxidation of the luminophore and co-reactant, where the co-reactant can either be directly oxidised at the electrode or through mediated oxidation. Mediated oxidation is observed when the co-reactant cannot be oxidised directly via heterogeneous electron transfer from the electroactive species to the electrode. Instead homogenous electron transfer between the oxidised luminophore and the co-reactant is more favourable. As such, mediated oxidation will preferentially proceed. The co-reactant radical ions formed via these oxidation process, then rapidly decompose producing a species with high reductive power. Reactions between this highly reductive species and the oxidised luminophore produce the excited state, which is responsible for the observed emission. This emission process typically results in the reformation of the luminophore, allowing for it to proceed in further ECL reactions, hence gifting the technique its enhanced sensitivity.[9-11, 16, 26]

The reductive-oxidation pathway follows the same basic principles as the oxidative-reduction mechanism, where a cathodic potential is applied, resulting in the reduction of the luminophore and co-reactant either directly or via mediated reduction. The radicals produced then decompose, here forming highly oxidative species, which then react with the reduced luminophore to produce the excited state responsible for the observed emission.[9-11, 16, 26]

The formation of the excited state for both mechanistic pathways can instead proceed via ion annihilation. This occurs between the oxidised or reduced luminophore, formed via heterogenous electron transfer to or from the electrode, and a secondary reduced or oxidise luminophore species formed via the homogeneous electron transfer between the luminophore and the highly reductive or oxidative species formed via the co-reactant radical decomposition.[10]

In order for co-reactant ECL to proceed, the co-reactant must meet a number of criteria. These include, good solubility and stability within a wide range of solvents, exhibit fast electron transfer kinetics, display limited or no ECL emission themselves and do not interfere or quench the ECL response of the luminophore itself.[23, 26] Utilisation of the co-reactant pathway often addresses some of the limitations faced by annihilation systems. Of particular note is the ability of co-reactant ECL to be used for the analysis of species which undergo irreversible oxidation or reduction or where the oxidised or reduced

species are not stable enough to undergo the annihilation mechanism.[10] What's more, the oxidative-reduction pathway allows for the prevention of molecular oxygen quenching, increasing the ECL signal obtained, ultimately increasing sensitivity. While the proportional nature of ECL intensity with co-reactant or luminophore concentration, allows for direct quantitative analysis of the co-reactant or a luminophore tagged species.[23, 26] However, in contrast to the annihilation mechanism, only the luminophore is typically regenerated whilst the co-reactant is consumed. As such the number of measurement cycles that can be performed upon a single sample are limited.[10]

Scheme 2.2: General mechanism for the oxidative-reduction and reductive-oxidation co-reactant ECL systems

Reaction Process	Oxidative-reduction	Reductive-oxidation
Redox reactions	$R - e^- \rightarrow R^{\bullet +}$ $C - e^- \rightarrow C^{\bullet +}$	$R + e^- \rightarrow R^{\bullet -}$ $C + e^- \rightarrow R^{\bullet -}$
Mediated redox processes	$R^{\bullet +} + C \rightarrow R + C^{\bullet +}$	$R^{\bullet -} + C \rightarrow R + C^{\bullet -}$
Homogenous chemical reactions	$C^{\bullet +} \rightarrow C_{red}$ $C_{red} + R \rightarrow R^{\bullet -} + P$	$C^{\bullet -} \rightarrow C_{ox}$ $C_{ox} + R \rightarrow R^{\bullet +} + P$
Excited state formation	$R^{\bullet +} + R^{\bullet -} \rightarrow R + R^*$ or $R^{\bullet +} + C_{red} \rightarrow R^* + P$	$R^{\bullet +} + R^{\bullet -} \rightarrow R + R^*$ or $R^{\bullet -} + C_{rox} \rightarrow R^* + P$
Light emission	$R^* \rightarrow R + h\nu$	$R^* \rightarrow R + h\nu$

Key:
R = luminophore, C = co-reactant, C_{red} = highly reducing co-reactant intermediate, C_{ox} = highly oxidising intermediate, P = product associated with co-reactant intermediate reactions

2.3 References

1. P. T. Kissinger and W. R. Heineman, *J. Chem. Ed.*, 1983, **60**, 702.
2. G. A. Mabbott, *J. Chem. Ed.*, 1983, **60**, 697.
3. D. A. Brownson and C. E. Banks, in *The handbook of graphene electrochemistry*, Springer, London, 2014, ch. 2, pp. 23-77.
4. N. Elgrishi, K. J. Rountree, B. D. McCarthy, E. S. Rountree, T. T. Eisenhart and J. L. Dempsey, *J. Chem. Ed.*, 2017, DOI: 10.1021/acs.jchemed.7b00361.
5. A. J. Bard, L. R. Faulkner, J. Leddy and C. G. Zoski, *Electrochemical methods: fundamentals and applications*, wiley New York, 1980.
6. A. L. Eckermann, D. J. Feld, J. A. Shaw and T. J. Meade, *Coord. Chem. Rev.*, 2010, **254**, 1769-1802.
7. A. R. Eckert, J.-S. Hsiao and S. E. Webber, *J. Phys. Chem.*, 1994, **98**, 12025-12031.
8. A. J. Bard, L. R. Faulkner, J. Leddy and C. G. Zoski, in *Electrochemical methods: fundamentals and applications*, wiley New York, New York, 1980, vol. 2, ch. 18, pp. 736 - 766.
9. M. M. Richter, *Chem. Rev.*, 2004, **104**, 3003-3036.
10. W. Miao, *Chem. Rev.*, 2008, **108**, 2506-2553.
11. L. Hu and G. Xu, *Chem. Soc. Rev.*, 2010, **39**, 3275-3304.
12. S. Parveen, M. S. Aslam, L. Hu and G. Xu, in Electrogenerated chemiluminescence: protocols and applications, Springer, New York, 2013, ch. 1, pp. 1-10.
13. W. J. Abbey, R. Bhartia, L. W. Beegle, L. DeFlores, V. Paez, K. Sijapati, S. Sijapati, K. Williford, M. Tuite, W. Hug and R. Reid, *Icarus*, 2017, **290**, 201-214.
14. X.-Y. Yang, C.-Y. Xu, B.-Q. Yuan and T.-Y. You, *Chin. J. Anal. Chem.*, 2011, **39**, 1233-1237.
15. A. Zhang, C. Miao, H. Shi, H. Xiang, C. Huang and N. Jia, *Sens. Actuators B*, 2016, **222**, 433-439.
16. M. Rizwan, N. Mohd-Naim and M. Ahmed, *Sensors*, 2018, **18**, 166.
17. Y. Gao, Y. Tian and E. Wang, *Anal. Chim. Acta*, 2005, **545**, 137-141.
18. L. Jianguo, C. Yuan and J. Huangxian, *Electroanalysis*, 2007, **19**, 1569-1574.
19. B. Yuan, C. Zheng, H. Teng and T. You, *J. Chromatogr. A*, 2010, **1217**, 171-174.
20. O. Ramdani, J. P. Metters, L. C. S. Figueiredo-Filho, O. Fatibello-Filho and C. E. Banks, *Analyst*, 2013, **138**, 1053-1059.
21. C. K. P. Truong, T. D. D. Nguyen and I.-S. Shin, *BioChip J.*, 2019, **13**, 203-216.
22. N. J. Kearney, C. E. Hall, R. A. Jewsbury and S. G. Timmis, *Anal. Commun.*, 1996, **33**, 269-270.
23. R. Pyati and M. M. Richter, Annual Reports Section "C" (Physical Chemistry), 2007, **103**, 12-78.
24. D. M. Hercules, *Science*, 1964, **145**, 808-809.
25. K. S. V. Santhanam and A. J. Bard, *J. Am. Chem. Soc.*, 1965, **87**, 139-140.
26. S. Parveen, M. S. Aslam, L. Hu and G. Xu, in Electrogenerated chemiluminescence: protocols and applications, Springer, New York, 2013, ch. 2, pp. 15-28.
27. J. Tellinghuisen, Berlin, Heidelberg, 1987.
28. Z. Liu, W. Qi and G. Xu, *Chem. Soc. Rev.*, 2015, **44**, 3117-3142.

CHAPTER THREE

CHARACTERISATION OF METAL ELECTROCHEMILUMINOPHORES

“The way to get started is to quit talking and begin doing”

Walt Disney

3.1 Introduction

The electrochemical and optical properties of the metal luminophores utilised for ECL reactions can be interrogated to provide an insight into their electronic and structural properties. Understanding such properties of the metal luminophores required for ECL production can enhance our understanding of the ECL pathways responsible for the observed luminescence, in addition to their behaviour within an electrochemical environment.

The ruthenium (II) polypyridine complexes such as $[Ru(bpy)_3]^{2+}$, utilised throughout this body of work, have been almost exclusively employed for the production of ECL since it was first reported in 1972.[1] This orange luminophore is largely unmatched, producing high quantum yields within a range of solvent system, characteristics attributed to its extensive use over the past four decades.[2, 3] Surface modification, particularly through polymer films increases the electrochemical response of the redox active species at the electrode surface.[4] Polymer films allow for the creation of a multilayer deposition, enhancing the electrochemical response of a species with the movement of electrons between the electrode and the electroactive species proceeding via diffusion.[4] Nafion, a cation exchange polymer first reported by Rubinstein and Bard[5] in 1980, is still utilised today owing to its strong chemical resistance and biocompatibility.[5-7] Incorporation of charged species, such as the ruthenium complex used here, occur with ease due to the electrostatic interactions between the cationic $[Ru(bpy)_3]^{2+}$ and the anionic

sultanate groups within the Nafion polymer.[5-7] The polymer film containing the electroactive species can then be easily deposited upon the electrode surface.

The main objective of this chapter was to establish the electrochemical and spectroscopic properties of the surface modified electrode. A range of electrochemical measurements were performed to determine these characteristics such as the FWHM and diffusion coefficients. These values were then compared to the ideal values expected to evaluate the fabrication of the sensor.

3.2 Experimental

3.2.1 Materials

Tris (2,2′-bipyridyl)-dichlororuthenium(II) hexahydrate ($[Ru(bpy)_3]^{2+}].Cl_2.6H_2O$), lithium perchlorate ($LiClO_4$) and Nafion 117 (~ 5% mixture of lower aliphatic alcohols and water) were purchased from Sigma-Aldrich. Absolute ethanol (EtOH), acetonitrile (ACN) and methanol were purchased from VWR. All chemicals were used as received and all solutions were prepared in Milli-Q water (18 mΩ cm^{-1}).

3.2.2 Instrumentation

A CH instrument model 760D electrochemical analyser was used for all electrochemical and electrochemiluminescence measurements. GSI Technologies Electrochemical carbon screen-printed electrodes (SPE) with a 4 mm carbon working electrode, carbon counter electrode, and Ag quasi-reference electrode were used for all electrochemical measurements with a 100 µL sample volume. All electrochemical measurements were performed across a potential range of 0.5 to 1.3 V vs Ag, with a scan rate of 100 mV s^{-1}, and a sampling interval of 0.001 V. ECL emission was recorded via a Hamamatsu H10723-20 photomultiplier tube (PMT) enclosed within a light-tight Faraday cage. The PMT was positioned directly above the working electrode surface through the use of a specially designed sensor holder.

Ultraviolet (UV)-visible spectroscopy was performed in 50:50 ACN:H_2O at a concentration of 12.5 μM. Measurements were performed in a 1 cm path

length quartz cuvette and collected with a Cary 300 Bio UV/Vis spectrophotometer. Emission spectra were collected with a Cary Eclipse fluorescence spectrometer. Measurements were performed in a 1 cm quartz cuvette at a concentration of 0.5 mM in 50:50 (v/v) ACN:H_2O for room temperature spectra and at 5 μM in 4:1 (v/v) EtOH:MeOH for low temperature spectra. Low temperature spectra were collected using a custom-made quartz sample holder and cooled to 85 K using a OptistatDN Variable Temperature Liquid Nitrogen Cryostat.

3.2.3 Fabrication of $[Ru(bpy)_3]^{2+}$/Nafion ECL Sensor

The $[Ru(bpy)_3]^{2+}$/Nafion film was fabricated by the following procedure: 1 mM $[Ru(bpy)_3]^{2+}$ was prepared in 50:50 (v/v) EtOH:H_2O. A total of 5% w/v Nafion was diluted to a concentration of 0.4% w/v with 50:50 (v/v) EtOH:H_2O. To prepare a final film concentration of 0.5 mM $[Ru(bpy)_3]^{2+}$ in 0.2% w/v the above solutions were mixed in a 1:1 (v/v) ratio. Once prepared the film was stored at 4^{o}C. When required 7 μL of the film was drop cast onto the carbon working electrode and air-dried under darkness for two hours.This fabrication procedure was used throughout subsequent chapters.

3.3 Results and Discussion

3.3.1 Optical Properties

The UV-visible spectra of the $[Ru(bpy)_3]^{2+}$ complex demonstrated the expected trends for a $[Ru(N)_6]^{2+}$ coordination sphere, where N represents a ligand species, with the UV-visible spectra obtained consistent with those previously reported for $[Ru(bpy)_3]^{2+}$, refer to Figure 3.1.[8-13] The absorption bands at 450 and 420 nm can be assigned to the metal-to-ligand charge transfer (MLCT) between the t_{2g} d-orbitals on the ruthenium metal centre to the anti-bonding π^* orbital on the bipyridine ligand.[8-10, 12] The d-d transitions responsible for the complexes orange colouration are observed in the weak bands around 325 to 350 nm (highlighted in the inset of Figure 3.1 for clarity).[8-10, 12] The intense bands observed between 244 to 285 nm are the result of the π to π^* transitions associated with the bipyridine ligands.[8-10, 12]

The emission spectra of the ruthenium complex further confirms the complexes $[Ru(N)_6]^{2+}$ coordination sphere. Figure 3.2 shows the corrected photoluminescence spectra obtained for the complex at room temperature (293 K) and at 85 K. The emission spectra at room temperature gave the expected emission maximum at ~ 614 nm corresponding to emission from the triplet MLCT excited state, relaxing back to ground.[11, 13] At these higher temperatures the low lying triplet MLCT states behave as a single state due to sufficient thermal population producing one board emission. In contrast, the low temperature spectra reveal the vibrational fine structure of the complex, which is lost at higher temperatures as a result of thermal

broadening. The emission peaks observed within the low temperature spectra are consistent with prior literature for this complex.[9, 11-15] The fine vibrational structure observed can be assigned to the three closely spaced excited states with luminescence occurring from the ^{3}MLCT transitions.[9, 12, 14, 15] The emission maxima obtain at 85 K displays a characteristic blue shift. This shift has been previously reported and is associated with the rigidity of surrounding media at these low temperatures preventing the Franck-Condon excited state from completely relaxing within its emission lifetime.[9] As a result emission occurs from a higher energy level than when in solution.[9] All spectroscopic data obtained for $[Ru(bpy)_3]^{2+}$ is summarised in Table 3.1 alongside comparative literature values for the reported properties.

Table 3.1: Spectroscopic data for $[Ru(bpy)_3]^{2+}$ complex used in sensor fabrication

Absorbance[a] λ_{max} (nm)	Emission[b] λ_{max} (nm) (293 K)	Emission[b] λ_{max} (nm) (85 K)
285, 450	614	581
451[11]	618[11]	-
286, 450[13]	622[13]	581[13]

[a] measured in 50:50 (v/v) ACN:H_2O
[b] measured in 4:1 (v/v) EtOH:MeOH

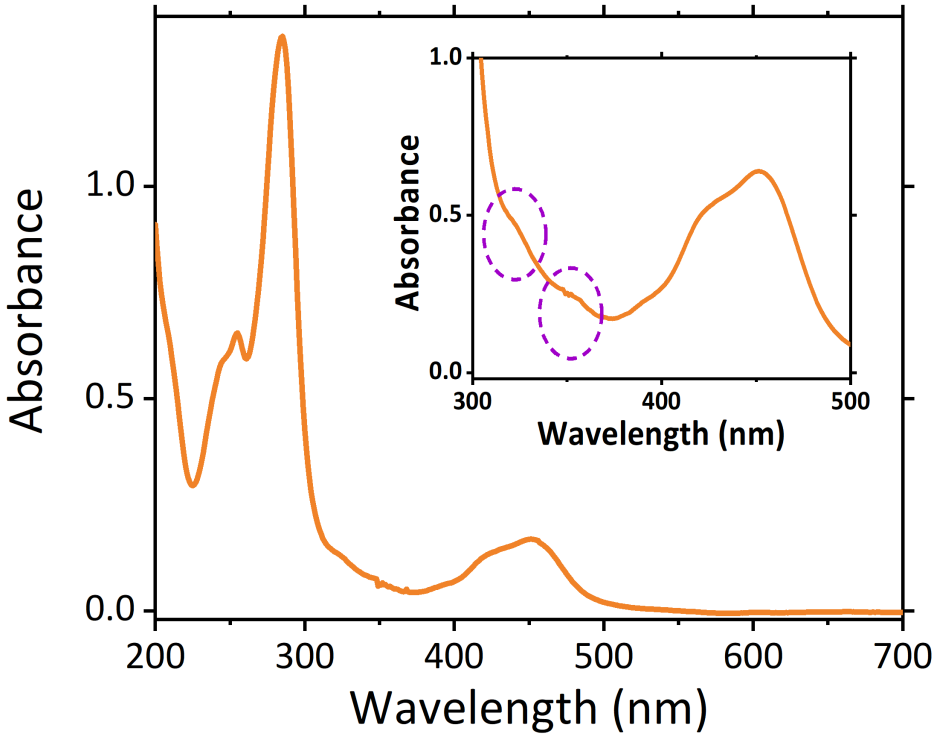

Figure 3.1: UV-visible absorbance spectra of 12.5 μM $[Ru(bpy)_3]^{2+}$ dissolved in 50:50 (v/v) ACN:H_2O recorded at room temperature. Inset highlights the weak bands at 325 and 350 nm with a 0.5 mM $[Ru(bpy)_3]^{2+}$ sample.

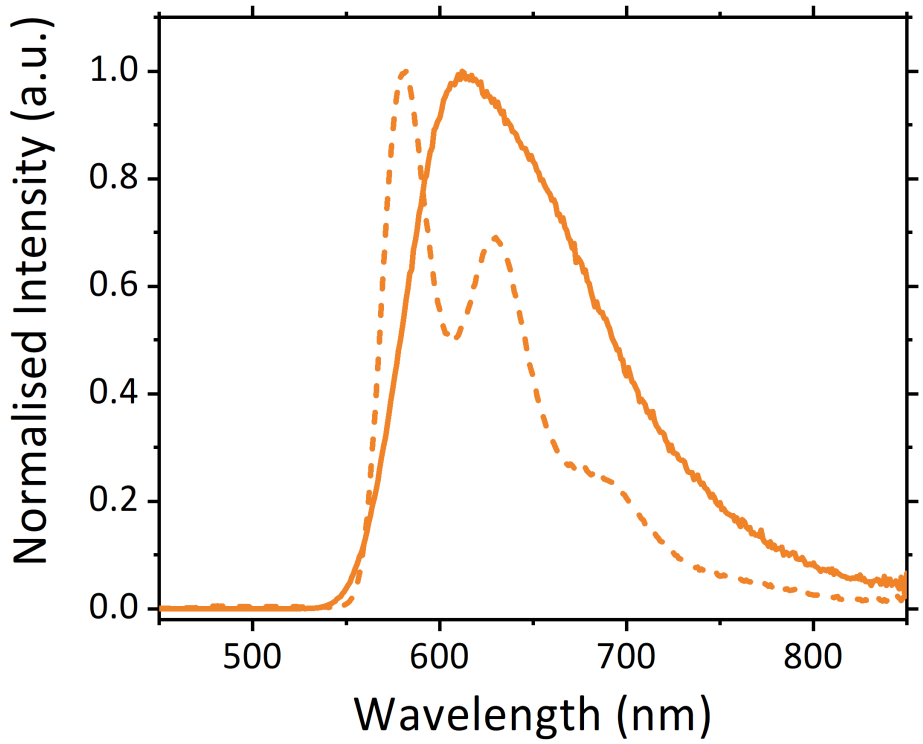

Figure 3.2: Normalised and corrected emission spectra of 5 μM $[Ru(bpy)_3]^{2+}$ dissolved in 4:1 (v/v) EtOH:MeOH with λ_{ex} of 290 nm at 293 K (solid) and 85 K (dashed).

Given the excellent correlation of the obtained spectroscopic data with those previously reported[8-15], confidence that the ruthenium complex chosen for sensor fabrication would behave as expected offering a reliable and sensitive ECL luminophore was achieved.

3.3.2 Electrochemical Properties

The electrochemical properties of the ruthenium complex were investigated for the most part when confined within Nafion, as this represents the conditions under which the complex would be utilised. To ensure the behaviour of the complex was not altered when $[Ru(bpy)_3]^{2+}$ was encapsulated within the cation exchange polymer, voltammograms were obtained within a solution, with 0.1 M NaCl as the supporting electrolyte and compared to the behaviour observed for the surface bound $[Ru(bpy)_3]^{2+}$. The typical CV's shown in Figure 3.3, display the expected anodic and cathodic peaks of the $Ru^{2+/3+}$ redox couple at +1.06 and +0.95 V vs Ag when confined to the electrode surface and +1.02 and +0.95 V vs Ag when in solution. Comparison of the redox potentials of the $Ru^{2+/3+}$ couple revealed that encapsulation of the ruthenium complex within the film does not negatively impact upon its redox behaviour. This is further confirmed through a comparison of the $E_{1/2}$ values of 0.99 V and 1.01 V for the complex within a solution-based system and Nafion, respectively.

Confident that encapsulation of the $[Ru(bpy)_3]^{2+}$ within the cation-exchange polymer does not negatively impact upon the redox characteristics of the luminophore, all further characterisation was performed with the luminophore bound to the working electrode surface.

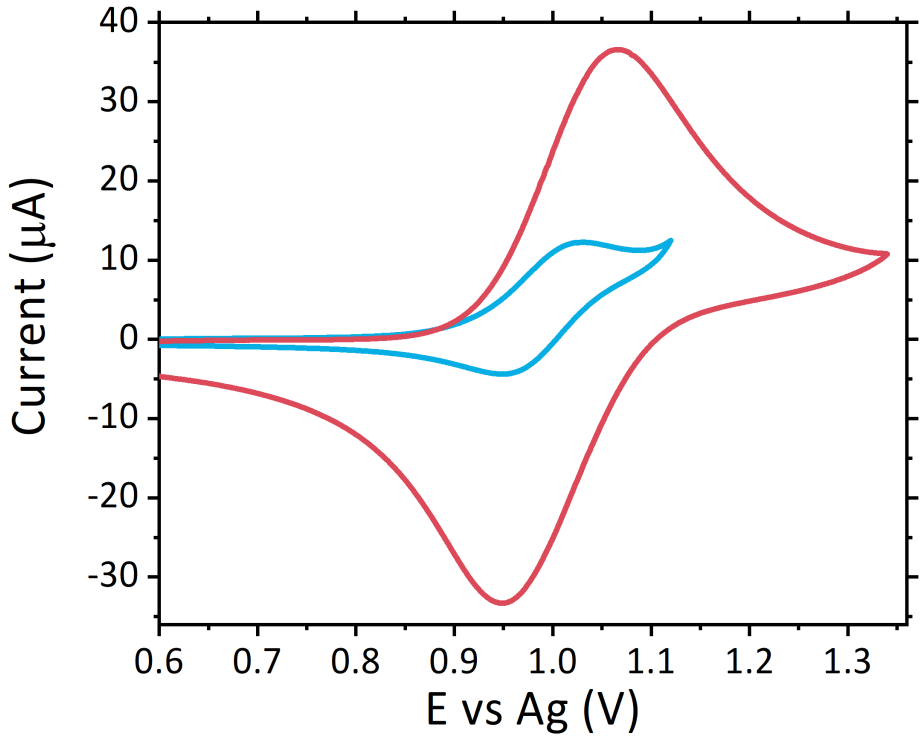

Figure 3.3: Typical CV's obtained for 0.5 mM $[Ru(bpy)_3]^{2+}$ within solution (blue) and confined to the electrode surface via the Nafion polymer (pink) with 0.1 M NaCl as the supporting electrolyte, at a scan rate of 100 mV s^{-1} on the 4 mm carbon working screen printed electrodes.

Figure 3.4 displays the typical voltammograms obtained for the ruthenium-modified electrodes with 0.1 M $LiClO_4$ as the supporting electrolyte across multiple scan rates. At sufficiently slow scan rates the peak-to-peak separation (ΔE_p), is close to zero, with the full width half-maximum (FWHM) close to the theoretical value of 90.6 mV for a one electron process of a surface-confined species.[16, 17] The broad non-gaussian peaks, nonzero ΔE_p and departure from the theoretical FWHM value for a one electron process highlights deviation from the ideal behaviour of surface confined species at higher scan rates. This behaviour is instead consistent with a system under semi-infinite diffusion control, rather than the typical finite diffusion behaviour observed for surface confined species. This however was not unexpected and has been previously reported for Nafion encapsulated $[Ru(bpy)_3]^{2+}$, with this semi-infinite diffusion behaviour attributed to the cluster-type structure of Nafion and slow mass transport through the film, accounting for the large ΔE_p values.[5, 18, 19] Semi-infinite diffusion was further established by the linear relationship observed for peak current against the square root of the scan rate, as shown by the Randles-Sevcik plot within the inset of Figure 3.4. In addition to this as the scan rate was increased, a subsequent increase in the peak-to-peak separation was observed, a characteristic intrinsic to freely diffusing species under semi-infinite diffusion control rather than surface bound species, where the peak-to-peak separation remains constant at approximately zero mV across all scan rates.[20] The kinetics of the forward and reverse reactions of the redox couple are assessed through the ratio of i_{pa}/i_{pc}. For a system, under electrochemical ideality, the ratio of i_{pa}/i_{pc} should

be at unity.[20] For all scan rates interrogated the $i_{pa}/i_{pc} \approx 1$, hence the sensor is seen to be operating under almost ideality, with the electrochemical reversibility of the sensor facilitating its reusability.

To investigate the variation intrinsic to sensor manufacture a number of characteristics within the voltammograms were interrogated across six measurements with the electrolyte solution. Comparison of the %RSD values across the E_{pa}, E_{pc}, I_{pa} and I_{pc} values revealed variations were observed with %RSD values for E_{pa} and E_{pc} of 1.6% and 1.5%. While more significant variations were observed within the anodic and cathodic peak currents at 3.2% and 5.0% respectively. Variation during sensor manufacturing is not entirely surprising given the drop casting methodology employed. Such methods likely lead to small inconsistencies within film thickness and working electrode coverage. Such inconsistencies likely account for the larger variations observed within the anodic and cathodic peak currents, where mass transport to the electrode surface is a major contributing factor within the obtained values. Variations in electrode manufacturer intrinsic to the screen printing process will also contribute to this variation, although primarily toward the potentials observed. Although variations are present within the sensor fabrication, these are within the typical accepted values within standard analytical methods and as such would not negatively impact sensor performance to a significant degree.

In addition to providing information on whether the analyte remains freely diffusing in solution, the Randles-Sevcik plots can also be used to determine the rate of charge transfer through the film leading to the conversion of the $Ru^{2+/3+}$ couple. The charge transfer coefficient (D_{CT}) describes the movement of charge through the film for systems under semi-infinite diffusion control, such as the sensor described herein. D_{CT} can be calculated from known parameters and those obtained from the Randles-Sevcik plots using equation 3.1. The D_{CT} values calculated further confirm the system is operating under semi-infinite diffusion control with the determined values in good agreement with those values previously reported for this system type.[17, 21]

$$D = \frac{(ip)^2 RT}{(0.4463 n C_0 A F)^2 n F v} = \left(\frac{slope}{0.4463 n F A C_0} \right)^2 \frac{RT}{nF} \quad \text{(equation 3.1)}$$

Table 3.2 contains a summary of the electrochemical properties of the surface confined $[Ru(bpy)_3]^{2+}$. The values reported, correspond to the voltammograms collected with a scan rate of 100 mV s^{-1}. The focus was placed upon this scan rate as it represents the scan rate which will be employed for all future measurements for analyte detection.

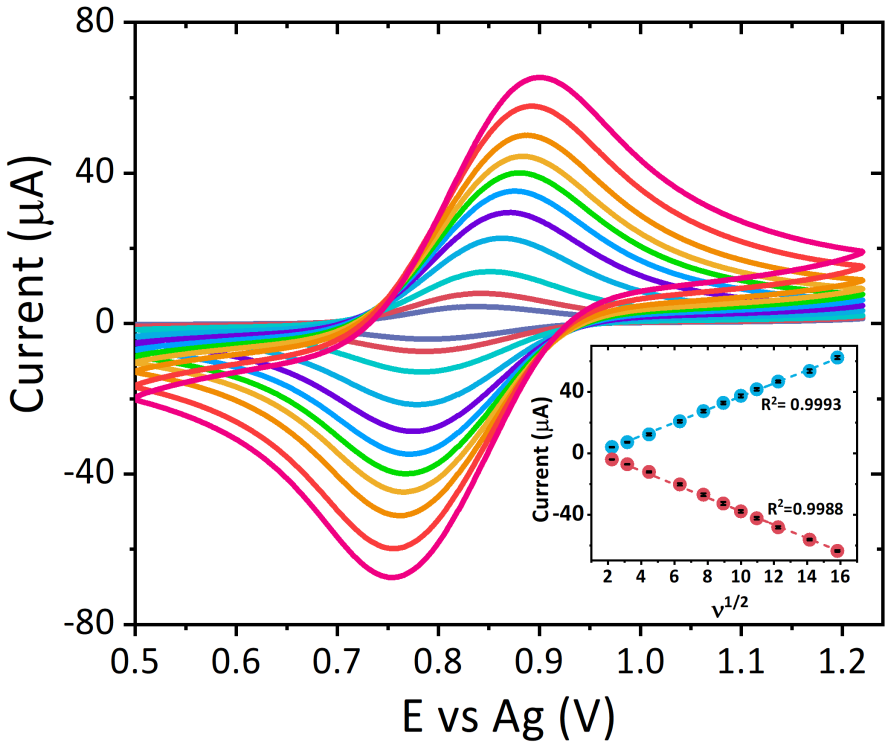

Figure 3.4: CV's showing the $Ru^{2+/3+}$ couple, for $[Ru(bpy)_3]^{2+}$-Nafion surface modified electrodes across a scan rate range of 5 to 250 mV s^{-1} in 0.1 M $LiClO_4$ over a potential range of 0.5 ≤ E ≤ 1.22 V vs Ag. Inset shows the linear dependance of current against $\boldsymbol{\nu}^{1/2}$.

Table 3.2: Electrochemical data for electrodes modified with $[Ru(bpy)_3]^{2+}$-Nafion film used in sensor fabrication at a scan rate of 100 mV s^{-1} with 0.1 M $LiClO_4$ as the supporting electrolyte.

E_{ox} vs Ag (V)	E_{red} vs Ag (V)	$E_{1/2}$ (V)	ΔE_p (mV)	D_{CT} Anodic (10^8 cm^2 s^{-1})	D_{CT} Cathodic (10^8 cm^2 s^{-1})	Ip_a/Ip_c
0.88	0.78	0.83	100	6.40	6.75	0.99

3.4 Conclusion

Electrochemical and optical characterisation of the ruthenium luminophore was performed and the results compared with the behaviour previously reported for this luminophore. Good agreement was observed for both the spectroscopic and electrochemical properties with those expected from prior literature. As such there was confidence that the use of this luminophore for sensor fabrication would provide a reliable ECL sensor.

The electrochemical properties of the $[Ru(bpy)_3]^{2+}$ were assessed both within the traditional solution-based system and when encapsulated within the film, and demonstrated that encapsulation of the luminophore within the cation exchange polymer did not negatively impact upon its redox behaviour. As such electrode modification with Nafion would provide a suitable methodology for binding of the redox centre to the electrode surface. The electrochemical and spectroscopic properties of the luminophore demonstrated its suitability for use within the sensor design. Fabrication of the sensor with $[Ru(bpy)_3]^{2+}$ encapsulated within cation exchange polymer Nafion produced a sensor that displayed almost ideal electrochemical behaviour. Efficient regeneration of the Ru^{2+} species makes this design ideal for ECL based sensors, where high intensity and hence sensitivity can be obtained due to regeneration of the electroactive luminophore species producing a large number of photons per measurement cycle. Furthermore, efficient regeneration of the redox centre provides a multi-use sensor which is both cost effective and minimises reagent consumption.

3.5 References

1. N. E. Tokel and A. J. Bard, Journal of the American Chemical Society, 1972, **94**, 2862-2863.
2. M. M. Richter, *Chemical Reviews*, 2004, **104**, 3003-3036.
3. Z. Liu, W. Qi and G. Xu, *Chemical Society Reviews*, 2015, **44**, 3117-3142.
4. C. M. A. Brett and A. M. C. F. O. Brett, in *Surface Engineering: Surface Modification of Materials*, eds. R. Kossowsky and S. C. Singhal, Springer Netherlands, Dordrecht, 1984, DOI: 10.1007/978-94-009-6216-3_42, pp. 656-664.
5. I. Rubinstein and A. J. Bard, Journal of the American Chemical Society, 1980, **102**, 6641-6642.
6. Z. Guo and S. Dong, *Anal. Chem.*, 2004, **76**, 2683-2688.
7. P. Bertoncello, L. Dennany, R. J. Forster and P. R. Unwin, *Anal. Chem.*, 2007, **79**, 7549-7553.
8. M. J. Cook, A. P. Lewis, G. S. G. McAuliffe, V. Skarda, A. J. Thomson, J. L. Glasper and D. J. Robbins, *Journal of the Chemical Society, Perkin Transactions 2*, 1984, DOI: 10.1039/P29840001293, 1293-1301.
9. P. Innocenzi, H. Kozuka and T. Yoko, *The Journal of Physical Chemistry B*, 1997, **101**, 2285-2291.
10. H. Rensmo, S. Lunell and H. Siegbahn, Journal of Photochemistry and Photobiology A: Chemistry, 1998, **114**, 117-124.
11. G. J. Barbante, C. F. Hogan, D. J. D. Wilson, N. A. Lewcenko, F. M. Pfeffer, N. W. Barnett and P. S. Francis, *Analyst*, 2011, **136**, 1329-1338.
12. W. Thompson David, A. Ito and J. Meyer Thomas, *Journal*, 2013, **85**, 1257.
13. L. C. Soulsby, D. J. Hayne, E. H. Doeven, D. J. D. Wilson, J. Agugiaro, T. U. Connell, L. Chen, C. F. Hogan, E. Kerr, J. L. Adcock, P. S. Donnelly, J. M. White and P. S. Francis, *Physical Chemistry Chemical Physics*, 2018, **20**, 18995-19006.
14. J. V. Caspar and T. J. Meyer, Journal of the American Chemical Society, 1983, **105**, 5583-5590.
15. D. Saha, S. Das, S. Karmakar, S. Dutta and S. Baitalik, *RSC Adv.*, 2013, **3**, 17314-17334.
16. A. J. Bard, L. R. Faulkner, J. Leddy and C. G. Zoski, *Electrochemical methods: fundamentals and applications*, wiley New York, 1980.
17. E. J. O'Reilly, T. E. Keyes, R. J. Forster and L. Dennany, *Analyst*, 2013, **138**, 677-682.
18. I. Rubinstein and A. J. Bard, Journal of the American Chemical Society, 1981, **103**, 5007-5013.
19. Y. Qu, X. Liu, X. Zheng and Z. Guo, *Analytical Sciences*, 2012, **28**, 571-576.
20. N. Elgrishi, K. J. Rountree, B. D. McCarthy, E. S. Rountree, T. T. Eisenhart and J. L. Dempsey, *Journal of Chemical Education*, 2017, DOI: 10.1021/acs.jchemed.7b00361.
21. E. J. O'Reilly, T. E. Keyes, R. J. Forster and L. Dennany, *Electrochem. Commun.*, 2018, **86**, 90-93.

CHAPTER FOUR

UTILISATION OF AN ELECTROCHEMILUMINESCENCE SENSOR FOR ATROPINE DETERMINATION IN COMPLEX MATRICES

“Science indeed. One dummy trying to knock off another dummy with a bit of a stick”

Merlin (Sword in the Stone 1963)

This chapter comprises of publication:

K. Brown (primary author and principal investigator), M. McMenemy, M. Palmer, M. J. Baker, D. W. Robinson, P. Allan and L. Dennany, *Anal. Chem.*, 2019, **91**, 12369-12376.

DOI: 10.1021/acs.analchem.9b02905

Abstract

A major challenge within forensic science is the development of accurate and robust methodologies that can be utilised on-site for detection at crime scenes and can be used for the analysis of multiple complex sample types. The recent expansion of electrochemical sensors to tackle this hurdle has resulted in sensors that can perform analysis without any pretreatment required. Given the vast array of samples that are submitted for forensic analysis, this can pose a major challenge for all electrochemical sensors, including electrochemiluminescent (ECL)-based sensors. Within this chapter, the capacity of an ECL-based sensor to address this challenge and it's potential to detect and quantify atropine within a wide range of samples directly, including herbal material and spiked commercial drinks is demonstrated. This developed portable platform demonstrates satisfactory analytical parameters with linearity across a concentration range of 0.75 to 100 μM, reproducibility of 1.9%, repeatability of 8.3%, and a detection limit of 0.75 μM. The sensor displays good selectivity toward alkaloid species and, in particular, the hallucinogenic tropane alkaloid functionality within complex matrices. This portable sensor provides rapid detection alongside low cost and operational simplicity, thus, providing a basis for the exploitation of ECL-based sensors within the forensic arena.

4.1 Introduction

The exploitation of illicit substances continues to be an international concern further exacerbated by the ever changing nature of the global drug market. The monitoring and detection of such substances has become particularly challenging with the increasing presence of novel psychoactive substances (NPS).[1-3] Traditional methodologies such as high performance liquid chromatography mass spectrometry (HPLC-MS) and gas chromatography mass spectrometry (GC-MS) remain the gold standard laboratory based analytical techniques within forensic analysis. However, there is a growing need for rapid, sensitive and inexpensive detection systems for in-field analysis of both illicit substances and poisons within clinical and law enforcement environments.[4] The main screening methods currently in use, which primarily consist of colorimetric presumptive tests whose colour changes indicate the presence of a specific drug class, are often inadequate for NPS. Moreover, their poor selectivity hinders their reliability across all drug classes.[4] Furthermore, these screening methods cannot be ascribed effectively to all forensic samples, limiting their use in-field. Electrochemical platforms such as electrochemiluminescence (ECL) can address these challenges, presenting a unique opportunity to address the current gap in forensic practices for the rapid and crude identification of illicit and poisonous substances.

Atropine is a tropane alkaloid found within certain plants of the *solanaceus* family, including *Datura* and *Atropa belladonna*. Its anticholinergic

hallucinogenic behaviour, due to its antagonist actions toward the acetylcholine receptors, makes the tropane alkaloid ideal as a poison, while its hallucinogenic effects make it appealing as a recreational drug.[5] Atropine is today considered one of the most important tropane alkaloids for medicinal purposes, where it is employed for the treatment of Parkinson's disease[6, 7], to slow down the progression of myopia[8] and as a treatment for organophosphate poisoning.[9] In contrast to other popular naturally occurring recreational drugs, such as cannabis, atropine and sister tropane alkaloid scopolamine producing species remain largely unregulated in many countries; indeed, pharmaceutics containing the tropane alkaloid can often be obtained without a medical prescription.[5]

The use of atropine as a poison is not a novel concept as is highlighted by the 1994 case of Dr Paul Agutter. Dr Agutter, a biology professor at Edinburgh Napier University, attempted to murder his wife by spiking her gin and tonic with the deadly tropane alkaloid. Agutter subsequently attempted to divert suspicion by lacing multiple bottles of tonic, before returning the poisoned bottles to the supermarket shelf, resulting in mass panic when a number of people in the Edinburgh area fell ill.[10]

As previously mentioned, traditional methods for the identification of atropine and scopolamine, a structurally similar compound also found within *Datura*, typically involve HPLC[11], HPLC-MS[12] and GC-MS analysis.[11, 12] However, these methods suffer from significant instrument cost, lack of compatibility

with the optimal extraction solvents, and poor portability. Furthermore, the complexity of such techniques requires the operator to have expert working knowledge, posing a significant limitation for in-field or at scene testing. Exploration of ECL and cyclic voltammetry (CV) approaches both independently and as hyphenated systems have been reported for the detection of these alkaloid species.[6, 13-16] Although detection limits reported by these methods are typically higher than those achieved by HPLC-MS and GC-MS, (μM compared with nM) the versatility, portability and ease of use of electrochemical methods make their use appealing, particularly toward in-field applications. In addition, when considering the atropine concentrations of 0.35 mM to 1 mM[6] employed by Paul Agutter in his murder attempt did not result in any fatalities, it becomes apparent that the higher concentrations required for effective poisoning and to induce the onset of symptoms could thus be easily detected utilising basic electrochemical sensors.[6]

Although current electrochemical techniques have been applied to a wide variety of different sample matrices, including urine[15, 17-19], blood[17, 19] pharmaceutical preparations[6, 16, 18, 20-23] and non-ideal buffers such as Coca-Cola®[6], to date no one has reported the direct detection of atropine within *Datura* plant species without prior separation strategies[13, 14, 21] or lengthy extraction procedures employed to isolate the tropane alkaloid species.[22]

Within this chapter a proof-of-concept for the potential application of an ECL based detection strategy, utilising atropine as a model drug species, within

several potential forensic sample matrices was demonstrated. For the first time, the ability to directly detect a species within plant material through mechanical application onto an electrode surface was achieved. This eliminated the need to perform any extraction procedures, thus, providing a proof-of-concept for an in-field portable sensor utilising *Datura* to highlight potential applications of ECL sensors as drug screening tools with minimal sample preparation.

4.2 Experimental

4.2.1 Materials

Tris (2,2' – bipyridyl) – dichlororuthenium (II) hexahydrate ($[Ru(bpy)_3].Cl_2.6H_2O$), atropine sulfate monohydrate, lithium perchlorate ($LiClO_4$), mexiletine hydrochloride and Nafion 117 (~ 5 % mixture of lower aliphatic alcohols and water) were purchased from Sigma Aldrich. Absolute EtOH was purchased from VWR chemicals. All chemicals were used as received. All solutions were prepared in Milli-Q water (18 mΩ cm^{-1}). *Datura* plant species were grown from seed in house and harvested as required. *Solanum lycopersicum* (tomato plant), Coca-Cola® and tonic water were commercially purchased.

4.2.2 *Instrumentation*

The electrochemical instrumentation and electrode materials used were previously described within section 3.2.2.

All chromatographic analysis was performed using an Agilent 1200 series LC-MSD with a fixed variable wavelength detector set at 214 nm, coupled to an Agilent 6130 quadrupole mass spectrometer with electrospray and atmospheric-pressure chemical ionisation. An Aglient poroshelll 120 Å EC-C-18, 4.5 x 7.5 mm column at a column temperature of 40°C was used. A sampling volume of 5 µL of the extract was injected under a flow rate of 1 mL min^{-1} with a total analysis time of 18 minutes. Analytes were eluted using a gradient flow profile of 0.1 % v/v formic acid and water (mobile phase

A) and 0.1 % v/v formic acid and acetonitrile (mobile phase B). The flow profile used is detailed within Table 4.1.

Table 4.1: LC-MS gradient flow profile details, mobile phase A is 0.1%v/v formic acid water and mobile phase B is 0.1%v/v formic acid acetonitrile.

Time (minutes)	Mobile Phase A Composition (%)	Mobile Phase B Composition (%)
0	95	5
1.48	95	5
8.50	0	100
13.50	0	100
18.00	95	5

4.2.3 Fabrication of $[Ru(bpy)_3]^{2+}$ / Nafion ECL Sensor

The $[Ru(bpy)_3]^{2+}$/Nafion film modified carbon paste screen printed electrode was fabricated following the same procedure as described within section 3.2.3.

4.2.4 Preparation of Datura and Tomato Plant Samples for Electrochemical Analysis

Datura and *Solanum lycopersicum* (tomato plant) material (used as a negative control) were either extracted prior to analysis or analysed directly from harvest. Extractions were performed on approximately 50 mg of air-dried plant material through ultrasonication in 10 mL of aqueous $LiClO_4$ adjusted to pH 8 for 30 minutes. For direct detection within plant material,

Datura or tomato leaf was mechanically applied to the modified electrode surface and 100 μL of electrolyte cast on top to provide the required conductance.

4.2.5 Preparation of Datura and Tomato Plant Samples for LC-MS Analysis

Datura extracts for LC-MS analysis were prepared by extracting 50 mg of air-dried plant material in 10 mL of methanol and 1 mL of mexiletine hydrochloride as an internal standard at a concentration of 0.7 mM was added. Extractions were performed via ultrasonication at room temperature for 40 minutes. Pre-concentration was performed via evaporation of the extract to a final volume of 3 mL, from which a 1 mL portion of the extract was passed through a 0.2 μm PTFE filter to remove any solid particulates.

4.3 Results and Discussion

4.3.1 ECL Detection of Atropine

In contrast to previous studies[6, 17-19, 22] here atropine displayed no distinctive electrochemical behaviour at the concentrations of interest upon unmodified carbon screen printed electrodes across the potential range of interest, refer to Figure 4.1. However, at higher concentrations, within the mM range, an anodic peak at +0.89 V was observed (see Figure 4.2). Atropine has previously been shown to produce an ECL response in the presence of the traditional luminophore $[Ru(bpy)_3]^{2+}$, proceeding through a mediated oxidation mechanism as observed for alternative amine species of similar structure.[15, 23-28] This mediated oxidation proceeds via the homogeneous electron transfer between the Ru^{3+} generated in-situ and atropine present within the solution. The occurrence of the mediated oxidative process resulting in the oxidation of atropine and the subsequent ECL response can be further confirmed by interrogation of the CV signals observed at the ruthenium modified electrode. As the concentration of atropine increases, the oxidation peak produced by the Ru^{3+} species is observed to grow, while the reduction peak corresponding to the regeneration of the Ru^{2+} species decreases, as shown within Figure 4.2. This behaviour is consistent with electrochemical reactions which are mediated by Ru^{3+} centres.[29] As the oxidation route for atropine is kinetically unfavourable upon the electrode surface, it primarily proceeds via homogeneous electron transfer to the Ru^{3+} centres to generating the ECL emission shown within Figure 4.3. As a result of the consumption of the Ru^{3+} centres through atropine's mediate oxidation

process, there are fewer Ru^{3+} species available for the reduction process leading to the regeneration of the Ru^{2+} species during the reverse scan, resulting in the reduction current decreasing as the atropine concentration and hence consumption of Ru^{3+} increases.

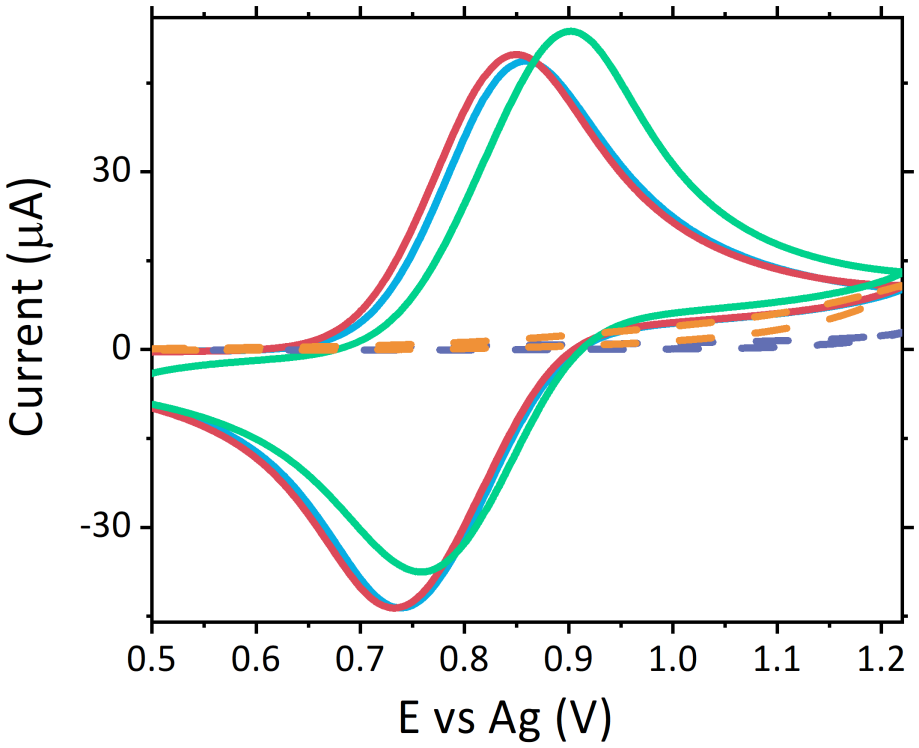

Figure 4.1: Typical CV responses obtained from an unmodified SPE carbon electrode with 50 µM atropine sulfate (orange) and without (purple), ruthenium film modified electrode with no co-reactant (blue) and in the presence of 50 µM atropine sulfate (pink), and 1 mM atropine sulfate (green) at a scan rate of 100 mV s^{-1} over the potential range 0.5 ≤ E ≤ 1.22 V vs Ag with 0.1 M $LiClO_4$ as the electrolyte.

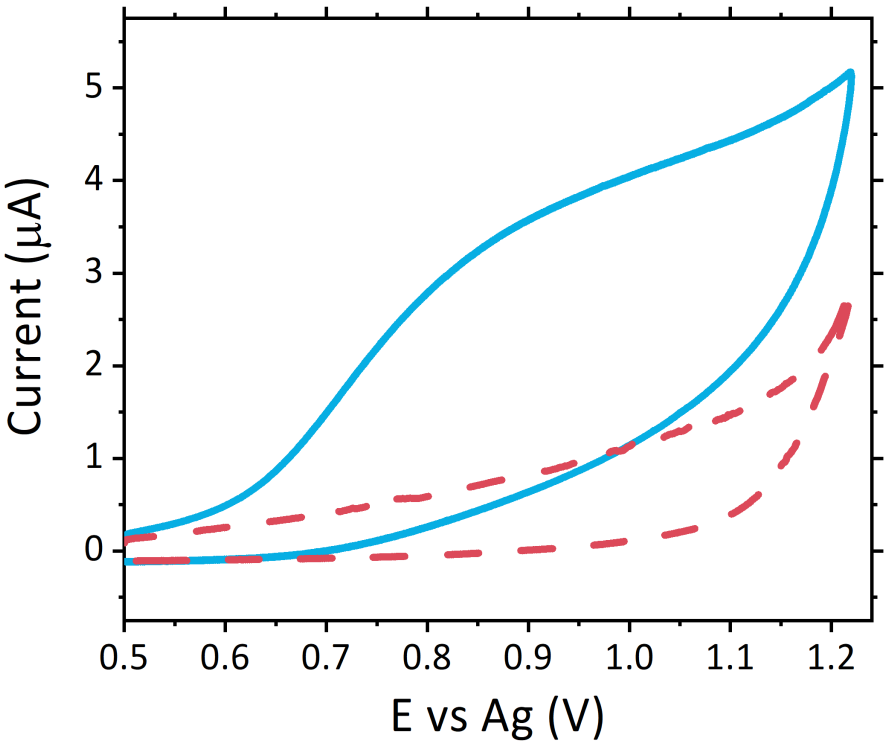

Figure 4.2: CV response of atropine at a concentration of 2.5 mM at an unmodified carbon SPE (blue solid line), at a scan rate of 100 mV s^{-1} across a potential range of 0 ≤ E ≤ 1.22 V vs Ag with 0.1 M $LiClO_4$ as the supporting electrolyte (pink dashed line).

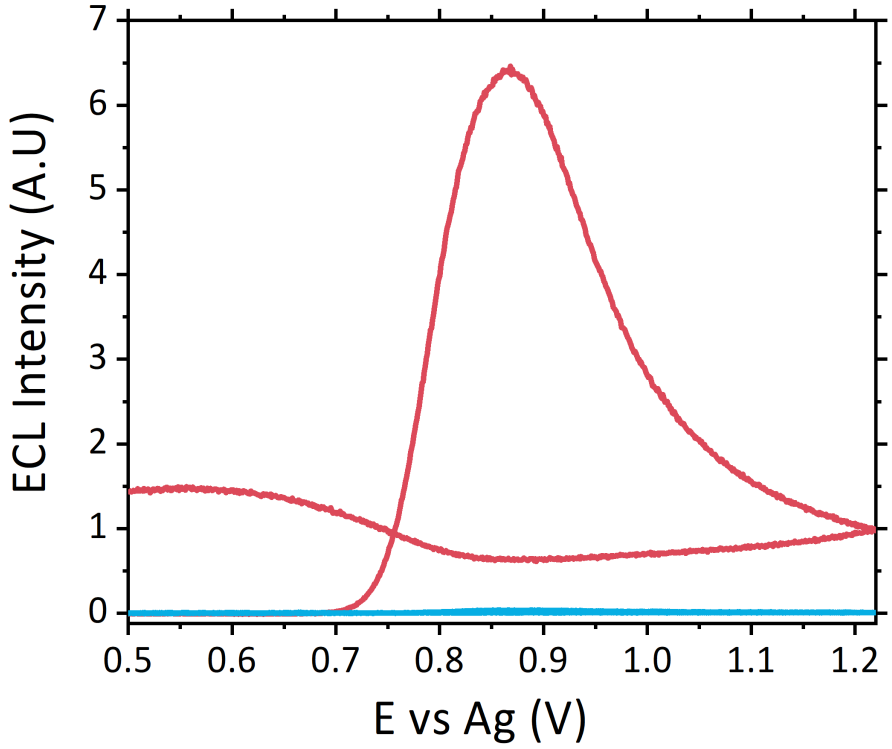

Figure 4.3: ECL signals recorded with film modified electrodes with no co-reactant (blue) and with 50 μM atropine sulfate (pink) at a scan rate of 100 mV s^{-1} over the potential range 0.5 ≤ E ≤ 1.22 V vs Ag with 0.1 M $LiClO_4$ as the supporting electrolyte and a PMT setting of 0.5 V.

Mechanisms recently suggested for the production of atropines' ECL emission, propose a cyclic reaction mechanism, which sees the regeneration of atropine alongside Ru^{2+} centres.[16] However, instead the oxidation of atropine is observed to be chemically irreversible where the electro-oxidation of atropine results in the generation of formaldehyde and likely formation of a secondary amine at the tropane ring system as a result of oxidative *N*-dealkylation. The presence of formaldehyde was confirmed through the Hehner's test,[30, 31] where prior to electrochemical measurements atropine containing samples produced a negative result, but following the generation of ECL, a violet ring was formed at the interface between the milk and H_2SO_4 containing trace amounts of potassium persulfate. Hence confirming the generation of formaldehyde following electrochemical measurements as a result of the irreversible chemical bond breakage within the parent compound. The proposed oxidative-reduction mechanism for the generation of ECL emission is shown within in equations (4.1) to (4.5), where the Ru^{3+} species generated at the electrode surface oxidises atropine following equation (4.2), forming the highly reducing intermediated, atropine• (a neutral radical species (b)). This intermediate then acts as the necessary co-reactant generating the excited Ru^{2+}* state through homogenous electron transfer, which in turn generates the imminium cation (c) as the product. Oxidative *N*-dealkylation, shown in scheme 4.1, then occurs generating formaldehyde (f) and the secondary amine species noratropine (e) via hydrolysis producing (d) and subsequent decomposition of the imminium cation. This de-alkylation mechanism is consistent with those previously reported by Leroy *et al.*[20] and

Bagheri *et al.*[18] for the electro-oxidation of atropine via CV and with those observed for the electrochemical oxidation of tropanes and aliphatic tertiary amines.[32, 33]

Scheme 4.1: Schematic detailing the electrolytic oxidative *N*-dealkylation mechanism for atropine during the ECL process.

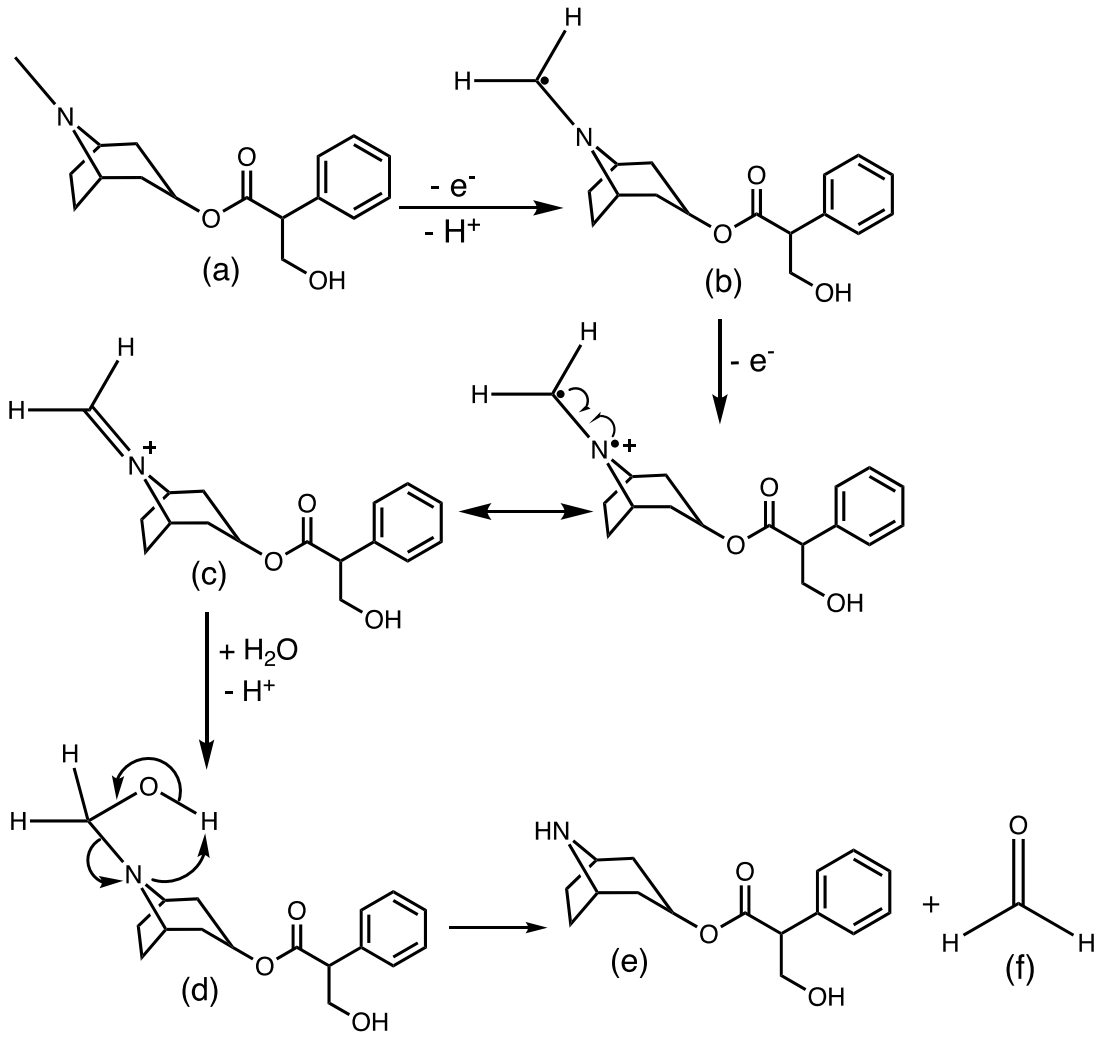

$$[Ru(bpy)_3]^{2+} \leftrightarrow [Ru(bpy)_3]^{3+} + e^- \quad (4.1)$$

$$[Ru(bpy)_3]^{3+} + atropine \rightarrow [Ru(bpy)_3]^{2+} + atropine^{+\bullet} \quad (4.2)$$

$$atropine^{+\bullet} \rightleftharpoons atropine^{\bullet} \quad (4.3)$$

$$[Ru(bpy)_3]^{3+} + atropine^{\bullet} \rightarrow [Ru(bpy)_3]^{2+*} + (f) + (e) \quad (4.4)$$

$$[Ru(bpy)_3]^{2+*} \rightarrow [Ru(bpy)_3]^{2+} + h\nu \quad (4.5)$$

4.3.2 Effect of pH on ECL Response

pH is widely accepted to influence the ECL response of atropine and similar amine species, where the greatest signal is obtained at values close to its pKa.[15, 16, 23, 27] The influence of pH was investigated between pH 5 and 11 with an atropine concentration of 50 μM. The ECL signal intensity was observed to increased from pH 5 to 8, reaching a maximum at pH 8, close to the reported pKa value of 9.85. As such, this pH was chosen as the optimum pH at which all further analysis was performed.[34] A further increase in pH values above pH 8 resulted in a dramatic decrease in signal intensity, before an increase was again observed at pH 11, see Figure 4.4. Upon reaching pH 9 the greater alkaline conditions likely lead to a signal decrease as a result of the quenching effect from the side reaction between the hydroxyl anions and the generated $[Ru(bpy)_3]^{3+}$.[15] The subsequent increase in signal intensity at pH 11 and the broadening of the emission peak at this pH, suggests the emergence of a second electroactive species. The appearance of this second species is thought to be the result of the base catalysed degradation of atropine in the presence of high concentrations of hydroxide ions, likely

leading to the formation of tropine and tropic acid.[35] Subsequent investigations of each of the degradation products revealed tropine to be a suitable co-reactant for the generation of ECL, refer to Figure 4.5. This is not surprising given the tropane functionality, contained within tropine's structure, is responsible for the ECL emission of atropine. Hence it becomes highly likely that tropine will likely follow the same oxidative *N*-dealkylation mechanistic pathway as described within scheme 4.1.

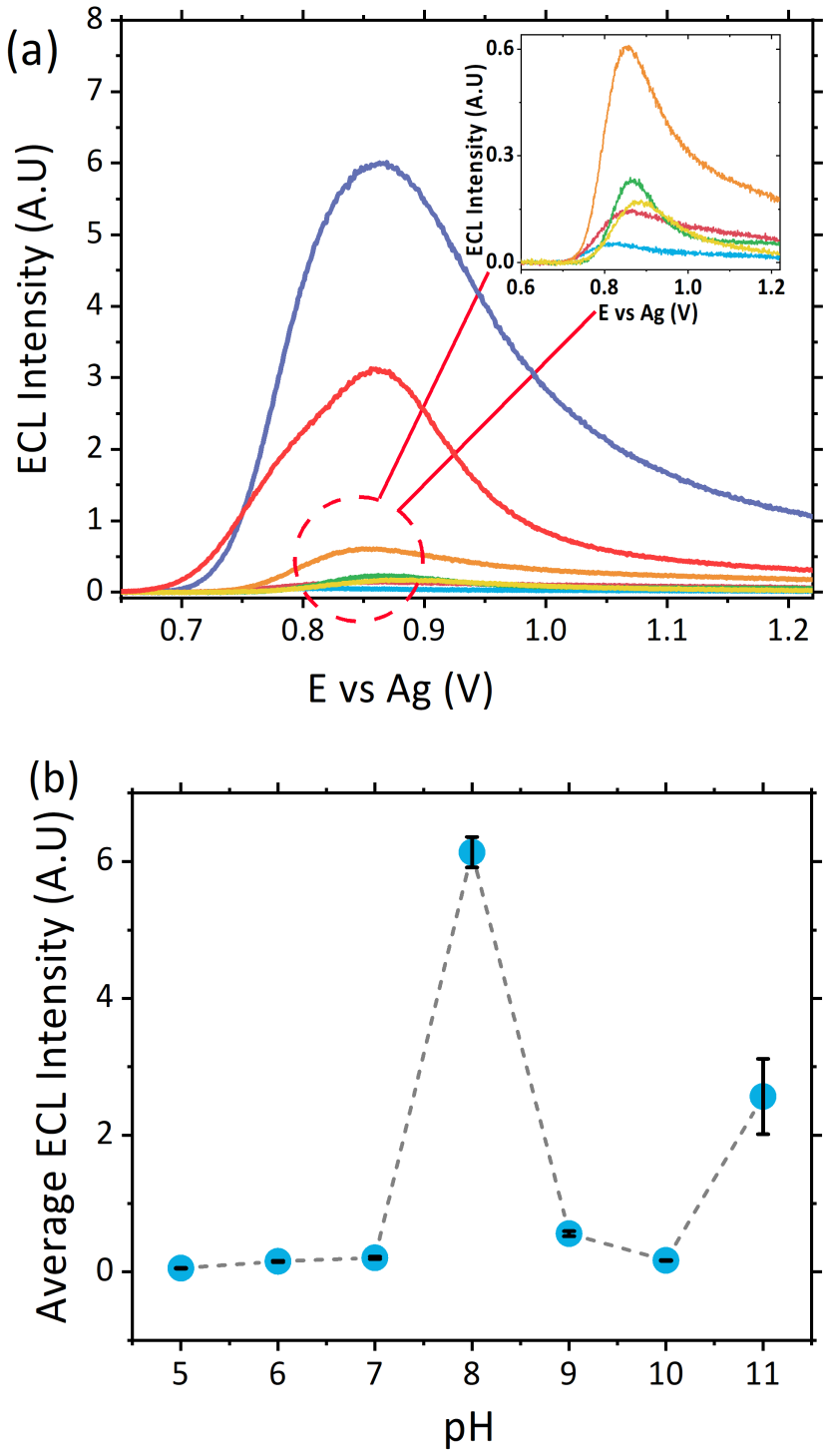

Figure 4.4: (a) ECL response of 50 μM atropine sulfate between pH 5 - 11 at a scan rate of 100 mV s^{-1} over the potential range 0.5 ≤ E ≤ 1.22 V vs Ag at a PMT setting of 0.5 V with 0.1 mM $LiClO_4$ as the electrolyte. (b) Trend in ECL response with pH, where each point represents the mean of the maximum ECL intensity at n=3 with error bars comprising of ± 1SD across these measurements.

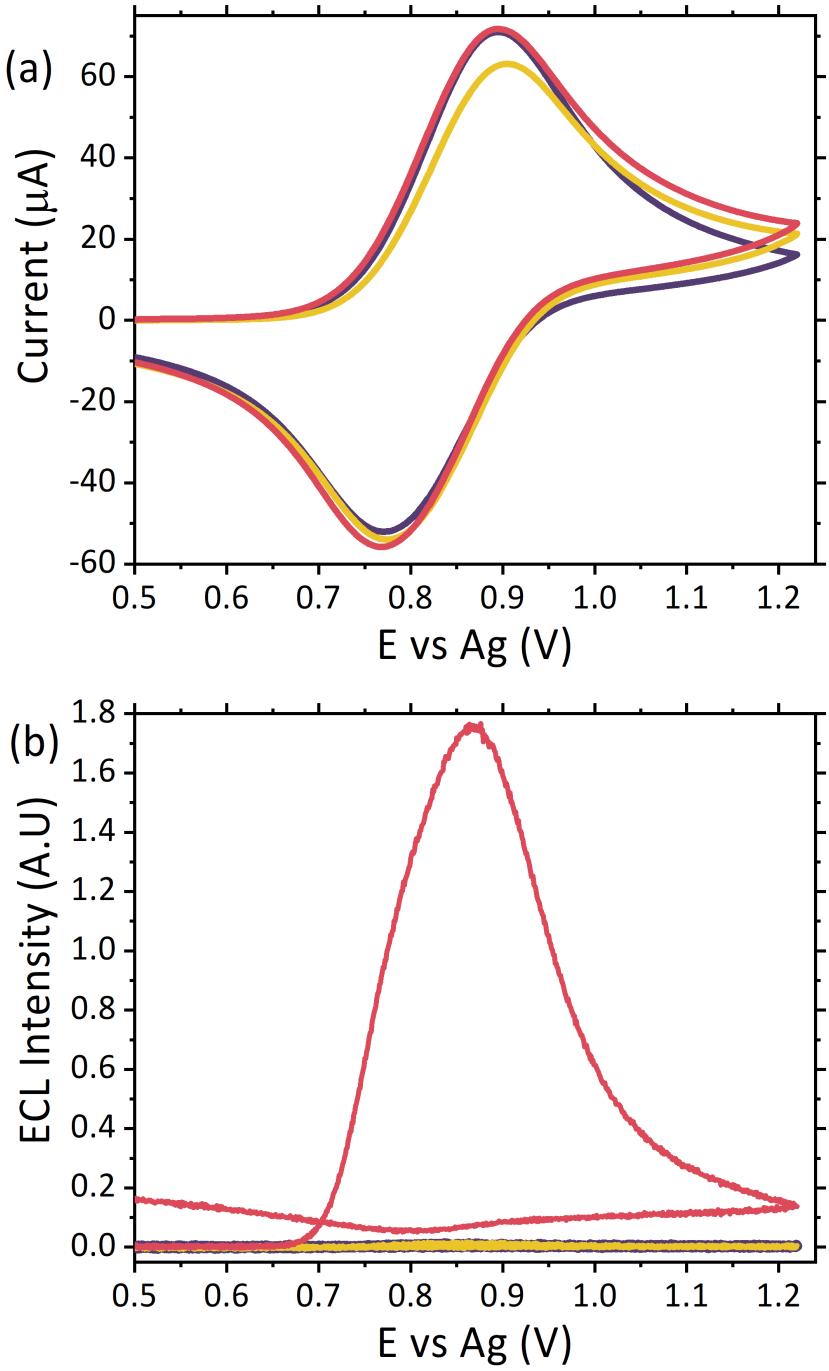

Figure 4.5: (a) CV responses of 50 µM tropic acid (yellow) and 50 µM tropine (red) with $[Ru(bpy)_3]^{2+}$ modified electrodes at a scan rate of 100 mV s^{-1} over the potential range 0.5 ≤ E ≤ 1.22 V vs Ag with pH 8 adjusted 0.1 M $LiClO_4$ as the supporting electrolyte. (b) corresponding ECL signals from (a) at a PMT setting of 0.45 V. The purple trace in both (a) and (b) is of a $[Ru(bpy)_3]^{2+}$ modified electrode under the same parameters within blank electrolyte.

4.3.3 Influence of Atropine Concentration

The impact of atropine concentration upon ECL response was investigated across a concentration range of 0.75 to 100 μM, comparable to the ranges previously reported for the detection of atropine via electrochemical[6, 15, 16, 22] and chemiluminescence methodologies.[36] Furthermore this concentration range covers the typical values observed within a variety of *Datura* species.[37] As atropine concentration was increased the ECL signal correspondingly increased as shown within Figure 4.6. Alongside the increase in signal intensity, a shift in peak maximum potential is observed with atropine concentration. This potential shift although unexpected can likely be attributed to a combination of the following effects: first, when ruthenium becomes the rate limiting reagent, the Ru^{3+} centres required for the mediated oxidation of atropine are consumed at a rate greater than they can be produced via heterogeneous oxidation at the electrode surface.[38] Second, with more atropine available to undergo the irreversible oxidation process, a slight shift in the pH of the solution immediately surrounding the electrode surface can occur, as a result of the increased concentration of the electro-generated by-products: noratropine and formaldehyde. These effects are consistent with previous reports, which also observed a shift in the λ_{ECLmax} upon graphite electrodes.[39] This only stands to highlight the impact even a slight pH change at the inner Helmholtz layer can have. Overall the response at maximum intensity was observed to be linearly proportional to atropine concentration with a coefficient R^2 value of 0.997 (Figure 4.6 inset), with a detection limit of 0.75 μM (S/B=3). To calculate the measurement variance

associated with each of the sensors' independent variables (instrumentation, electrode and measurement day) and represent this as a relative standard deviation (RSD) the methodology previously employed by Nordon *et al.*[40] was utilised, which allowed for the RSD of each variable to be independently determined. Six subsequent measurements upon the same electrode (instrument variation), sample analysis across six different electrodes (electrode variation) and analysis of the same sample across six different days (measurement day variation) was performed. Once measurements were performed the variation for each independent variable was determined through the employment of the standard mathematical procedure[40], whereby the value determined for electrode variation excludes the contribution from instrument variation and measurement day excludes the contribution from electrode and instrument variation. The resultant RSD values for each was determined as 4.1%, 1.9% and 8.3% for instrument, electrode and measurement days respectively.

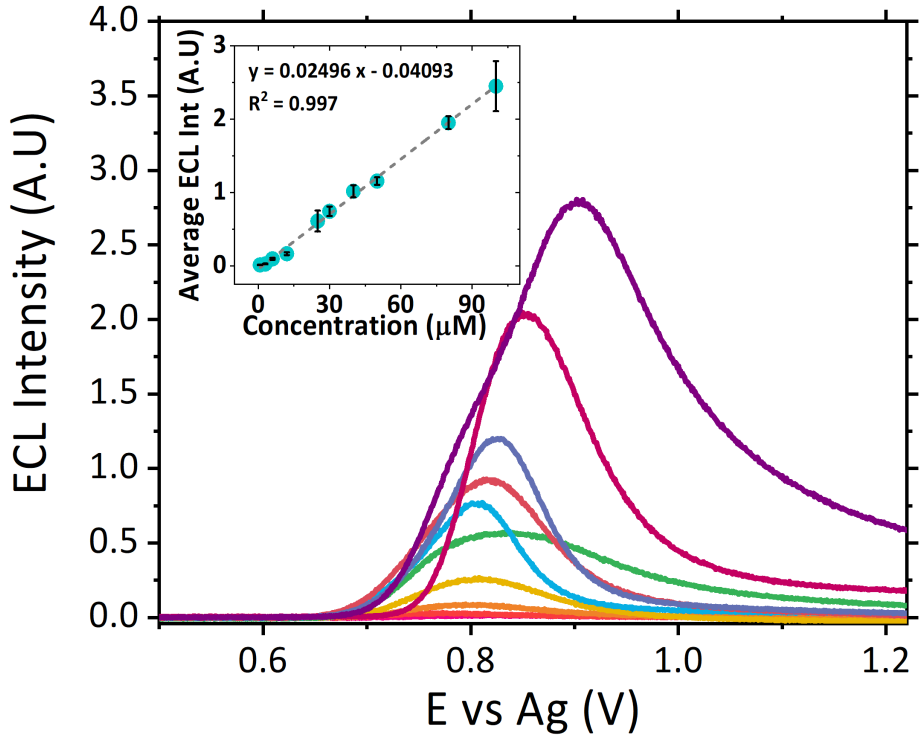

Figure 4.6: Dependence of ECL signal on atropine sulfate concentration between 0.75 to 100 μM in pH 8 0.1 M $LiClO_4$ at a scan rate of 100 mV s^{-1} across a potential range of 0.5 ≤ E ≤ 1.22 V vs Ag at a PMT setting of 0.45 V. Inset shows the trend of maximum ECL signal against atropine sulfate concentration.

4.3.4 Sample Analysis

To demonstrate the wide potential scope of applications possible with the developed sensor, analysis of a variety of different complex matrices encountered within “real world” scenarios was performed, including plant material and drink samples. Here for the first time a direct analysis method of *Datura* plant extracts alongside herbal material through mechanical application to the electrode surface without any prior separation or extraction techniques was performed. Despite a large number of species present alongside the tropane alkaloids, as demonstrated by the absorbance profile of the LC-MS analysis performed upon the leaf material (see Figure 4.7), no interfering peaks were observed in either the CV (see Figures 4.8a and 4.8b) or ECL analysis performed upon the extracts (Figure 4.9a) or via mechanical voltammetry technique (Figure 4.9b) outside of the potential region for the oxidation of the tropane alkaloid species, with an ECL signal observed at approximately the same potential as observed for atropine sulfate within the $LiClO_4$ electrolyte. To ensure the signals obtained were not impacted, or the result of the vast number of co-species present alongside the alkaloid within the complex herbal matrix, leafs obtained from a tomato plant were used as a negative control. Tomato plants originate from the same plant family as *Datura*, the *solanaceous* family, but do not contain the hallucinogenic compounds of interest: atropine and scopolamine. Despite the control species not containing the hallucinogenic tropane alkaloids, a slight signal is still observed. This is believed to arise as a result of the naturally occurring glycoalkaloids found within all members of the *solanaceous* family.[41, 42] The

particular glycoalkaloid found within tomato plants is the steroid alkaloid tomatine, which contains the electroactive piperidine alkaloid functionality.[41, 42] It is therefore proposed that this functionality will result in the observed ECL signal, as is reported for other structurally similar amine species.[15, 24-28, 43] The emission onset of tomatine is observed to commence at a lower potential than atropine, attributed to the oxidation occurring at the secondary amine within the piperidine alkaloid rather than a tertiary amine, as is present within the tropane alkaloid functional groups.

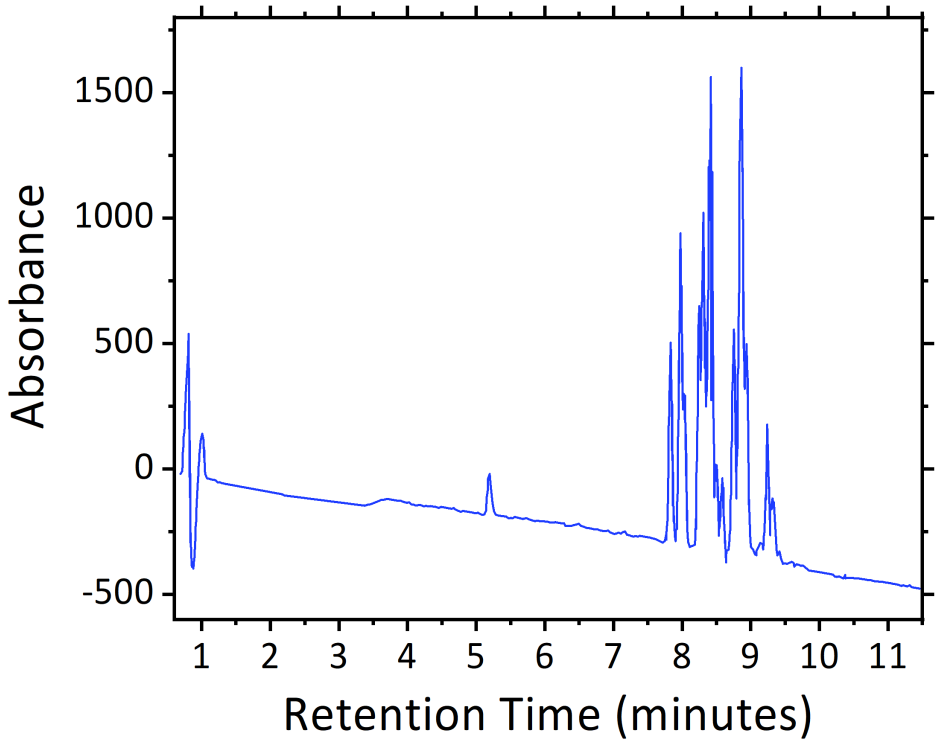

Figure 4.7: Chromatogram of *Datura* leaf extracts, obtained during LC-MS analysis with methanol as the extraction solvent, with a detection λ of 214 nm, gradient flow with mobile phase A of 0.1%v/v formic acid water and mobile phase B of 0.1% v/v formic acid acetonitrile.

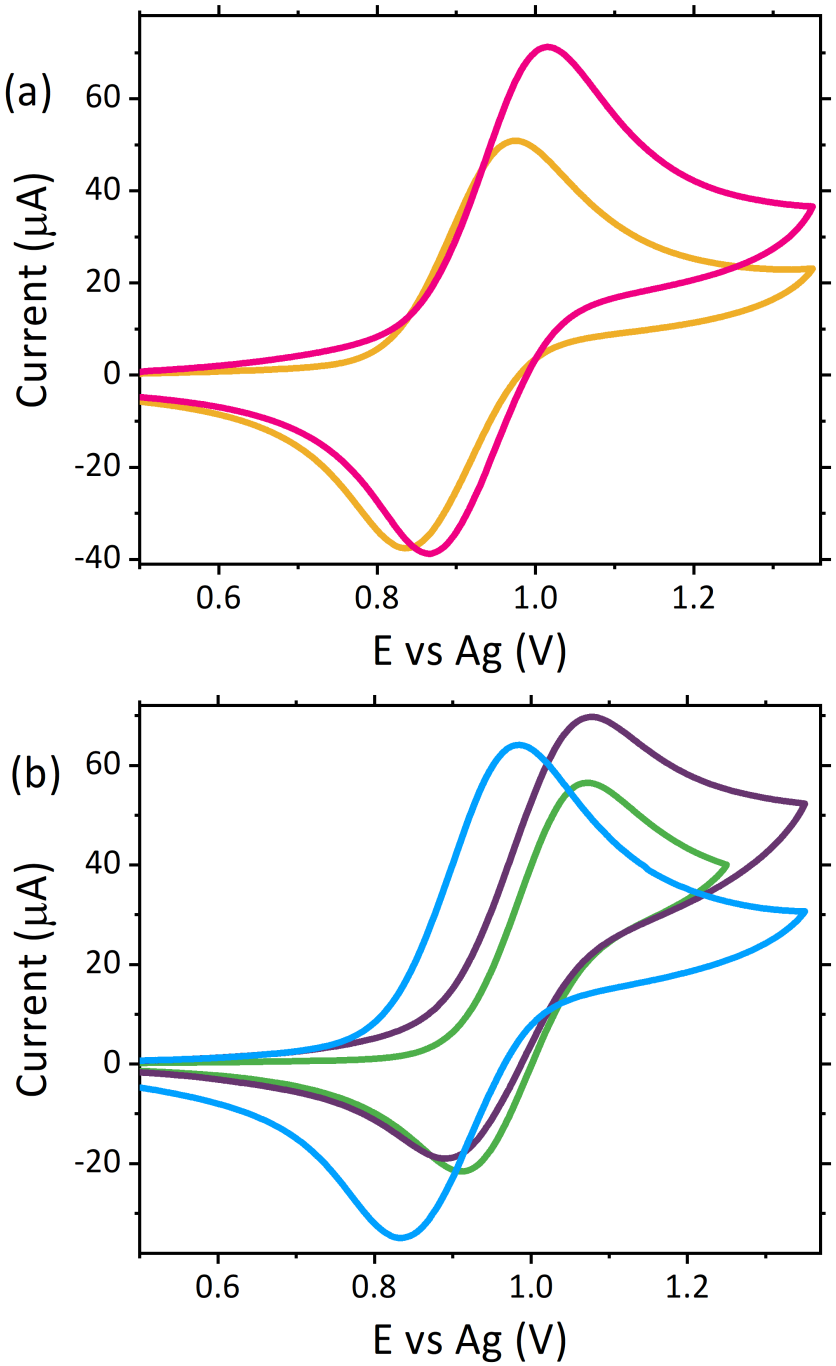

Figure 4.8: CV responses obtained for (a) *Datura* leaf (pink) and tomato leaf (yellow) extracts and (b) mechanical application of mature *Datura* leaf (green), young *Datura* leaf (purple) and tomato leaf (blue) with $[Ru(bpy)_3]^{2+}$-modified electrode at a scan rate of 100 mV s^{-1} over the potential range $0.5 \leq E \leq 1.36$ V vs Ag with 0.1 M $LiClO_4$ as the extraction solvent and supporting electrolyte.

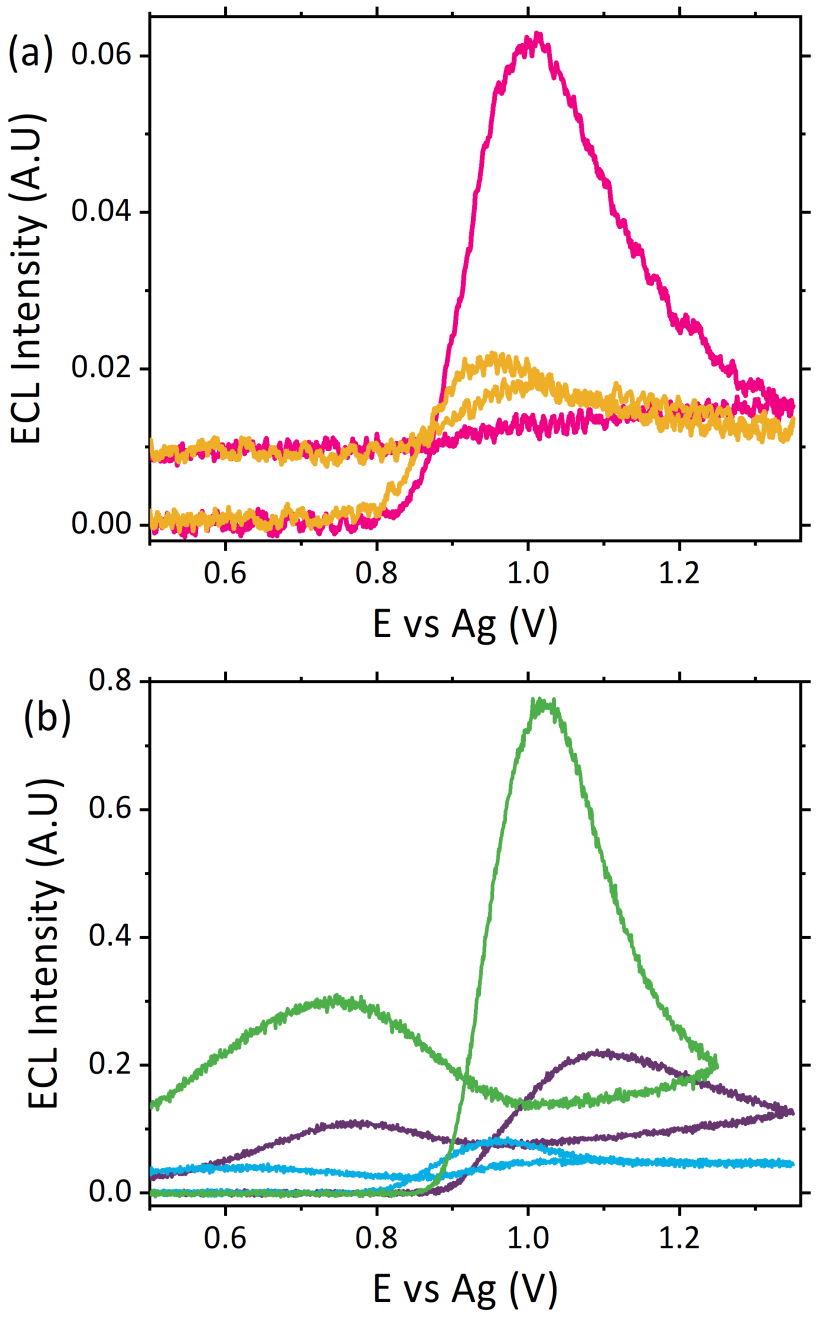

Figure 4.9: Corresponding ECL responses for Figure 4.8, obtained for (a) *Datura* leaf (pink) and tomato leaf (yellow) extracts and (b) mechanical application of mature *Datura* leaf (green), young *Datura* leaf (purple) and tomato leaf (blue) with $[Ru(bpy)_3]^{2+}$-modified electrode at a scan rate of 100 mV s^{-1} over the potential range $0.5 \leq E \leq 1.36$ V vs Ag with 0.1 M $LiClO_4$ as the extraction solvent and supporting electrolyte and a PMT setting of 0.45 V.

To further assess the selectivity of the developed sensor an interferent study was conducted utilising other naturally occurring alkaloids known to be present within *Datura* species. These potential interferents included scopolamine, the second hallucinogenic tropane alkaloid present within Datura and the naturally occurring alkaloid solanine present within all plants of the *solanaceous* family. These were assessed against the signals observed for tomatine, $LiClO_4$, atropine sulfate and from the *Datura* herbal material and can be found within Figure 4.10. The signals obtained from the solanine species was comparable to that observed for the pH 8 $LiClO_4$ blank, and, as such can be considered a negligible signal and hence can be considered to not interfere with the ECL signal obtained from the herbal material. The tomatine signal, however was slightly larger at an intensity of 0.05 A.U. This greater intensity may be attributed to the secondary amine functionality compared with the tertiary amine found within solanine. Thus to account for the impact of naturally occurring glycoalkaloids present may have upon the observed ECL signal from *Datura*, the predicted concentrations reported within Table 4.2 were corrected by subtracting this threshold response from the overall ECL signal intensity observed for the herbal material. This does represent a limitation of the proposed system; however, this is outweighed by the potential screening ability of this portable ECL approach and the rapid results that can be obtained, especially considered along with the employment of a threshold signal to negate impact from the naturally occurring alkaloids.

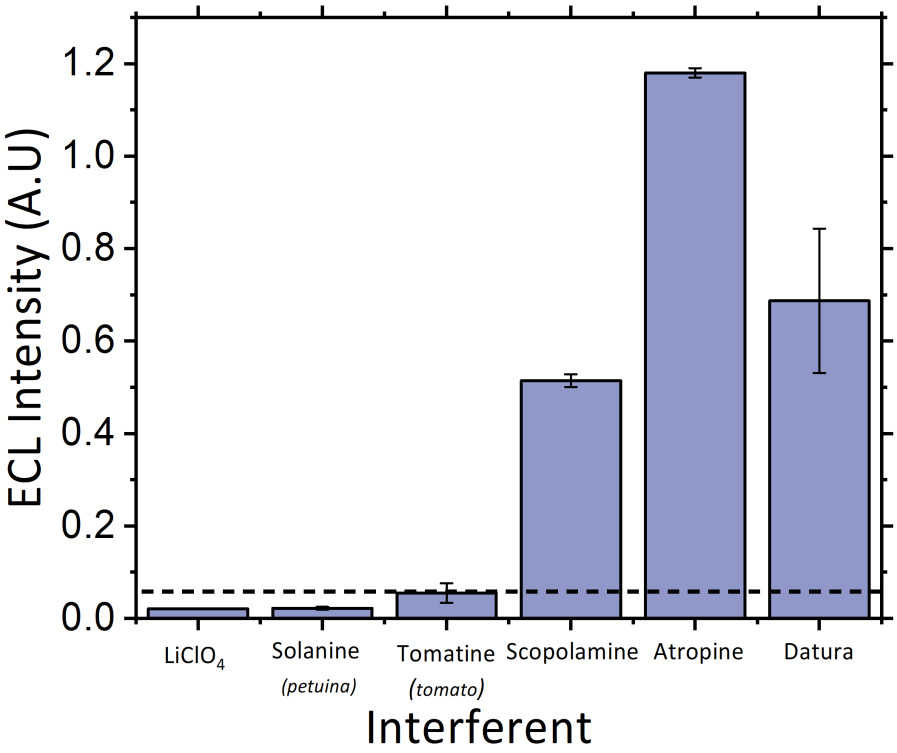

Figure 4.10: Maximum ECL responses observed using the proposed sensor in the presence of different naturally occurring species found within herbal material of the *solanaceous* family compared against the signals observed for atropine sulfate in $LiClO_4$ and Datura. The dotted line represents the threshold signal used to correct calculated concentrations of the alkaloids within the herbal material analysed. Each bar represents the mean of the maximum ECL intensity at n=3 with error bars comprising of ± 1SD.

Table 4.2: Uncorrected and corrected alkaloid concentrations estimated from extracts (E) and mechanically applied samples (M) obtained from ECL analysis of tomato and young and mature *Datura* plants, where corrections were performed through subtraction of the tomatine threshold signal.

Sample	ECL Intensity (A.U.)	Corrected ECL Intensity (A.U)	Uncorrected [alkaloid] (μM)	Corrected [alkaloid] (μM)
Tomato leaf (E)	0.0213	0	2.49	0
Tomato leaf (M)	0.0818	0	4.92	0
Datura (E)	0.0539	0.0357	3.07	3.80
Mature *Datura* (M)	0.683	0.591	29.0	25.3
Young *Datura* (M)	0.303	0.249	13.8	11.6

Although this current study focuses upon the detection of atropine, it can be clearly seen from Figure 4.10 that closely related tropane alkaloid compound, scopolamine, also generates a significant ECL emission. We know from the LC-MS analysis (see Figure 4.11) of the *Datura* material that both atropine and scopolamine are present, where both species were identified through the presence of their pseudo-molecular ion fragments at 290 m/z and 304 m/z for atropine and scopolamine respectively. These two compounds only differ by the presence of a single epoxide group within scopolamine and are, as such, observed to oxidise at almost indistinguishable potentials. Although scopolamine is observed to typically oxidise at a slightly later potential than atropine under CV interrogation. Therefore, it is highly likely that the ECL

signals observed from the herbal material analysed are likely a combination of the emission from both tropane alkaloids, atropine and scopolamine, acting as suitable co-reactants. Examination on how to interrogate and extrapolate the impact to the overall signal which scopolamine would contribute and the ability to differentiate between the two species is under investigation. Despite this likely interferent effect, as the signals obtained within the herbal material lie within the same potential range identified for both atropine and scopolamine, confident identification of the presence of hallucinogenic tropane alkaloids within this material was made. Adding further confidence is the significantly larger signal observed within the herbal material compared with those obtained for the other naturally occurring non-hallucinogenic glycoalkaloids present within members of the *solanaceous* family, thus ensuring the observed signals are not a result of the other species naturally found within herbal material.

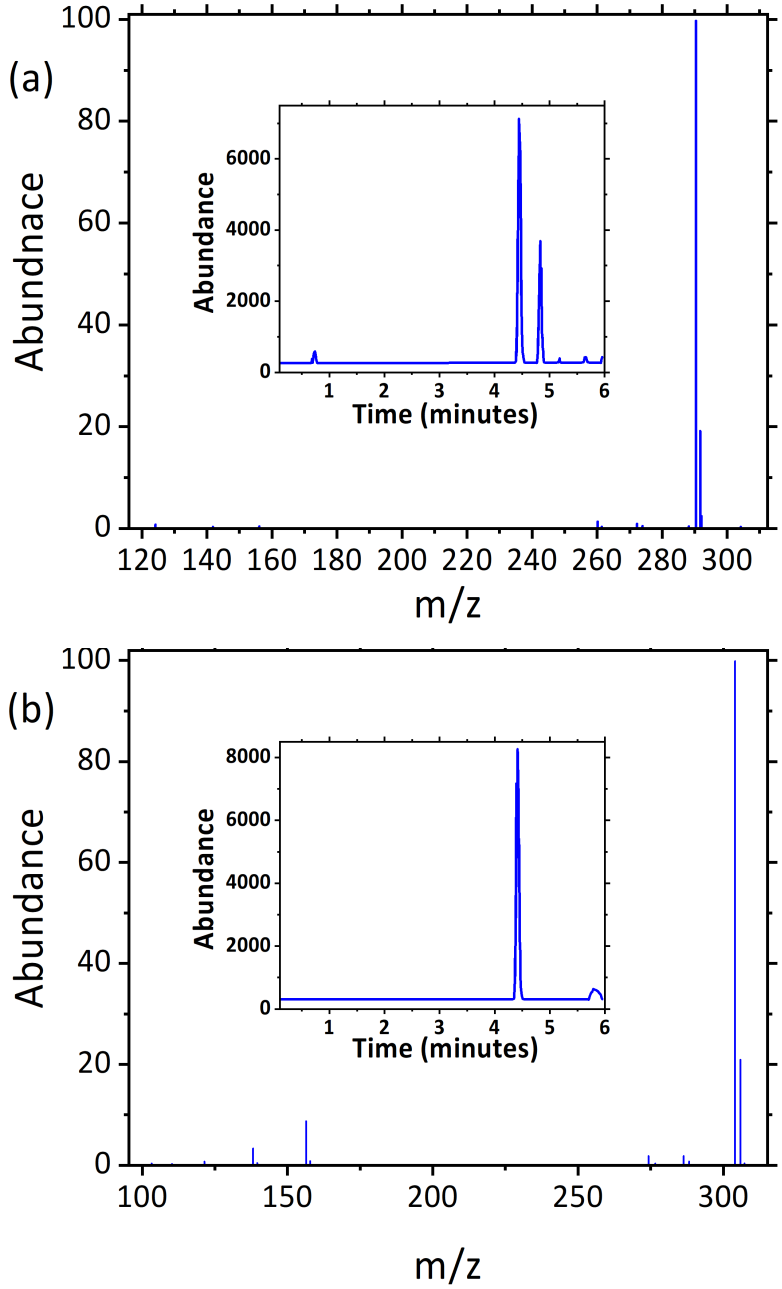

Figure 4.11: (a) mass spectrum of atropine found within *Datura* leaf extract during LC-MS analysis, where pseudo-molecular ion at 290 m/z ratio was used for identification. Inset shows the extracted ion chromatogram over 290:292 m/z for the leaf extract. (b) mass spectrum of scopolamine found within *Datura* leaf extract during LC-MS analysis, where pseudo-molecular ion at 304 m/z ratio was used for identification. Inset shows the extracted ion chromatogram over 304:306 m/z for the leaf extract.

An alternative complex matrix used, in the form of commonly encountered carbonated drinks, was performed to further simulate a “real-world" scenario, which may be employed within a forensic case, such as potential drink spiking. Coca-Cola®, a common mixer and tonic water, the drink chosen by Paul Agutter in the attempted murder of his wife, were spiked to a final concentration of 50 μM atropine sulfate. To emphasise the field applicability of this protocol, spiked drink samples were diluted with the electrolyte to produce an ideal sample matrix and analysed alongside neat pH adjusted samples that replicate a potential “real-world” matrix. The natural acidity of Coca-Cola® and tonic water, at approximately pH 2, prevented the detection of atropine within raw unadjusted samples; refer to Figure 4.12 and Figure 4.13. for the corresponding CV and ECL signals. As demonstrated in Figure 4.4, at acidic pH values, minimal ECL signal is obtained for atropine, attributed to the protonated form of the alkaloid dominating at these pH values. As such, it was necessary to adjust the drink matrices to more alkaline pH values to facilitate detection.

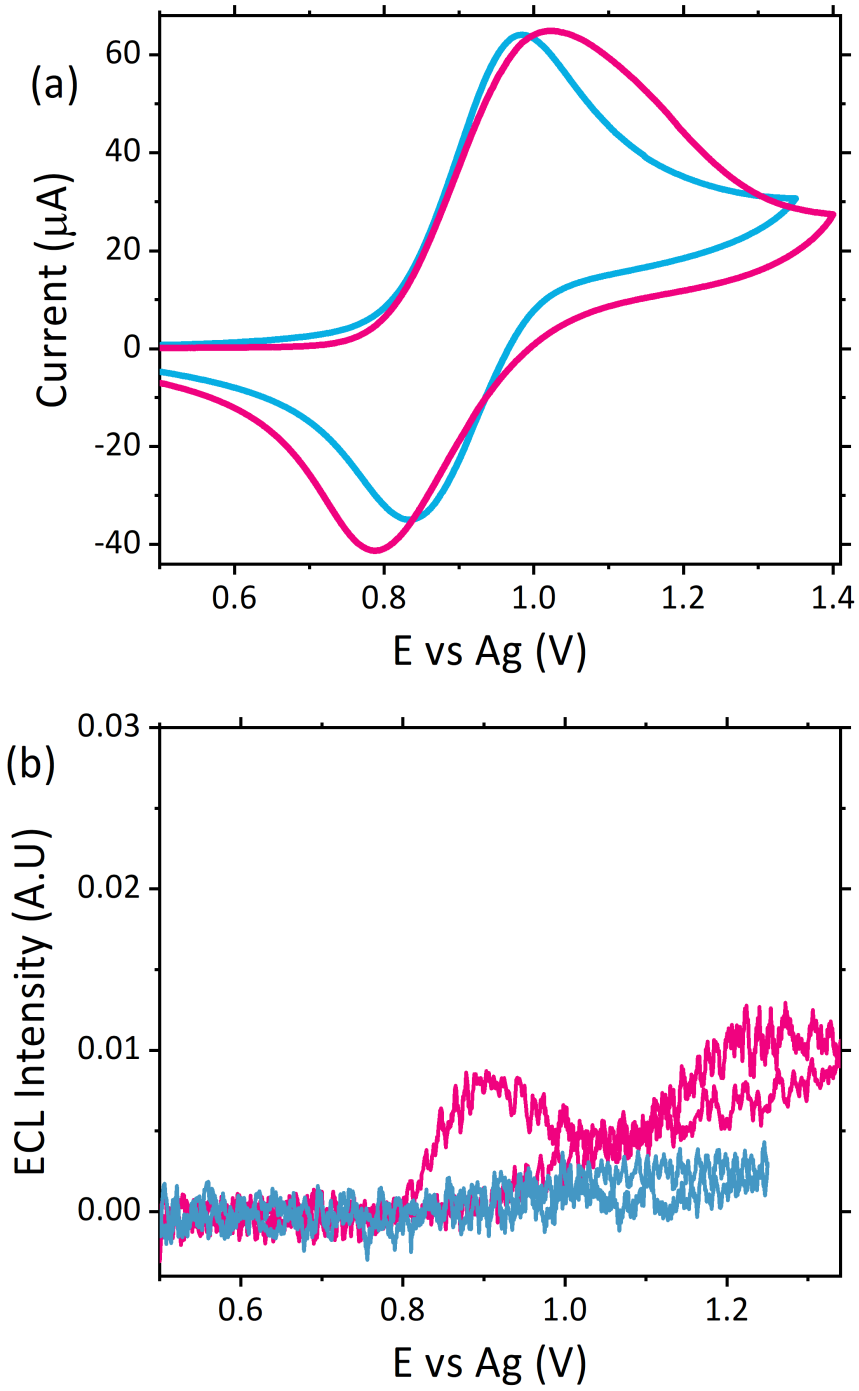

Figure 4.12: CV responses of raw Coca-Cola® (blue) and raw Coca-Cola® spiked with 50 µM atropine sulfate (pink) with $[Ru(bpy)_3]^{2+}$ modified electrode at a scan rate of 100 mV s^{-1} over the potential range 0.5 ≤ E ≤ 1.36 V vs Ag. (b) corresponding ECL signals from (a) at a PMT setting of 0.45 V.

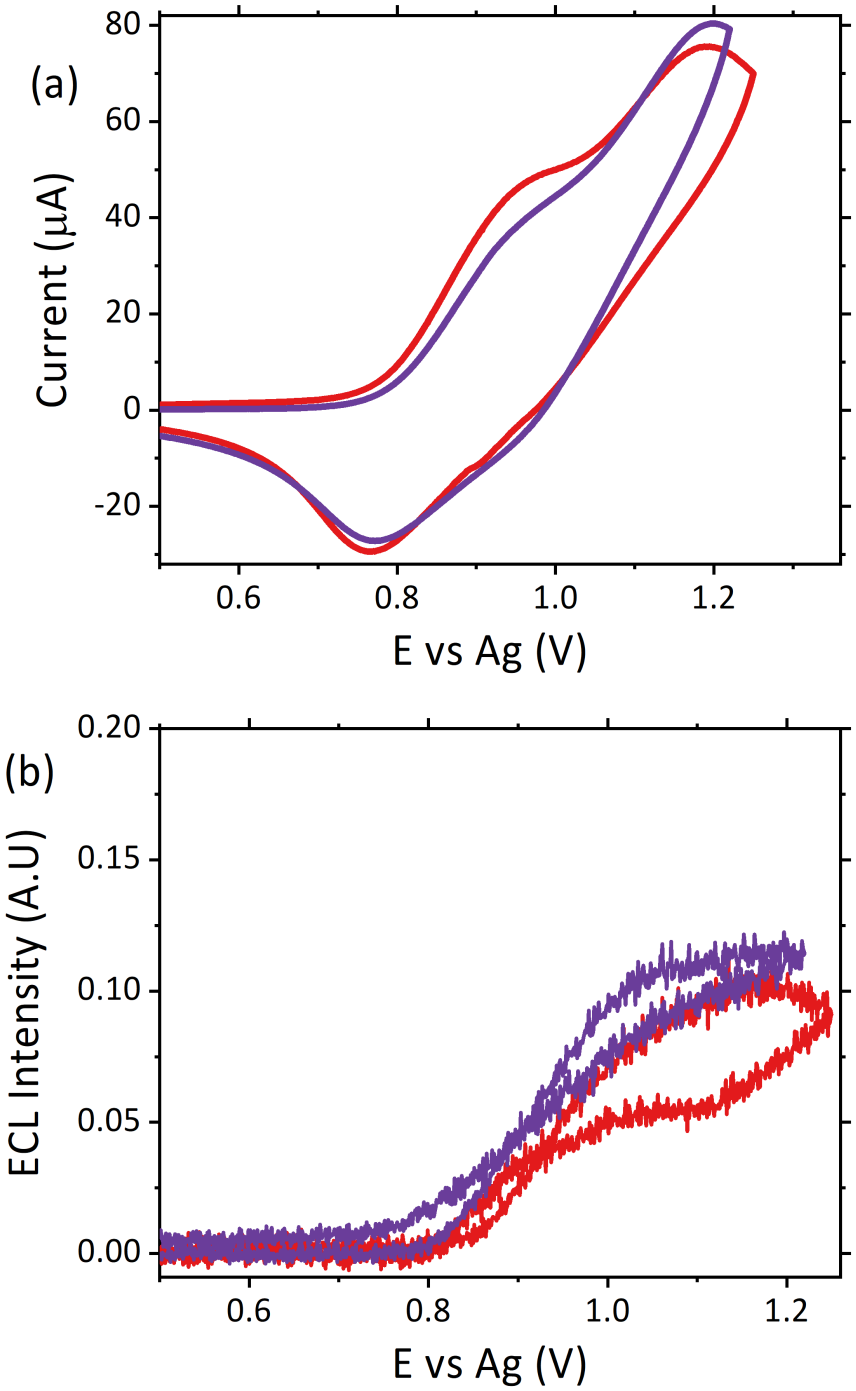

Figure 4.13: CV responses of raw tonic water (red) and raw tonic water spiked with 50 µM atropine sulfate (purple) with $[Ru(bpy)_3]^{2+}$ modified electrode at a scan rate of 100 mV s^{-1} over the potential range 0.5 ≤ v ≤ 1.25 V vs Ag. (b) corresponding ECL signals from (a) at a PMT setting of 0.45 V.

By diluting the drink samples in a 1:1 v/v ratio with the electrolyte, recoveries of 99% and 96% were obtained for Coca-Cola®, and tonic water, respectively. This demonstrated a high degree of accuracy, with the ECL sensor producing recoveries above the 95% threshold typically required for analytical methodologies. Analysis of neat pH adjusted samples demonstrated the ability of the drink matrices to provide the necessary conductivity to perform electrochemical measurements. As can be seen in Figure 4.14, the ECL obtained from the neat samples displayed a slightly shifted and lower intensity signal. This is likely the consequence of the non-ideal characteristics of this matrix, including higher solution resistance to charge transfer. As such, the recoveries obtained for the neat drink samples were below the typical 95% threshold value at 85% and 84% for Coca-Cola® and tonic respectively; concentrations calculated for all samples are reported in Table 4.3. Previously, Ramdani *et al.*[6] have reported the detection of atropine in diluted diet Coca-Cola® via CV but failed to identify atropine in tonic water as a result of interference from the electroactive alkaloid, quinine. As shown in Figure 4.14 (b) the influence of quinine can be almost negated by the employment of ECL alongside CV. The diluted tonic water displayed no significant interference from quinine at pH 8. However, it is likely that at alternative pH values a greater interference effect may be observed. The non-spiked neat tonic water displays a larger signal, compared with the diluted blank. This can likely be attributed to the higher concentration of quinine present in the non-dilute sample. This interference effect in combination with the non-ideal matrix effects previously discussed could account for the lower recovery

obtained within neat tonic water samples. Despite the lower recoveries obtain this protocol has shown its strength for detection of atropine within non-ideal matrices with minimal sample preparation required and, as such, makes an ideal candidate for alternative screening methodologies for employment within a forensic arena. However, the reliance upon the pH of samples does present a significant limitation to the proposed protocol toward field employment, where the ability to accurately adjust samples to a specified pH would be challenging. As a screening protocol, however, the ability to accurately quantify samples is not required, and as such a wide range of pH values, as shown by Figure 4.4, would result in an indicative signal, warranting further testing. As such it hoped this protocol could be applied to a range of different drink matrices across a range of pH values.

Table 4.3: Calculated atropine sulfate concentrations and % recoveries obtained from ECL analysis of spiked pH 8 Coca-Cola® and tonic water samples. Where neat denotes pH adjusted matrices and diluted denotes samples containing additional electrolyte.

Sample	Avg. Calculated [atropine] (μM)	%recovery
Neat Coca-Cola®	42.3	85
Diluted Coca-Cola®	49.3	99
Neat tonic water	42.1	84
Diluted tonic water	47.9	96

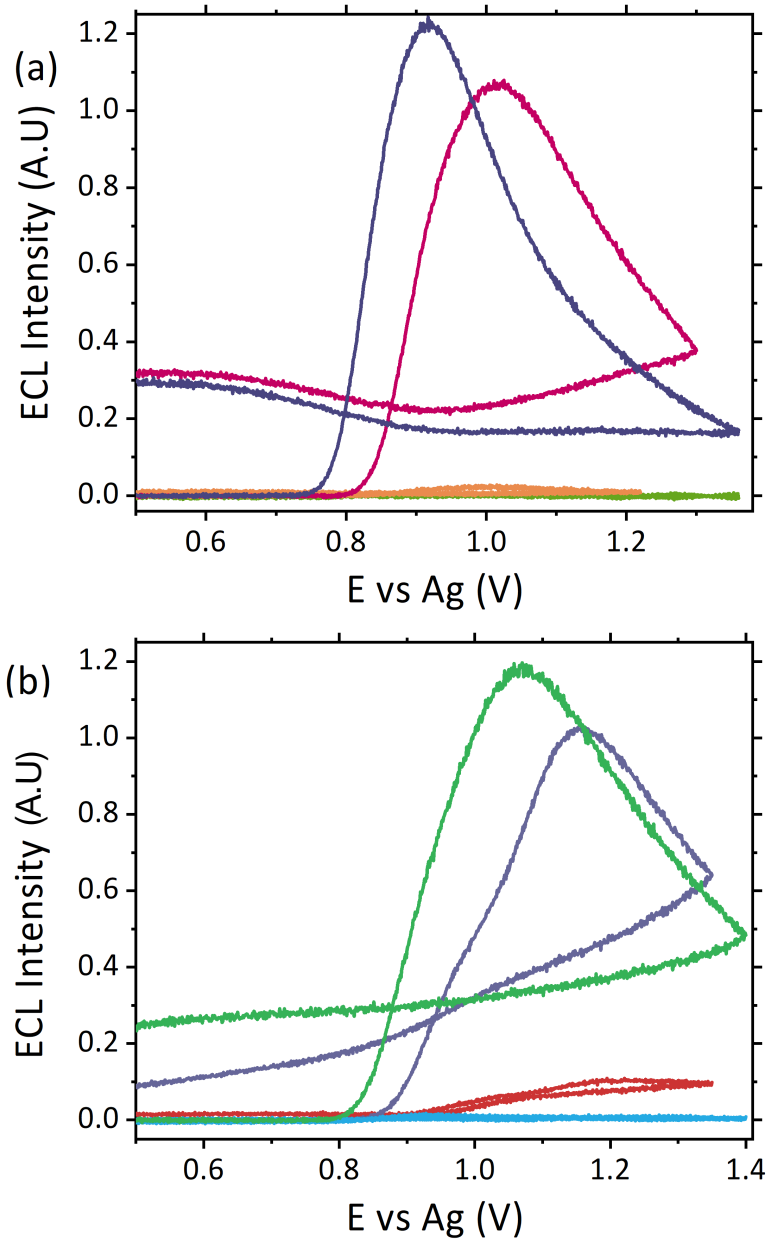

Figure 4.14: ECL responses obtained for (a) neat pH 8 Coca-Cola® without (orange) and with 50 µM atropine sulfate (pink), and $LiClO_4$ diluted pH 8 Coca-Cola® without (lime) and with 50 µM atropine sulfate (purple) and (b) neat pH 8 tonic water without (red) and with 50 µM atropine sulfate (purple), and $LiClO_4$ diluted pH 8 tonic water without (blue) and with 50 µM atropine sulfate (green) on $[Ru(bpy)_3]^{2+}$- modified electrodes at a scan rate of 100 mV s^{-1} over the potential range $0.5 \leq E \leq 1.4$ V vs Ag at a PMT setting of 0.45 V.

4.4 Conclusions

In this chapter the ability of a simple Nafion-$[Ru(bpy)_3]^{2+}$ film modified screen-printed carbon electrode sensor for the detection of atropine within a variety of complex sample matrices was demonstrated. In spite of the complex nature of the plant-based material, no significant interference effects were observed, despite the vast number of species present within such material. The developed sensor demonstrates a degree of selectivity toward alkaloid species, with a preference toward tropane alkaloids observed. Although a slight signal is observed for other naturally occurring glycoalkaoids found within herbal material, these signals can be considered negligible when compared with the hallucinogenic tropane alkaloids of interest, and as such, these naturally occurring alkaloids can be used as a threshold value above which it can be determined if hallucinogens are indeed present or not. The current methodology, however, does show limited selectivity between different tropane alkaloid species, as is apparent when comparing the emission signals between atropine and scopolamine. Further work is ongoing, with the hope of understanding the impact that scopolamine has on the detected signal within herbal material. However, this initial proof-of-concept demonstrates an appropriate screening method for the identification of hallucinogenic tropane alkaloids within herbal material. For the first time direct analysis of a species within its native form with differentiation between mature and young plants *Datura* via ECL achieved. This proposed protocol would negate the need to perform complex, expensive, and lengthy extraction procedures prior to analysis, making it ideal for field employment.

In addition to this, analysis of atropine within complex matrices of Coca-Cola® and tonic water, with and without the addition of electrolyte, with good % recoveries was achieved. Not only does this demonstrate the ability of ECL to be applied to non-ideal matrices, but also the ability to detect emission through coloured matrices, without any interference effects. These new methodologies would be ideal for future implementation into field analysis where often a rapid result is required with access to limited knowledge or facilities. However, the limited selectivity currently observed between species within the same class, and a dependence on pH to obtain emission may require samples to be pH-adjusted in-field prior to analysis. Despite this, these initial results have shown promise for the use of ECL sensors for the direct detection of species within their native form. This is a concept we are continuing to explore and hope to expand past atropine and scopolamine through the investigation of potential techniques that could be employed to improve the selectivity of the developed sensor in order to differentiate between compounds within the same class, such as atropine and scopolamine.

4.5 References

1. J. Tettey and C. Crean, *Philos. Trans. R. Soc., B*, 2015, **370**, 20140265.
2. L. Shaw and L. Dennany, *Curr. Opin. Electrochem.*, 2017, **3**, 23-28.
3. United Nations Publication, World Drug Report 2018, https://www.unodc.org/wdr2018/prelaunch/WDR18_Booklet_1_EXSUM.pdf, (accessed 9th October, 2018).
4. C. Banks and J. Smith, *The Analytical Scientist*, 2016, 41-43.
5. S. Reichert, C. Lin, W. Ong, C. C. Him and S. Hameed, *Canadian family physician Medecin de famille canadien*, 2017, **63**, 369-370.
6. O. Ramdani, J. P. Metters, L. C. S. Figueiredo-Filho, O. Fatibello-Filho and C. E. Banks, *Analyst*, 2013, **138**, 1053-1059.
7. P. Srivanitchapoom, S. Pandey and M. Hallett, *Parkinsonism & related disorders*, 2014, **20**, 1109-1118.
8. J. Gwiazda, Optometry and vision science : official publication of the American Academy of Optometry, 2009, **86**, 624-628.
9. M. Eddleston, N. A. Buckley, P. Eyer and A. H. Dawson, *The Lancet*, 2008, **371**, 597-607.
10. D. Johnson, Atropine, https://www.chemistryworld.com/podcasts/atropine/6546.article, (accessed 9th November, 2018).
11. B. Dräger, J. Chromatogr. A, 2002, **978**, 1-35.
12. S. Auriola, A. Martinsen, K.-M. Oksman-Caldentey and T. Naaranlahti, *J. Chromatogr. B: Biomed. Sci. Appl.*, 1991, **562**, 737-744.
13. L. Jianguo, C. Yuan and J. Huangxian, *Electroanalysis*, 2007, **19**, 1569-1574.
14. B. Yuan, C. Zheng, H. Teng and T. You, *J. Chromatogr. A*, 2010, **1217**, 171-174.
15. X.-Y. Yang, C.-Y. Xu, B.-Q. Yuan and T.-Y. You, *Chin. J. Anal. Chem.*, 2011, **39**, 1233-1237.
16. A. Zhang, C. Miao, H. Shi, H. Xiang, C. Huang and N. Jia, *Sens. Actuators B*, 2016, **222**, 433-439.
17. N. F. Atta, A. Galal and R. A. Ahmed, *Int. J. Electrochem. Sci*, 2012, **7**, 10365-10379.
18. H. Bagheri, S. M. Arab, H. Khoshsafar and A. Afkhami, *New J. Chem.*, 2015, **39**, 3875-3881.
19. A. A. Ensafi, P. Nasr-Esfahani, E. Heydari-Bafrooei and B. Rezaei, *Talanta*, 2015, **131**, 149-155.
20. P. Leroy and A. Nicolas, *J. Pharm. Biomed. Anal.*, 1987, **5**, 477-484.
21. Y. Gao, Y. Tian and E. Wang, *Anal. Chim. Acta*, 2005, **545**, 137-141.
22. R. A. Dar, P. K. Brahman, S. Tiwari and K. S. Pitre, *Colloids Surf., B*, 2012, **91**, 10-17.
23. Q. Xiang, X. D. Yang and Y. Gao, *Adv. Mater. Res.*, 2014, **989-994**, 1007-1010.
24. C. Song and J. Zhang, in *PEM Fuel Cell Electrocatalysts and Catalyst Layers: Fundamentals and Applications*, ed. J. Zhang, Springer London, London, 2008, DOI: 10.1007/978-1-84800-936-3_2, pp. 89-134.
25. Q. Cai, L. Chen, F. Luo, B. Qiu, Z. Lin and G. Chen, *Anal. Bioanal. Chem.*, 2011, **400**, 289-294.
26. M. D. Meti, S. T. Nandibewoor and S. A. Chimatadar, *Synth. React. Inorg., Met.-Org., Nano-Met. Chem.*, 2014, **44**, 263-272.
27. J. McGeehan and L. Dennany, *Forensic Sci. Int.*, 2016, **264**, 1-6.

28. F. Takahashi, S. Nitta, R. Shimizu and J. Jin, *Forensic Tox.*, 2018, **36**, 185-191.
29. R. J. Forster and C. F. Hogan, *Anal. Chem.*, 2000, **72**, 5576-5582.
30. O. Rosenheim, *Analyst*, 1907, **32**, 106b-108.
31. C. C. Fulton, Industrial & Engineering Chemistry Analytical Edition, 1931, **3**, 199-200.
32. L. C. Portis, V. V. Bhat and C. K. Mann, *J. Org. Chem.*, 1970, **35**, 2175-2178.
33. B. L. Laube, M. R. Asirvatham and C. K. Mann, *J. Org. Chem.*, 1977, **42**, 670-674.
34. W. D. Dettbarn, E. Heilbronn, F. C. G. Hoskin and R. Kitz, *Neuropharmacology*, 1972, **11**, 727-732.
35. P. Zvirblis, I. Socholitsky and A. A. Kondritzer, *J. Am. Pharm. Assoc.*, 1956, **45**, 450-454.
36. P. A. Greenwood, C. Merrin, T. McCreedy and G. M. Greenway, *Talanta*, 2002, **56**, 539-545.
37. B. Boros, Á. Farkas, S. Jakabová, I. Bacskay, F. Kilár and A. Felinger, *Chromatographia*, 2010, **71**, 43-49.
38. S. M. Oja and B. Zhang, *ChemElectroChem*, 2016, **3**, 457-464.
39. L.-H. Shen, H.-N. Wang, P.-J. Chen, C.-X. Yu, Y.-D. Liang and C.-X. Zhang, *J. Food Drug Anal.*, 2016, **24**, 199-205.
40. A. Nordon, A. Mills, R. T. Burn, F. M. Cusick and D. Littlejohn, *Anal. Chim. Acta*, 2005, **548**, 148-158.
41. M. Friedman, *J. Chromatogr. A*, 2004, **1054**, 143-155.
42. M. Friedman, C. E. Levin, S.-U. Lee, H.-J. Kim, I.-S. Lee, J.-O. Byun and N. Kozukue, *J. Agric. Food Chem.*, 2009, **57**, 5727-5733.
43. Y. Xu, Y. Gao, H. Wei, Y. Du and E. Wang, *J. Chromatogr. A*, 2006, **1115**, 260-266.

CHAPTER FIVE

ELECTROCHEMILUMINESCENT SENSORS AS A SCREENING STRATEGY FOR PSYCHOACTIVE SUBSTANCES WITHIN BIOLOGICAL MATRICES

“Giving up is for rookies”

Philoctetes (Hercules 1997)

This chapter comprises of publication:

K. Brown (primary author and principal investigator), C. Jacquet, J. Biscay, P. Allan and L. Dennany, Analyst, 2020, **145**, 4295-4304.

DOI: 10.1039/D0AN00846J

Abstract

With the rapid growth and appearance of novel psychoactive substances (NPS) onto the global drug market, the need for alternative screening methodologies for implementation within clinical environments is substantial. The immunoassay methods currently in use are inadequate for this new drug trend with the potential for misdiagnosis and subsequent administration of incorrect patient treatment increased. This chapter illustrates a strong proof-of-concept for the use of electrochemiluminescence (ECL) as a screening methodology for NPS, using the hallucinogenic compound scopolamine as a model compound. A low cost, easy-to-use and portable sensor has been developed and successfully employed for the detection of scopolamine at clinically relevant concentrations within a variety of biological matrices, including human pooled serum, urine, artificial saliva and sweat, without any prior sample preparation required. Moreover, assessment of the sensor's potential as a point-of-care wearable device was performed with sample collection from the surface of skin, demonstrating its capability for the qualitative identification of scopolamine despite collection of only minimal sample volumes off the skin's surface. The developed sensor exhibits a strong proof-of-concept toward the employment of such ECL sensors as point-of-care devices, where the sensor's ease of use and removal of time-consuming and complex sample preparation methods will ultimately increase its usability by physicians, widening the avenues where ECL sensors could be employed.

5.1 Introduction

Despite the global implementation of increased legislative controls to negate the use of novel psychoactive substances (NPS), they remain prevalent both within the drug community and market. NPS are typically designed to mimic the effects of traditional illicit substances but with an altered chemical structure, they were frequently outwith the control of the implemented drug legislation. Unsurprisingly, this resulted in an increased popularity amongst users as a result of their accessibility.[1-3] Despite their design to mimic the user effects of traditional drug substances they are often found to induce unexpected and unwanted side effects. Current knowledge regarding the pharmacological or pharmacokinetic mechanisms of these substances is limited; moreover, the continuous growth of NPS structural variations make it almost impossible for authorities or practitioners to maintain a working knowledge. The lack of understanding surrounding the pharmacokinetics of these substances is a significant problem; with no information on their bioavailability, elimination half-life, psychoactive effects, potency and toxicity available, life threatening side effects and fatalities are common.[4-6]

One of the most notable issues related to NPS use is the current lack of adequate screening protocols. The immunoassay methods typically utilised for the screening of traditional illicit substances, particularly within emergency rooms, are in adequate for the detection of NPS, often generating “false negative” or “false positive” results, indicating the consumption of a traditional illicit substance over an NPS, as a result of the structural similarities or

pharmacological targets of NPS to traditional drugs. As such clinicians, toxicologists, emergency physicians and forensic practitioners have been required to turn to alternative techniques for the screening of these substances. However, these alternative techniques available often include laborious and expensive detection methods utilising mass spectrometry, a technique not suited for screening methodologies, especially when combine with the rapid appearance of new NPS and lack of reference materials available for their identification.[4-7] This is especially relevant when considering the availability of such methods to emergency room physicians. Mass spectrometry is not only expensive to perform and maintain, but requires skilled personnel, time consuming sample preparation and available reference standards, all of which are not commonly available within a typical emergency room. Moreover, physicians require rapid answers to determine patient treatment to ensure any further health risks are minimised. As such, there is an urgent requirement for new screening methodologies to address this gap. Although required for a number of fields, there is a particular interest to focus upon methodologies appropriate for physicians, where the requirement for ease-of-use, low cost and rapid analysis is key.

Electrochemiluminescence (ECL) may hold a viable solution to this problem. ECL is a powerful technique with increased development in recent years resulting in its wide application across a number of different fields. ECL and other electrochemical (EC) based techniques have become popular within medical device and bioanalytical fields, largely owing to their significant

benefits over the more traditional techniques.[8-10] Primarily ECL and EC offer simplified instrumentation, increased operational simplicity and improved sensitivity. Uniquely the luminescence generated by ECL is controlled via the application of an applied external potential, negating the need for an external light source in contrast to alternative luminescence techniques. Removing this requirement allows for compact and lightweight instrumentation, ideal for portable or point-of-care devices. Furthermore, the cost of ECL instrumentation over the traditional analytical techniques of gas chromatography mass spectrometry (GC-MS) or liquid chromatography mass spectrometry (LC-MS), required for the identification of NPS such as scopolamine, is drastically decreased. Not only is the initial outlay cost of instrumentation vastly decreased, but the maintenance and operational costs are also significantly lower and do not require a dedicated instrument suite. In addition the minimal sample preparation and rapid analysis times, intrinsic to ECL, ensure it satisfies all requirements for use by emergency room physicians.[8-11] ECL based sensors therefore hold significant potential as viable alternatives to the current screening techniques employed within emergency rooms, particularly for NPS but also for the screening of the traditional illicit substances.

Scopolamine, a naturally occurring tropane alkaloid, is produced by members of the *solanaceous* family. Much like atropine, its sister tropane alkaloid and biosynthetic precursor, scopolamine has a history of recreational abuse attributed to its anticholinergic hallucinogenic effects. Despite its

hallucinogenic properties' scopolamine remains largely uncontrolled in a number of countries, where the tropane alkaloid producing plants are easily accessible, found even within domestic gardens.[12] Scopolamine is not only utilised for its hallucinogenic effects, but also for its suspected aphrodisiac, amnesic and submissive actions upon the user. These properties are likely related to the recent increase in the use of scopolamine for drug facilitate crimes, including sexual assaults, robberies and attempted murder.[12-17] Scopolamine's, often unknown, toxicity poses an increased risk to users, with unintentional poisonings and fatalities commonly reported despite the low amounts consumed. This was apparent in 2009, when an epidemic of scopolamine poisonings were reported in Oslo after the date-rape drug Rohypnol™ was adulterated with the tropane alkaloid[13]; while in 2018, Spain reported a number of drug facilitate crimes involving scopolamine.[18] Furthermore, the use of scopolamine as an incapacitating drug has been utilised among the South-American countries for decades.[12-18] Scopolamine's reported half-life is approximately 1 hour, reaching its maximum concentration approximately 20 minutes after ingestion of a therapeutic dose, equivalent to a 0.5 mg tablet.[19] One of the significant challenges when investigating the use of illicit substances within criminal activity, such as drug facilitated sexual assault, is the rapid metabolism and excretion of the compounds, making their detection after the matter extremely challenging. Under emergency room scenarios, however, with patients presenting with symptoms, it is probable that such substances are still within the detection window. Despite limited human studies upon the pharmacology and

pharmacokinetics of scopolamine, it has been successfully detected within the urine of different mammals between 24 to 106 hours following ingestion with a wide range of dosage percentages observed across different species.[16, 19, 20] However, the animal studies fail to provide the required knowledge on the excretion and metabolism pathways of scopolamine. The few human studies available indicate that scopolamine is rapidly removed from the blood and distributed around the body prior to liver metabolism, where less than 5% of the parent compound is renally excreted with, on average, an 8-hour half-life. Secondary drug excretion of scopolamine is suspected with reports of the parent compound found within hair, feces and breath.[19-21]

With scopolamine abuse increasing, a screening methodology capable of offering rapid detection is thus necessary. This chapter discusses the use of the previously described (chapter four) basic ruthenium based electrochemiluminescent sensor developed utilising screen-printed electrodes, which offers rapid detection with minimal sample preparation and volumes at a low cost. For the first time, the ability to detect scopolamine not only via ECL but also within complex biological matrices including, human serum, urine, artificial saliva and artificial sweat has been achieved. What's more, successful replication of sensor application to the surface of the skin was achieved and despite significantly low volumes of hallucinogen present, an easily identifiable signal was observed. By removing the requirement for sample preparation of biological fluids prior to analysis, it is hoped that such a

sensor would be ideal for implementation within emergency rooms, although also appropriate for a range of different fields, where physicians would be able to perform analysis bedside obtaining the rapid answers they require for patient treatment. A strong proof-of-concept for not only the developed sensor but for the use of ECL based devices for employment as point-of-care or in-field sensors has been demonstrated. These sensors could be easily used out with a laboratory environment by non-experts. The cost of this analysis in comparison to the mass spectrometry techniques currently employed for screening of NPS, such as scopolamine, is a significant advantage of such a design and stand to offer a viable alternative screening methodology that currently does not exist.

5.2 Experimental

5.2.1 Materials

Tris (2,2′-bipyridyl)-dichlororuthenium(II) hexahydrate ($[Ru(bpy)_3]\cdot Cl_2\cdot 6H_2O$), (–)-scopolamine hydrobromide trihydrate (Sc-HBr), lithium perchlorate ($LiClO_4$), urea, lactic acid, human pooled serum, Surine™ and 117 Nafion (~5% mixture of lower aliphatic alcohols and water) were purchased from Sigma-Aldrich. Absolute EtOH, arctic acid, aluminium chloride ($AlCl_4$) and sodium chloride (NaCl) were purchased from VWR Chemicals. All chemicals were used as received. All solutions were prepared in Milli-Q water (18 mΩ cm^{-1}). Artificial saliva (Bioténe® oral balance gel) and synthetic skin were commercially purchased and used as received.

5*.2.2 Instrumentation*

The electrochemical instrumentation and electrode materials used were previously described within section 3.2.2.

5.2.3 Fabrication of $[Ru(bpy)_3]^{2+}$ / Nafion ECL Sensor

The [Ru(bpy)3]2+/Nafion film modified carbon paste screen printed electrode was fabricated following the same procedure as described within section 3.2.3.Prior to sample measurements, to ensure a stable signal, electrodes were preconditioned by performing three subsequent CV cycles over the potential range of interest within the electrolyte solution to achieve a stable signal. For biological fluid analysis preconditioning was performed within the

respective matrix. For off-skin sample analysis no preconditioning was performed.

5.2.4 Preparation of Biological Samples

All samples were prepared via spiking of the selected matrix with the required volume of 5 mM scopolamine hydrobromide prepared in H_2O to produce the desired concentration. Human pooled serum samples were stored at -80^{o}C and fully defrosted at room temperature prior to spiking and measurement. Artificial sweat was prepared following the ISO 3610-2 guidance.[22, 23] Artificial saliva and synthetic urine were commercially purchased and spiked with scopolamine as required.

5.3 Results and Discussion

5.3.1 ECL Detection of Scopolamine

Tropane alkaloids, scopolamine and atropine, have demonstrated the ability to reliably behave as co-reactants producing ECL through the oxidative-reduction pathway.[24-26] As previously observed for atropine (chapter four), scopolamine's limited redox activity, results in minimal oxidation of the species upon unmodified carbon electrode surfaces. At significantly higher concentrations a measurable oxidation signal can be obtained, with irreversible oxidation occurring at +1.3 V vs Ag, see Figure 5.1a. At the concentrations of interest, however, direct electrochemical oxidation is not sufficient for viable detection methods. However, in the presence of $[Ru(bpy)_3]^{2+}$, mediated oxidation of the tropane group via the electrogenerated Ru^{3+} species, facilities light emission through the oxidative-reduction pathway with a maximum ECL intensity observed at +0.9 V, see Figure 5.1b. The ECL mechanism undertaken by scopolamine is believed to follow a similar pathway to that observed in analytical studies of other structurally similar amine species.[25, 27, 28] Currently there is limited literature available on the electrochemical detection of scopolamine itself. Da Costa Oliveira *et al.*[29] and Florea *et al.*[30], have previously reported the direct electrochemical detection of scopolamine utilising boron doped diamond and graphite screen printed electrodes respectively. To date the detection of scopolamine via ECL has largely been achieved through the employment of prior separation strategies[31-33], with its use as a direct detection method minimal.[25, 26]

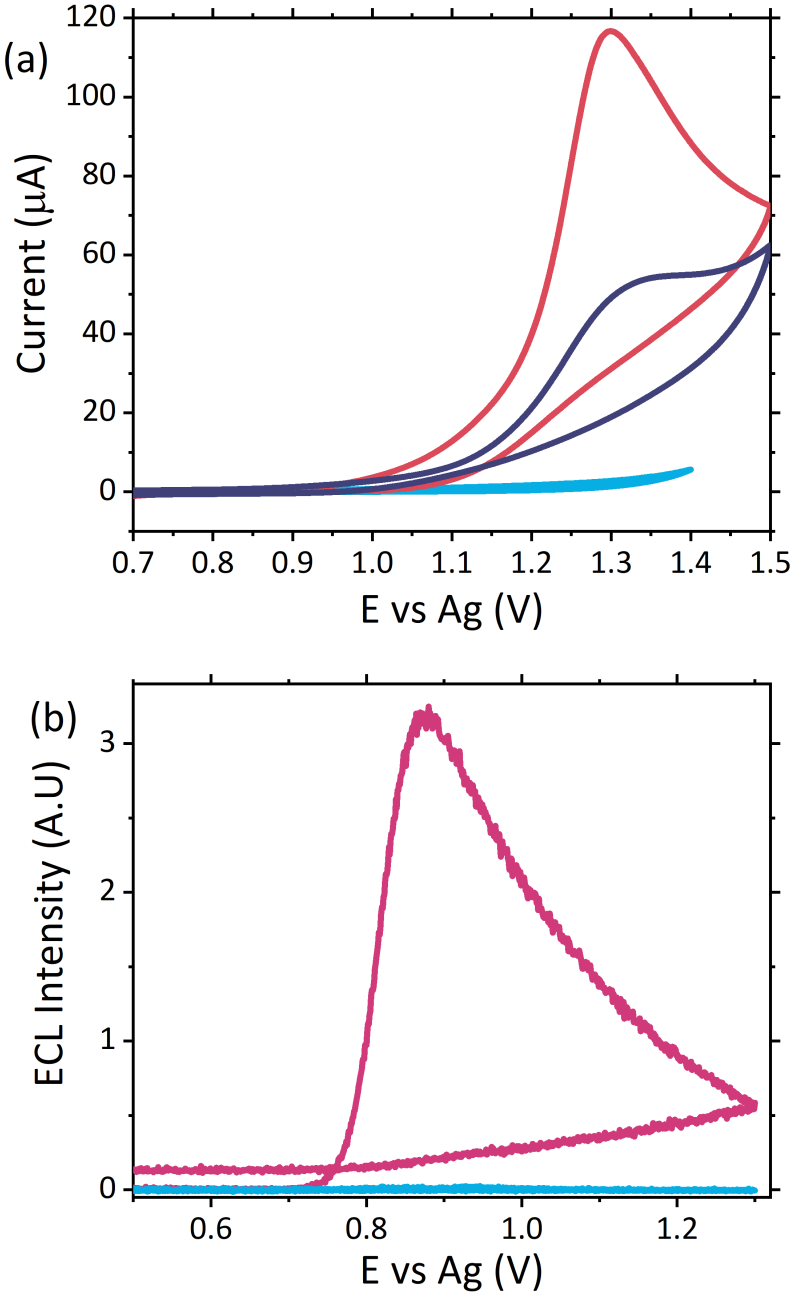

Figure 5.1: (a) CV responses of 0.1 M $LiClO_4$ (blue), 1.25 mM (purple) and 2.5 mM (pink) scopolamine hydrobromide at an unmodified carbon SPE and (b) ECL response of 0.1 M $LiClO_4$ (blue) and 50 µM scopolamine hydrobromide (pink) at a $[Ru(bpy)_3]^{2+}$ film modified carbon working electrode. Both measurements were collected at scan rate of 100 mV s^{-1} across a potential range of $0.5 \leq E \geq 1.5$ V vs Ag at a PMT setting of 0.4 V, with $LiClO_4$ as the supporting electrolyte.

Scheme 5.1: Mechanism for the oxidative *N*-dealkylation responsible for the ECL emission of scopolamine (a) leading to the formation of norscopolamine (e) and formaldehyde (f)

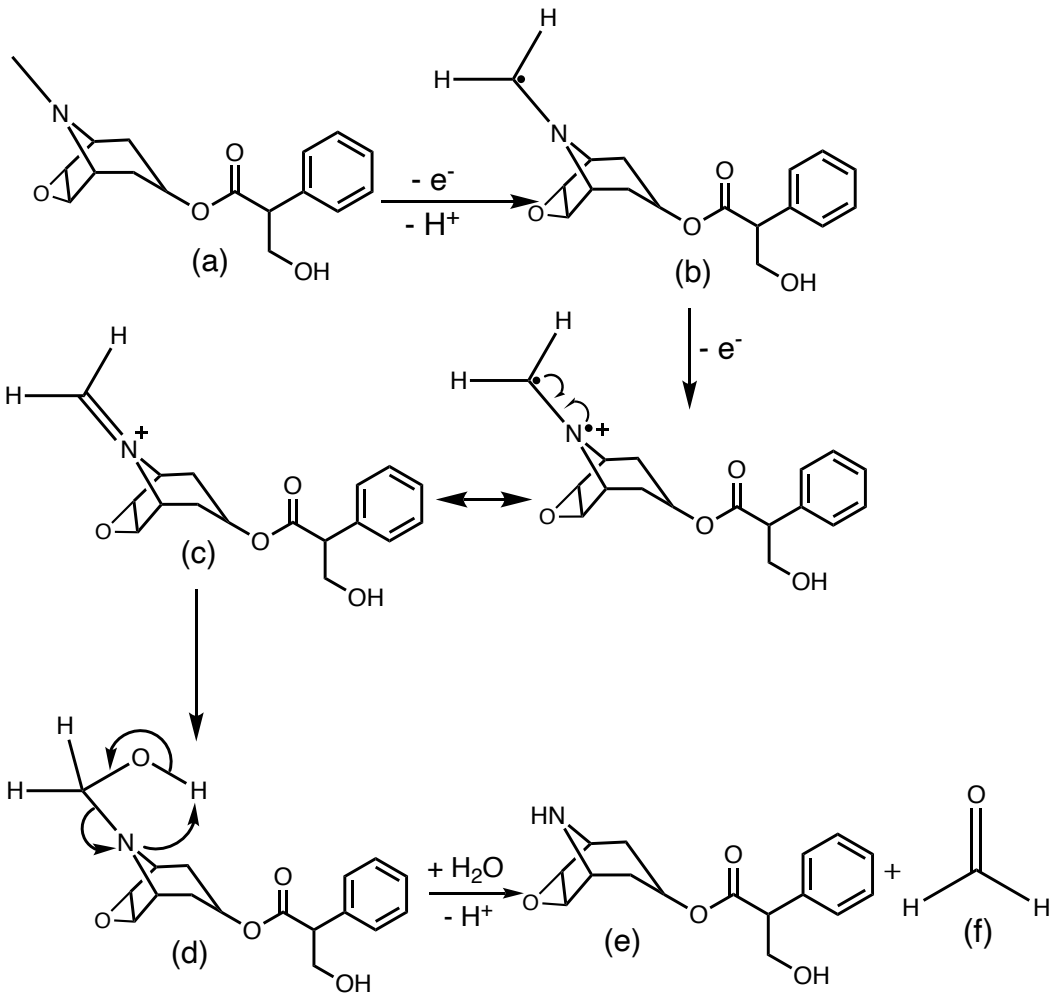

The structural similarities, typically indistinguishable oxidation potentials and chemically irreversible electro-oxidation of scopolamine generating by-product formaldehyde, suggests that it follows the same oxidative *N*-dealkylation mechanism as previously proposed for atropine, refer to section 4.3.1.[25] This mechanism based upon those observed for structurally similar tropanes[34] and tertiary aliphatic amines[35] is responsible for the ECL emission of scopolamine. The irreversible oxidation observed can be attributed to the electrolytic degradation of scopolamine, forming a secondary amine species at the tropane ring (norscopolamine) alongside formaldehyde. The oxidative-reduction mechanism proposed is summarised within scheme 5.1 and equations (5.1) to (5.5). The Ru^{3+} species generated at the electrode surface during the forward potential sweep (5.1) is required for the subsequent mediated oxidation of scopolamine following (5.2), which generates the highly reducing intermediate scopolamine• (a neutral radical species) (5.3). This scopolamine radical (b) then undergoes homogenous electron transfer with the remaining Ru^{3+} species to produce the excited Ru^{2+*} species, which upon relaxation emits a photon of a characteristic wavelength in this case 614 nm. Following this homogenous electron transfer reaction, the imminium cation (c) formed decomposes via hydrolysis and subsequent *N*-dealkylation generating formaldehyde and the secondary amine species, norscopolamine (e).

$$[Ru(bpy)_3]^{2+} \leftrightarrow [Ru(bpy)_3]^{3+} + e^- \quad (5.1)$$

$$[Ru(bpy)_3]^{3+} + scopolamine \rightarrow [Ru(bpy)_3]^{2+} + scopolamine^{+\bullet} \quad (5.2)$$

$$scopolamine^{+\bullet} \rightleftharpoons scopolamine^{\bullet} \quad (5.3)$$

$$[Ru(bpy)_3]^{3+} + scopolamine^{\bullet} \rightarrow [Ru(bpy)_3]^{2+*} + (f) + (e) \quad (5.4)$$

$$[Ru(bpy)_3]^{2+*} \rightarrow [Ru(bpy)_3]^{2+} + h\nu \quad (5.5)$$

The dependence of ECL signal intensity with sample pH is dictated by the molecule's dissociation mechanism. pH determines whether the oxidisable form of the molecule is dominant under different pH conditions. Chapter four discusses the trend observed for atropine's ECL intensity with varying pH. As expected scopolamine displayed a similar trend as seen for atropine and other structurally similar amine species, refer to Figure 5.2.[25, 26, 36, 37] As such, the maximum ECL intensity was obtained at pH 8 close to the compounds pKa of 7.75.[38] Moreover, measurable signals were obtained across the entire pH range investigated for scopolamine, although to varying intensities. The ability to obtain a measurable signal across a range of pH values presented a unique opportunity to utilise this intrinsic characteristic of the sensor for the analysis of biological fluids, where samples with a range of pH values would be encountered.

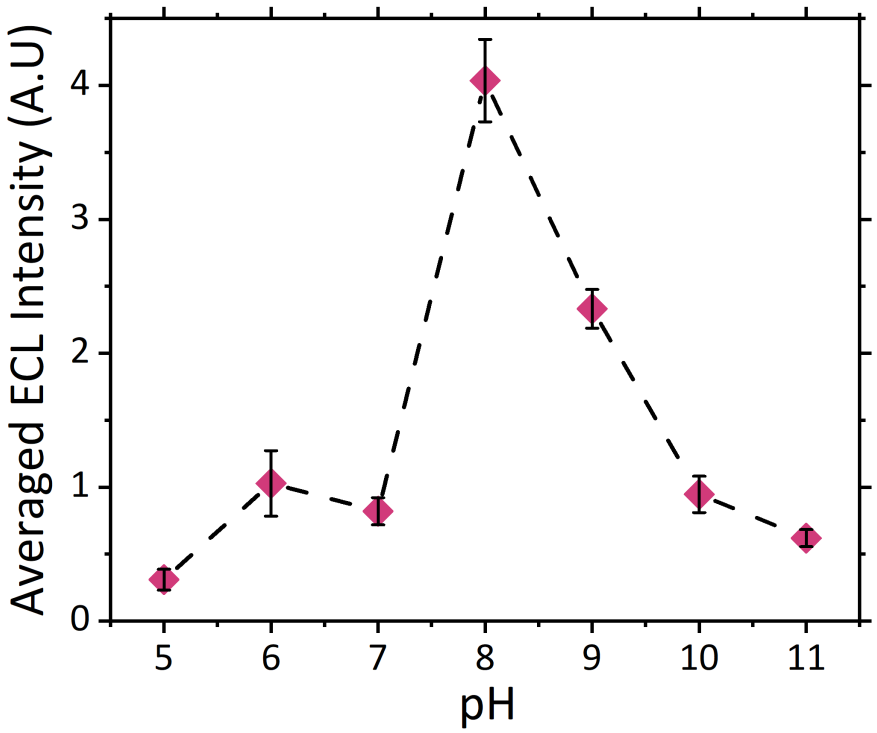

Figure 5.2: Trend in ECL intensity with pH for scopolamine hydrobromide prepared in 0.1 M $LiClO_4$ at the desired pH. Measurements were collected at a scan rate of 100 mV s^{-1} across $0.5 \leq E \leq 1.36$ V vs Ag at a PMT setting of 0.6 V. Each point represents the mean of the maximum ECL intensity at n=3 with error bars comprising of ± 1SD across these measurements.

5.3.2 Biological Fluid Analysis

The $[Ru(bpy)_3]^{2+}$ film SPE sensor utilised here for the analysis of biological fluid samples has previously demonstrated satisfactory analytical performance (refer to section 4.3.3), offering suitable detection limits, sub μM, and the required precision, with electrode reproducibility of 1.9% and repeatability of 8.3%. As such, the designed sensor offers an ideal analysis tool for the screening of biological fluids for illicit substance detection.

5.3.2.1 Human Pooled Serum Analysis

The dose of scopolamine administered for criminal and predatory use has been reported between 0.99 and 6.23 μM in blood (0.0003 to 0.00189 mg mL^{-1}), which is approximately 50 to 3000 times the typical therapeutic dose from a single dermal slow release patch administered over a 24 hour period, resulting in an approximate therapeutic blood concentration of 0.99 nM ($3.0x10^{-7}$ μg mL^{-1}).[14, 15, 39] Despite the therapeutic concentration of approximately 0.99 nM lying out with the detection limits achievable with this current screening methodology, such low concentrations would not induce the adverse symptoms which would result in users requiring emergency treatment. As such, there is currently no significant demand for emergency room screening protocols to operate within the nM region.

No sample preparation was performed on serum samples, which were analysed neat. Neat serum was spiked to give a final concentration of 1 μM scopolamine hydrobromide. Once spiked with the hallucinogen, the serum

sample was analysed directly upon the ruthenium modified electrodes. Figure 5.3a shows a comparison of the voltammograms obtained with the ruthenium modified electrodes. Despite the complexity and likely resistance to charge transfer of neat serum, the voltammograms obtained demonstrate its ability to offer the conductivity necessary for use as a suitable electrochemical matrix. This is confirmed through the comparable peak-to-peak separations of the $Ru^{2/3+}$ redox couple within serum and a typical supporting electrolyte of 0.1 M $LiClO_4$, with ΔE_p values of 136 mV for serum and 134 mV for 0.1 M $LiClO_4$ achieved. The difference in the E0, E_{pa} and E_{pc} values can be attributed to the use of the non-isolated quasi-reference electrode comprising of screen-printed silver paste, in contrast to the typical isolate Ag/AgCl reference utilised within standard cell setups.

Analysis of neat serum revealed that species intrinsic to the matrix produced a measurable signal, within the potential range of interest to that of scopolamine. This is not entirely surprising given the complex composition of serum, containing a wide variety of amino acids and proteins, which have been previously shown to produce ECL with the $[Ru(bpy)_3]^{2+}$ luminophore.[40-44] Previous ECL analysis within extracted and purified serum has demonstrated a similar ECL response from serum when analysed with $[Ru(bpy)_3]^{2+}$ luminophore.[45] Further analysis of four of the common amino acids; proline, tryptophan, glutamine and lysine, with the developed sensor and a supporting electrolyte of $LiClO_4$, confirmed their ability to behave as suitable ECL co-reactants, refer to Figure 5.4. As such, ruthenium based ECL

sensors' specificity will be negatively impacted within biological fluids, due to the presence of free amino acids. Although under ideal electrochemical conditions these free amino acids produced intensities comparable to scopolamine see Figure 5.4, when compared to the signal intensity observed within raw serum (see Figure 5.3b) there is a significant visual difference between the neat matrix and that of 0.1 μM scopolamine. This background response intrinsic to serum can likely be attributed to the low concentration of free amino acids present within the serum, which generates this response. A brief investigation across six pooled serum samples demonstrated a degree of variation in the intrinsic background signal, shown within Figure 5.5. With an RSD of 17% across pooled serum samples, there is in turn a high likelihood of the background serum response varying across individuals. This variation could be influenced by an individual's health, whether blood collection was performed fed or fasted or prescribed medication. To establish a thorough understanding of this variation, a comprehensive clinical study is required, although beyond the scope of this current proof-of-concept study it would be erroneous to not consider the potential impact this could have. Although variation was observed across the pooled serum samples a threshold signal of 0.498 A.U. could be established lying well below the lowest concentration of 0.1 μM analysed at an intensity of 1.23 A.U. However, this by no means represents a true threshold value, as clinical studies across a range of individuals would be required to establish this.

The use of raw serum as a sample matrix without performing any prior purification procedures poses an increased risk of false identification within biological fluids. However, the significant visual difference observed between the matrix without the hallucinogen and with a clinically relevant concentration displays a strong premise for its use as a screening tool for serum samples. Screening protocols rely upon qualitative identification, a prerequisite met by this proposed methodology. Even at significantly low scopolamine concentrations of 0.5 μM and 0.1 μM, both of which lie below scopolamine's LD_{50} at an approximate concentration of 6.23 μM[39], an easily identifiable difference between neat serum and that containing the hallucinogen is observed, refer to Figure 5.3b. Analysis of the ECL signal in Figure 5.3b also reveals a shift in the potential at which the maximum ECL intensity is observed. This phenomenon is something which has been previously observed with increasing concentrations of co-reactants at the ruthenium sensor (chapter 4 section 4.3.3).[25, 26] As such, it is likely this observed shift can be attributed to the two main effects previously reported[25, 26, 46]; ruthenium becoming the rate limiting reagent and a pH alternation at the inner Helmholtz plane close to the electrode surface. As the ruthenium within the sensor becomes the rate limiting reagent, oxidation of the species required to produce ECL becomes more difficult with the luminophore consumed at a rate quicker than it can be produced. Secondly, as higher concentrations of scopolamine are present, there is a greater concentration of the oxidative *N*-dealkylation by-products, formaldehyde and norscopolamine, resulting in a shift in pH at the inner Helmholtz plane. The

signal observed at 0.1 μM lies at the limit of detection (LOD), where the LOD was determined at 3 times the blank signal observed from neat serum. As such with a low LOD confidence in the sensor's ability to operate as a qualitative screening tool at clinically relevant concentrations is provided.

Despite the frequent use of blood and subsequently serum for drug detection, the need to separate serum from blood prior to analysis still poses a significant limitation. Furthermore, the collection of blood from a patient is still considered an invasive procedure. The extraction of serum from the collected whole blood matrix requires time consuming sample preparation, specialist equipment and expertise. As such this fails to meet the requirement for point-of-care devices for use by physicians. Although the ability to overcome this sample preparation step through the use of whole blood samples offers a possible solution, the limited penetration of visible light through whole blood prevents detection of the electrogenerated luminescence from the ruthenium complex with an emission maximum at 614 nm.[47]

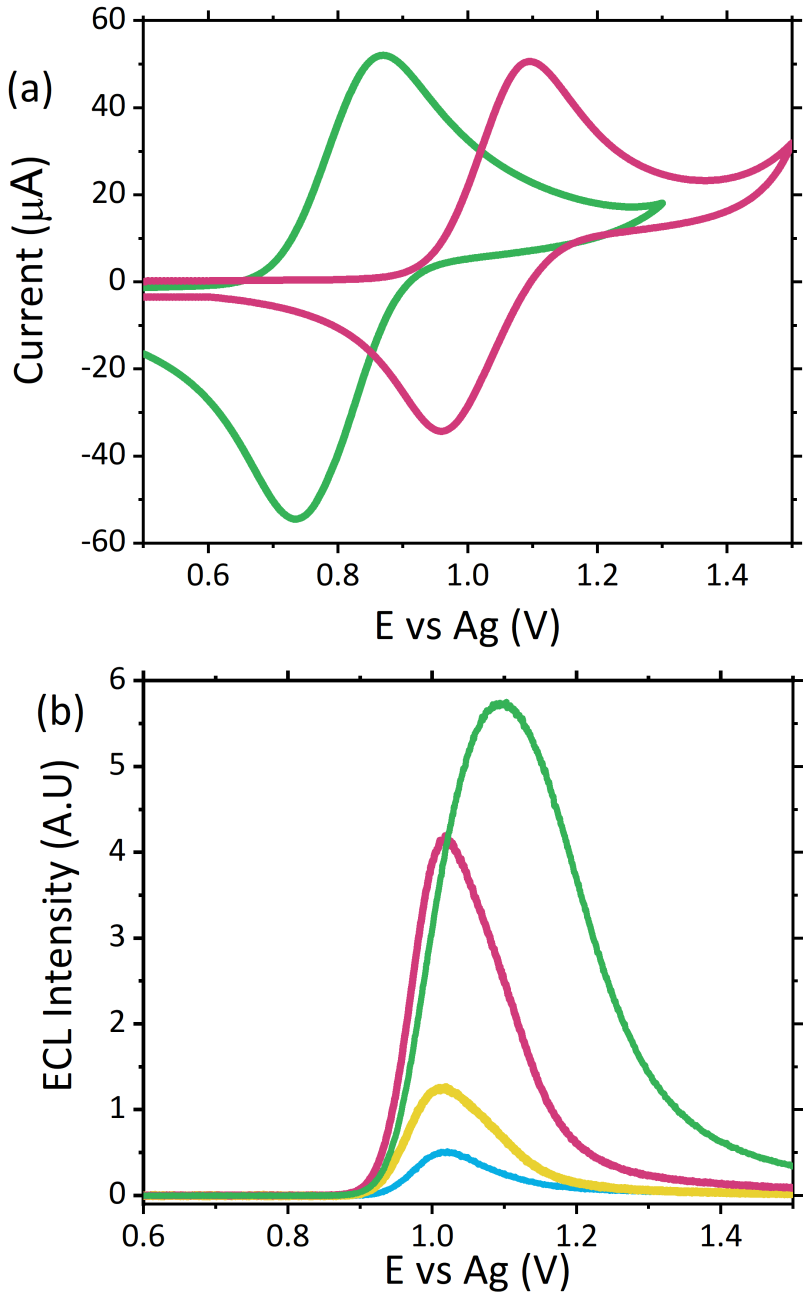

Figure 5.3: (a) CV of $Ru^{2+/3+}$ redox couple in $[Ru(bpy)_3]^{2+}$ film with comparable ΔE_p values in 0.1 M $LiClO_4$ (green) and neat serum (pink) and (b) ECL responses of neat serum (blue) and 1 μM (green), 0.5 μM (pink) and 0.1 μM (yellow) scopolamine hydrobromide in human pooled serum collected with the $[Ru(bpy)_3]^{2+}$ film modified carbon working electrode at a scan rate of 100 mV s^{-1} across a potential range of $0.5 \leq E \geq 1.5$ V vs Ag and a PMT setting of 0.48 V. The use of the quasi-reference electrode accounts for the difference in the E0 values.

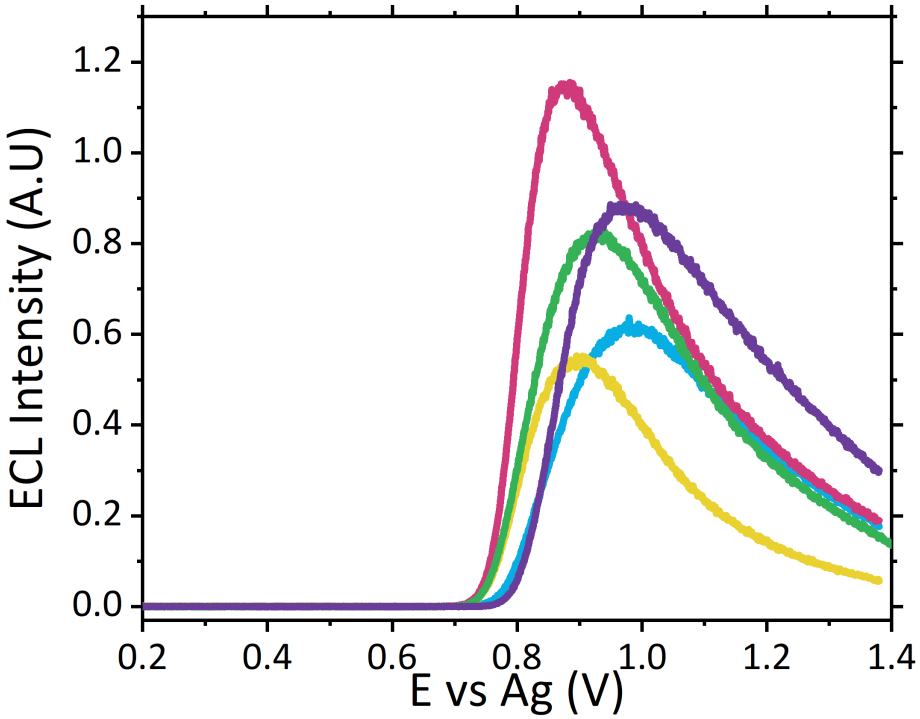

Figure 5.4: ECL responses of 50 μM scopolamine hydrobromide (purple), 60 μM tryptophan (blue), 600 μM glutamine (yellow), 300 μM lysine (pink) and 300 μM proline (green) at a $[Ru(bpy)_3]^{2+}$ film modified carbon working electrode collected at a scan rate of 100 mV s^{-1} across a potential range of $0.2 \leq E \geq 1.4$ V vs Ag at a PMT setting of 0.4 V.

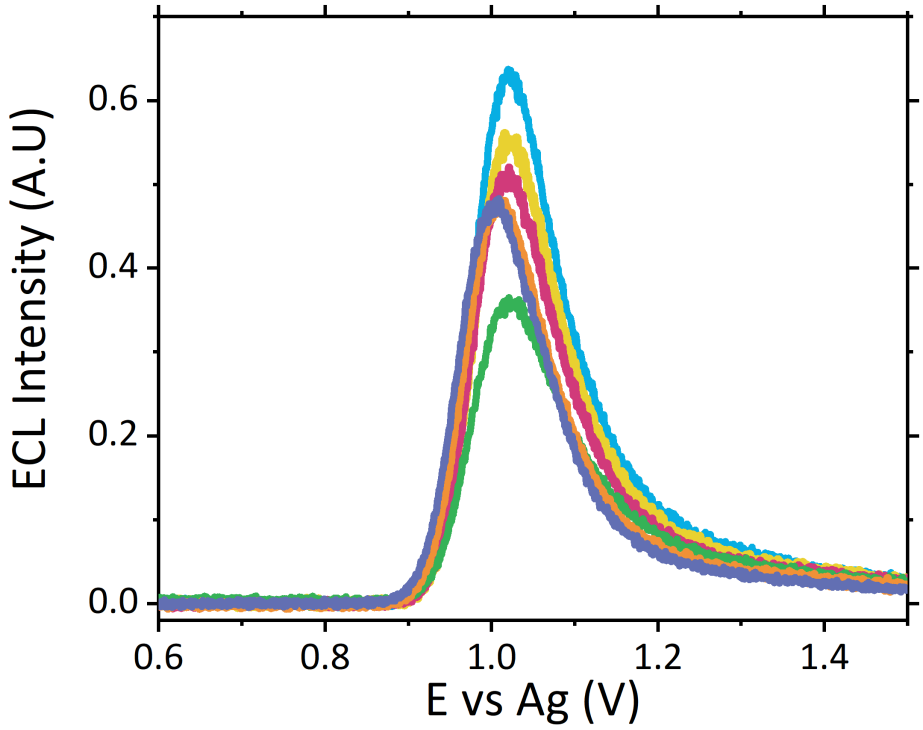

Figure 5.5: ECL responses of six neat pooled serum samples collected with the $[Ru(bpy)_3]^{2+}$ film modified carbon screen printed working electrode at a scan rate of 100 mV s^{-1} across a potential range of 0.6 ≤ E ≥ 1.5 V vs Ag and a PMT setting of 0.48 V.

5.3.2.2 Urinary Analysis

With limited pharmacological studies on scopolamine available, little is known regarding its metabolism and excretion pathways. However current studies suggest scopolamine undergoes a first pass metabolism, with ~ 5% of the parent drug renally excreted. As such, it was important to assess sensor performance within this matrix. As with serum, no sample preparation was performed, with all samples analysed neat within Suirne™ without dilution or purification. In contrast to serum, urine produced an anodic peak at +1.11 V vs Ag at the unmodified carbon electrode surface, see Figure 5.6a. Previous electrochemical analysis of urine displayed a similar oxidation peak at +1.0 V vs Ag/AgCl[29] and was attributed to the presence of uric acid, which has previously been shown to undergo oxidation at carbon electrodes.[29, 48] The same anodic peak is observed at the ruthenium modified electrode, at +1.16 V vs Ag, refer to Figure 5.6a, and as such obscures the reversible $Ru^{2+/3+}$ couple normally observed. The ECL response of the urine matrix, shown in Figure 5.6b, displays significant background signal from the matrix, comparable to that observed in serum. Previous analysis of urine via ruthenium based ECL has documented the occurrence of a background emission from the matrix[49-51], as such the emission observed here is not unexpected. Although the presence of uric acid produced the oxidation peak within the CV, it has been previously demonstrated that uric acid behaves as an ECL quencher toward the tripropylamine $[Ru(bpy)_3]^{2+}$ system and hence it is not assumed to be responsible for the emission peak observed within the blank urine matrix.[51, 52] Similarly, urea and ascorbic acid are also known to

effectively quench emission from $[Ru(bpy)_3]^{2+}$ generated ECL during urinary analysis.[51-53] As such it is believed that the emission signal intrinsic to the urine matrix is instead related to the presence of lactic acid and creatinine, both of which have previously been shown to produce ECL emission with ruthenium luminophores.[41, 54-56] Scopolamine hydrobromide was spiked into the urine matrix at a range of clinically relevant concentrations from 0.5 to 6 μM. As can be seen within Figure 5.6b, a distinct visual difference across all concentrations was apparent, with 6 μM at an intensity ~ 5.3 times that of the blank. In comparison to the serum matrix, sensitivity was reduced, with the LOD ten times greater than that of serum. It is thought this could be related to competing reactions as a result of the presence of the known quenchers of ascorbic acid, urea and uric acid. Signals obtained at 0.5 μM and 1 μM lie below that of the typical analytical standard of three times the blank intensity. However, if a threshold signal could instead be established, then signals above this value could be attributed to presence of the hallucinogen, facilitating qualitative identification. Initial studies established the threshold at 0.7 A.U across three electrode measurements. However further investigation would be warranted to determine whether this value would be affected from person to person variation from clinical human urinary samples. As such, despite urine's position as the most frequently used toxicological sample for drug detection and negates the requirement for sample extraction, as is required for serum from whole blood, the reduced sensitivity as a result of the competing quenching reactions would limit its use as a point-of-care device in its current format.

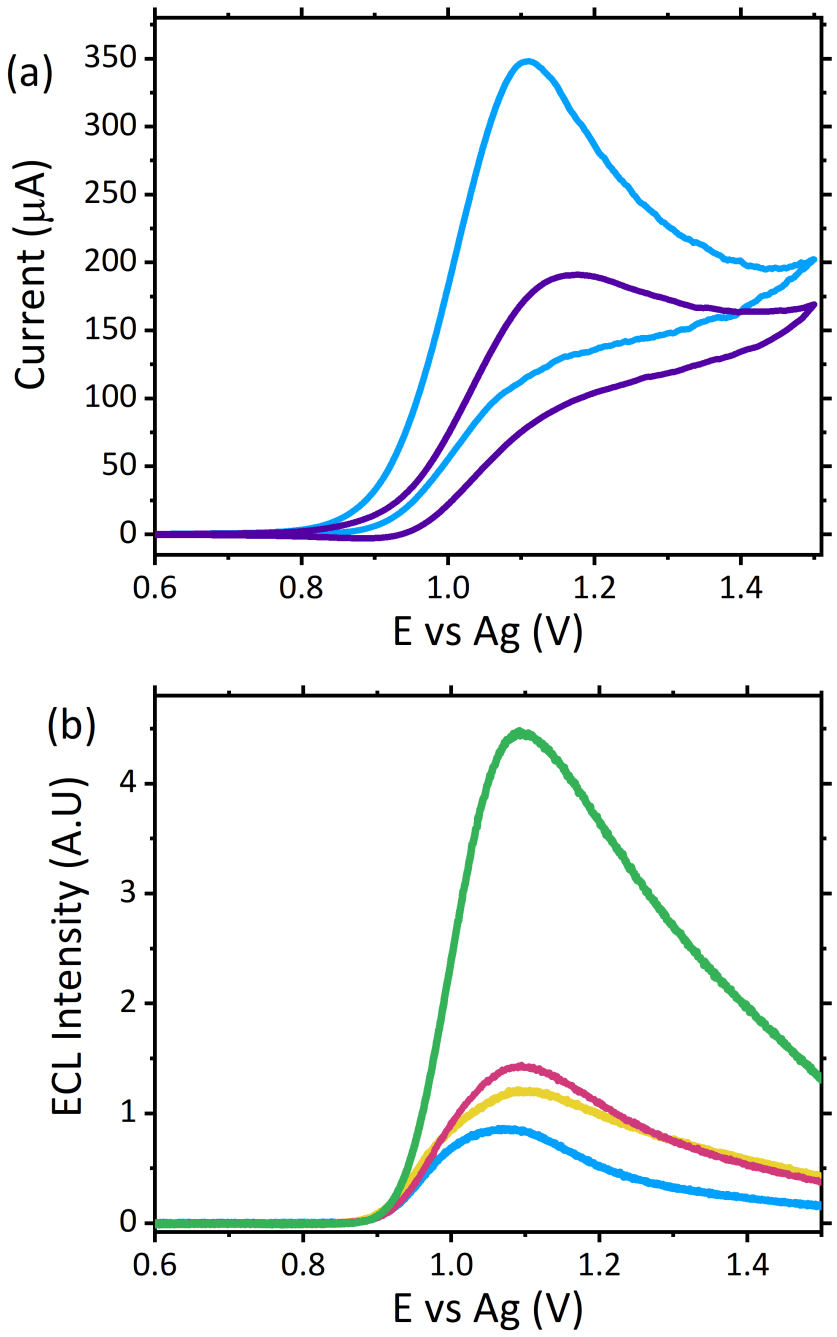

Figure 5.6: (a) CV responses of Surine™ on unmodified carbon SPE (blue) and Surine™ on $[Ru(bpy)_3]^{2+}$ film modified carbon working electrode (purple) and (b) ECL responses of Surine™ (blue) and Surine™ spiked with 6 μM (green), 1 μM (pink) and 0.5 μM(yellow) scopolamine hydrobromide with the $[Ru(bpy)_3]^{2+}$ film modified carbon working electrode. Both measurements were collected at a scan rate of 100 mV s^{-1} across a potential range of $0.5 \leq E \geq 1.5$ V vs Ag and a PMT setting of 0.48 V.

5.3.2.3 Analysis of Artificial Saliva

A potential alternative biological matrix that could easily be collected from a patient presenting with symptoms is saliva. Saliva offers a number of advantages over blood and serum as a sample matrix. Collection of saliva can be considered less invasive for patients. What's more saliva, unlike blood, would not require sample preparation prior to analysis, with visible light able to easily penetrate through the matrix for analyte detection. Previous analysis of saliva via ECL has been reported, however they have required either buffer dilution or incorporation into an immunoassay format, rather than a direct detection method, as proposed within this chapter.[55, 57-59]

The compatibility of the proposed ECL sensor for direct saliva analysis was investigated through the use of artificial saliva, containing a number of the active enzymes naturally present within human saliva. Neat artificial saliva was not observed to produce a significant ECL emission as shown within Figure 5.7a. This is in contrast to human serum and urine (refer to Figure 5.3b and Figure 5.6b), whereas a result of the free amino acids, lactic acid and creatinine notable ECL responses from the biological matrix is observed. This, therefore, suggests that the enzymes present within saliva do not behave as suitable co-reactants toward the ruthenium complex utilised within this sensor design. When the artificial saliva sample was spiked with high scopolamine concentrations at 10 μM, a clear visual difference between the neat matrix and that which contains the hallucinogen was observed, refer to Figure 5.7a. However, this concentration is greater than what would be

clinically observed, as such the concentration was decreased to 1 μM to established the sensor's potential for clinical translation. Despite this significant concentration decrease, again a distinct visual difference between the blank biological matrix and that containing the hallucinogen is observed. In contrast to serum, where a LOD of 0.1 μM was obtained, here the LOD will be approximately ten times greater, comparable to urinary analysis, with the 1 μM intensity observed at four times that of the blank. This poorer sensitivity within saliva could be attributed to the poorer electron transfer kinetics observed within this matrix as a result of its higher viscosity. As such, as can be seen through interrogation of the CV (refer to Figure 5.7b), the ruthenium redox couple displays flatter and broader peaks with an increased ΔE_p at 399 mV. This increase in ΔE_p is likely related to the increased resistance of the more viscous matrix toward charge transfer. As such, a large Ohmic drop will be observed, contributing to the large peak-to-peak separation observed. Thus, with the poorer electron transfer kinetics present within this viscous matrix, the decreased sensitivity compared with serum is not surprising. However, the unmistakable difference in ECL intensity at 1 μM does nevertheless meet the requirements for use as a qualitative tool for identification of the hallucinogen within saliva at clinically relevant concentrations. As such, the ECL sensing platform does meet the prerequisites for use as a saliva screening tool without any pre-treatment or purification required.

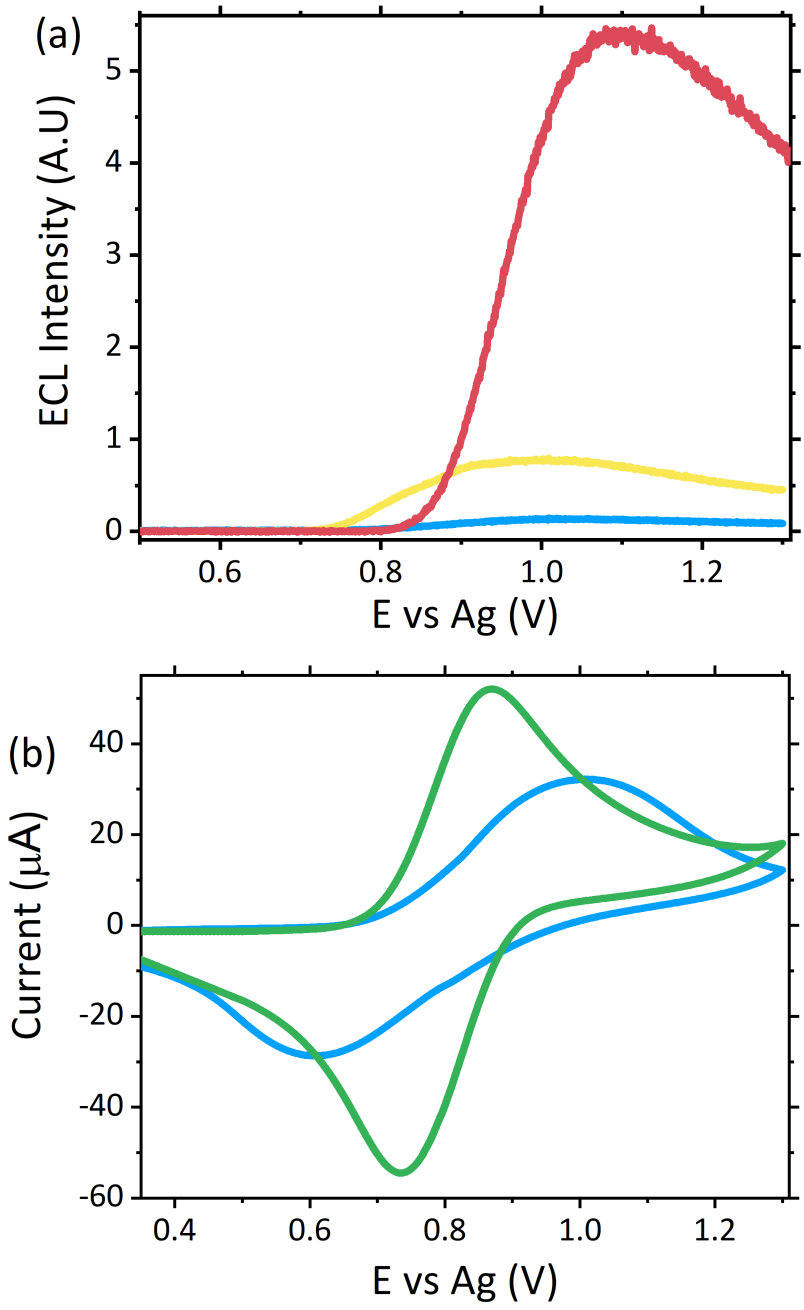

Figure 5.7: (a) ECL responses of artificial saliva (blue) and artificial saliva spiked with 10 μM (pink) and 1 μM (yellow) scopolamine hydrobromide and (b) CV responses of 0.1 M $LiClO_4$ (green) and neat artificial saliva (blue). All measurements were collected on $[Ru(bpy)_3]^{2+}$ film modified carbon working electrode at a scan rate of 100 mV s^{-1} across a potential range of $0.2 \leq E \geq 1.3$ V vs Ag and a PMT setting of 0.48 V.

5.3.2.4 Analysis of Artificial Sweat

With serum, saliva and urine providing suitable matrices for the ECL analysis of biological fluids, the potential for the use of sweat provided a promising avenue. The ability to use sweat for drug screening would offer a minimally invasive technique, which could offer a viable alternative matrix for emergency room physicians. Patients experiencing significant hallucinogenic symptoms, under severe distress or intubated due to respiratory issues could make the collection of serum, urine or saliva for physicians challenging, particularly when rapid results are required. Thus, sweat which can be easily collected from the skin's surface offers a practical alternative. As with the previous matrices, sweat itself did possess a small intrinsic signal, likely related to the presence of the different biological and salt components, including lactic acid, previously reported to produce an ECL emission.[60-62]

Figure 5.8a displays the ECL response observed when scopolamine was present within artificial sweat at a concentration of 10 μM. Comparable to that observed within the saliva, a significant visual difference between the neat matrix and that containing the hallucinogen was observed. Furthermore, when the concentration was decreased to the clinically relevant concentration of 1 μM, a distinct visual difference at an intensity 3.4 times greater than the blank matrix signal allowed for the clear differentiation between the natural matrix and when the hallucinogen was present. As such, this methodology allowed for confident identification of scopolamine within sweat. However, prior to implementation as a point-of-care device, it would again be necessary

to establish a threshold signal which would account for person to person variation and any further potential interferents as a result of the consumption of medications, alcohol or any other substances a patient may have consumed or applied to their skin. As such, to confidently establish such a threshold value further investigation is warranted as with the other matrices investigated.

To obtain the signals shown within Figure 5.8a a casting volume of 100 μL was employed. However, in reality the volume of sweat that would be collected from an individual's skin would indeed be far less. A wearable or surface applied sensor would therefore offer the most appropriate system for future point-of-care devices and also facilitate continuous real time patient monitoring. To determine the feasibility of this current sensor design for incorporation into a wearable device, the sensor was assessed for the collection and detection of scopolamine off synthetic skin. To perform these measurements synthetic skin was either soaked in blank sweat or sweat spiked with scopolamine for approximately 30 minutes, after which the skin was then removed. The skin coated with the corresponding sweat samples was then placed within a petrie dish to provide a flat surface to facilitate the mechanical wiping of the modified electrode. The electrode was slowly wiped across the surface of the skin by hand a total of three times to collect the sample, visually ensuring full electrode coverage prior to analysis. The geometry of the SPE is ideal for such applications due to the close proximity of all three electrodes, with a total area of 33 mm^2 requiring sample coverage.

While the flexible polymer support allows for the electrode to be manipulated with ease avoiding any damage to the electrode surfaces during this process. Despite a significant reduction in the volume of sample present upon the electrode surface, as can be seen within Figure 5.8b, the sample containing the hallucinogen can still be confidently identified from the blank sweat, at a signal intensity ~ 47 times greater.

As such, a strong proof-of-concept for the developed ECL sensor for employment as a wearable point-of-care device was demonstrated. However further investigation is once more warranted to establish whether the reported design is indeed appropriate for clinical translation. Human trials would offer the greatest understanding and knowledge regarding potential clinical translation. However, the toxicity of scopolamine and potential side effects at the required levels would prevent such trials from involving scopolamine, in turn preventing the attainment of genuine sweat samples from human skin following indigestion, metabolism and execration of the drug. Nevertheless, the successful use of ruthenium based ECL sensors for the analysis of human sweat on the skin and off surfaces have been recently reported[61, 62], and as such provides a degree of confidence that the proposed sensor detailed within this chapter would be fundamentally viable for clinical employment.

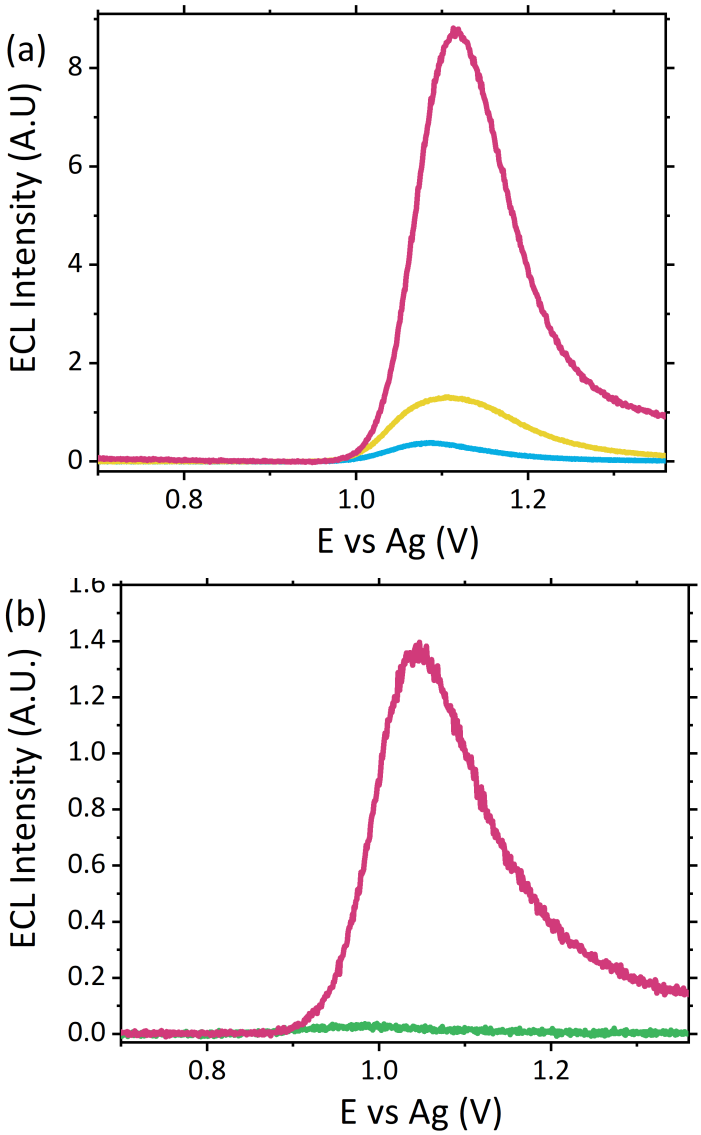

Figure 5.8: (a) ECL responses of artificial sweat (blue) and artificial sweat spiked with 10 μM (pink) and 1 μM (yellow) scopolamine hydrobromide with the $[Ru(bpy)_3]^{2+}$ film modified carbon screen printed working electrode at a scan rate of 100 mV s^{-1} across a potential range of 0.5 ≤ E ≥ 1.36 V vs Ag and a PMT setting of 0.48 V. (b) ECL responses of artificial sweat (green) and artificial sweat spiked with scopolamine hydrobromide (pink) collected off synthetic skin via mechanical wiping of the $[Ru(bpy)_3]^{2+}$ film modified carbon screen printed working electrode collected at a scan rate of 100 mV s^{-1} across a potential range of 0.5 ≤ E ≥ 1.36 V vs Ag and a PMT setting of 0.6 V.

5.4 Conclusion

A portable electrochemiluminescent sensor has been successfully developed for the detection of tropane alkaloid scopolamine within a variety of complex biological matrices. Utilising disposable screen-printed electrodes modified with a simple Nafion-$[Ru(bpy)_3]^{2+}$ film, a low-cost alternative to the complex instrumentation currently utilised for analysis of such samples is offered. This chapter details a qualitative sensor for the screening of the consumption of non-traditional drugs, such as novel psychoactive substances, alongside common illicit substances that may be encountered within a hospital emergency room. Within such clinical environments, an easily obtained and rapid “yes or no” answer is often required, a criterion met by the proposed methodology. Despite the complex nature of matrices such as serum, urine, saliva and sweat, no significant interference effects, which negatively impacted upon the qualitative analysis at clinically relevant concentrations, were observed. As such the ability to confidently distinguish between neat matrices and those containing the hallucinogen was possible. What’s more, the requirement for complex, time-consuming and costly sample extraction procedures, that would require specialist facilities and knowledgeable experts in a variety of sample extraction techniques, was removed. Further to this, a simplistic sensing system capable of detecting low volumes of a species from a biological surface such as artificial skin was developed. The proof-of-concept demonstrated within this chapter is strong, however further testing of the sensor is warranted. Although this contribution only discusses the identification of scopolamine, previous reports have demonstrated how this

sensor alongside similar systems have been employed for the detection of other structurally similar amines, including atropine and methamphetamine.[25, 26, 37] As such, this sensor could be applied for the detection of species other than scopolamine within these biological matrices with ease. However, this also proposes a question of potential interference effects from structurally similar species. Further investigations into the impact of other commonly consumed substances such as medication, nicotine or alcohol would therefore also be pertinent. Current investigations into the ability to negate the interference effects from structurally similar species such as amino acids and atropine are on-going and includes an examination of alternative metal luminophores and the exploitation of pH controlled ECL, with preliminary results suggesting the ability to switch off emission from interfering species is possible.[26] Ultimately, enhancing the specificity of the sensor would only stand to improve its design and hence increase its potential toward clinical translation. Current analysis has been performed on simulated scenarios utilising artificial sweat, skin and saliva. In order to gain a greater understanding of the applicability of the current sensor design for employment within patient care, it would be necessary to test the sensor upon clinical samples obtained following scopolamine consumption. The toxicity of scopolamine makes testing of the sensor under real-world conditions challenging. To combat this, there is the potential to utilise more commonly encountered species that produce ECL emission within the same potential region. Compounds with structural similarities, such as sister tropane alkaloid atropine, have been previously reported to produce similar

ECL signals within the same potential region.[25, 26] As such, the use of a structurally similar species such as nicotine, another alkaloid known to produce an ECL signal within sweat[62] could offer a viable solution, for the assessment of additional interferent effects on the sensor due to other components excreted within sweat or saliva, not considered within this current contribution. Nevertheless, the current sensor design within the contribution demonstrates a promising avenue toward the expansion of ECL based sensors as point-of-care devices.

5.5 References

1. J. Tettey and C. Crean, *Philos. Trans. R. Soc., B*, 2015, **370**, 20140265.
2. L. Shaw and L. Dennany, *Curr. Opin. Electrochem.*, 2017, **3**, 23-28.
3. United Nations Publication, World Drug Report 2018, https://www.unodc.org/wdr2018/prelaunch/WDR18_Booklet_1_EXSUM.pdf, (accessed 9th October, 2018).
4. A. Helander, M. Bäckberg, P. Hultén, Y. Al-Saffar and O. Beck, *Forensic Sci. Int.*, 2014, **243**, 23-29.
5. M. Fagiola, T. Hahn and J. Avella, *J. Anal. Toxicol.*, 2018, **42**, 562-569.
6. K. E. Grafinger, M. E. Liechti and E. Liakoni, *Br. J. Clin. Pharmacol.*, 2019, DOI: 10.1111/bcp.14115.
7. O. Beck, L. Rausberg, Y. Al-Saffar, T. Villen, L. Karlsson, T. Hansson and A. Helander, *Drug Test. Anal.*, 2014, **6**, 492-499.
8. M. M. Richter, *Chem. Rev.*, 2004, **104**, 3003-3036.
9. W. Miao, *Chem. Rev.*, 2008, **108**, 2506-2553.
10. C. K. P. Truong, T. D. D. Nguyen and I.-S. Shin, *BioChip J.*, 2019, **13**, 203-216.
11. A. J. Bard, L. R. Faulkner, J. Leddy and C. G. Zoski, *Electrochemical methods: fundamentals and applications*, wiley New York, 1980.
12. S. Reichert, C. Lin, W. Ong, C. C. Him and S. Hameed, *Canadian family physician Medecin de famille canadien*, 2017, **63**, 369-370.
13. O. M. Vallersnes, C. Lund, A. K. Duns, H. Netland and I.-A. Rasmussen, *Clin. Toxicol.*, 2009, **47**, 889-893.
14. E. Le Garff, Y. Delannoy, V. Mesli, V. Hédouin and G. Tournel, *Forensic Sci. Int.*, 2016, **261**, e17-e21.
15. K. J. Lusthof, I. J. Bosman, B. Kubat and M. J. Vincenten-van Maanen, *Forensic Sci. Int.*, 2017, **274**, 79-82.
16. L. Fernández-López, M. Falcón Romero, G. Prieto-Bonete, C. Pérez-Martínez, J. Navarro-Zaragoza, D. Suarez and A. Luna Maldonado, *Forensic Sci. Int.*, 2018, **287**, e10.
17. BBC News, Woman in court over alleged murder and poisoning, https://www.bbc.co.uk/news/uk-england-london-51123944, (accessed 6th April, 2020).
18. J. Sáiz, T. D. Mai, M. L. López, C. Bartolomé, P. C. Hauser and C. García-Ruiz, *Sci. Justice*, 2013, **53**, 409-414.
19. U. D. Renner, R. Oertel and W. Kirch, *Ther. Drug Monit.*, 2005, **27**, 655-665.
20. H. Chen, Y. Chen, H. Wang, P. Du, F. Han and H. Zhang, *Talanta*, 2005, **67**, 984-991.
21. S. F. Malamed, in *Sedation (Fifth Edition)*, ed. S. F. Malamed, Mosby, Saint Louis, 2010, DOI: https://doi.org/10.1016/B978-0-323-05680-9.00029-1, pp. 316-354.
22. S. Caporali and U. Bardi, *Corrosion*, 2012, **68**, 025001-025001.
23. International Organization for Standardization, ISO 3160-2:2015 Watch-Cases and Accessories — Gold Alloy Coverings — Part 2: Determination of Fineness, Thickness, Corrosion Resistance and Adhesion, 2015.
24. A. Zhang, C. Miao, H. Shi, H. Xiang, C. Huang and N. Jia, *Sens. Actuators B*, 2016, **222**, 433-439.
25. K. Brown, M. McMenemy, M. Palmer, M. J. Baker, D. W. Robinson, P. Allan and L. Dennany, *Anal. Chem.*, 2019, **91**, 12369-12376.
26. K. Brown, C. Jacquet, J. Biscay, P. Allan and L. Dennany, *Anal. Chem.*, 2020, **92**, 2216-2223.
27. A. Devadoss, L. Dennany, C. Dickinson, T. E. Keyes and R. J. Forster, *Electrochem. Commun.*, 2012, **19**, 43-45.

28. R. Russell, A. J. Stewart and L. Dennany, *Anal. Bioanal. Chem.*, 2016, **408**, 7129-7136.
29. T. da Costa Oliveira, M. H. P. Santana, C. E. Banks, R. A. A. Munoz and E. M. Richter, *Electroanalysis*, 2019, **31**, 567-574.
30. A. Florea, J. Schram, M. de Jong, J. Eliaerts, F. Van Durme, B. Kaur, N. Samyn and K. De Wael, *Anal. Chem.*, 2019, **91**, 7920-7928.
31. Y. Gao, Y. Tian and E. Wang, *Anal. Chim. Acta*, 2005, **545**, 137-141.
32. L. Jianguo, C. Yuan and J. Huangxian, *Electroanalysis*, 2007, **19**, 1569-1574.
33. B. Yuan, C. Zheng, H. Teng and T. You, *J. Chromatogr. A*, 2010, **1217**, 171-174.
34. B. L. Laube, M. R. Asirvatham and C. K. Mann, *J. Org. Chem.*, 1977, **42**, 670-674.
35. L. C. Portis, V. V. Bhat and C. K. Mann, *J. Org. Chem.*, 1970, **35**, 2175-2178.
36. L. Dennany, Z. Mohsan, A. L. Kanibolotsky and P. J. Skabara, *Faraday Discuss.*, 2014, **174**, 357-367.
37. J. McGeehan and L. Dennany, *Forensic Sci. Int.*, 2016, **264**, 1-6.
38. J. Sangster, *LOGKOW Data Base*, Sangster Res Lab, Montreal, Quebec, Canada, 1994.
39. C. L. Winek, W. W. Wahba, C. L. Winek and T. W. Balzer, *Forensic Sci. Int.*, 2001, **122**, 107-123.
40. L. Dennany, E. J. O'Reilly, T. E. Keyes and R. J. Forster, *Electrochem. Commun.*, 2006, **8**, 1588-1594.
41. H. Hosono, W. Satoh, J. Fukuda and H. Suzuki, *Sens. Actuators B*, 2007, **122**, 542-548.
42. J. Perła-Kaján, T. Twardowski and H. Jakubowski, *Amino Acids*, 2007, **32**, 561-572.
43. K. Mariño, R. Saldova, B. Adamczyk and P. M. Rudd, in *Carbohydrate Chemistry: Volume 37*, The Royal Society of Chemistry, 2012, vol. 37, pp. 57-93.
44. H. Xie, X. Li, L. Zhao, L. Han, W. Zhao and X. Chen, *Sens. Actuators B*, 2016, **222**, 226-231.
45. Y. Hu, W. Xu, J. Li and L. Li, *Luminescence,* 2012, **27**, 63-68.
46. L.-H. Shen, H.-N. Wang, P.-J. Chen, C.-X. Yu, Y.-D. Liang and C.-X. Zhang, *J. Food Drug Anal.*, 2016, **24**, 199-205.
47. A. J. Stewart, J. Hendry and L. Dennany, *Anal. Chem.*, 2015, **87**, 11847-11853.
48. J. L. Owens, H. A. Marsh and G. Dryhurst, *J. Electroanal. Chem. Interfacial Electrochem.*, 1978, **91**, 231-247.
49. X. Sun, J. Liu, W. Cao, X. Yang, E. Wang and Y. S. Fung, *Anal. Chim. Acta*, 2002, **470**, 137-145.
50. Y.-M. Liu, W. Tian, Y.-X. Jia and H.-Y. Yue, *ELECTROPHORESIS*, 2009, **30**, 1406-1411.
51. Y. Tao, X. Zhang, J. Wang, X. Wang and N. Yang, *J. Electroanal. Chem.*, 2012, **674**, 65-70.
52. J. Ballesta-Claver, R. Rodríguez-Gómez and L. F. Capitán-Vallvey, *Anal. Chim. Acta*, 2013, **770**, 153-160.
53. F. Takahashi and J. Jin, *Luminescence*, 2008, **23**, 121-125.
54. W. Satoh, H. Hosono and H. Suzuki, *Anal. Chem.*, 2005, **77**, 6857-6863.
55. J. Ballesta Claver, M. C. Valencia Mirón and L. F. Capitán-Vallvey, *Analyst*, 2009, **134**, 1423-1432.
56. D. An, Z. Chen, J. Zheng, S. Chen, L. Wang, Z. Huang and L. Weng, *Food Chem.*, 2015, **168**, 1-6.

57. Z.-Y. Shang, C.-F. Han and Q.-J. Song, *Chin. J. Anal. Chem.*, 2014, **42**, 904-908.
58. Z. Zhou, L. Xu, S. Wu and B. Su, *Analyst*, 2014, **139**, 4934-4939.
59. Y. Yao, H. Li, D. Wang, C. Liu and C. Zhang, *Analyst*, 2017, **142**, 3715-3724.
60. X. Cai, J. Yan, H. Chu, M. Wu and Y. Tu, *Sens. Actuators B*, 2010, **143**, 655-659.
61. M.-M. Chen, S.-B. Cheng, K. Ji, J. Gao, Y.-L. Liu, W. Wen, X. Zhang, S. Wang and W.-H. Huang, *Chem. Sci.*, 2019, **10**, 6295-6303.
62. S. Li, Y. Lu, L. Liu, S. S. Low, B. Su, J. Wu, L. Zhu, C. Li and Q. Liu, *Sens. Actuators B*, 2019, **285**, 34-41.

CHAPTER SIX

TALE OF TWO ALKALOIDS: pH CONTROLLED ELECTROCHEMILUMINESCENCE FOR DIFFERENTIATION OF STRUCTURALLY SIMILAR COMPOUNDS

“This is either madness … or brilliance”

“It’s remarkable how often those two traits coincide”

Orland Bloom and Johnny Depp

As Will Turner and Jack Sparrow

(Pirates of the Caribbean: The Curse of the Black Pearl 2003)

This chapter comprises publication:

K. Brown (primary author and principal investigator), C. Jacquet, J. Biscay, P. Allan and L. Dennany, *Anal. Chem.*, 2020, **92**, 2216-2223.

DOI: 10.1021/acs.analchem.9b04922

Abstract

Electrochemiluminescence (ECL) has increased in popularity as a result of its inherent advantages, including but not limited to portability, simplicity of use, reduced reagent consumption and low operational costs. However, these significant advantages are often over shadowed as a result of its limited specificity. With intrinsically broad emissions, ECL lacks the definition observed with other available analytical techniques. Moreover, species with similar functional groups are observed to display indistinguishable electrochemical behaviour, thus typically emitting within the same potential region. Within this chapter the ability to utilise pH controlled ECL to identify the presence of two individual species within a mixed sample was achieved. The potential of this methodology to quantify scopolamine in the presence of sister tropane alkaloid atropine, a known ECL interferent, was illustrated. Previously the two alkaloids could not be distinguished through a single analysis technique without the employment of a separation strategy. pH controlled ECL is a simple approach to improve the specificity of a basic $[Ru(bpy)_3]^{2+}$ film based sensor. By exploiting molecular characteristics, such as pKa, the ability to fine-tune this methodology to facilitate identification of analytes previously exhibiting indistinguishable ECL emission was achieved. Thus, by improving specificity, while maintaining operational simplicity and inexpensive design, the potential power of ECL for the identification of structurally similar compounds has been highlighted. Further improvements upon specificity, such as demonstrated within this contribution, only stands to further future applications of ECL sensors across a range of different fields.

6.1 Introduction

The ability to identify compounds with confidence is a fundamental concept within analytical chemistry. Often analysis of samples, regardless of the field, requires the detection of compounds based upon their structural properties. This can range from impurity analysis in pharmaceutics to identification of illicit substances within a forensic context. As analytical chemistry moves toward greater portability, the requirement to simplify instrumentation, minimise cost and decrease reagent consumption has become a key driving force during the method development phase.[1-3] Electrochemiluminescence (ECL) satisfies a number of these criteria.[4-7] By combining the advantages of electrochemistry with photoluminescence, ECL stands out from other analytical techniques. Unlike its counterparts ECL produces luminescence without the requirement of an external light source, vastly simplifying the instrumentation required, allowing it to be packaged within light weight portable systems.[4-8] With the recent advances in both electrochemical (EC) and ECL systems the ability to negate the need for potentiostats, by utilising mobile phones to apply the required voltage has been demonstrated alongside the use of their in-built cameras as the detector, thus producing low cost, portable and operationally simple devices.[9, 10]

As the technology to perform ECL progresses one significant limitation remains. Specificity has long plagued both EC and ECL techniques. The principles upon which both techniques operate suffer from a lack of specificity as a result of the redox chemistry across functional groups remaining largely

similar.[5] One commonly encountered functional group which are known to suffer from this lack of specificity found within amine containing species. A large number of amine containing compounds have been shown to behave as strong ECL co-reactants. However, their redox chemistry and hence emission mechanisms remain largely similar and thus their signals are observed within the same potential region.[5, 11-15] This can make identification of a specific species problematic and can limit identification to high level functional group classification. Furthermore, similar species such as tropane alkaloids, which contain a tertiary nitrogen group within their tropane ring, are also observed to emit within this region and thus further complicate class identification.[16-18] Therefore it has been necessary, until now, to employ separation strategies such as chromatography or capillary electrophoresis (CE) prior to EC or ECL detection, such that analytes which are structurally similar are identified via their retention or migration times.[19-22]

A number of methodologies have been recently established to improve the specificity of EC and ECL techniques. These largely focus upon the addition of a secondary species to modify the electrode surface. Commonly employed methods include the addition of biological recognition molecules such as single stranded apatmers[23-25] and antibodies[8, 26] but can also include non-biological materials such as Schiff bases,[27, 28] carbon nanotubes,[29] fluorescent probes[30] and specifically designed metal complexes.[31, 32] Biological species in particular demonstrate a high degree of selectivity toward the molecule of interest. These can be specifically designed to

interact with one particular species. Following this interaction, a “signal on” or “signal off” approach is observed. When the target analyte is present, the ECL probes are either released from the electrode surface, thus resulting in a decrease in ECL intensity, or are brought closer to the electrode surface thus facilitating the commencement of electrochemistry, resulting in the increase or appearance of a signal.[23, 25] Alternative biological based approaches investigate the incorporation of the recognition group into the co-reactant species rather than the electrode surface. This technique showed promise and offered a simpler methodology than the electrode modification procedures previously employed.[33]

Although the aforementioned mention techniques have demonstrated a high degree of specificity, making them powerful modification strategies, they are both complex and expensive to perform. In contrast, this chapter discusses a simple strategy to increase ECL specificity without requiring the inclusion of additional species to the electrode surface, bar the necessary luminophore. Despite their almost identical chemical structure and electrochemical properties, it has been possible to differentiate between two tropane alkaloids, atropine sulfate and scopolamine hydrobromide. By effectively switching off emission from atropine, while maintaining scopolamine’s emission, the ability to quantify scopolamine in the presence of atropine becomes possible. Exploiting the difference in pKa values and subsequently adjusting sample pH accordingly, emission from a basic $[Ru(bpy)_3]^{2+}$ ECL sensor can be tuned to provide greater specificity. Furthermore, unlike the

biological or chemical modifications, which require expertise to perform, this simple system can be easily adapted to accommodate a range of skills levels across a number of fields, thus further widening its applications. In addition, by avoiding the use of the selective reagents, the developed sensor can be applied to a wide range of different species without requiring a complete redesign of electrode modification procedures. By negating the requirement for a separation strategy prior to detection, instrument and operational simplicity in addition to portability are maintained, all of which will only stand to further encourage the use of such a basic ECL sensing system. Moreover, expansion of pH controlled ECL to a more extensive range of compound classes will only stand to further enhance the possible applications for this combination of techniques, thus, illustrating the potential of such a strategy to the wider analytical community.

6.2 Experimental

6.2.1 Materials

Tris (2,2′-bipyridyl)-dichlororuthenium(II) hexahydrate ($[Ru(bpy)_3]\cdot Cl_2\cdot 6H_2O$), atropine sulfate monohydrate, (–)-scopolamine hydrobromide trihydrate (Sc-HBr), lithium perchlorate ($LiClO_4$), and 117 Nafion (~5% mixture of lower aliphatic alcohols and water) were purchased from Sigma-Aldrich. Absolute EtOH was purchased from VWR Chemicals. All chemicals were used as received. All solutions were prepared in Milli-Q water (18 mΩ cm^{-1}).

6.*2.2 Instrumentation*

The electrochemical instrumentation and electrode materials used were previously described within section 3.2.2.

6.2.3 Fabrication of $[Ru(bpy)_3]^{2+}$ / Nafion ECL Sensor

The [Ru(bpy)3]2+/Nafion film modified carbon paste screen printed electrode was fabricated following the same procedure as described within section 3.2.3. Prior to sample measurements, electrodes were preconditioned through the performance of three subsequent CV cycles over the potential range of interest within the electrolyte solution to achieve a stable signal.

6.3 Results and Discussion

6.3.1 ECL Detection of Atropine and Scopolamine

The ability of a simple ruthenium film-based ECL sensor to reliably detect tropane alkaloids atropine sulfate and scopolamine hydrobromide both within ideal and complex matrices without the requirement for any sample preparation was previously demonstrated within chapters four and five.[18] One of the major limitations facing single luminophore ECL analysis systems is the lack of specificity offered as a result of the broad spectral responses observed. Species with similar functionalities display similar redox behaviour, and as a result, they often produce emission at similar potentials.[5] Small structural differences have however been observed to result in slight variations of redox potentials. This becomes apparent when examining atropine and scopolamine. The two tropane alkaloids possess almost identical chemical structures, as shown within Figure 6.1a. However, CV and subsequent ECL analysis of both species individually have shown that the potential at which oxidation occurs differs for each analyte. The CVs for both are shown within Figure 6.1b and Figure 6.1c with atropine observed at a slightly earlier potential of +0.89 V compared with +1.30 V observed for scopolamine at unmodified carbon electrodes. The ECL maximums, were observed to display slight potential differences via their individual interactions with the $Ru^{2+/3+}$ redox couple resulting in +0.83 and +0.89 V for atropine and scopolamine, respectively. This mediated oxidation process is consistent with reported ECL mechanistic pathways for alkaloids.[16-18, 34] It is believed that these slight differences arise due to the influence of the additional epoxide

group present within scopolamine's structure. Quantum calculations performed upon both species have shown that the E_{HOMO} for atropine (–9.590 eV[35]) is slightly higher than that observed for scopolamine (–9.780 eV).[35] Furthermore, Marquez *et al.*[36] also reported that E_{HOMO} for scopolamine exists at lower energies than other alkaloid species including cocaine and tropane.[36] With the distance between the epoxide group and the nitrogen of the tropane ring only 2.47 Å,[37] it is proposed that redistribution of the electron density could result in an inductive effect toward the positive nitrogen within the tropane ring system, thus stabilising the cation. As such the HOMO for scopolamine will be observed at a lower energy than atropine, which has no additional electron donating groups present and thus requires the application of more positive potentials to promote electro-oxidation.[35-37] A comparable trend has been previously reported for similar species including amino acids where the presence of different functional groups was seen to influence the oxidation potentials as a result of the difference in E_{HOMO}.[11, 38, 39] This slight potential difference is also observed within the ECL intensity of the alkaloids, see Figure 6.2a, with atropine's ECL maximum observed at +0.83 V and scopolamine at +0.89 V. The lower onset of ECL has previously been observed for atropine[18] and can be attributed to the formation of a radical species to similar mechanisms outlined previously within chapters four and five.[40, 41] Despite the different oxidation potentials of atropine and scopolamine, when a mixed sample is analysed, the two individual peaks cannot be identified, as shown in Figure 6.2b. This is not unusual since the broad spectral response observed as a consequence of ECL emission does

not offer the distinctive peaks observed in other analytical techniques. Moreover, the oxidative-reduction ECL mechanism, responsible for their ECL emission is almost identical, since both compounds contain the same tropane alkaloid functionality, responsible for their electrochemical behaviour. Furthermore, they also follow the same oxidative *N*-dealkylation degradation pathways, similar to those observed for other structurally similar amine species.[16-18, 42-44] As such, the ability to differentiate between these structurally similar species in addition to other structurally similar amine species utilising single luminophore ECL alone is extremely challenging.

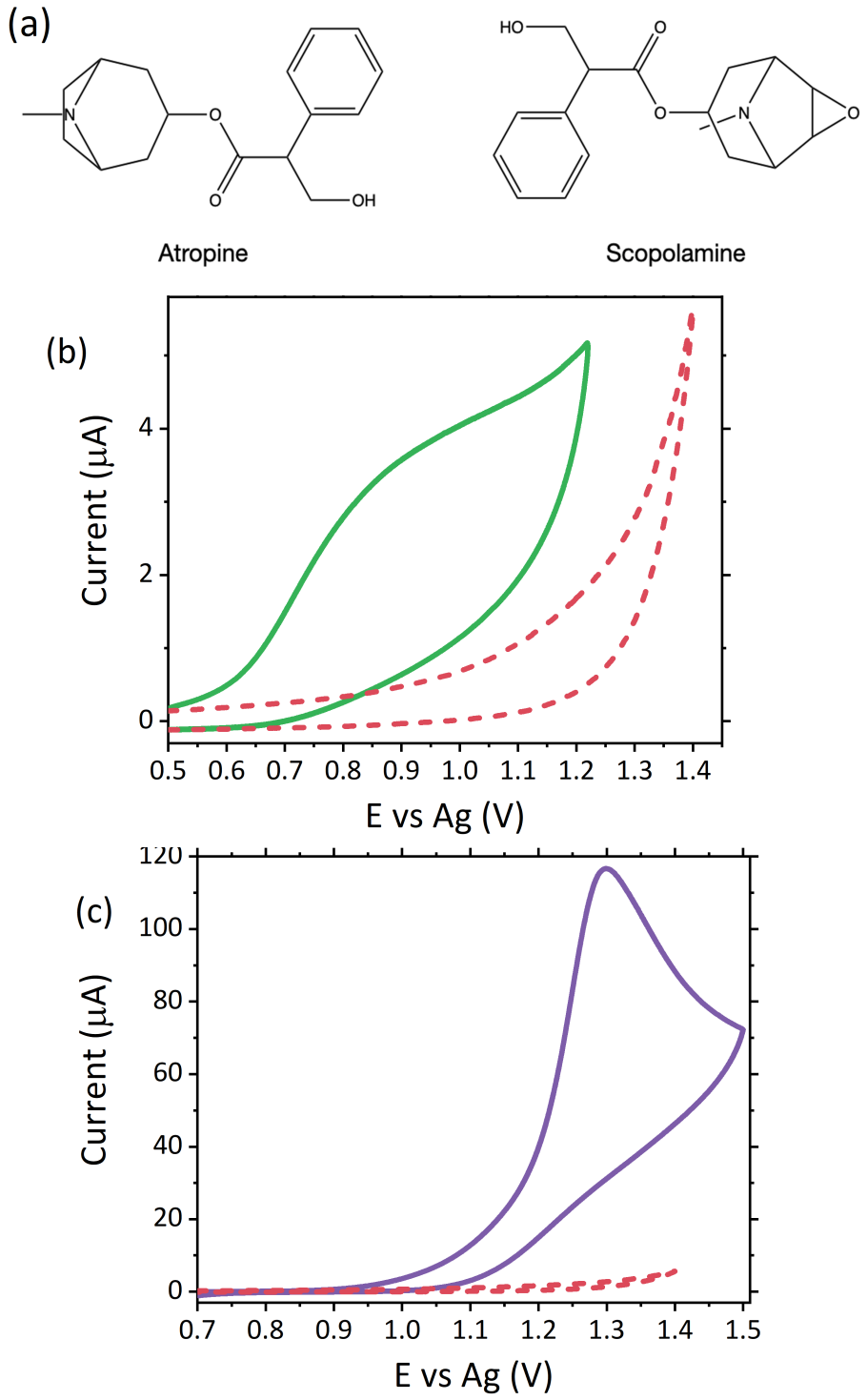

Figure 6.1: (a) Chemical structure of tropane alkaloids atropine and scopolamine and CV response of (b) 2.5 mM atropine sulfate (green) and (c) 2.5 mM scopolamine hydrobromide (purple) with 0.1 M $LiClO_4$ (pink) as the supporting electrolyte at unmodified carbon screen-printed electrodes at a scan rate of 100 mV s^{-1} across $0.5 \leq E \leq 1.5$ V vs Ag.

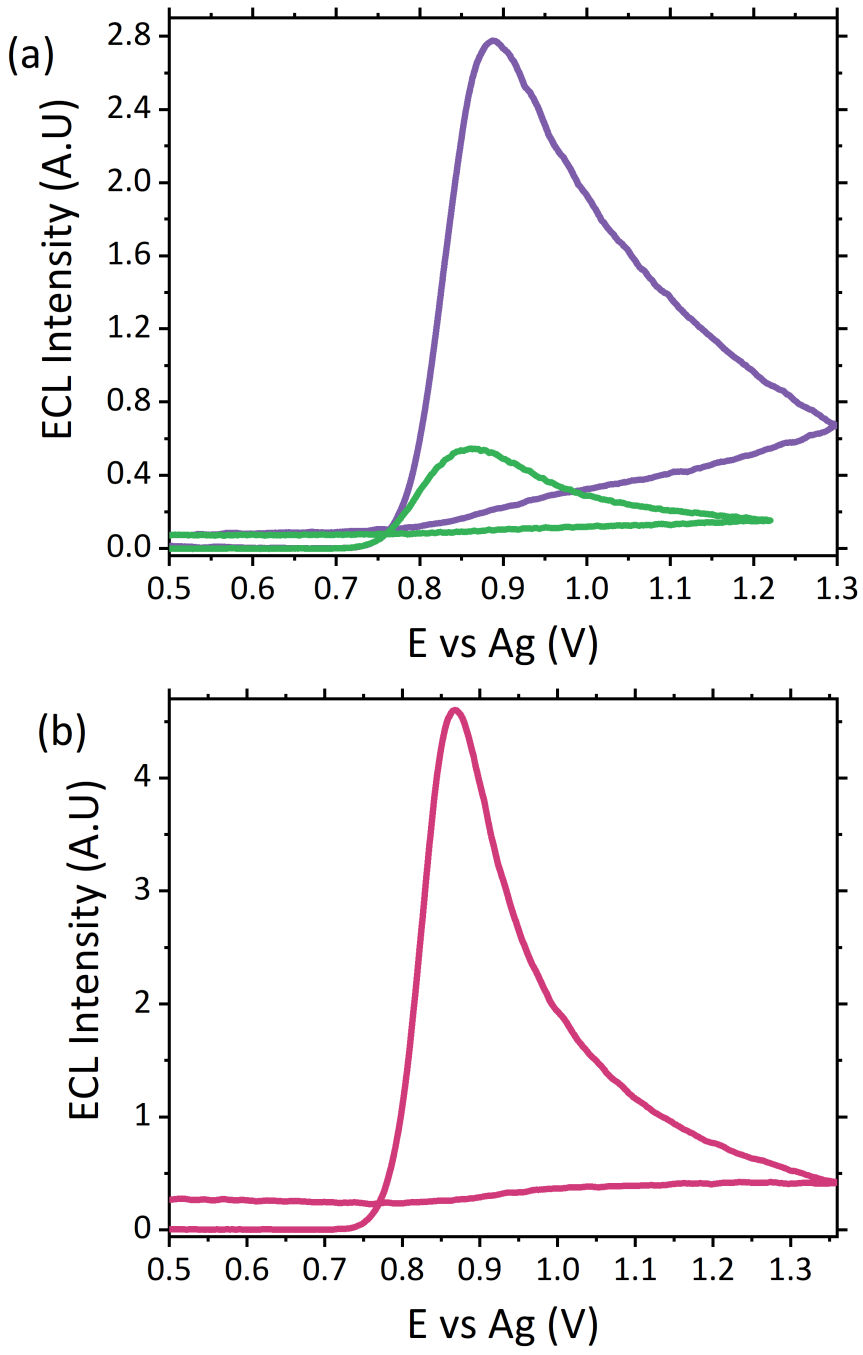

Figure 6.2: ECL responses of (a) atropine sulfate (green) and scopolamine hydrobromide (purple) and (b) a mixed atropine sulfate and scopolamine hydrobromide sample all collected with ruthenium modified carbon electrodes in pH 8 $LiClO_4$ at a scan rate of 100 mV s^{-1} across $0.5 \leq E \leq 1.3$ V vs Ag at a PMT setting of 0.6 V.

6.3.2 pH Impact on ECL Intensity

It is well-known that pH significantly influences the intensity of ECL emission, as a result of whether the oxidisable form of the analyte is dominant under that particular pH. As such, the greatest emission intensities are observed close to the pKa values of the species.[14, 16-18, 45] pH analysis of atropine[18] (refer to chapter four Figure 4.4) has shown a negligible emission is observed at acidic pH values, with the minimal signal between pH 5 and 7, before a dramatic increase is seen at pH 8.[18] In contrast, pH analysis of scopolamine hydrobromide (refer to chapter five Figure 5.2) revealed that a measurable signal is observed across all pH values. This includes the acidic pH values, with an increase in signal observed at both pH 6 and pH 8. Despite the almost identical structure of the two alkaloids, their pKa values are notably different, with atropine reported at a pKa of 9.85[46] and scopolamine hydrobromide at 7.6.[47] The difference in pKa and subsequently, the proportion of free base species present at different pH values thus presents the opportunity to exploit this difference to facilitate the identification of the alkaloids separately within mixed samples. Scopolamine's lower pKa and hence lower basicity compared with atropine results in more of its non-pronated, and hence oxidisable form, present at lower pH values. In fact, the proportion of free base scopolamine present at a physiological pH of 7.4 is reported to be 70 times more than atropine under the same conditions.[37] Thus, it is therefore not surprising when directly comparing the ECL intensity dependance with pH for both species that there are obvious pH ranges where

emission from one species can in essence be switched off. Interestingly contrasting the behaviour observed in ECL, there is no observable impact observed within the CVs as a result of changes in pH, refer to Figure 6.3a and Figure 6.3b. This is most likely due to the $Ru^{2+/3+}$ redox couple being the predominant feature observed within the voltammograms, refer to Figure 6.4. It becomes clear when examining the ECL intensity dependence with pH for each species that acidic pH values offer the best compromise between negating the signal response from atropine and obtaining the maximum signal from scopolamine, refer to Figure 6.5. As such the optimum pH identified for the detection of scopolamine in the presence of atropine was determined at pH 6. In contrast, scopolamine is observed to emit a considerable signal at all pH values investigated where atropine emits. Although it could be thought that pH 11 would offer a viable pH to optimise atropine emission and negate scopolamine emission, as previously discussed within chapter four, emission at this pH is due to the catalysed degradation of atropine under these alkaline conditions, leading to the formation of tropine and tropic acid.[18, 48] As such, this degradation prevented quantification of atropine when in the presence of scopolamine, with the inability to accurately control the concentration of atropine remaining at this pH. Furthermore, tropine is also found to behave as a suitable co-reactant and hence able to produce a measurable ECL response, and as such will contribute to the observed signal. Therefore, the proportion of the signal caused by tropine compared with atropine could not be discerned.[18]

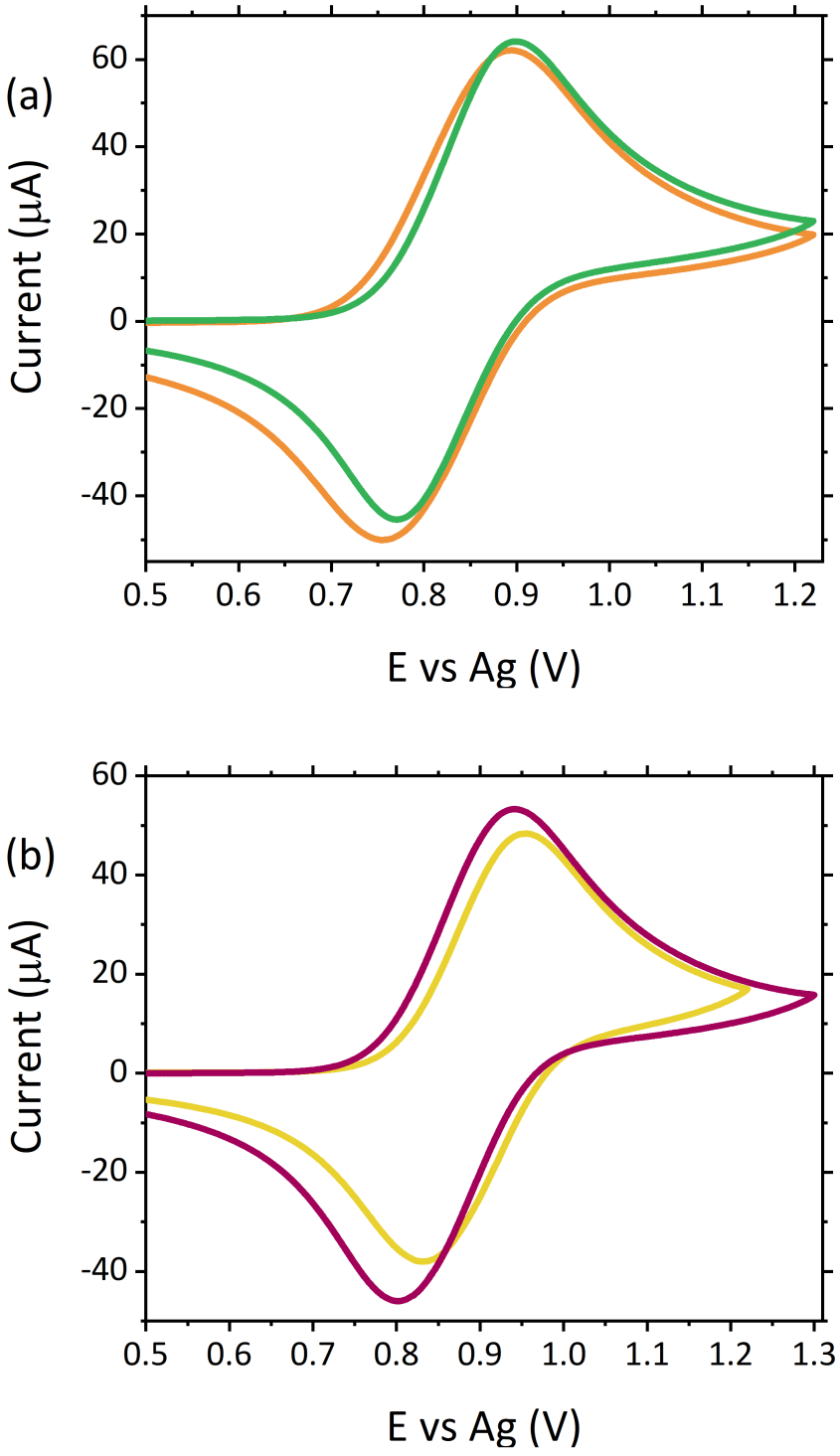

Figure 6.3: CV responses for (a) 50 µM atropine sulfate at pH 6 (orange) and pH 8 (green) and (b) 50 µM scopolamine hydrobromide at pH 6 (yellow) and pH 8 (pink), at a scan rate of 100 mV s^{-1} across a potential range of $0.5 \leq E \leq 1.30$ V vs Ag with 0.1 M $LiClO_4$ as the electrolyte.

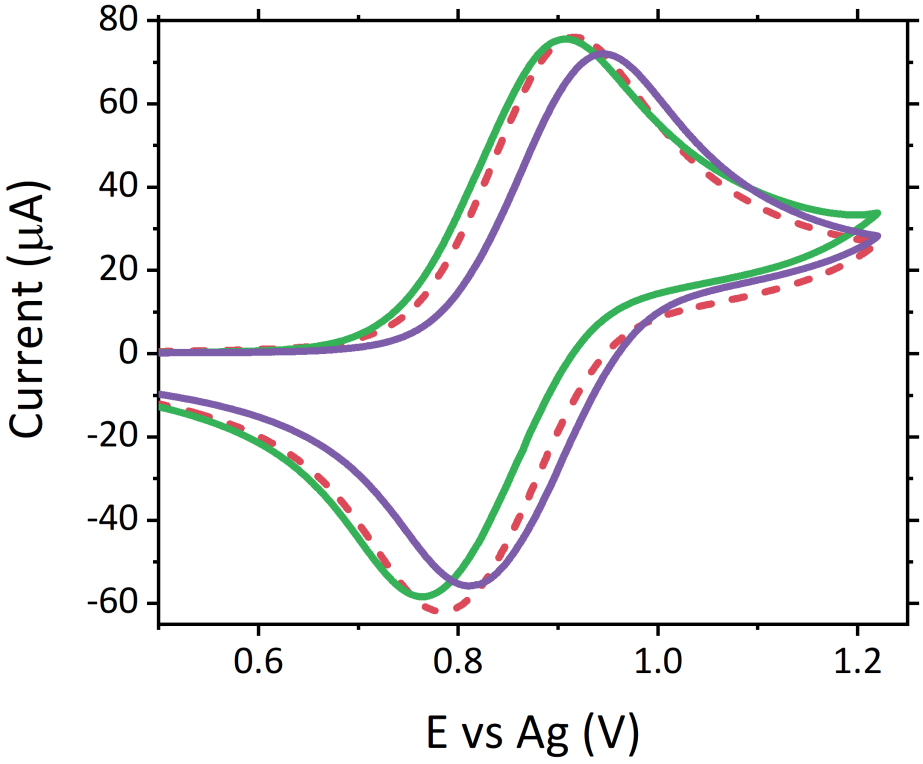

Figure 6.4: CV responses of 50 µM atropine sulfate (green), 50 µM scopolamine hydrobromide (purple) and 0.1 M $LiClO_4$ (pink) at $[Ru(bpy)_3]^{2+}$ film modified screen-printed carbon electrodes at a scan rate of 100 mV s^{-1} in 0.1 M $LiClO_4$ electrolyte across $0.5 \leq E \leq 1.22$ vs Ag.

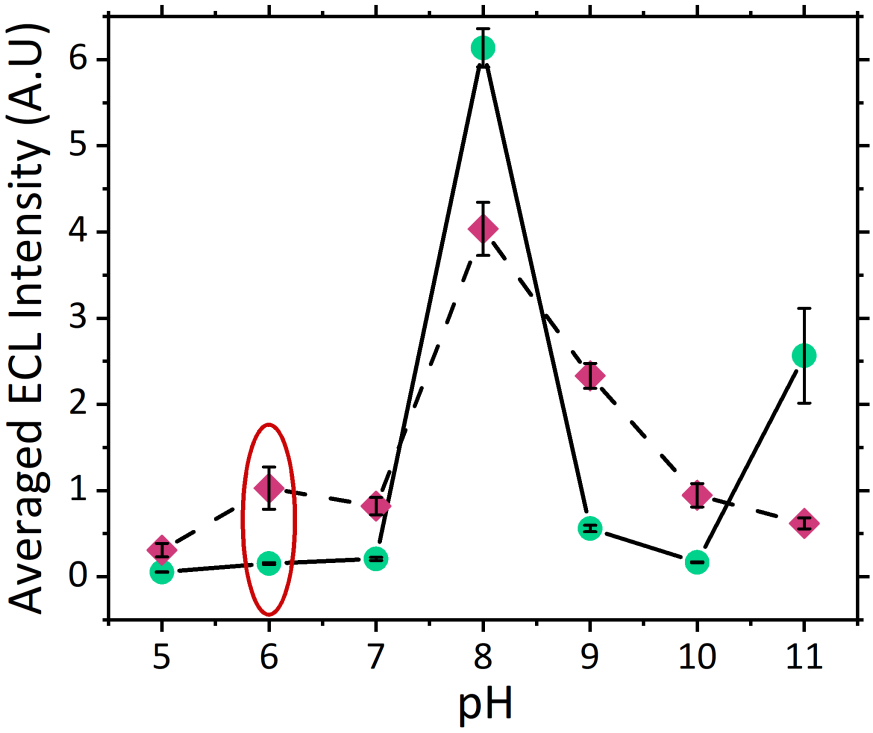

Figure 6.5: Comparison of ECL intensities with pH for atropine sulfate (green) and scopolamine hydrobromide (pink), with pH 6 highlighted as the optimum pH for differentiation. Both species were prepared in 0.1 M $LiClO_4$ at the desired pH. Measurements were collected at a scan rate of 100 mV s^{-1} across $0.5 \leq E \leq 1.36$ V vs Ag at a PMT setting of 0.45 V for atropine sulfate and 0.6 V for scopolamine hydrobromide. Each point represents the mean of the maximum ECL intensity at n=3 with error bars comprising of ± 1SD across these measurements.

6.3.3 Analytical Performance

Prior to the analysis of mixed samples, it was necessary to prepare suitable calibration curves at the chosen pH values. The optimum pH for the determination of scopolamine in the presence of atropine was chosen as pH 6. Although there are other pH values that resulted in greater ECL intensities, pH 6 produced the greatest difference in ECL response between the two alkaloids, as such it would be ideally suited to discriminate the presence of scopolamine over atropine. At other pH values, the contribution from atropine's ECL emission would not make quantification of scopolamine possible. pH 10 was also considered, but the atropine response was larger than that observed for pH 6 where it was negligible, in addition, pH 10 lies close to the region where alkaline degradation of atropine is observed.

Thus, a calibration curve was prepared for scopolamine hydrobromide at pH 6. The $[Ru(bpy)_3]^{2+}$ film SPE sensor utilised within this study has previously demonstrated satisfactory analytical performance (refer to section 4.3.3), including an electrode reproducibility of 1.9% and repeatability of 8.3% and was observed to exhibit the same behaviour here.[18] The limit of detection (LOD) for each calibration was calculated as 0.418 and 0.440 μM for pH 6 and 8, respectively, based upon the standard deviation of the y intercept and slope of the regression line.[49] The influence of scopolamine hydrobromide concentration upon ECL intensity at pH 6 was investigated across a range of 0.625–250 μM. As analyte concentration was increased the ECL intensity

was observed to linearly increase in proportion with the maximum ECL response between 0.625 and 100 μM with a coefficient R^2 value of 0.999, see the inset of Figure 6.6a. Above 100 μM, a plateau effect was observed (see Figure 6.6b) which prevented quantification above this concentration. This plateau effect is not unsurprising and is a previously reported limitation of ECL.[18, 50] At higher analyte concentrations, the consumption of ruthenium(III) becomes the limiting step, where it is consumed at a rate quicker than it can be produced. As such, a point is reached when the ECL intensity will no longer increase as analyte concentration increases.[18, 50] To tackle this, the ruthenium concentration present could be increased within the film or a dilution factor taken into account. However, the concentrations of scopolamine and atropine likely to be encountered within any "real-world" scenario would be far lower, with concentrations typically ranging between 0.99 to 20 μM in biological or herbal material samples; therefore, it was not currently necessary to concentrate upon the quantification of these higher concentrations.[51-54]

A second calibration curve was also prepared at pH 8, the optimum pH where maximum ECL intensity is observed for each analyte. The same concentration range as for pH 6 was investigated, with a linearly proportional response observed with scopolamine concentration at a maximum ECL intensity with a R^2 value of 0.995, see Figure 6.7a inset. In contrast to pH 6, at pH 8 the linear range was only observed between 0.625 and 50 μM, see Figure 6.7a. Above 50 μM, the previously described plateau effect, was

observed (refer to Figure 6.7b). At concentrations above 80 µM, scopolamine at pH 8, a decrease in the ECL intensity can be observed. This may partly be a result of the more easily oxidisable form at this pH undergoing direct oxidation at the electrode surface, generating the electro-*N*-dealkylation species (norscopolamine). The formation of norscopolamine would result in a decrease in the concentration of the ECL co-reactant, scopolamine, and therefore result in a decrease in ECL production. This can be attributed to a far greater proportion of scopolamine being present in its non-protonated and hence oxidisable form at this pH. Thus, ruthenium(III) becomes the limiting reagent at a much lower total concentration due to a higher proportion of scopolamine species present, which are able to undergo ECL. As can be seen in both Figure 6.6a and Figure 6.7a, in addition to the ECL intensity increasing with scopolamine concentration, a slight shift in the potential of maximum response is observed. This effect is not unexpected and is consistent with prior literature where a shift is observed at both ruthenium modified carbon electrodes and unmodified graphite electrodes.[18, 55] This shift can likely be attributed to two effects. As the concentration of scopolamine is increased and the concentrations at which ruthenium(III) becomes the limiting reagent reached, it becomes more difficult to produce the oxidised species required to undergo ECL. Moreover, as more scopolamine is present and undergoes the irreversible ECL mechanisms, a greater concentration of the byproducts, norscopolamine and formaldehyde, are produced leading to a shift in the pH of the sample within the inner Helmholtz plane close to the surface of the electrode.[18, 50, 55] With no significant response from atropine

observed at pH 6, its presence would not impact the ability to identify the presence of scopolamine within a mixed sample. While at pH 8, the onset of ECL production from atropine and hence increased total signal intensity would indicate the presence of a second co-reactant, here atropine. Therefore, it is necessary to have measurements for scopolamine at both pH values to identify the presence of both alkaloids. Without both sets of data, an indication of the total alkaloid presence could be made but identification of the number of alkaloids presence would not be possible.

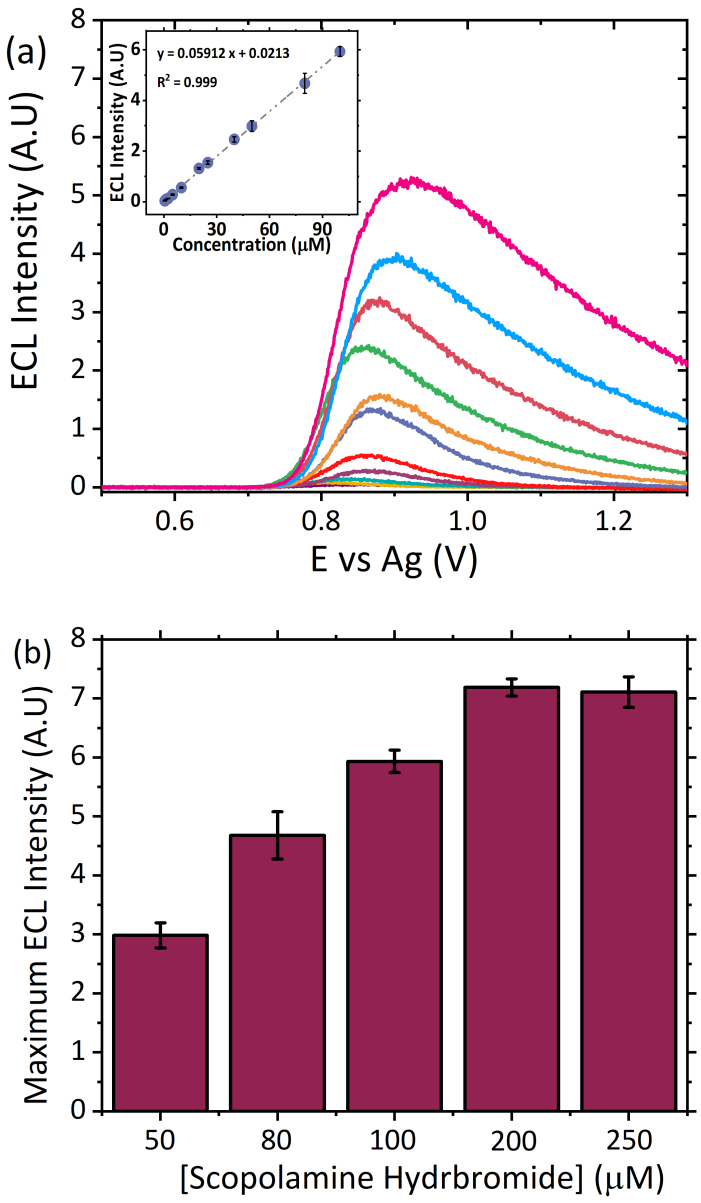

Figure 6.6: (a) Dependence of ECL intensity with scopolamine hydrobromide concentration at pH 6 between 0.625 and 100 µM. Inset shows the trend of maximum ECL intensity against scopolamine hydrobromide concentration and (b) maximum ECL intensities recorded for scopolamine hydrobromide at pH 6 between 50 to 250 µM demonstrating a plateau in ECL response observed when ruthenium becomes the limiting reagent. All samples were prepared in 0.1 M $LiClO_4$ and measured at a scan rate of 100 mV s^{-1} across $0.5 \leq E \leq 1.26$ V vs Ag at a PMT setting of 0.6 V. Each point represents the mean of the maximum ECL intensity at n=3 with error bars comprising of ± 1SD across these measurements.

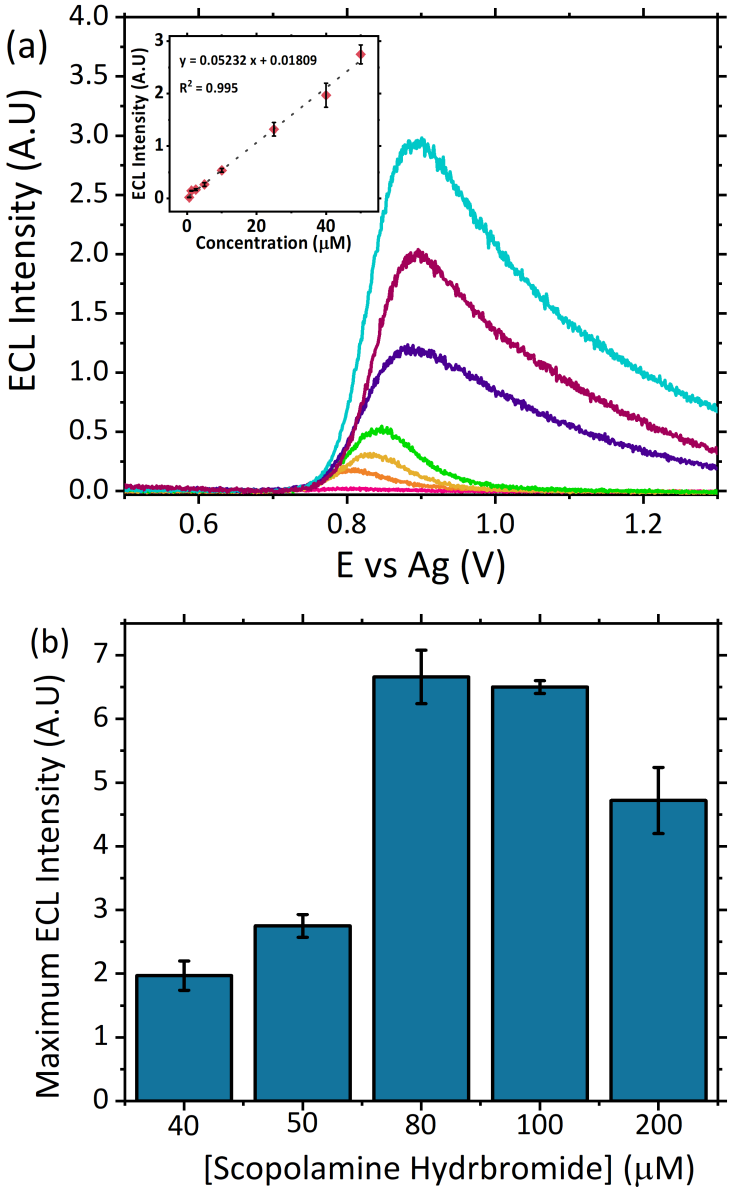

Figure 6.7: (a) Dependence of ECL intensity with scopolamine hydrobromide concentration at pH 8 between 0.625 and 50 µM. Inset shows the trend of maximum ECL intensity against scopolamine hydrobromide concentration and (b) maximum ECL intensities recorded for scopolamine hydrobromide at pH 8 between 40 to 200 µM demonstrating a plateau in ECL response observed when ruthenium becomes the limiting reagent. All samples were prepared in 0.1 M $LiClO_4$ and measured at a scan rate of 100 mV s^{-1} across $0.5 \leq E \leq 1.26$ V vs Ag at a PMT setting of 0.6 V. Each point represents the mean of the maximum ECL intensity at n=3 with error bars comprising of ± 1SD across these measurements.

6.3.4 Mixed Alkaloid Sample Analysis

To establish whether the analyte pKa could be exploited to successfully quantify individual analytes that possess similar ECL emission mechanisms within the same sample matrix, the two tropane alkaloids atropine and scopolamine were used as model compounds within this proof-of-concept study. Samples containing both alkaloids were prepared and measured at pH 6, where only scopolamine emission was expected, pH 8 where both species produce the greatest ECL intensity, and pH 11 where atropine's emission over scopolamine is the greatest. The scopolamine concentration was kept constant in both pH 6 and 8 samples at 50 μM while the atropine sulfate concentration was varied between 12.5 and 100 μM. For pH 11, concentrations were reversed, with atropine maintained at 50 μM and scopolamine varied between 12.5 and 100 μM. Assessment of the ECL signal intensity due to the presence of atropine was made by comparing the calculated concentrations of scopolamine hydrobromide at both pH 6 and 8 to the known concentrations added. Scopolamine hydrobromide concentrations were calculated using the relevant calibration curves constructed for each pH, see Figure 6.6 and Figure 6.7, the results of which are summarised within Table 6.1. In order to establish whether a sample contained only scopolamine or if another alkaloid was present, in this case atropine, it is necessary to obtain the information for the expected scopolamine signal both at pH 6 and 8 of pure standards. These can then be used as system standards, in a similar manner as is performed for more traditional analytical techniques such as HPLC.

The ECL intensity of the pH 8 samples demonstrated a trend of increasing ECL intensity as the atropine concentration increased between 12.5 and 50 μM. After this, a decrease in overall ECL intensity was observed, refer to Figure 6.8a. This decrease is not unexpected and can be attributed to the ruthenium(III) species becoming the rate limiting reagent. At pH 8, the free base or non-pronated form of both species will be the dominant form present. Previously, 50 μM scopolamine hydrobromide was observed as the maximum concentration which produced an increasing ECL intensity with an increase in concentration. Above 50 μM, the ECL intensity was no longer dependent upon the scopolamine concentration, and thus 50 μM was the maximum concentration that could be accurately quantified. Thus, with scopolamine hydrobromide at its maximum quantifiable concentration and atropine sulfate also present at its maximum linearly dependent concentration of 100 μM, it is thus not unsurprising that a decrease in overall ECL intensity was observed. As can be seen within Table 6.1, the concentration of scopolamine calculated within mixed samples at pH 8 is far greater than the 50 μM present. Furthermore, an examination of the ECL signals, such as those shown in Figure 6.8b, demonstrate that the total ECL signal observed for the mixed alkaloid sample is not the result of the direct addition of the two individual signals for atropine and scopolamine at this pH. As such, the ECL intensity of scopolamine hydrobromide cannot be corrected by direct subtraction of the atropine signal.

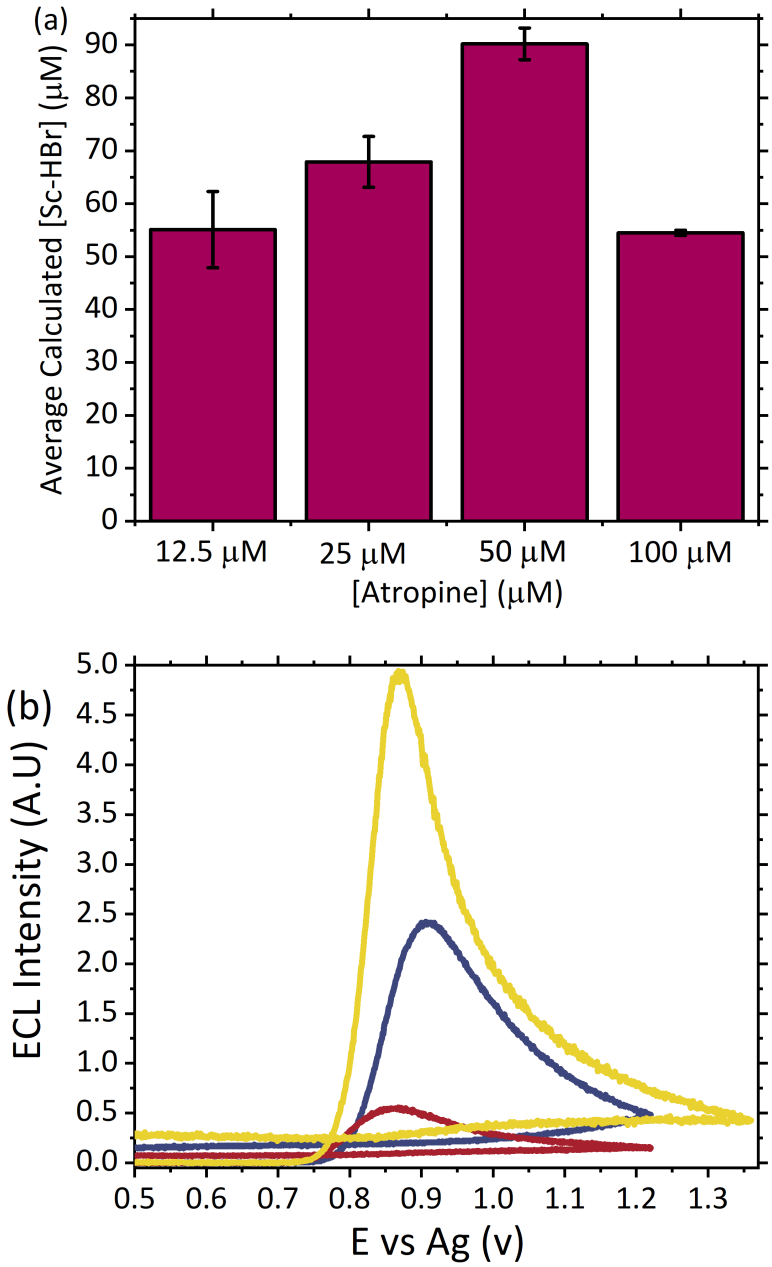

Figure 6.8: (a) Calculated scopolamine hydrobromide (Sc-HBr) concentrations in the presence of varying concentrations of atropine sulfate at pH 8. Concentrations calculated based upon maximum ECL intensity. (b) ECL responses of 50 μM atropine sulfate (pink), 50 μM scopolamine hydrobromide (purple), and 50 μM atropine sulfate and scopolamine hydrobromide (yellow) in pH 8 0.1 M $LiClO_4$ as the electrolyte and measured at a scan rate of 100 mV s^{-1} across $0.5 \leq E \leq 1.36$ V vs Ag at a PMT setting of 0.6 V

In contrast, analysis at pH 6 displayed no increase in total ECL intensity despite the increasing concentrations of atropine sulfate present, see Figure 6.9a. Furthermore, the examination of the signals obtained for 50 µM scopolamine are almost identical to those observed for the mixed samples, see Figure 6.9b. Table 6.1 contains a summary of the scopolamine concentrations calculated at pH 6 and demonstrates that, despite the presence of increasing concentrations of atropine, the calculated scopolamine concentrations remain constant at approximately 50 µM, hence, demonstrating a good accuracy of the developed methodology. This promising result demonstrated that by exploiting the difference in pKa values, compounds with similar chemical structures and hence ECL emission mechanisms can be successfully quantified within a mixed sample where more than one species produces an ECL response.

Table 6.1: Summary of atropine sulfate concentrations added and scopolamine hydrobromide concentrations calculated at each pH.

pH	[atropine] (µM)	[scopolamine] added (µM)	average calculated [scopolamine] (n=3) (µM)
6	12.5	50	49.7
6	25	50	50.8
6	50	50	49.3
6	100	50	50.3
8	12.5	50	55.1
8	25	50	67.9
8	50	50	90.2
8	100	50	54.5

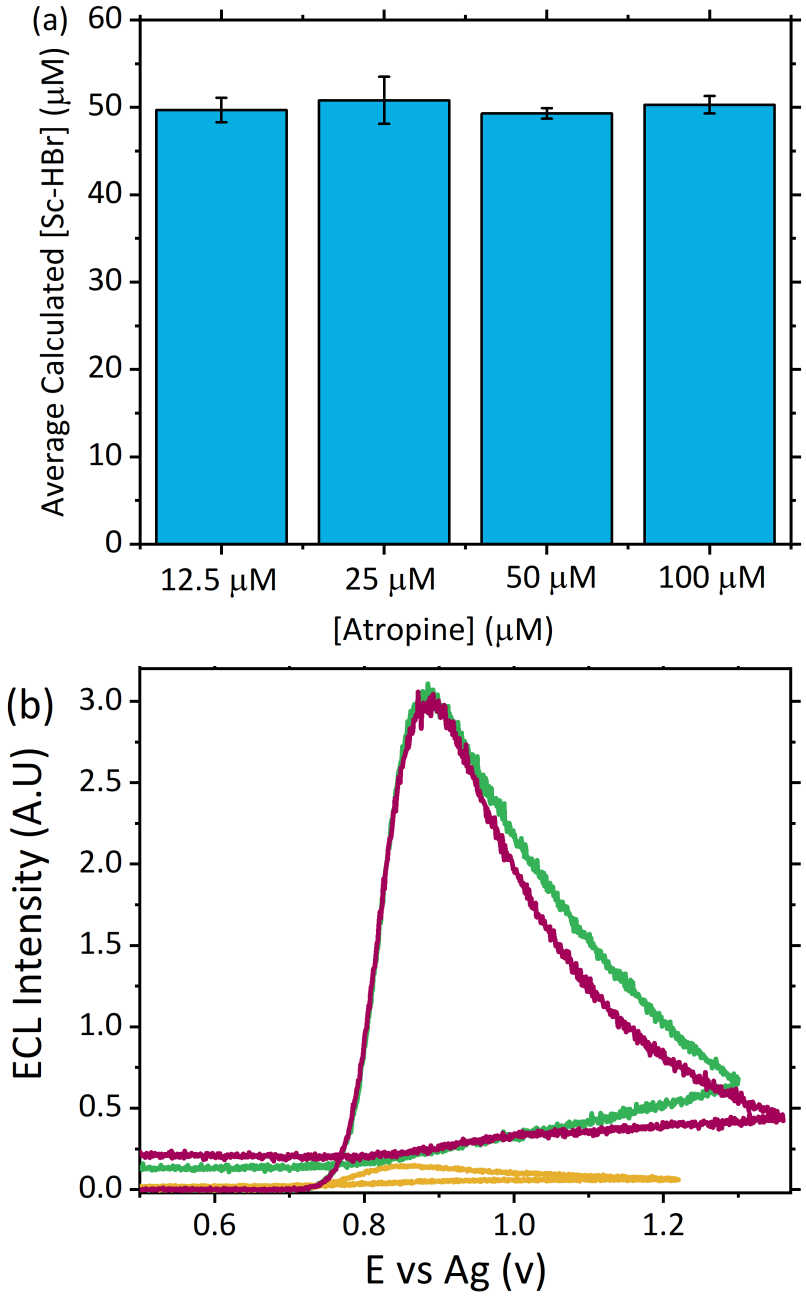

Figure 6.9: (a) Calculated scopolamine hydrobromide (Sc-HBr) concentrations in the presence of varying concentrations of atropine sulfate at pH 6. Concentrations calculated based upon maximum ECL intensity. Each bar represents the mean of the maximum ECL intensity at n=3 with error bars comprising of ± 1SD across these measurements. (b) ECL responses of 50 μM atropine sulfate (yellow), 50 μM scopolamine hydrobromide (green), and 50 μM atropine sulfate and scopolamine hydrobromide (pink) in pH 6 0.1 M $LiClO_4$ as the electrolyte and measured at a scan rate of 100 mV s^{-1} across $0.5 \leq E \leq 1.36$ V vs Ag at a PMT setting of 0.6 V.

As previously discussed, when samples at pH 11 were analysed, the base catalysed degradation of atropine to the ECL active degradation product, tropine, prevented accurate quantification at this pH. However, with scopolamine producing minimal emission intensity of 0.34 A.U at pH 11, the presence of a secondary species can be confidently determined; in this case, atropine is producing the observed signal increase, refer to Figure 6.10. Due to the significant increase in signal intensity when atropine is present in addition to scopolamine at pH 11, pH controlled ECL can be adequately used as a screening protocol to identify the number of species present in a potential mixed sample. Moreover, although in this current contribution the ability to quantify multiple species present is not possible, the potential for future application of chemometric modelling utilising ECL signals has been identified. By analysing samples at pH 6 and subsequently pH 11, the presence of both tropane alkaloids can be identified. Using pH 6 to negate emission from atropine, the concentration of scopolamine can be confidently determined. It is then probable that when the concentration of scopolamine is known, a calibration model could be constructed incorporating this known concentration. Chemometric modelling would then facilitate the removal of the signal contribution from scopolamine, thus allowing for the determination of the proportion of the signal attributed solely to atropine. Using this model, it would then be possible to determine the concentration of atropine present within the unknown sample.

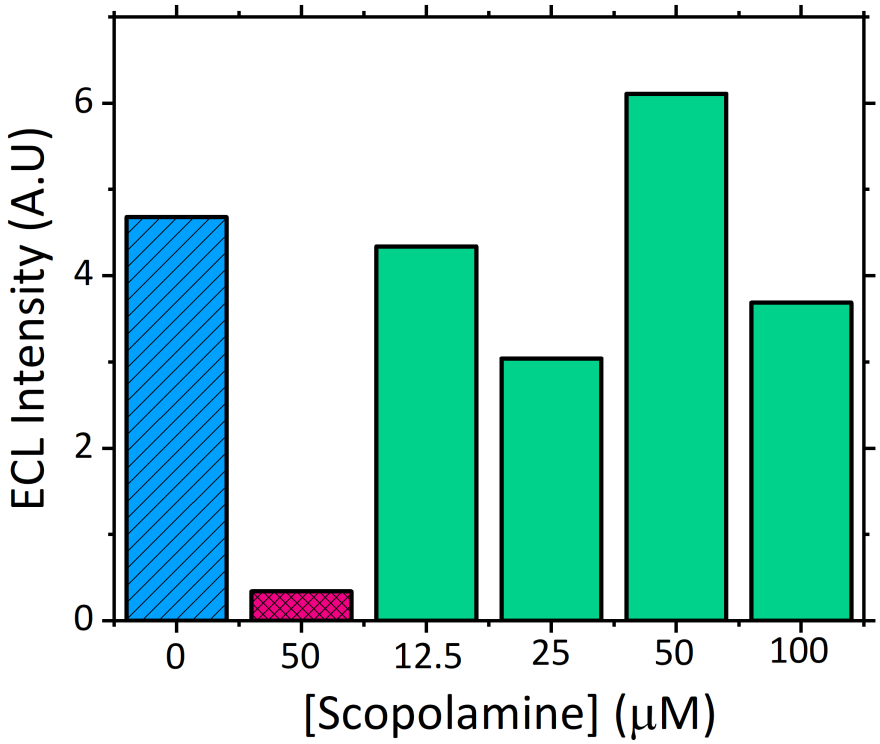

Figure 6.10: ECL intensity with varying concentrations of scopolamine hydrobromide in the presence of 50 μM atropine sulfate at pH 11 (green). The pink bar represents the ECL intensity observed 50 μM scopolamine hydrobromide only at pH 11. The blue bar represents the ECL intensity observed for 50 μM atropine sulfate only at pH 11.

6.4 Conclusion

Within this chapter the ability to identify between almost identical chemical structures through a basic $[Ru(bpy)_3]^{2+}$ based ECL sensor was demonstrated for the first time. Prior to this, species similar in structure, such as the two tropane alkaloids used here, could not be differentiated from one another via ECL without employing either separation strategies prior to detection or complex sample extraction and purification procedures to physically separate out individual components of a mixture.[20, 56] ECL has long suffered from limited specificity as a result of its broad emission spectra leading to indistinctive peaks with groups of compounds such as amines, all producing emission within the same potential region. In chapters four and five the same basic $[Ru(bpy)_3]^{2+}$ sensor was used. Chapter four, which discusses the detection of atropine within herbal plant material, highlighted the inability of the designed sensor to distinguish whether atropine, scopolamine or both were responsible for the observed signal.[18] By utilising pH and exploring the difference in pKa the developed methodology could be used to qualitatively determine whether a single species or multiple are responsible for the observed signal. Furthermore, although unable to quantify both tropane alkaloids at this time, this pH controlled ECL strategy can be successfully used for the quantification of scopolamine within a mixed sample containing various concentrations of atropine. Both tropane alkaloids as mentioned above have been previously shown to emit within the same potential region and thus are known to cause interference for qualifying or quantifying the alkaloids individually, when they are within the same matrix. This chapter has

shown that by closely studying the impact of pH upon ECL emission, a region can be identified where a single species' emission can in essence be switched off facilitating the qualification or quantification of the remaining emitting species. Although this is a promising step forward to increase the specificity offered by ECL, further development is still required. Although here scopolamine could be accurately quantified in the presence of atropine, the reverse could not be successfully performed. It, therefore, stands that the same problem would be encountered for other compound groups. However, it is hoped that the application of chemometric modelling to overcome this limitation would allow for the quantification of more species in the future. This chapter solely focused upon the tropane alkaloid family, and thus other groups of structurally similar compounds must be also investigated in the same manner to understand the wider applicability of the pH controlled ECL. While the initial studies reported within are promising and despite ECL possessing a number of advantages in comparison to its rivals, its limited specificity is currently hindering applications of the technique among the wider analytical community. As such, alternative methods to further improve its specificity are imperative if ECL is to become a more widely employed technique.

6.5 References

1. L. Shaw and L. Dennany, *Curr. Opin. Electrochem.*, 2017, **3**, 23-28.
2. W. R. de Araujo, T. M. G. Cardoso, R. G. da Rocha, M. H. P. Santana, R. A. A. Muñoz, E. M. Richter, T. R. L. C. Paixão and W. K. T. Coltro, *Anal. Chim. Acta*, 2018, **1034**, 1-21.
3. F. Chemat, S. Garrigues and M. de la Guardia, *Curr. Opp. Green Sust. Chem.*, 2019, DOI: https://doi.org/10.1016/j.cogsc.2019.07.007.
4. A. J. Bard, L. R. Faulkner, J. Leddy and C. G. Zoski, *Electrochemical methods: fundamentals and applications*, wiley New York, 1980.
5. M. M. Richter, *Chem. Rev.*, 2004, **104**, 3003-3036.
6. W. Miao, *Chem. Rev.*, 2008, **108**, 2506-2553.
7. C. K. P. Truong, T. D. D. Nguyen and I.-S. Shin, *BioChip J.*, 2019, **13**, 203-216.
8. E. J. O'Reilly, P. J. Conroy, S. Hearty, T. E. Keyes, R. O'Kennedy, R. J. Forster and L. Dennany, *RSC Adv.*, 2015, **5**, 67874-67877.
9. J. L. Delaney, E. H. Doeven, A. J. Harsant and C. F. Hogan, *Anal. Chim. Acta*, 2013, **803**, 123-127.
10. E. H. Doeven, G. J. Barbante, A. J. Harsant, P. S. Donnelly, T. U. Connell, C. F. Hogan and P. S. Francis, *Sens. Actuators B*, 2015, **216**, 608-613.
11. L. Dennany, E. J. O'Reilly, T. E. Keyes and R. J. Forster, *Electrochem. Commun.*, 2006, **8**, 1588-1594.
12. P. Pastore, D. Badocco and F. Zanon, *Electrochim. Acta*, 2006, **51**, 5394-5401.
13. D. An, Z. Chen, J. Zheng, S. Chen, L. Wang, Z. Huang and L. Weng, *Food Chem.*, 2015, **168**, 1-6.
14. J. McGeehan and L. Dennany, *Forensic Sci. Int.*, 2016, **264**, 1-6.
15. A. J. Stewart, K. Brown and L. Dennany, *Anal. Chem.*, 2018, **90**, 12944-12950.
16. X.-Y. Yang, C.-Y. Xu, B.-Q. Yuan and T.-Y. You, *Chin. J. Anal. Chem.*, 2011, **39**, 1233-1237.
17. A. Zhang, C. Miao, H. Shi, H. Xiang, C. Huang and N. Jia, *Sens. Actuators B*, 2016, **222**, 433-439.
18. K. Brown, M. McMenemy, M. Palmer, M. J. Baker, D. W. Robinson, P. Allan and L. Dennany, *Anal. Chem.*, 2019, **91**, 12369-12376.
19. W. Cao, J. Liu, H. Qiu, X. Yang and E. Wang, Electroanalysis: An International Journal Devoted to Fundamental and Practical Aspects of Electroanalysis, 2002, **14**, 1571-1576.
20. Y. Gao, Y. Tian and E. Wang, *Anal. Chim. Acta*, 2005, **545**, 137-141.
21. L. Jianguo, C. Yuan and J. Huangxian, *Electroanalysis*, 2007, **19**, 1569-1574.
22. B. Yuan, C. Zheng, H. Teng and T. You, *J. Chromatogr. A*, 2010, **1217**, 171-174.
23. G. Bozokalfa, H. Akbulut, B. Demir, E. Guler, Z. P. Gumus, D. Odaci Demirkol, E. Aldemir, S. Yamada, T. Endo, H. Coskunol, S. Timur and Y. Yagci, *Anal. Chem.*, 2016, **88**, 4161-4167.
24. R. Oueslati, C. Cheng, J. Wu and J. Chen, *Biosens. Bioelectron.*, 2018, **108**, 103-108.
25. J. Gao, Z. Chen, L. Mao, W. Zhang, W. Wen, X. Zhang and S. Wang, *Talanta*, 2019, **199**, 178-183.
26. J. Zhou, N. Gan, F. Hu, T. Li, H. Zhou, X. Li and L. Zheng, *Sens. Actuators B*, 2013, **186**, 300-307.

27. L. S. de Oliveira, M. A. Balbino, M. M. T. de Menezes, E. R. Dockal and M. F. de Oliveira, *Microchem. J.*, 2013, **110**, 374-378.
28. L. de Oliveira, A. dos Santos Poles, M. Balbino, M. Teles de Menezes, J. de Andrade, E. Dockal, H. Tristão and M. de Oliveira, *Sensors*, 2013, **13**, 7668.
29. L. Asturias-Arribas, M. A. Alonso-Lomillo, O. Domínguez-Renedo and M. J. Arcos-Martínez, *Anal. Chim. Acta*, 2014, **834**, 30-36.
30. H. Xie, X. Li, L. Zhao, L. Han, W. Zhao and X. Chen, *Sens. Actuators B*, 2016, **222**, 226-231.
31. A. J. Stewart, J. Hendry and L. Dennany, *Anal. Chem.*, 2015, **87**, 11847-11853.
32. H. J. Kim, K.-S. Lee, Y.-J. Jeon, I.-S. Shin and J.-I. Hong, *Biosens. Bioelectron.*, 2017, **91**, 497-503.
33. H. Li, A. C. Sedgwick, M. Li, R. A. R. Blackburn, S. D. Bull, S. Arbault, T. D. James and N. Sojic, *Chem. Comm.*, 2016, **52**, 12845-12848.
34. A. Florea, J. Schram, M. de Jong, J. Eliaerts, F. Van Durme, B. Kaur, N. Samyn and K. De Wael, *Anal. Chem.*, 2019, **91**, 7920-7928.
35. K. Shalabi, Y. Abdallah, H. M. Hassan and A. Fouda, *Int. J. Electrochem. Sci*, 2014, **9**, 1468-1487.
36. M. J. Márquez, M. A. Iramain and S. A. Brandán, *Int. J. Soc. Res. Methodol.*, 2018, **12**, 97-140.
37. H. Weinstein, S. Srebrenik, S. Maayani and M. Sokolovsky, *J. Theor. Biol.*, 1977, **64**, 295-309.
38. L. He, K. A. Cox and N. D. Danielson, *Anal. Lett.*, 1990, **23**, 195-210.
39. V. S. Sastri, in *Underground Pipeline Corrosion*, ed. M. E. Orazem, Woodhead Publishing, 2014, DOI: https://doi.org/10.1533/9780857099266.1.166, pp. 166-211.
40. W. Miao, J.-P. Choi and A. J. Bard, *J. Am. Chem. Soc.*, 2002, **124**, 14478-14485.
41. M. Sentic, M. Milutinovic, F. Kanoufi, D. Manojlovic, S. Arbault and N. Sojic, *Chem. Sci.*, 2014, **5**, 2568-2572.
42. L. C. Portis, V. V. Bhat and C. K. Mann, *J. Org. Chem.*, 1970, **35**, 2175-2178.
43. B. L. Laube, M. R. Asirvatham and C. K. Mann, *J. Org. Chem.*, 1977, **42**, 670-674.
44. L. Dennany, E. J. O'Reilly, P. C. Innis, G. G. Wallace and R. J. Forster, *Electrochim. Acta*, 2008, **53**, 4599-4605.
45. Q. Xiang, X. D. Yang and Y. Gao, *Adv. Mater. Res.*, 2014, **989-994**, 1007-1010.
46. W. D. Dettbarn, E. Heilbronn, F. C. G. Hoskin and R. Kitz, *Neuropharmacology*, 1972, **11**, 727-732.
47. F. J. Muhtadi and M. M. A. Hassan, in *Analytical Profiles of Drug Substances*, ed. K. Florey, Academic Press, 1990, vol. 19, pp. 477-551.
48. P. Zvirblis, I. Socholitsky and A. A. Kondritzer, *J. Am. Pharm. Assoc.*, 1956, **45**, 450-454.
49. A. Shrivastava and V. Gupta, *Chronicles of Young Scientists*, 2011, **2**, 21-25.
50. S. M. Oja and B. Zhang, *ChemElectroChem*, 2016, **3**, 457-464.
51. C. L. Winek, W. W. Wahba, C. L. Winek and T. W. Balzer, *Forensic Sci. Int.*, 2001, **122**, 107-123.
52. B. Boros, Á. Farkas, S. Jakabová, I. Bacskay, F. Kilár and A. Felinger, *Chromatographia*, 2010, **71**, 43-49.
53. E. Le Garff, Y. Delannoy, V. Mesli, V. Hédouin and G. Tournel, *Forensic Sci. Int.*, 2016, **261**, e17-e21.

54. K. J. Lusthof, I. J. Bosman, B. Kubat and M. J. Vincenten-van Maanen, *Forensic Sci. Int.*, 2017, **274**, 79-82.
55. L.-H. Shen, H.-N. Wang, P.-J. Chen, C.-X. Yu, Y.-D. Liang and C.-X. Zhang, *J. Food Drug Anal.*, 2016, **24**, 199-205.
56. R. A. Dar, P. K. Brahman, S. Tiwari and K. S. Pitre, *Colloids Surf., B*, 2012, **91**, 10-17.

CHAPTER SEVEN

CONCLUSIONS AND FUTURE WORK

“We keep moving forward, opening new doors and doing new things, because we’re curious and curiosity keeps leading us down new paths”

Walt Disney

ECL sensors have shown great promise for the sensing of a variety of target molecules, including those of forensic and diagnostics relevance. The intrinsic benefits of ECL offer a technique applicable to a variety of environments owing to its simplified instrumentation, minimal sample volumes and flexible choice of electrode material. Its wider acceptance within the analytical community in recent years has only been heightened by these benefits alongside the commercial availability of portable systems and disposable screen printed electrodes. Moreover, recent advancements have seen the incorporation of the technique into wearable sensors, appropriate for point-of-care devices offering continuous patient monitoring. Due to technological advancements, a recent shift in the necessary equipment required to perform ECL was been witnessed with reports upon the utilisation of smartphone devices as viable alternatives to traditional potentiostats, with in-built camera systems utilised as an alternative detector. Further advancements will ultimately only decrease the instrumentation costs while further enhancing portability. Both of which stand to only increase the accessibility of the technique to the wider analytical community, in turn offering significant benefits in the progression of such methodologies toward NPS screening strategies.

The utilisation of $[Ru(bpy)_3]^{2+}$ as the luminophore species, which has been utilised within ECL sensing systems since its inception in the 1960's, facilitates the development of sensors with superb sensitivity, in addition to the provision of a wide knowledge base upon which to draw. The ability of

the $[Ru(bpy)_3]^{2+}$ luminophore to operate within both the anodic and cathodic potential regions allows for its utilisation for both oxidative-reduction and reductive-oxidation mechanisms, alongside the annihilation pathway. Moreover, its compatibility within both organic and aqueous systems makes it ideal for implementation across a variety of complex matrix analysis, with particular interest in biological fluids. As a result of these characteristics, the $[Ru(bpy)_3]^{2+}$ luminophore is well positioned for ECL sensing systems concerned with the detection of a vast array of compounds.

Such reasons lead to its inclusion within this work which aimed to establish the feasibility of a basic $[Ru(bpy)_3]^{2+}$ based ECL sensor for the detection of tropane alkaloids within a variety of complex matrices, applicable to a forensic environment. Tropane alkaloids, atropine and scopolamine where chosen not only due to their hallucinogenic properties and criminal abuse but to exploit their almost identical chemical structures, for the assessment of the ability of an ECL sensor for individual identification of structurally similar compounds. A feat not previously achieved solely through ECL, as a result of its inherent lack of specificity from its broad emission spectrum. Such a characteristic is vital for techniques employed within forensic screening procedures, particularly with regard to NPS detection.

The developed sensor utilised carbon paste screen printed electrodes upon a flexible polymer substrate. The carbon working electrode was selectively modified through the drop casting of a film containing $[Ru(bpy)_3]^{2+}$

encapsulated within the cation exchange polymer Nafion. Optimum concentration of the luminophore species was determined to be 0.5 mM when contained within a 0.2% w/v Nafion film, with a 50:50 v/v EtOH:H_2O solvent system. This combination produced a film which displayed almost ideal electrochemical behaviour under interrogation, revealing a ΔE_p close to zero at sufficiently slow scan rates for the $Ru^{2+/3+}$ redox coupled and a FWHM close to the theoretical value of 90.6 mV for a one electron process. At higher scan rates, the departure from this ideality were observed, however this was not unexpected, but rather consistent with previous behaviour reported of Nafion encapsulated $[Ru(bpy)_3]^{2+}$. Encapsulation of the $[Ru(bpy)_3]^{2+}$ species facilitated employment of the sensor within a variety of matrices, with desorption of the luminophore species from the electrode surface negated hence maximising the sensitivity of the sensing system. Utilisation of disposable SPE was fundamental, not only due to their ease of translation into real-world applications including forensic analysis, but they allowed for the use of minimal samples volumes, key for samples of high toxicity or indeed forensic case samples.

Assessment of the sensor for the detection of tropane alkaloids, atropine and scopolamine, revealed their limited electrochemical behaviour upon unmodified carbon electrodes, thus preventing their detection solely through electrochemical methods. Incorporation of the ruthenium luminophore facilitated their detection via mediated oxidation, leading to ECL emission via the oxidative-reduction pathway. The mechanism for each alkaloid was

determined, with confirmation of the oxidative *N*-dealkylation process through the detection of the by-product formaldehyde. Both alkaloids displayed similar ECL emissions in regard to their position and shape, however scopolamine's $ECL_{\lambda max}$ was observed to produce a higher ECL intensity at slightly later oxidation potential, likely related to its greater electrochemical behaviour over atropine. pH analysis of both species revealed that they follow the same general trend, consistent with other structurally similar amines, with the greatest ECL intensity observed at values close to their pKa. Initial investigations identified that both alkaloids were suitable for analysis via the ECL electrochemical sensor developed here, thus making them ideal model compounds for use within this proof-of-concept study for the screening of NPS.

The developed ECL sensing system demonstrated satisfactory analytical performance; with an instrument precision of 4.1%, electrode variability of 1.9% and measurement day reproducibility of 8.3%. Detection limits were achieved down to forensically and clinically relevant concentrations of 0.75 μM and 0.44 μM at pH 8 for atropine and scopolamine respectively. As such the sensor could be applied for the detection of the alkaloids within a variety of complex matrices including herbal material, commercial drinks and biological fluids with confidence.

The ability to perform ECL analysis within commercial drink samples would offer rapid results to forensic investigators for cases of suspected drink

spiking, in addition to commercial applications. Direct analysis of atropine within tonic water and Coca-Cola® demonstrated a good correlation between experimental and theoretical values, despite the complex matrix. This demonstrates the ability of the sensor to provide ECL analysis within a non-ideal electrochemical matrix with no significant detriment observed, in spite of the greater resistance to charge transfer within these matrices alongside the presence of additional species. The ability to reliably detect ECL emission from within a coloured matrix, with no interference from the matrix background, was also observed. This finding implied the strong possibility to use light emitting techniques such as ECL for the screening of coloured samples, a limitation often reported within current forensic screening methodologies. As such, the samples matrices which can be screened for NPS presence would be expanded through the application of this sensing system.

Direct analysis of plant or herbal based material is a key achievement with direct relevance toward NPS detection. Often NPS are deposited upon herbal material prior to their distribution. Employed presumptive tests are frequently incompatible with such complex matrices, the development of this disposable ECL sensor combats this limitation by demonstrating the ability to reliably detect an alkaloid response within native plant species despite the large number of alternative compounds present. Here *Datura* leaf material, in which both alkaloids naturally occur, was mechanically applied to the modified electrode surface producing a response. As such, extraction

procedures were negated, making this methodology ideal for implementation outwith a laboratory facility. The signals obtained were used to distinguish between young and mature plants, highlighting a sensitivity toward alkaloid concentration. Furthermore, a singular response was observed despite the large number of co-species present within such a complex material. A degree of specificity toward tropane alkaloids was therefore displayed, further demonstrated through analysis of tomato plant material which produced a negligible signal, despite originating from the same parent plant family as *Datura* (solanaceous) and hence containing glycoalkaloid species.

Forensic cases often involve biological samples. In addition, the lack of knowledge surrounding NPS and their pharmacology can pose a significant problem for physicians treating patients under emergency situations. As such, it would be prudent for any sensing system developed for such applications within this field to be applicable for use within biological matrices. ECL's history of application within medicinal diagnostics typically involves complex extraction procedures or the employment of biological recognition molecules adhered to the electrode surface. This however is not suited towards in-field or point-of-care applications, where rapid answers are required at minimal cost with limited facilities available. Assessment of the developed sensor demonstrated the ability to detect the tropane alkaloids within biological matrices, most notably without any prior sample preparation procedures required, a key focus during sensor development. Despite the removal of the extraction and purification procedures previously

necessary, the ECL system was able to qualitatively detect scopolamine within serum, urine, saliva and sweat at clinically relevant concentrations. Furthermore, a proof-of-concept for the direct application of the sensor to the skin's surface revealed superb sensitivity and robustness, identifying the alkaloid despite collection of only minimal sample volumes from a roughened surface via an abrasive voltammetry method, without detriment to the electrodes surface.

The current sensor design within this body of work demonstrated a promising avenue toward the expansion of portable ECL systems for employment as screening methodologies alongside point-of-care devices. For the first time abrasive ECL was successfully demonstrated and revealed compatibility with range of biological fluids, herbal material and commercial drinks with no prior preparations required. Therefore, the methodologies and ECL sensor described within this work indicates a strong premise for the employment of portable ECL sensors within forensic and biomedical arenas. Such fields require rapid results, often with access to limited knowledge or facilities. Although a strong concept is shown within, one key issue remains. The intrinsic lack of specificity offered through ECL. This inherent characteristic poses an undisputed limitation of the sensor for the employment as a screening methodology within such environments. Initial progress has been made toward improved specificity within this body of work, through the development of pH controlled ECL. Here the ability switch off emission from one species, while maintaining that of the secondary

species was achieved. Atropine and scopolamine's almost identical chemical structures made them ideal for this investigation, with the tropane alkaloids displaying indistinguishable electrochemical behaviour and hence ECL mechanism. By alternating the pH of the sample matrix it became possible, at low pH values, to switch off emission from atropine. This allowed for the quantification of scopolamine within samples containing both alkaloids, with a good correlation observed between the theoretical concentrations and that measured. This was the first employment of such a methodology to improve ECL specificity and it is hoped its use can be expanded past these alkaloid species and improve the acceptance of ECL within forensic and biomedical environments.

Although this current work displayed satisfactory and promising results of the designed sensor for the detection of tropane alkaloids, full assessment of its performance across a range of different compounds, including more popular NPS classes, is required. Despite synthetic cannabinoids amongst the most prevalent NPS classes, there is to date limited literature available upon their electrochemical detection. This is in spite of their core structure containing functional groups ideal for electrochemical techniques. As such, it would be prudent to assess any ECL sensing system for the detection of this class. Moreover, this body of work demonstrated the capability of the developed sensor for abrasive ECL towards herbal material analysis, as such this design lends itself well to the detection of synthetic cannabinoids, commonly distributed on such material. It is hoped the strong proof-of-

concept shown by this sensing system could be easily applied to alternative species with minimal adaptions required. As ruthenium can be used in both the cathodic and anodic potential regions, it makes its employment here ideal for such an application. Furthermore, a greater study upon the variation intrinsic to biological fluids would be required. Although outside the scope of this research it would be prudent to determine person to person variation, in order to gain a full understanding of the impact towards the intrinsic background signals recorded. Such an understanding would allow for the confident assignment of a threshold value, above which the presence of a foreign species would be assigned. A study of this kind should include a thorough investigation of potential interferents including the impact of fast or feed state, common medications and other legal psychoactive substances including nicotine and alcohol.

However further investigations into improved specificity remains necessary. Although the developed pH controlled ECL displayed a promising initial step, it requires the user to possess an in-depth knowledge of the target species, its pKa and its ECL response. Hence, this technique in its current formate is not as yet applicable as a screening methodology or for use by non-experts. It therefore becomes pertinent to investigate further techniques which can address this limitation. The employment of alternative metal luminophores has begun to show potential for such applications. Alternative species based upon iridium or osmium metal centred complexes have displayed a degree of selectivity toward different species. However little knowledge or

understanding of the mechanisms behind this selectivity are currently known and therefore far more in-depth studies are indeed required. Alongside the alternative specificity offered and compared with the traditional ruthenium based luminophore, these iridium and osmium complexes are observed to emit at different wavelengths and display alternative colours. As such the possibility to develop a multi-electrode array system is presented. This kind of system could offer colour controlled ECL sensors facilitating the identification of multiple species within a singular matrix. The development of such a sensor would be the ultimate system to address the current specificity hurdle, offering a sensing system appropriate for employment within a variety of forensic and clinical environments. Hence, the need for new screening methodologies appropriate for NPS detection would be addressed, while the acceptance of ECL sensors across the analytical community and beyond would be widened.